

SOME OXIDATIVE ADDITION REACTIONS OF  
GROUP IVB COMPOUNDS TO  
TRANSITION METAL COMPOUNDS

by

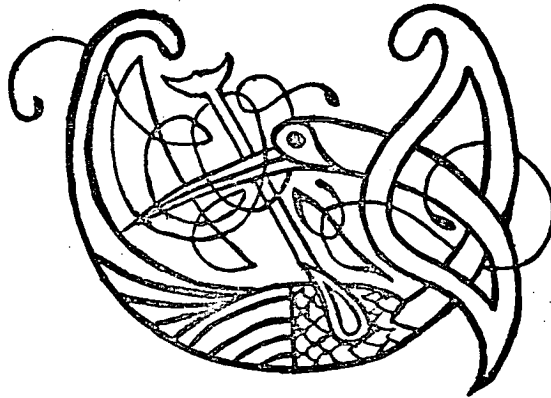
Thomas Earle Fraser

A Thesis presented for the degree of Doctor of Philosophy  
University of Edinburgh

December 1977



TO MY MOTHER  
AND MY BROTHER



### Acknowledgements

I would like to thank Professor E.A.V. Ebsworth for giving me the opportunity to do this research and for his constant help and encouragement during my term as his student.

I would also like to thank Dr. S. Cradock and Dr R. Perutz for their help and advice during this work. Without the help of Dr. D.W.H. Rankin, the electron diffraction studies would not have been possible and I would like to thank him for his help in that area.

I would like especially to thank Dr. F. Reed for his willingness to impart his expertise in the preparation and handling of the air sensitive iridium compounds, and to Mr S.D.G. Henderson for his patience and perseverance during my long apprenticeship on the vacuum line. I would also like to express my gratitude to all my co-workers for their support during the three years.

Further, I would like to thank Professor D.W.J. Cruickshank and Dr. B. Beagley of U.M.I.S.T. for providing the facilities for the collection of the electron diffraction data and Mrs V. Ulbrecht for running the samples.

Finally I would like to thank the S.R.C. and N.A.T.O. for financing this research and the University of Edinburgh for providing the laboratory facilities.

This dissertation has not been submitted, in part or in whole, for any degree at this or any other university. A superficial study of the reactions of  $MH_3X$  (M:Si,Ge ; X:H,Cl,Br,I) with  $IrH(CO)(PPh_3)_3$  was made as a part of a final year project, but these reactions have been repeated and studied in more detail for the purposes of this work. As far as I am aware, this research is original and is my own work; where this is not so, credit has been given.

Thomas E. Fraser

### Summary

In Part One of this thesis, compounds formed by the oxidative addition of  $\text{MH}_3\text{X}$  (M:Si,Ge; X:H,F,Cl,Br,I) and  $\text{H}_3\text{SiMH}_3$  (M:C,Si) to  $\text{Ir}(\text{CO})\text{X}(\text{PEt}_3)_2$  (X:Cl,I) or  $\text{IrH}(\text{CO})(\text{PPh}_3)_3$ , and additions of  $(\text{SiH}_3)_2\text{Z}$  (Z:O,S,Se) and  $(\text{SiH}_3)_3\text{P}$  to  $\text{Ir}(\text{CO})\text{I}(\text{PEt}_3)_2$ , are described and characterised by n.m.r. spectroscopy and, where possible, by infra-red spectroscopy and analysis for C and H.

In Part Two, analogous reactions were attempted by allowing Group IVB compounds to react with  $\text{Et}_3\text{PAuX}$  (X:Cl,I) and  $(\text{Et}_2\text{P}(\text{CH}_2)_2)_2\text{Au}_2$ . Conclusive proof of oxidative addition was not obtained, but several unusual reactions were observed and attempts are made in the text to account for the observations made during these reactions.

In Part Three, determinations of the structure, in the gas phase, of an ylide compound (trimethyl(methylene)phosphorane), similar to that used in the preparation of the dimeric gold compound studied in Part Two, by electron diffraction, is described. Also, the gas phase structure of the related ylide (hexamethylcarbodiphosphorane) is studied by electron diffraction, using two mathematical models to describe the molecule: one model (Model A) assumes a fixed conformation, whereas the other (Model B) assumes free rotation within the molecule. The structures derived are discussed in terms of the way in which they reflect the nature of the ylide bonds in the molecules.

## CONTENTS

	Page
<b>Part One</b>	
<b>Iridium Reactions</b>	
<b><u>Chapter 1</u> Introduction to Iridium Work</b>	<b>1</b>
1.1 Mechanisms	
1.2 Oxidative Addition Reactions Involving Iridium Complexes	9
1.3 Oxidative Addition in Catalysis	15
1.4 Nuclear Magnetic Resonance Spectroscopy	19
<b><u>Chapter 2</u> Additions of <math>MH_3X</math> (M:Si,Ge; X:H,F,Cl,Br,I)</b>	<b>27</b>
2.1 Additions to $Ir(CO)X(PET_3)_2$ (X:Cl,I)	27
2.1.1 Reactions Involving Oxidative Addition Only	30
Figure 2a	33
2.1.2 Oxidative Addition Reactions Involving Halide Exchange	46
2.1.3 Trends in n.m.r. Parameters	51
2.2 Additions to $IrH(CO)(PPh_3)_3$ (n.m.r. study)	54
2.2.1 Results of the $^{31}P$ n.m.r. Study	55
2.2.2 Results of the $^{19}F$ Study	62
2.3 Conclusions on Additions of $MH_3X$	64
<b><u>Chapter 3</u> Additions of <math>H_3SiMH_3</math> (M:C,Si)</b>	<b>68</b>
3.1 Additions to $Ir(CO)Cl(PET_3)_2$	68
3.1.1 Addition of $Si_2H_6$	68
3.1.2 Addition of $H_3SiCH_3$	69
3.2 Additions to $IrH(CO)(PPh_3)_3$	70
3.2.1 Addition of $Si_2H_6$	71
3.2.2 Addition of $H_3SiCH_3$	76
3.3 Conclusions from $H_3SiMH_3$ Addition Reactions	82

<u>Chapter 4</u>	Additions of $(\text{SiH}_3)_2\text{Z}$ (Z:O,S,Se) to $\text{Ir}(\text{CO})\text{I}(\text{PET}_3)_2$	84
4.1	Additions of $(\text{SiH}_3)_2\text{O}$	85
4.2	Additions of $(\text{SiH}_3)_2\text{S}$ and $(\text{SiH}_3)_2\text{Se}$	86
4.3	Conclusions from $(\text{SiH}_3)_2\text{Z}$ Addition Reactions	91
<u>Chapter 5</u>	Additions of $(\text{SiH}_3)_3\text{P}$ to $\text{Ir}(\text{CO})\text{I}(\text{PET}_3)_2$	96
5.1	Reaction of Excess $(\text{SiH}_3)_3\text{P}$	97
5.2	1:2 Molar Reaction of $(\text{SiH}_3)_3\text{P}$ with $\text{Ir}(\text{CO})\text{I}(\text{PET}_3)_2$	100
5.3	1:3 Molar Reaction of $(\text{SiH}_3)_3\text{P}$ with $\text{Ir}(\text{CO})\text{I}(\text{PET}_3)_2$	101
5.4	Conclusions from $(\text{SiH}_3)_3\text{P}$ Addition Reactions	103
Appendices to Part. One		
(a)	Reactions of $\text{H}_2\text{S}$ and $\text{H}_2\text{Se}$ with $\text{Ir}(\text{CO})\text{Cl}(\text{PET}_3)_2$	108
(b)	A Homonuclear Decoupling Experiment. on $\text{IrH}(\text{CO})\text{I}(\text{PET}_3)_2\text{SiH}_2\text{Br}$	110
(c)	2:1 Molar Reaction of $\text{SiH}_4$ with $\text{Ir}(\text{CO})\text{Cl}(\text{PET}_3)_2$	112
Part Two		
Gold Reactions		
<u>Chapter 6</u>	Attempted Oxidative Addition Reactions of Group IVB Compounds to $\text{Et}_3\text{PAuX}$ (X:Cl,I) and $(\text{Et}_2\text{P}(\text{CH}_2)_2)_2\text{Au}_2$	113
6	Introduction to Gold Work	113
6.1	Reactions of Group IVB Hydrides and Halides with $\text{Et}_3\text{PAuX}$	114
6.2	Reactions of $\text{H}_3\text{SiMH}_3$ (M:C,Si) with $\text{Et}_3\text{PAuX}$	116
6.3	Reaction of $\text{SiH}_3\text{I}$ with $(\text{Et}_2\text{P}(\text{CH}_2)_2)_2\text{Au}_2$	118
Part Three		
Electron Diffraction Gas Phase Structure Determinations		
<u>Chapter 7</u>	Introduction to Electron Diffraction Methods	122
<u>Chapter 8</u>	Structure of Trimethyl(methylene)phosphorane	127
8.1	Model	129

8.2	Refinement and Results	130
8.3	Conclusions	131
<u>Chapter 9</u>	<u>Structure of Hexamethylcarbodiphosphorane</u>	141
9.1	Refinement Assuming Fixed Conformation of $P(CH_3)_3$ Units	143
9.1.1	Model A	143
9.1.2	Refinement and Results	144
9.2	Refinement Assuming Free Rotation of $P(CH_3)_3$ Units	154
9.2.1	Model B	154
9.2.2	Results	156
9.3	Conclusions	165
<u>Chapter 10</u>	<u>Experimental</u>	169
	Equipment	169
	Solvents and Preparations of Group IVB Compounds	172
	The sections and sub-sections in this chapter have been given the same numbers as the chapter and section to which they relate.	
	References	182
	Appendix - Published Papers	187



PART ONE

Chapter 1

Introduction to Iridium Work

## 1.1 Mechanisms

The term "Oxidative Addition" is a general one to cover various reactions where an increase in formal oxidation state of a system is accompanied by an increase in co-ordination number.

Co-ordination number	d electron configuration
8	$d^1, d^2$
6	$d^3, d^4, d^5, d^6$
5	$d^7, d^8$
4-square planar	$d^8$
4-tetrahedral	$d^{10}$
3	$d^{10}$
2	$d^{10}$

Table 1/1

Table 1/1 shows d electron configurations for transition metals and their associated co-ordination numbers. In order for an oxidative addition to occur, the transition metal system must be capable of supporting the increased co-ordination number associated with its increased oxidation state. The small molecule which oxidises the system generally adds as two ligands to the system and, in doing so, a bond within the small molecule is broken. Assigning the oxidation state of the metal in the system by assuming a closed valence shell on each ligand, the new ligands must both acquire two electrons to complete their valence shells. Two of these electrons will come from the bond which is broken within the small molecule, but the other two electrons must come from the metal system. The formal oxidation state of the metal must increase by two. To recapitulate: for such an

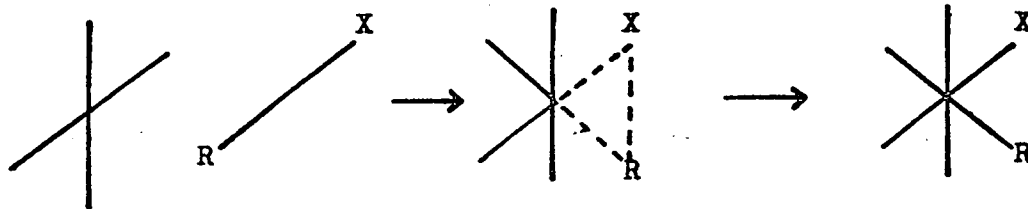
oxidation to occur, both the co-ordination number and the oxidation number of the metal in the system must increase by two (i.e. the formal number of d electrons must decrease by two). A system capable of undergoing such a reaction is the four co-ordinate  $d^8$  system, which would then go to a six co-ordinate  $d^6$  system.  $\text{Ir}(\text{CO})\text{Cl}(\text{PPh}_3)_2$  is a good example of such a system. A similar reaction could be achieved by the five co-ordinate  $d^8$  system, but this would require the loss of a ligand, at some stage in the reaction, to form the six co-ordinate species.  $\text{IrH}(\text{CO})(\text{PPh}_3)_3$  is a good example of this type of system.

This view of oxidative addition is derived from Crystal Field Theory. Molecular Orbital Theory uses a slightly different approach. Molecular Orbital Theory predicts that many transition metal complexes will follow the "Eighteen Electron Rule". These are the eighteen electrons required to fill the bonding and non-bonding orbitals which arise from the interaction of the atomic orbitals of the metal and the ligands. Compounds of  $d^8$  configuration, such as  $\text{Ir}(\text{CO})\text{Cl}(\text{PPh}_3)_2$  contain only sixteen electrons in the molecular orbitals and require two additional electrons to comply with the Eighteen Electron Rule. In the oxidative addition reaction these two electrons are supplied by the small molecule which adds to the system. The term "oxidative addition" is therefore ambiguous as it is not always clear just what is being oxidised.

There are several mechanisms which can be proposed for this type of reaction. These are:-

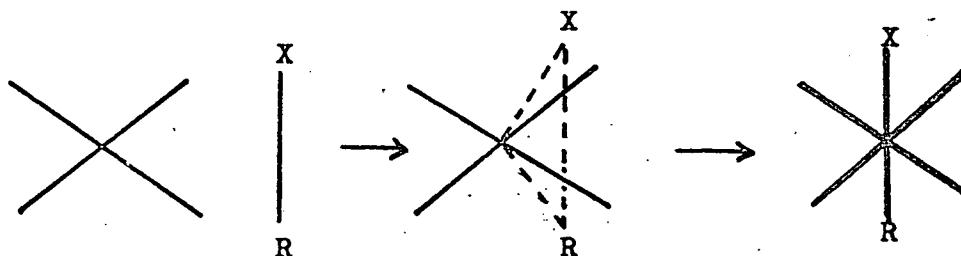
(a) The small molecule approaches the  $d^8$  species from above or below the plane of the metal complex. The two metal-ligand bonds parallel to the bond which is broken in the small molecule move

away from the small molecule as it approaches. A bond is broken within the small molecule and two bonds formed to the metal.



This mechanism would give what is termed a cis product in which the added ligands are mutually cis.

(b) The small molecule approaches the  $d^8$  system in the plane of the molecule with the bond within the small molecule, which is to be broken, perpendicular to this plane. There is no distortion out of the plane of the metal ligands. The bond in the small molecule is broken and two bonds to the metal are formed.

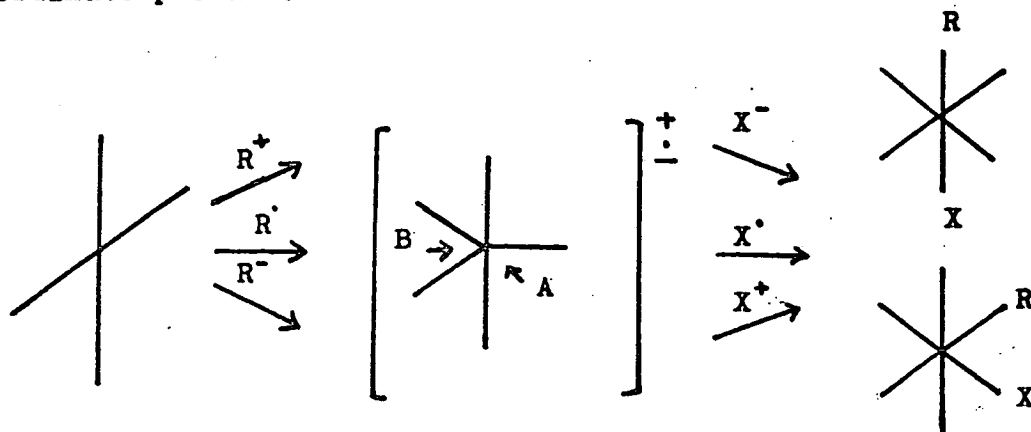


This mechanism would give a product which is termed a trans product in which the added ligands are mutually trans.

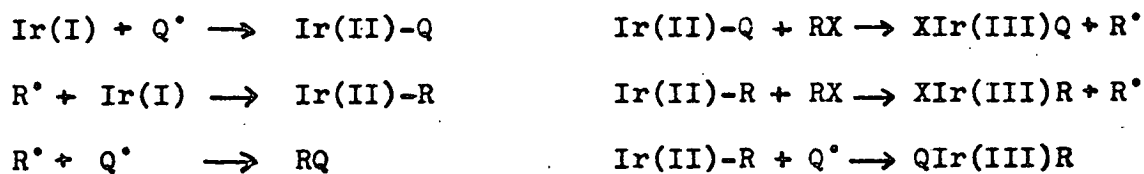
(a) and (b) are concerted processes with uncharged intermediates. They should therefore show second order rate expressions and be little influenced by the polarity of the solvent. Also if R is chiral, the chirality of R should be retained.

(c) The small molecule may, by homolytic or heterolytic cleavage of a bond, be broken into two fragments. One fragment of the molecule could then attack the square planar system of the metal to

form a five co-ordinate intermediate which would then be attacked by the other fragment of the small molecule to form the six co-ordinate product.



This mechanism can give both cis and trans addition, depending on whether the second fragment approaches the intermediate from route A or B respectively. The five co-ordinate intermediate is likely to undergo pseudo-rotation which could lead to the formation of further isomers. Mechanism (c) has been shown as a two stage process, but it is likely to involve initiation, propagation and termination: for example with radicals

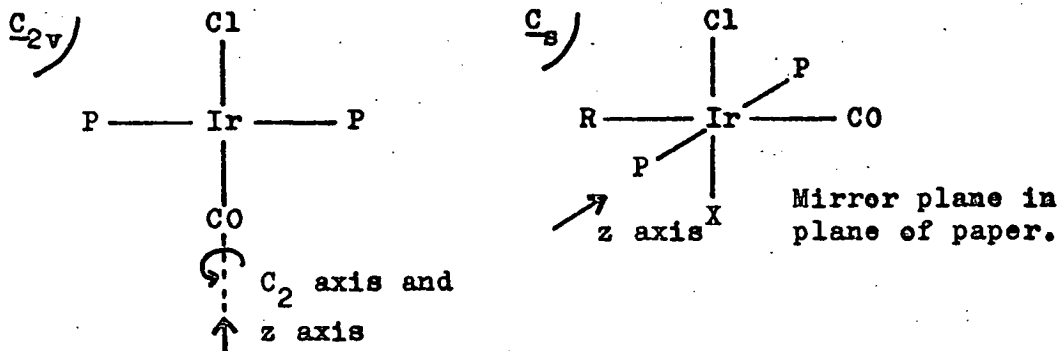


If R was a chiral centre, it is likely that it would undergo inversion due to an  $S_N2$  reaction at the carbon at the chiral centre or, if the R fragment had a finite lifetime, racemisation would occur. (c) would not show a simple second order rate expression and would be likely to be influenced by the polarity of the solvent. Also if a radical route is the mechanism used, the rate should be

increased by radical initiators and decreased by radical scavengers

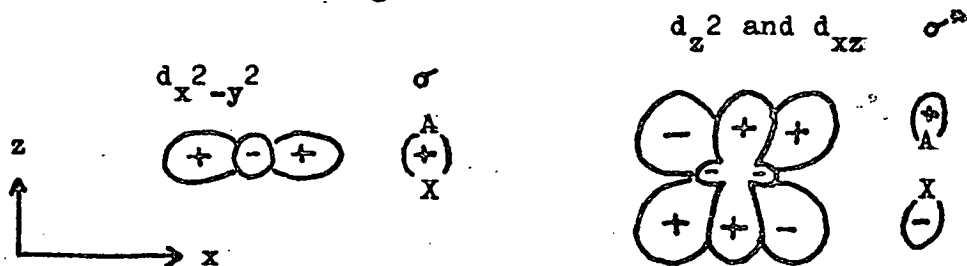
The mechanism for addition of a five co-ordinate  $d^8$  species is complicated by the loss of a ligand. If the ligand is lost before the addition, giving a four co-ordinate intermediate, which then undergoes the addition reaction, the reaction would be inhibited by an excess of the dissociating ligand, as the dissociation would be expected to be the rate determining step. The four co-ordinate intermediate would then go on to react by routes (a), (b), or (c). If the addition occurs before the dissociation, a seven co-ordinate intermediate would then be formed which would then eliminate a ligand. The formation of a seven co-ordinate intermediate would be expected to be the rate determining step and the rate of reaction would not be expected to be influenced by the presence of any free ligand. If the reaction was of a non-concerted type as with (c), a six co-ordinate intermediate would result. Whether or not this would then undergo attack by the remaining fragment of the small molecule or whether, if attack occurs, a charged or neutral ligand would be expelled, would depend on the polarity of the solvent.

A molecular orbital study of the simple oxidative addition reaction (i.e. to  $\text{Ir}(\text{CO})\text{Cl}(\text{PPh}_3)_2$ ) would be very useful for mechanistic considerations. Such a study is complicated by a change in overall symmetry during the reaction.  $\text{Ir}(\text{CO})\text{Cl}(\text{PPh}_3)_2$  has  $C_{2v}$  symmetry and has the z axis coincident with the  $C_2$  axis which lies along the carbonyl-iridium-chloride bond axis. After addition, both cis and trans isomers have  $C_s$  symmetry and the z axis is perpendicular to the mirror plane of the molecule, coinciding with the phosphorus-iridium-phosphorus bond axis.



Despite this complication, some qualitative observations can still be made on the concerted mechanisms (a) and (b). To simplify the discussion, only the addition of diatomics will be considered, but the argument may be extended to other small molecules by regarding them as diatomics with the atoms replaced by groups joined by the bond which is broken during the reaction.

In mechanism (a) the diatomic approaches via the vacant coordination sites perpendicular to the plane of the molecule as this would entail a minimum of steric hindrance. As the phosphines usually remain trans to each other throughout the reaction, the diatomic must normally approach with its molecular axis parallel to the  $d_z^2$  orbital. This would allow overlap between the filled  $d_{x^2-y^2}$  orbital and the filled  $\sigma$  bonding orbital of the diatomic. Overlap of the filled  $d_{xz}$  orbital and the empty  $\sigma^*$  anti-bonding orbital of the diatomic would also be possible and would be of great importance as any electron flow from the  $d_{xz}$  orbital into this anti-bonding orbital would tend to weaken the diatomic bond which is broken during the reaction.



In mechanism (b) the diatomic would approach the metal with its molecular axis bisected by the plane of the metal complex. It would approach between axes to minimise steric hindrance, but this route would still be more sterically hindered than that taken in mechanism (a). This would allow overlap to occur between the  $d_{yz}$  orbital and the  $\sigma$  bond of the diatomic, but in this case there is no  $d$  orbital which can interact with the  $\sigma^*$  anti-bonding orbital of the diatomic and so weaken the diatomic bond.

In considering addition it is worthwhile to look at the reverse reaction e.g. reductive elimination of  $H_2$  from  $IrH_2(CO)Cl(PPh_3)_2$ . Geoffrey and Pierantozzi have found that irradiation with U.V. light leads to a concerted elimination of  $H_2$  from  $IrH_2(CO)Cl(PPh_3)_2$ <sup>1</sup> and they offer the bonding scheme in figure 1a.

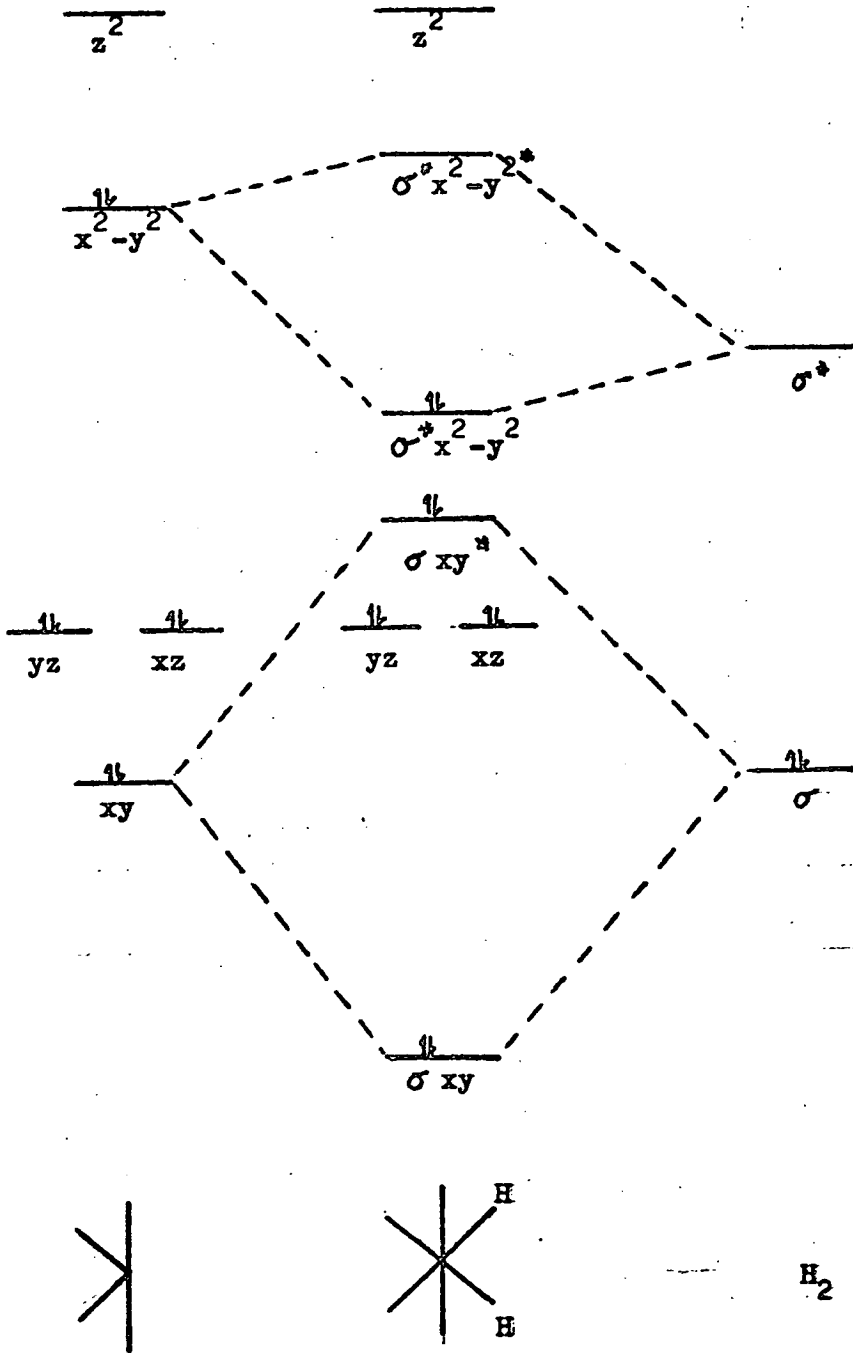
Geoffrey and Pierantozzi suggest that the elimination is due to promotion of an electron from  $\sigma^* x^2 - y^2$  to  $\sigma^* x^2 - y^2$ <sup>a</sup>. This gives a net non-bonding situation and the hydrogen dissociates from the metal. This would to some extent support the molecular orbital picture given above as  $\sigma^* x^2 - y^2$ <sup>a</sup> would have mainly metal character and this would represent a flow of  $\sigma^*$  electrons back into  $d_{xz}$  and so reverse mechanism (a).

This approach is appealing, but further evidence has shown that the initial excitation appears to be that of an electron associated with a phosphorus-iridium bond and that the dissociation is a secondary reaction.

It is difficult to discount any of the above mechanisms on purely theoretical grounds. It would be worthwhile to review these mechanisms in the light of the evidence from experimental work on these systems.



Figure 1a.



Geoffrey and Pierantezzi have used a different method of assigning the axes from that used in the text. The method of labelling used in the original article has been maintained in this figure, but this does not alter the above arguments.

Figure 1a Bending Scheme Suggested by Geoffrey and Pierantezzi <sup>1</sup>

## 1.2 Oxidative Addition Reactions Involving Iridium Complexes

A novel preparation of  $\text{trans-Ir(CO)Cl(PPh}_3)_2$  was described by Vaska and Di Luzio in 1961<sup>2</sup>. Due to the large amount of interest shown in this compound, especially by Vaska, it became generally known as Vaska's compound, although the compound was first made by a different route in 1959<sup>3</sup>. In the initial paper, Vaska and Di Luzio reported that Vaska's compound underwent oxidative addition of HCl to give a stable six co-ordinate species. This, Vaska reported, was in marked contrast with the unstable species generated by the analogous reaction with  $\text{trans-PtH(PEt}_3)_2\text{Cl}$ . With Vaska's compound it was possible to study the isomers produced by the oxidative addition of small molecules and, so it was hoped, to elucidate the mechanism, or mechanisms, of the reaction. Vaska went on to show that  $\text{H}_2$  and  $\text{Cl}_2$  also react in this way<sup>4</sup> and there have been many more reports of other small molecules which react in this way<sup>5</sup>.

In 1963  $\text{IrH(CO)(PPh}_3)_3$  was prepared from Vaska's compound<sup>6</sup>. This compound was not used in mechanistic work on oxidative addition due to the added complexity of the extra phosphine, but it was of great importance in the field of homogeneous catalysis and it is in this context that this compound will be discussed in the next section.

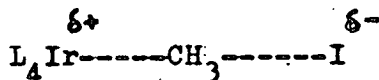
The synthesis of  $\text{IrH(CO)(PPh}_3)_3$  was overshadowed to some extent by Vaska's discovery, in the same year, of what is probably the most remarkable and best known property of Vaska's compound, which is its ability to combine reversibly with molecular oxygen<sup>7</sup>. Vaska was quick to point out the parallel between such behaviour and the action of haemoglobin in the bloodstream. He suggested that the oxygen adduct of Vaska's compound could be used as a model for the study

of oxygen carriers in complex biological systems. However study of  $\text{Ir}(\text{CO})\text{Cl}(\text{PPh}_3)_2 \cdot \text{O}_2$  itself was not easy due to its poor solubility. An X-ray determination of its structure<sup>8</sup> showed it to have an O-O distance of  $1.30 \pm 0.03 \text{ \AA}$  indicating an intermediate bond order between one (O-O in peroxide is about  $1.5 \text{ \AA}$ ) and two (O-O in  $\text{O}_2$  is  $1.21 \text{ \AA}$ ). The exact nature of the bonding of  $\text{O}_2$  to iridium and the formal oxidation state of the iridium is still a subject of some debate.

The investigation of the oxidative addition mechanism continued with a kinetic study of the additions of  $\text{H}_2$ ,  $\text{O}_2$  and  $\text{CH}_3\text{I}$ <sup>9</sup>. For  $\text{H}_2$  and  $\text{O}_2$  the reaction was found to be second order and the rate expression to be

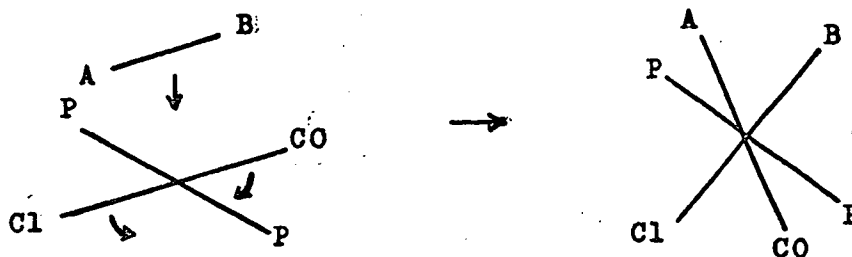
$$\text{Rate} = k(\text{Ir}(\text{CO})\text{X}(\text{PPh}_3)_2)(\text{A}) \quad \begin{array}{l} \text{X: Cl, Br, I} \\ \text{A: O}_2, \text{H}_2 \end{array}$$

The rate also depended on the nature of the halide X, being greatest when X is I and least when X is Cl. This can be understood, if addition is electrophilic, in terms of electron donation to the metal by the halide, which also increases from Cl to I. But with  $\text{CH}_3\text{I}$  the reaction was shown to be solvent dependant and the dependance on the halide X was reversed i.e. Cl faster than I. This led to postulating a transition state for this reaction of the type



A determination of the configuration of the isomers produced by the reaction of Vaska's compound with  $\text{HCl}$ ,  $\text{H}_2$ ,  $\text{X}_2$  and  $\text{CH}_3\text{I}$  was carried out using infra-red spectroscopy<sup>10</sup>. The conclusions were based on symmetry arguments and on the effect of the ligand trans to Cl on the Ir-Cl stretching frequency<sup>11</sup>. The results showed the

isomers to be of a type expected from cis addition, with the added ligands mutually cis and the phosphines mutually trans, confirming previous work and leading to the postulation of the following mechanism.

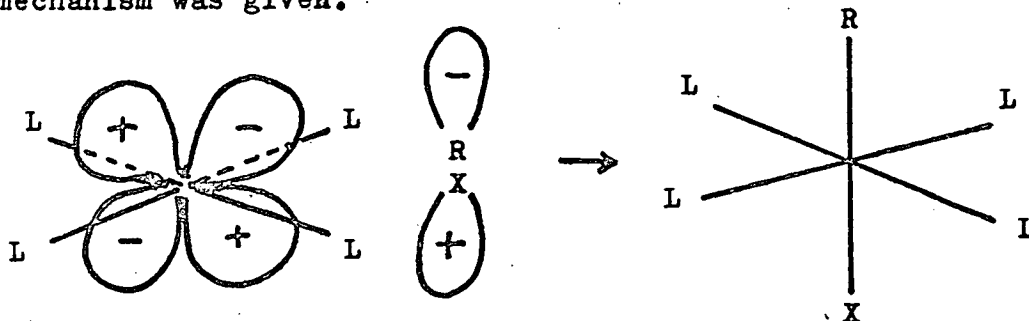


The conclusions, though straightforward, were in marked contrast with results obtained when dimethylphenylphosphine was substituted for triphenylphosphine<sup>13</sup>. In this case  $H_2$  underwent cis addition, but  $CH_3I$  underwent trans addition. In the analogous reaction with methylphenylphosphine, addition of  $X_2$  and  $CH_3I$  was trans and showed no solvent dependence, the reactions having been carried out in benzene and in glacial acetic acid<sup>14</sup>.

A simple cis mechanism no longer accounts for all these observations, which led to the question of whether there was such a thing as trans addition or whether apparent trans addition could be explained in terms of initial cis addition followed by rearrangement to give a product in which the added ligands were mutually trans. This idea was supported to some extent by work on the addition of allyl bromide to the dimethylphenylphosphine analogue of Vaska's compound<sup>15</sup>. Addition of allyl bromide to the complex gave a product apparently derived from trans addition, with mutually trans phosphines. Addition of allyl bromide in benzene gave an isomer apparently formed by cis addition, with mutually cis phosphines, but when this isomer was recrystallized from ethanol or chloroform the trans isomer was generated. It was postulated that

this rearrangement was made possible by halide dissociation and the resulting allyl-stabilised cation was isolated by dissolving either isomer in a methanolic solution of  $\text{NaBPh}_4$ . The presence of the allyl group may make this a special case and it would be unwise to extend any general conclusions to systems where an allyl-stabilised intermediate cannot be formed. It has been shown that the isomer produced on addition of  $\text{HX}$  to Vaska's compound also depends on the solvent used, being *cis* in the absence of solvent <sup>17</sup>, but giving "trans addition" isomers when subsequently dissolved. The proportion of *trans* to *cis* isomer depends on the solvent.

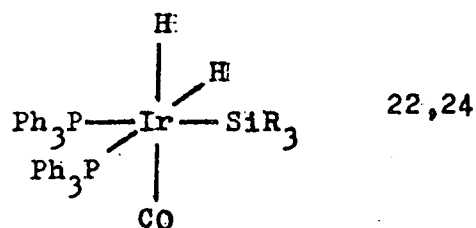
The reaction of  $\text{CH}_3\text{I}$  with Vaska's compound was singled out as being unusual <sup>9</sup>. If the transition state were of a linear type with an  $\text{S}_{\text{N}}2$  reaction at the carbon centre, then inversion at this centre should occur. It was reported that a chiral carbon centre showed retention of configuration on addition <sup>18</sup> and the following mechanism was given.



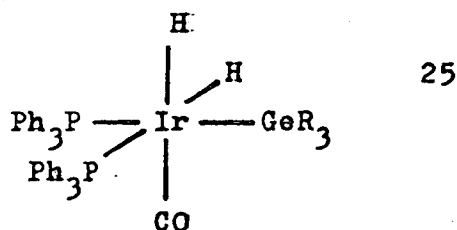
The results leading to this conclusion were interpreted on the premise that the cleavage of a carbon-iridium bond with  $\text{Br}_2$  went with retention of configuration at the carbon centre. This was questioned after it was found that bonds between carbon and several other metals were cleaved by  $\text{Br}_2$  with inversion at carbon <sup>19</sup>. Later work on related systems showed that racemisation of the

chiral molecule occurred and that the reaction was inhibited by galvanoxyl and promoted by benzoyl peroxide and  $O_2$ <sup>20,21</sup>, indicating a radical mechanism. If this were the case, the addition need not be concerted as the other reactions appear to be. Whereas with isomerisation of the allyl bromide adduct the five co-ordinate species needed for rearrangement is generated by dissociation of the six co-ordinate species, in this case one ligand may add initially to give a five co-ordinate species followed by addition of the other ligand as a second stage.

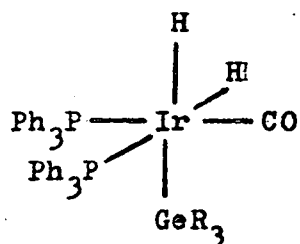
Addition of  $R_3SiH$  gave a hydride due to cleavage of the Si-H bond<sup>22</sup>. This has been shown to go with retention of configuration about the silicon<sup>23</sup>. If excess  $(EtO)_3SiH$  is added an exchange reaction occurs slowly to give  $R_3SiCl$  and a metal dihydride. This was assigned the structure



Analogous reactions were found to happen with  $R_3GeH$  (R: Me or Et) giving



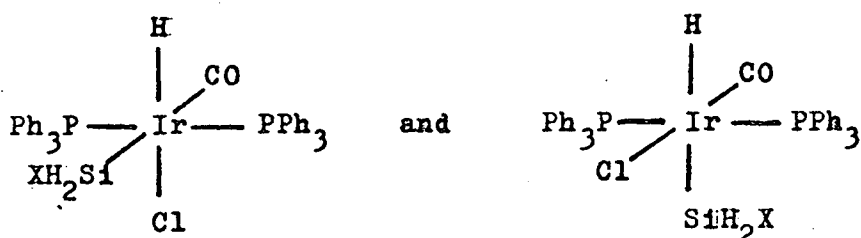
The structure



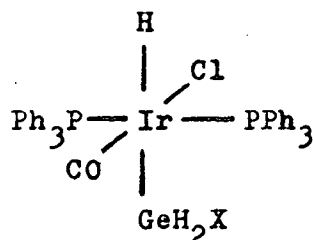
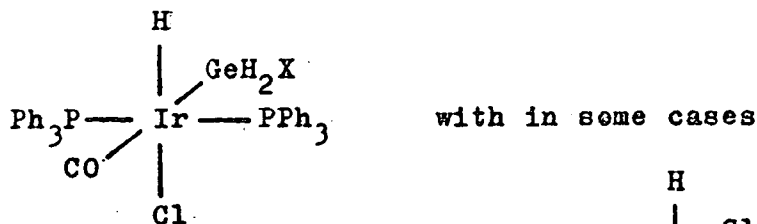
was dismissed due to the lack of

observable  $J_{\text{HirGeCH}}$ , but from results of work outlined in a later chapter it seems unlikely that such a coupling would be observed even if  $\text{IrH}$  were trans to  $-\text{GeR}_3$  and therefore this structure could still be considered.

Reactions with the less bulky  $\text{H}_3\text{SiX}$  and  $\text{H}_3\text{GeX}$  (X: H or halide) have been found to give only the initial reaction with no immediate exchange reaction of halide on iridium and hydride on silicon or germanium. Such a reaction only occurred at room temperature after several weeks. With  $\text{H}_3\text{SiX}$  the isomers produced were mainly assigned the structures



With  $\text{H}_3\text{GeX}$  the main isomer produced was



The silyl adducts were insoluble, but the germyl adducts were temporarily soluble, precipitating slowly over 30 minutes. It was suggested that this strange behaviour was due to some form of isomerisation of the initial product, such as phosphines going mutually cis, rendering the product insoluble. If this were the case, it would be another example of secondary rearrangement of an initial addition product.

It is unfortunate that these products are insoluble as the potentially reactive centres at  $-\text{SiH}_2\text{X}$  and  $-\text{GeH}_2\text{X}$  make these compounds very attractive as a field of study. As the nature of the ligand trans to the  $-\text{MH}_2\text{X}$  group would greatly influence its reactivity, it is important to know which isomers are present. It is therefore essential to obtain soluble products. In part, the following work was intended to extend our experience of these systems and hopefully contribute towards an answer to some of the questions posed.

### 1.3 Oxidative Addition in Catalysis

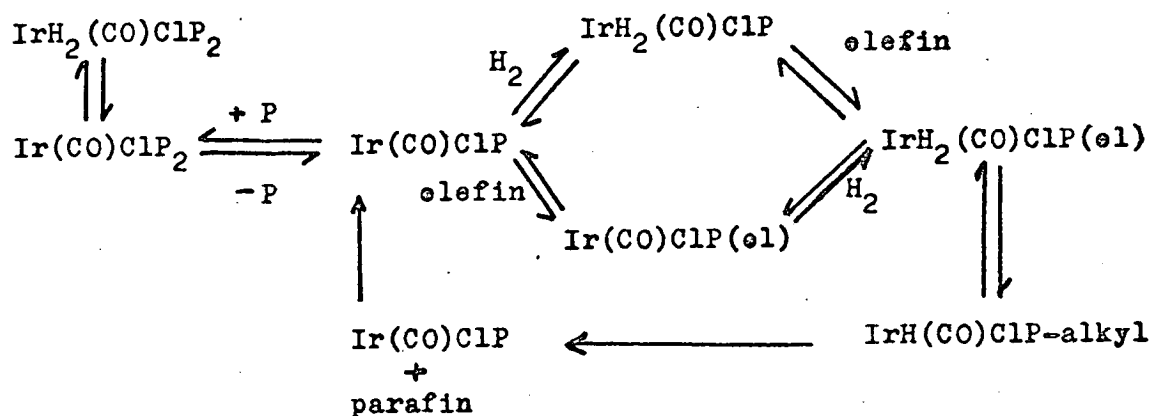
Work on oxidative additions of small molecules to Vaska's Compound and related compounds has given an insight into many of the mechanisms involved in homogeneous catalysis and so greatly increased the understanding of many of the general principles involved in this area. Not only have many iridium compounds proved to have catalytic activity, but many have given stable compounds where related metals (e.g. rhodium) do not and as a result have given an indication of the probable intermediates involved in the catalytic activity of the other metal compounds.

The principal areas in which Vaska's compound and closely related compounds have been of most use is in hydrogenation, isomerisation, deuteration and hydrosilation. All of these areas are closely inter related and so it is difficult to deal with each area





in the case of Vaska's compound, of  $\text{IrH}_2(\text{CO})\text{Cl}(\text{PPh}_3)_2$ , a well characterised species in work on oxidative additions, as essential in hydrogenation reactions. A kinetic study of the hydrogenation of maleic acid to succinic acid, catalysed by Vaska's compound, showed the reaction to be quite complex<sup>29</sup>. The reaction was found to go best in a highly co-ordinating solvent *N,N*-dimethyl acetamide and to be inhibited by excess phosphine. The following mechanism was proposed.

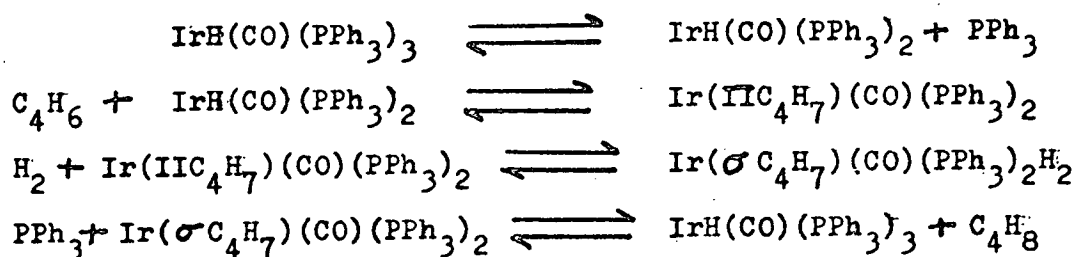


It may well be that the addition of hydrogen is the first step and that dissociation occurs from a six co-ordinate dihydride. The presence of a hydride ligand has been shown to weaken other bonds in the molecule notably those trans to the hydride<sup>30</sup>. One unexplained feature of the reaction was the acceleration by trace amounts of oxygen. The oxygen may itself be a catalyst or it may in some way activate Vaska's compound.

The rate of hydrogenation has been found to be accelerated forty fold by irradiation with U.V. light. The irradiation is only required to initiate the reaction which can proceed at the new rate in the dark<sup>31</sup>. A more recent development has been to anchor Vaska's compound to a diphenylphosphinated resin. This

pseudo-heterogeneous catalyst is found to increase the reaction rate more than 100 times as much as does a comparable homogeneous catalyst <sup>32</sup>.

$\text{IrH}(\text{CO})(\text{PPh}_3)_3$  was prepared by Vaska from Vaska's compound and shown to be a catalyst for the hydrogenation of ethylene <sup>33</sup>. This compound takes up both  $\text{C}_2\text{H}_4$  and  $\text{H}_2$  reversibly. Vaska postulated that a seven co-ordinate species was involved. Hydrogen uptake by the rhodium analogue of this compound had not been observed, but Vaska concluded, that hydrogen uptake was essential to the reactions of both compounds. The invocation of a seven co-ordinate species was found to be unnecessary in a later kinetic study of the hydrogenation of butene <sup>34</sup>. From this work it was concluded that the initial stage was not the addition of hydrogen, but of the alkene. The reaction gave a complicated rate equation due to many conflicting equilibria, but the essential reactions are listed here.



$\text{IrH}(\text{CO})(\text{PPh}_3)_3$  and  $\text{Ir}(\text{CO})\text{Cl}(\text{PPh}_3)_2$  have been shown to react with silyl <sup>45</sup> and trialkylsilyl species <sup>22</sup>. Hydrogen-deuterium exchange has been shown to be catalysed by  $\text{Ir}(\text{CO})\text{Cl}(\text{PPh}_3)_2$  <sup>23</sup> showing a degree of reversibility in these reactions.  $\text{IrCl}_3$  has been found to have some activity as a hydrosilation catalyst and silyl adducts of  $\text{Ir}(\text{CO})\text{Cl}(\text{PPh}_3)_2$  have been used as models of intermediates of Rh and Pt hydrosilation catalysts <sup>41</sup>, but neither of these iridium compounds has been successfully tested for activity as a hydro-

silation catalyst. One reason for this emission may be the low solubility of some of the silyl adducts, although low solubility would not be expected to be a handicap in catalysis. It is hoped that some of the compounds produced here will find use in this area.

#### 1.4 Nuclear Magnetic Resonance Spectroscopy (n.m.r.)

The growth in the use of nuclear magnetic resonance spectroscopy has been accompanied by a growing number of comprehensive texts on this subject. It is not the aim of this section to rival these texts, but rather to concentrate on specific terms and techniques, used in this work, with which the reader may be unfamiliar.

A compound must satisfy two conditions if it is to be studied by high resolution n.m.r. : it must be soluble and it must contain a spin active nucleus, preferably of spin  $I$  less than  $\frac{1}{2}$ . The nuclei which are made use of in this work are  $^1\text{H}$ ,  $^{31}\text{P}$  and  $^{19}\text{F}$ , all of which have  $I = \frac{1}{2}$ . The n.m.r. spectrum may be obtained by two methods. With the continuous wave method (C.W.) the area of the n.m.r. in which the observed nucleus resonates is scanned, by varying frequency or magnetic field, and the resonances are recorded, as they occur, during the scan. This method is used where nuclei of high sensitivity, such as  $^1\text{H}$ , are being observed and may also be of use with some of the less sensitive nuclei, such as  $^{19}\text{F}$ , but usually with some difficulty. In the case of low

sensitivity nuclei, such as  $^{31}\text{P}$ , the second method is generally used.

The second method of direct observation is the pulse or Fourier Transform method (F.T.) where the sample is pulsed with a single frequency in the region of the n.m.r. where the nuclei to be observed resonate. The free induction decay of the resonating nuclei is recorded and by means of a Fourier Transform from the time domain into the frequency domain, the n.m.r. is produced in a usable form. F.T. methods of obtaining n.m.r. are of most use in observing nuclei such as  $^{19}\text{F}$  and  $^{31}\text{P}$  and to some extent in recording n.m.r. of weak solutions of  $^1\text{H}$  samples, but in the last case the results obtained by F.T. are often no better than those obtained by C.W.

Once the spectrum has been recorded, a great deal of information may be obtained from the two basic parameters of n.m.r. which are chemical shift (measured in p.p.m.) and spin-spin coupling (measured in Hz.). Chemical shift will be discussed first and coupling, with its associated techniques, will be outlined in the last part of this section.

Chemical shifts are measured relative to a chosen standard for a particular nucleus. In the case of  $^1\text{H}$  the standard is tetramethylsilane (T.M.S.) whose protons are taken to resonate at 0 p.p.m. The chemical shift of a nucleus is influenced by its electronic environment: if a nucleus is heavily shielded by electrons it will tend to resonate at lower frequencies than would a nucleus which is lightly shielded. The chemical shift of a proton will therefore depend on its immediate chemical environment and to a lesser extent, on the overall chemical environment. Protons on silicon atoms tend

to resonate at positive chemical shifts, but hydrides on iridium tend to resonate at negative values. Protons on a silicon atom which is attached to iridium generally resonate at lower (sometimes as much as 1.5 p.p.m.) frequencies than the corresponding silyl system containing a proton rather than an iridium atom. The change in proton chemical shift of the protons on a free and bound silyl ligand depends on the metal involved, but with each metal a predictable change in chemical shift often emerges. So far only protons on the atom which is bound to the metal have been discussed.

The change in chemical shift on the binding of a molecule to a metal need not be the same (in magnitude or sign) for all protons on the molecule. A good example of this is triethylphosphine, which, when free, has a second order proton spectrum due to the resonance from the  $-CH_3$  part of the ethyl groups becoming closer to the resonances due to the  $-CH_2-$  parts at the magnetic field strengths of most common spectrometers. When the triethylphosphine is bound to iridium the  $-CH_2-$  resonances move to high frequency, but the  $-CH_3$  resonances move to low frequency. The change in chemical shift is not sufficient to eliminate the second order effects completely, but the pattern of resonances produced by the bound triethylphosphine is very different from that produced by free triethylphosphine.

As the chemical environment of a ligand is influenced by the trans ligand and to some extent by the cis ligands, so too is the chemical shift of the ligand. The generally accepted explanation for the negative chemical shifts of hydrides bound to a transition metal atom is that the hydride is shielded by electrons in the  $d_{xy}$  or  $d_{xz}$  or  $d_{yz}$  orbital on the metal. Any ligand which is trans to the

hydride and removes electrons (by  $\pi$  interaction) from the shielding  $d$  orbital will tend to make the hydride resonate to higher frequency. If the trans ligand increases the electron density in the shielding  $d$  orbital, the hydride will resonate to lower frequency. This is seen to be the case when a hydride trans to carbenyl on Ir(III) resonates to higher frequencies (-9 to -11 p.p.m.) than a hydride trans to halide (-15 to -20 p.p.m.).

Although these arguments have been illustrated with examples of proton n.m.r., empirically they apply equally to phosphorus n.m.r. and as the range of chemical shifts is larger than with proton n.m.r., compounds differing in a component quite far removed from the phosphorus atoms will still have a chemical shift difference of several p.p.m. For this reason, the phosphorus chemical shift of a compound may characterise it to the extent where its presence may be noted from future phosphorus spectra. The chemical shift of a phosphorus atom in a phosphine which is bound to iridium will depend on the oxidation state of the iridium. Triethylphosphine bound to Ir(I) resonates above 10 p.p.m. whereas, when bound to Ir(III) it resonates below -6 p.p.m.

#### Spin-Spin Coupling

Spin active nuclei in a molecule may couple. This coupling produces a splitting pattern on the resonances due to the nuclei involved. Unlike chemical shift, coupling is not influenced by magnetic field strength and the degree of coupling between any two nuclei A and B is a constant usually given the symbol  $J_{AQMB}$  where Q and M are atoms (if any) which connect A and B. The value of J is dependant on the gyromagnetic ratios of the nuclei (larger for  $^{31}\text{P}$  than for  $^1\text{H}$ ), the number of bonds separating the coupling

nuclei and the stereochemical arrangement of the nuclei. Coupling to one nucleus of spin  $\frac{1}{2}$  produces a doublet splitting. Coupling to two nuclei of spin  $\frac{1}{2}$  produces a triplet splitting. The more nuclei to which the resonating nucleus is coupled, the more complex the splitting pattern. From the pattern, it may be possible to deduce the number of spin active nuclei present in the molecule and their chemical or magnetic equivalence. The pattern is also dependant on the relative values of  $J$  and  $\Delta$  (the difference in the chemical shifts of the coupling nuclei). If two nuclei (e.g. phosphorus atoms) are mutually trans in a transition metal complex, they will be equivalent and give rise to a singlet resonance. If they are mutually cis, each trans to a different ligand, they will be inequivalent and appear as two doublets (due to mutual coupling of spin  $\frac{1}{2}$  nuclei) in the phosphorus spectrum. If the phosphorus nuclei resonate at two well separated chemical shifts ( $\Delta$  much larger than  $J$ ), then they constitute an AX-system and both lines of each doublet are of the same intensity, but as  $\Delta$  approaches the value of  $J$ , the outer lines of the two doublets decrease in intensity and the inner lines (those closest to each other) increase. This type of system is called an AB-system. When  $\Delta$  is of the same order of magnitude as  $J$ , the spectrum is said to be "second order".

The magnitude of the coupling constant is of great importance when the nuclei are on different ligands on a transition metal. Long range coupling between nuclei on trans ligands is often greater than between nuclei on cis ligands. This has some theoretical basis as coupling is conducted by electrons in the bonds between the atoms containing the nuclei and trans ligands



share more common s, p and d orbitals than do cis ligands; but the real basis is empirical: two bond  $J_{\text{PIrH}}$  is ca. 120Hz. for trans ligands, but less than 20Hz for cis ligands; two bond couplings  $J_{\text{HIrH}}$  for cis ligands are of the order of 2-3Hz., but three bond couplings  $J_{\text{HIrMH}}$  are rarely observed, whereas three bond couplings  $J_{\text{HIrMH}}$  for trans ligands are of the order of 2-3Hz.

Spin-spin coupling can be a useful property, but it can also cause problems. The simple example given above of the phosphorus spectrum of an AX-system could only be discussed in such simple terms if H-P coupling was ignored. The phosphorus atoms in a real system would probably be contained in a phosphine of the type  $\text{PR}_3$  where R is an alkyl or aryl group and the phosphorus-phosphorus coupling would be obscured by a multitude of couplings to the protons in the R groups and protons in the remainder of the complex. This problem can be overcome by a technique known as broad band decoupling. In this technique, a broad range of frequencies in the range of the resonances of the offending nuclei is applied to the system while collecting the n.m.r. spectrum thereby eliminating coupling to nuclei which resonate in this range. By decoupling all the protons in the complex (proton decoupling), it would be possible to observe  $J_{\text{PIrP}}$ .

It may not be advantageous to decouple the entire proton spectrum. If, for example, only the positive frequencies in the proton spectrum are irradiated, coupling to the metal hydrides might not be affected and so could be observed in the phosphorus spectrum. This would yield information on the number of protons directly bound to iridium (one hydride gives a doublet splitting etc.) and on the relative configuration of phosphorus and hydrogen atoms around iridium (a

phosphorus atom trans to a hydride will couple to a greater degree than a phosphorus atom cis to a hydride). This technique of selective irradiation is referred to, in this work, as off-resonance decoupling. Sometimes it is possible to decouple only the region associated with the R groups and it is possible to observe coupling to all other protons in the complex.

By using a single frequency and low power, it is possible to irradiate single peaks within a resonance. This technique is often called tickling. Suppose that a metal hydride H is coupled to another proton H' and that both H and H' are coupled to a phosphorus atom P. If a line in the H resonance is tickled, a line in the H' resonance will be affected. Both of these transitions share a common spin state of P and not only is proton-proton coupling confirmed, but also valuable information about the relative signs of  $J_{PH}$  and  $J_{PH'}$  is gained. This type of experiment is called homonuclear spin decoupling. If the resonances observed and tickled arise from nuclei of different types (e.g. P and H), this is called heteronuclear spin decoupling. Heteronuclear spin decoupling gives similar information to homonuclear spin decoupling, but is also useful in correlating peaks in the phosphorus spectrum to peaks in the proton spectrum when several products are present. If the proton spectrum is observed while scanning frequencies in the phosphorus region of the spectrum, a series of various phosphorus frequencies will be collected which affect various peaks in the proton spectrum. These frequencies may be transformed into chemical shifts by use of the equation

$$\delta = \frac{\nu_{\text{obs}} - \nu_{\text{standard}}}{\nu_{\text{standard}}}$$

This provides a means of obtaining a phosphorus spectrum (or the spectrum of any other spin active nucleus if it is coupled to protons) indirectly. The problem with indirect observation via proton resonances is that proton decoupling cannot be used and as a result, the peaks of the indirectly observed spectrum are broad and the chemical shifts gained are not very accurate: frequencies over the range of 30Hz. on either side of the accurate sharp peak observed in the proton decoupled directly obtained spectrum will affect the proton spectrum and in this way errors of  $\pm 1$  p.p.m. or over are not uncommon when indirect observation is used. However, this is the only method which is available for observing certain nuclei (e.g. isotopes of Ag and Rh) which, because they resonate at low frequencies, are technically difficult to observe directly.

CHAPTER 2

Additions of  $\text{SiH}_3\text{X}$  and  $\text{GeH}_3\text{X}$  ( $\text{X}:\text{H},\text{F},\text{Cl},\text{Br},\text{I}$ )

to  $\text{Ir}(\text{CO})\text{X}(\text{PEt}_3)_2$  ( $\text{X}:\text{Cl},\text{I}$ )

and  $\text{IrH}(\text{CO})(\text{PPh}_3)_3$

## 2.1 Reactions of $\text{Ir}(\text{CO})\text{X}(\text{PPh}_3)_2$ (X: Cl, I) and $\text{MH}_3\text{X}$

(X: H, Cl, Br, I) (M: Si, Ge)

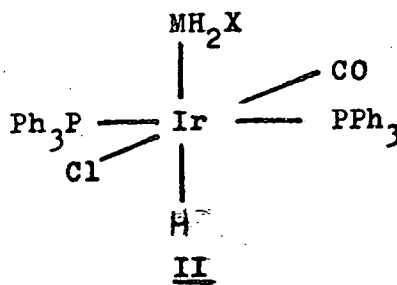
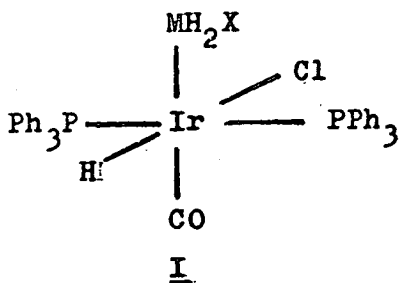
The reactions of  $\text{Ir}(\text{CO})\text{Cl}(\text{PPh}_3)_2$  with  $\text{R}_3\text{MH}$  (M: Si, Ge; R: alkyl or aryl) have been studied before<sup>22-25</sup>. These compounds are of interest for reasons outlined in the introduction and for possible synthetic use. The reactions of  $\text{Ir}(\text{CO})\text{Cl}(\text{PPh}_3)_2$  with  $\text{H}_3\text{MX}$  (M: Si, Ge; X: H, Cl, Br, I) have also been investigated<sup>45</sup>. These are of more potential importance as, from a synthetic point of view, there is not only the reactivity of the iridium-silicon bond to be considered; unlike the alkyl species which are shrouded by their bulky substituents and rendered effectively inert, there is also the likelihood of reactivity at the hydrogen-silicon bonds of the bound ligands. The influence of the ligand trans to the bound silyl makes it important to know the exact configuration of the species produced by these reactions<sup>11</sup>. This is most readily done by use of n.m.r. which also makes the protons on the silicon and germanium atoms important as details of the structure can be obtained from the resonances of these protons.

The work on the species formed from  $\text{Ir}(\text{CO})\text{Cl}(\text{PPh}_3)_2$  and  $\text{MH}_3\text{X}$  was impeded by insolubility. Many of the conclusions regarding the characterisation of the products of these reactions were based on vibrational data and so are tentative. The reaction of  $\text{SiH}_3\text{X}$  (X: H, Cl, Br, I) with  $\text{Ir}(\text{CO})\text{Cl}(\text{PPh}_3)_2$  were slow and required 1-2 days to reach completion; the products were white solids which were insoluble in benzene. The reactions of  $\text{GeH}_3\text{X}$  and  $\text{Ir}(\text{CO})\text{Cl}(\text{PPh}_3)_2$  were also investigated in benzene. Where

X was H, reaction was slow and the solid product was insoluble in benzene, but where X was Cl, Br or I the reaction was rapid and gave a soluble product, which slowly precipitated out and could not be redissolved. The soluble species was characterised by n.m.r. and by vibrational studies. The silyl and germyl reactions and the isomers produced are listed below. The gradual precipitation of the germyl halide species was hard to explain. Saturation of the solution was discounted as the precipitation took 30 minutes to begin and proceeded over an hour. It was postulated that this was due to some form of isomerisation in which the phosphines changed from being mutually trans to being mutually cis. No corroborative evidence, however, such as a change in the vibrational spectra from soluble to insoluble species, was presented.

Isomers Produced by Reaction of  $MH_3X$  with  $Ir(CO)Cl(PPh_3)_2$  <sup>45</sup>

M	X	Isomer
Si	H	I
Si	Cl	I and II
Si	Br	I
Si	I	I
Ge	H	I and II
Ge	Cl	I
Ge	Br	I
Ge	I	I



The addition reactions of silyl and germyl halides were accompanied by exchange reactions, where a light halide on the iridium exchanged for a heavier halide on the silicon or germanium. Such exchange is not unexpected where a square planar metal system is involved. In reactions involving square planar complexes of platinum, it is not unusual for a halide exchange reaction to go to completion before an addition reaction takes place. It is also possible for exchange to occur with the six co-ordinate product of the addition reaction (presumably by an  $I_a$  or  $I_d$  process). In the case of reactions with  $\text{Ir}(\text{CO})\text{Cl}(\text{PPh}_3)_2$ , halide exchange in the six co-ordinate situation is extremely slow, but exchange in the square case does occur to an appreciable degree, although to a lesser extent than with similar platinum complexes<sup>16</sup>. This would seem to be due to a slower rate of exchange in the iridium cases.

In an attempt to overcome the insolubility problem, another compound similar to  $\text{Ir}(\text{CO})\text{Cl}(\text{DPh}_3)_2$ , but which gave more soluble products, was sought.  $\text{Ir}(\text{CO})\text{Cl}(\text{PEt}_3)_2$  is similar in its reactions to  $\text{Ir}(\text{CO})\text{Cl}(\text{PPh}_3)_2$ , but, as  $\text{PEt}_3$  is a more basic phosphine than  $\text{PPh}_3$ , the reactions of  $\text{Ir}(\text{CO})\text{Cl}(\text{PEt}_3)_2$  tend to be faster and, in the case of oxygen uptake, tend to be irreversible.  $\text{Ir}(\text{CO})\text{Cl}(\text{PEt}_3)_2$  could not be made by the standard route<sup>46</sup> as the iridium trichloride supplied gave a low and impure yield of  $[\text{Ir}(\text{CO})_2\text{Cl}_2]^-$  to which  $\text{PEt}_3$  has to be added to give the required product. An alternative route for the preparation of  $\text{Ir}(\text{CO})\text{Cl}(\text{PEt}_3)_2$  which gave a better yield was found. This preparation is described in the experimental section. Unlike  $\text{Ir}(\text{CO})\text{Cl}(\text{PPh}_3)_2$ ,  $\text{Ir}(\text{CO})\text{Cl}(\text{PEt}_3)_2$  forms an

oxygen adduct in the solid phase and may only be handled for short periods in air, which does not facilitate experimental work. The advantage in using  $\text{Ir}(\text{CO})\text{Cl}(\text{PEt}_3)_2$  is in its solubility (and the solubility of its six co-ordinate derivatives) in common solvents. This property allows the use of n.m.r. which greatly facilitates characterisation of the products.

As with  $\text{Ir}(\text{CO})\text{Cl}(\text{PPh}_3)_2$ , halide exchange reactions would be expected to occur between  $\text{Ir}(\text{CO})\text{Cl}(\text{PEt}_3)_2$  and silyl and germyl halides. In some cases exchange did occur. It was felt to be unwise to bring a further possible complication to these reactions by using halogenated solvents. In the cases where exchange was felt to be unlikely, benzene was used as solvent and in the cases where there was a possibility of exchange, toluene was used to allow observation of the reaction at low temperatures. Where the n.m.r. spectrum of the system was to be observed, these solvents were used in a 99% deuterated form.

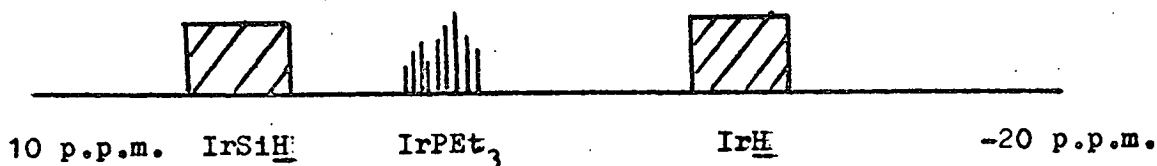
Halide exchange reactions tend to complicate the analysis of the addition reactions. For simplicity, it is therefore proposed to deal first with reactions in which exchange is not involved and then, armed with this data, to go on to reactions where halide exchange is also apparent.

#### 2.1.1 Reactions involving oxidative addition only.

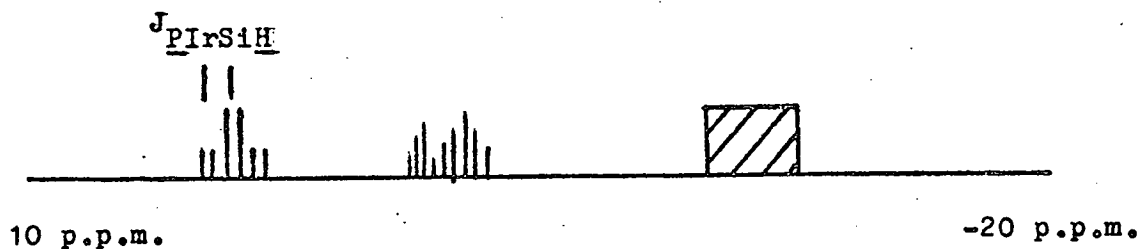
The reaction of  $\text{Ir}(\text{CO})\text{Cl}(\text{PEt}_3)_2$  with  $\text{SiH}_4$  was carried out in benzene at room temperature. The reaction was rapid and the yellow colour of the  $\text{Ir}(\text{CO})\text{Cl}(\text{PEt}_3)_2$  disappeared within a few minutes to give a clear colourless solution. The proton n.m.r. spectrum of this solution contains three sets of



resonances: those associated with protons on a silicon atom (3 - 5 p.p.m.), those associated with the ethyl groups of the phosphine (0.5 - 2.0 p.p.m.) and those associated with a proton on the iridium (less than -6 p.p.m.).

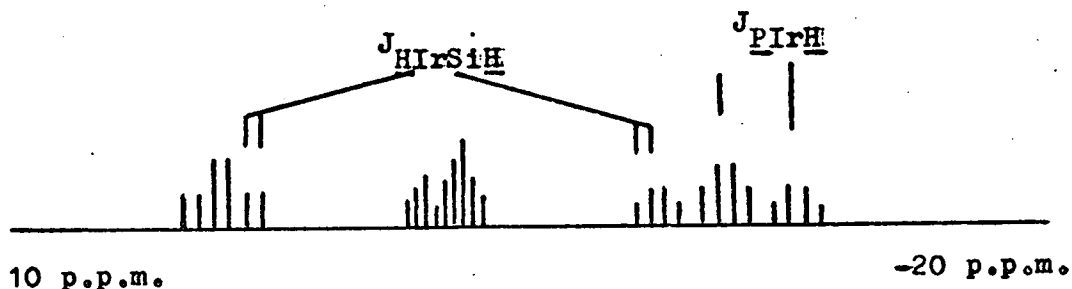


The resonances due to the protons on the ethyl groups of the phosphines show second order effects and do not yield much information apart from their overall pattern which indicates that the phosphine molecules are bound to a metal. The resonance due to the protons on the silicon appears as a triplet of doublets.



The triplet coupling is due to equivalent, or near equivalent, phosphorus atoms and may be collapsed by irradiating in the phosphorus region of the spectrum. For the phosphines to be apparently equivalent with respect to the silyl protons they must both be cis to the silyl group. The doublet splitting is probably due to coupling with a hydride on the iridium.

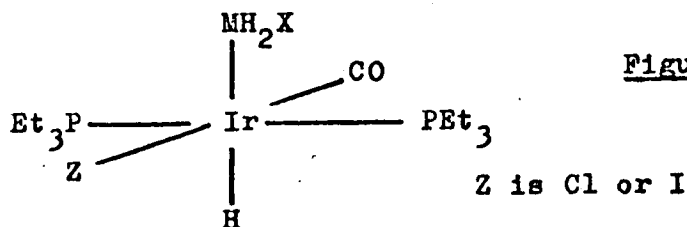
The resonance due to the hydride on the iridium takes the form of a triplet of quartets.



The triplet coupling, as with the silyl resonances, is due to the phosphines and is collapsed by a frequency corresponding to the same phosphorus chemical shift as that which collapsed the triplet coupling on the silyl protons. The quartet coupling is of the same magnitude as the doublet coupling on the silyl resonances and is thought to be due to three equivalent protons on the silicon. The chemical shift of the  $IrH$  resonance indicates that it could be trans to carbonyl<sup>38,39</sup>, but the observation of  $H-Ir-Si-H$  coupling suggests that it is trans to the silyl group.  $R_3Si-$  has a similar effect on  $Ir-Cl$  stretching frequencies to carbonyl and, although it is not wise to draw parallels between chemical shift patterns of hydrides on different metals, the  $PtH$  resonance of  $trans-HPt(PCy_3)_2(SiH_3)$  occurs at much higher frequencies than other platinum hydrides such as  $trans-HPt(PCy_3)_2Cl$  and it is therefore not unusual that there should be this coincidence between the chemical shift of  $IrH$  trans to carbonyl and trans to silyl.

The phosphorus n.m.r. contains a singlet, when proton decoupled, with  $^{13}C$  and  $^{29}Si$  satellites. This confirms that the phosphines are equivalent and mutually trans. The phosphorus resonance

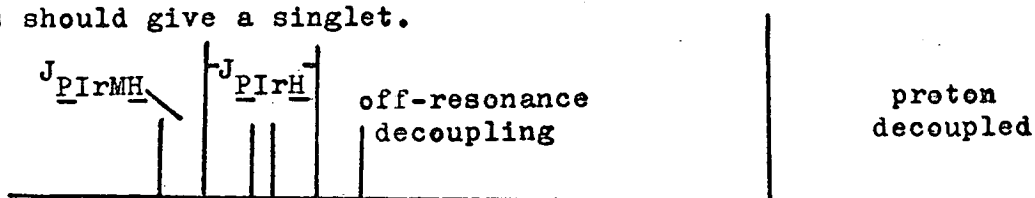
\* Cy: cyclohexyl



The above type of isomer is designated an A-type isomer. Its salient feature is that the added ligands (H- and-MH<sub>2</sub>X) are mutually trans.

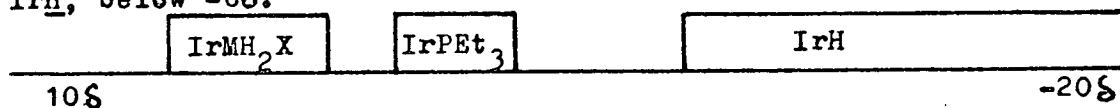
### <sup>31</sup>P n.m.r.

The phosphorus atoms are magnetically inequivalent. However, when the protons of the ethyl groups are decoupled (off-resonance decoupling), the phosphorus atoms become equivalent in all respects and should give a doublet (due to IrH) of triplets (due to two MH). When totally proton decoupled, the phosphorus atoms should give a singlet.

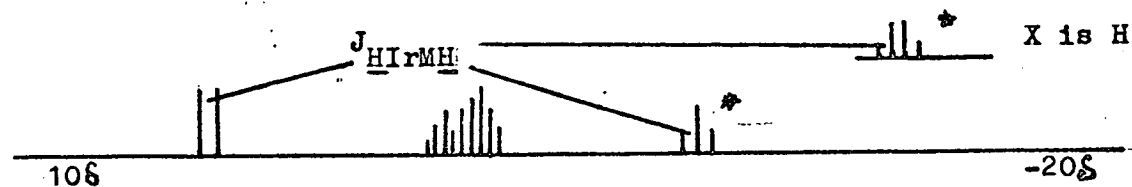


### <sup>1</sup>H n.m.r.

The proton spectrum of the A-type isomer should contain resonances due to the ethyl groups, 0δ to 1.5δ, due to MH, 2δ to 6δ, and due to IrH, below -6δ.



As IrH is trans to the MH<sub>2</sub>X group, IrH should couple to MH to give a doublet splitting on the MH<sub>2</sub> resonance and a triplet splitting on the IrH resonance (or a quartet when X is H).



The phosphorus atoms are equivalent with respect to IrH and MH and should give a triplet splitting on both resonances.

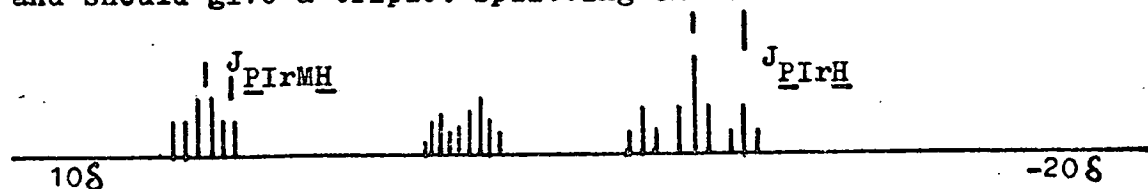


Figure 2a n.m.m. Spectra Expected from an A-type Isomer

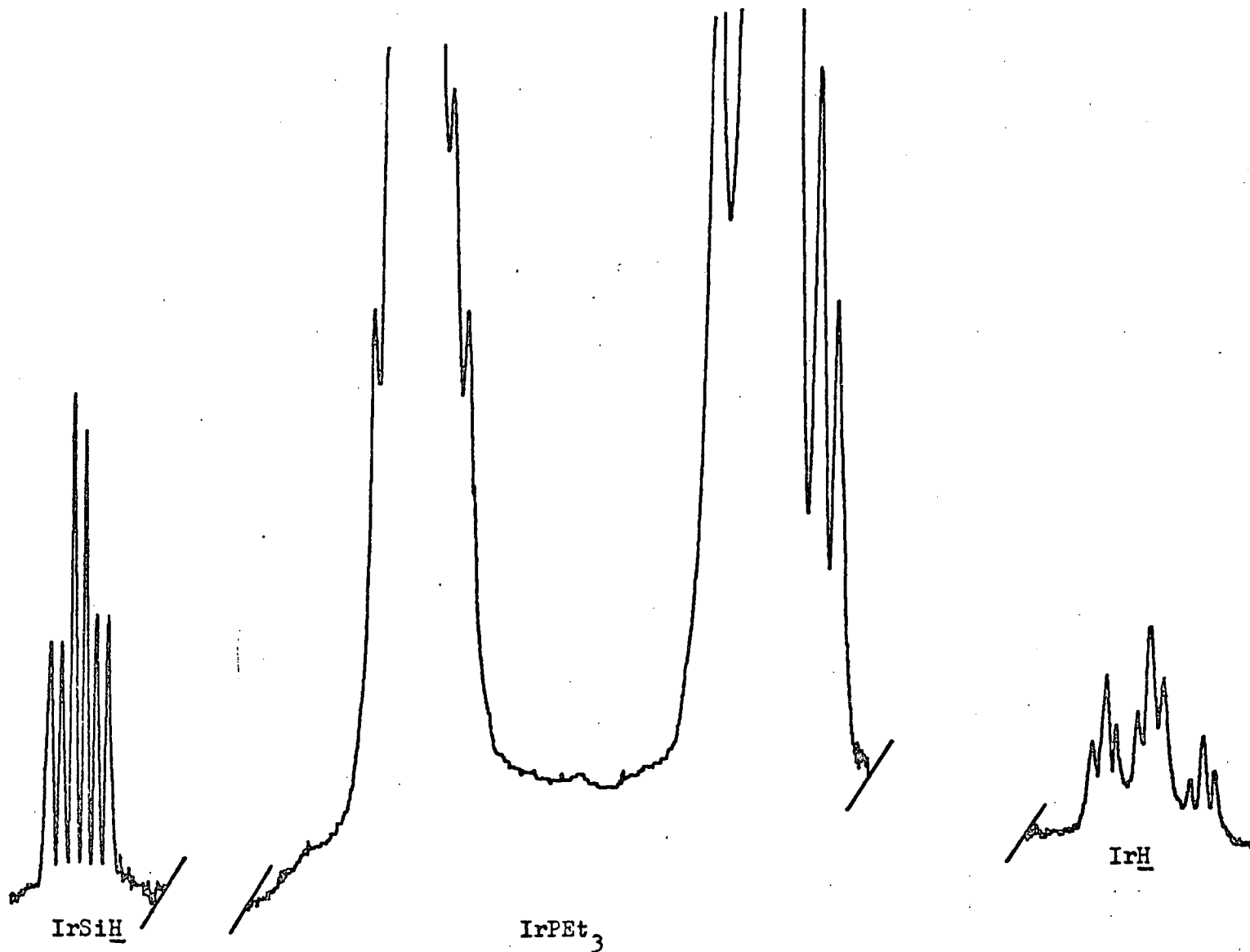


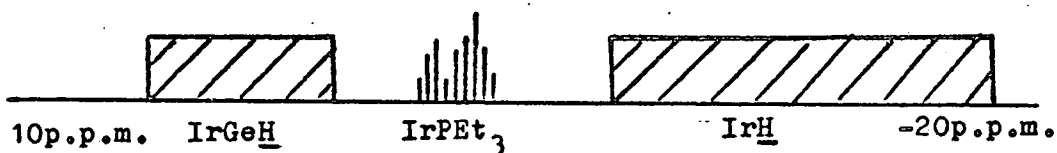
Figure 2b  $^1\text{H}$  spectrum of  $\text{IrH}(\text{CO})\text{I}(\text{PET}_3)_2\text{SiH}_2\text{Cl}$

- a typical spectrum of an A-type isomer.

occurs in the region expected for triethylphosphine bound to Ir(III).

Figure 2a defines an A-type isomer and gives a stepwise schematic account of the kind of n.m.r. spectrum expected from such an isomer. Comparison of the last schematic spectrum above with the last schematic spectrum in figure 2a indicates that the reaction of  $\text{Ir}(\text{CO})\text{Cl}(\text{PEt}_3)_2$  with  $\text{SiH}_4$  has given rise to an A-type isomer with mutually trans phosphines, silyl group trans to metal hydride and chloride trans to carbonyl.

The reaction of  $\text{Ir}(\text{CO})\text{Cl}(\text{PEt}_3)_2$  with  $\text{GeH}_4$ , as with the previous reaction, was done in benzene at room temperature. The rate of reaction was similar to that observed in the previous reaction; the yellow colour of  $\text{Ir}(\text{CO})\text{Cl}(\text{PEt}_3)_2$  was discharged within minutes to give a pale yellow solution. The proton n.m.r. spectrum of this solution contained two sets of resonances associated with protons on a germanium atom, two sets of resonances due to hydrides on a metal atom and resonances due to the ethyl groups of triethylphosphine, which, from the pattern, appear to be bound to a metal.



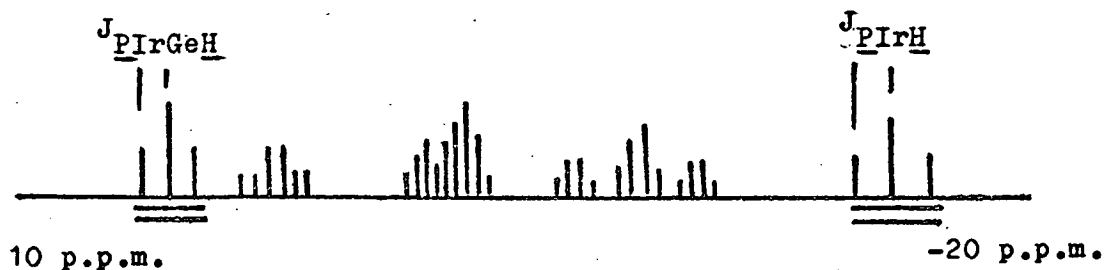
The  $\text{GeH}$  resonance to lower frequency appears as a triplet of doublets and the  $\text{IrH}$  resonance to higher frequency as a triplet of quartets. The triplet couplings are due to the phosphorus atoms which are equivalent, or nearly equivalent, to both  $\text{IrH}$

and  $\text{GeH}$  and must therefore be cis to both groups. The triplet couplings on both sets of resonances are collapsed by irradiating at frequencies corresponding to the same phosphorus chemical shift and are therefore associated with the same metal system. The doublet and quartet couplings are of the same magnitude; the quartet coupling is probably due to three equivalent germyl protons, the doublet coupling being due to the metal hydride. The metal hydride resonance occurs at a chemical shift associated with a hydride trans to carbonyl <sup>38,39</sup>, but due to the presence of coupling to the germyl protons, it is thought to be trans to the germyl group.



Comparison of the resonances underlined in the schematic spectrum above with the final spectrum in figure 2a, shows that resonances are due to an A-type isomer; mutually trans phosphines, germyl trans to hydride and chloride trans to carbonyl.

The other resonances in the proton n.m.r. spectrum take the form of triplets.



Both triplet couplings are collapsed by irradiating at frequencies corresponding to the same phosphorus chemical shift. This chemical shift differs from that used to collapse the triplet couplings in the A-type isomer which is present and it can therefore be assumed that the simple triplet resonances in the proton spectrum belong to a system which is independent of the A-type isomer. The resonance due to  $\text{IrH}$  is at a chemical shift commonly found for hydride trans to chloride and there are no other features in the n.m.r. to contradict this.

Comparison of the resonances underlined in the last schematic spectrum above with the final spectrum in figure 2c, shows these resonances to be due to what figure 2c defines as a B-type isomer; mutually trans phosphines, hydride trans to chloride and germyl trans to carbonyl.

The phosphorus spectrum shows a singlet for both isomers, when proton decoupled, confirming that the phosphines are mutually trans. From the phosphorus n.m.r. spectrum, the ratio of A-type isomer to B-type isomer is about 1:2. The larger peak (i.e. that for the B-type isomer) has  $^{13}\text{C}$  satellites; satellites could not be resolved on the resonance due to the second isomer. Both resonances occur in a region associated with triethylphosphine bound to Ir(III).

The reaction between  $\text{Ir}(\text{CO})\text{Cl}(\text{PEt}_3)_2$  and  $\text{SiH}_3\text{Cl}$  was not expected to be complicated by halide exchange as the halogen on the silicon and iridium are the same. The reaction was observed at low temperatures in toluene; the addition reaction began at about  $-40^\circ\text{C}$ . At this temperature the reaction was slow. The reaction mixture was brought up to room temperature

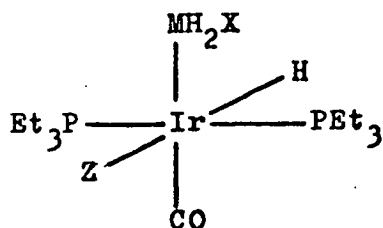


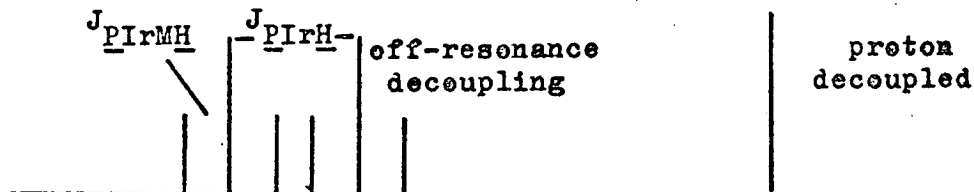
Figure 2c

Z is Cl or I

The above isomer has been designated as an B-type isomer. Its salient feature is that the added ligands are mutually cis (i.e. H- cis to  $-MH_2X$ ).

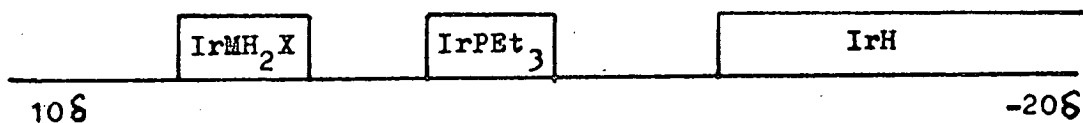
### $^{31}P$ n.m.r.

The phosphorus atoms are magnetically inequivalent, but when the protons of the ethyl groups are decoupled (off-resonance decoupling), the phosphorus atoms become equivalent in all respects and should give a doublet (due to  $IrH$ ) of triplets (due to  $-MH_2X$ ). When totally proton decoupled, the phosphorus atoms should give a singlet.



### $^1H$ n.m.r.

The proton spectrum should contain resonances due to the ethyl groups,  $0\delta$  to  $1.5\delta$ , due to  $MH$ ,  $2\delta$  to  $6\delta$ , and due to  $IrH$ , below  $-6\delta$ .



As the  $MH_2X$  group and  $IrH$  are mutually cis, any proton-proton coupling should be negligible or zero. The phosphorus atoms are equivalent with respect to  $MH_2X$  and  $IrH$  and should give a triplet splitting on both resonances.

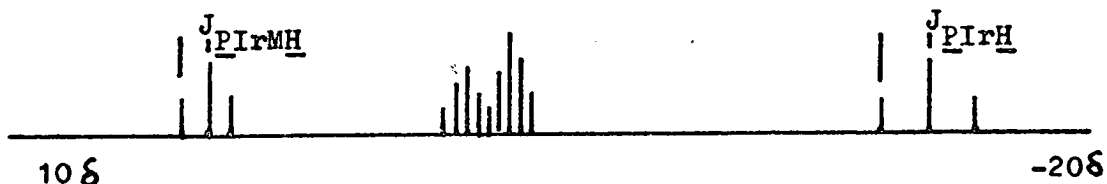


Figure 2c n.m.r. Spectra Expected from a B-type Isomer



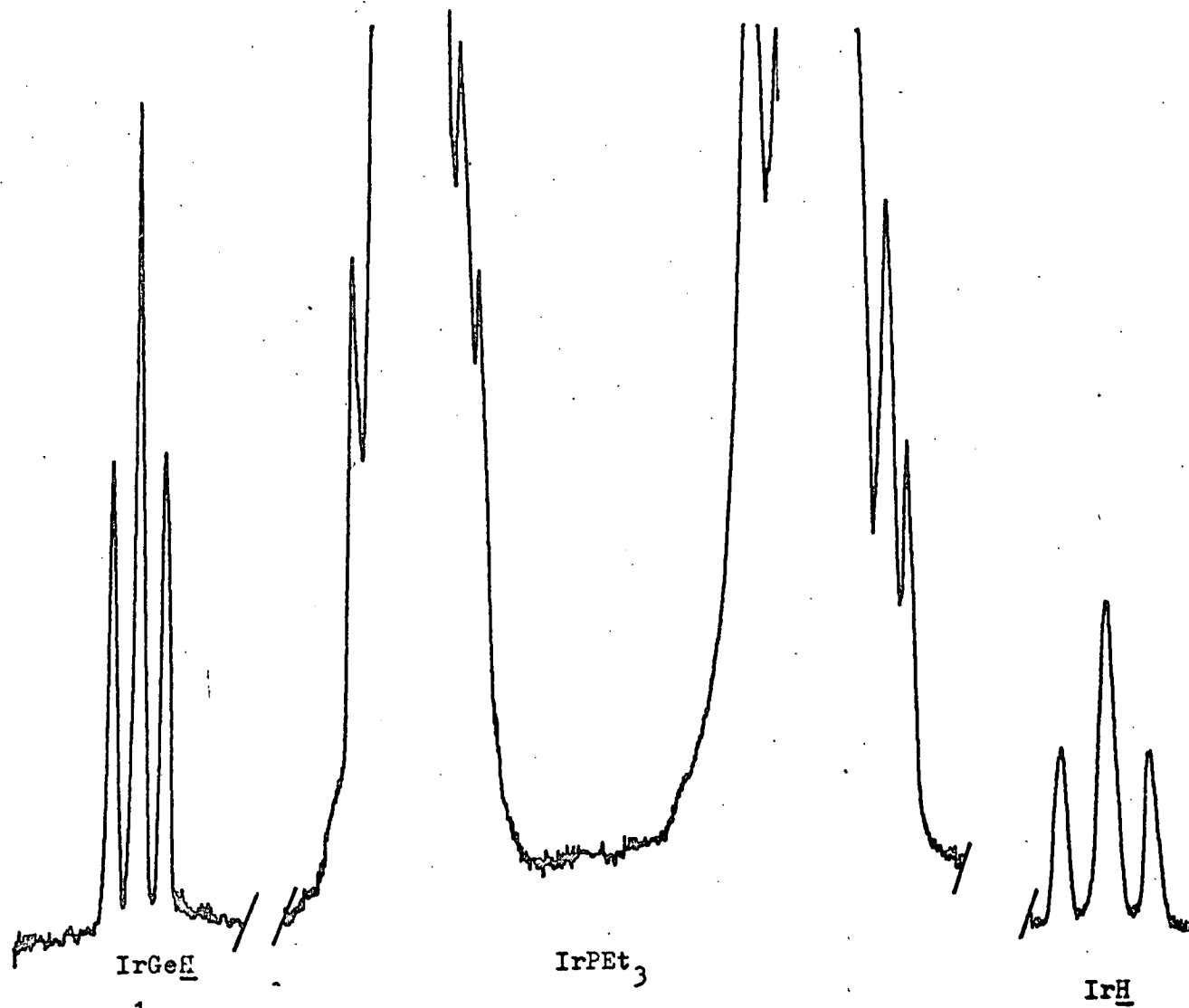


Figure 2d  $^1\text{H}$  spectrum of  $\text{IrH}(\text{CO})\text{I}(\text{PET}_3)_2\text{GeH}_2\text{Cl}$   
- a typical spectrum of a B-type isomer.

and the reaction was complete within minutes to give a clear colourless solution. The phosphorus n.m.r. contains a singlet, when proton decoupled, in the region associated with triethylphosphine bound to Ir(III). Off-resonance decoupling converts this to a doublet of triplets.

The proton n.m.r. spectrum gives a triplet of doublets in the  $\text{SiH}$  region and a triplet of triplets in the  $\text{IrH}$  region. From these n.m.r. spectra it is possible to assign an A-type structure to this product (see fig. 2a).

The proton n.m.r. spectrum of the solution also contained a triplet at a chemical shift associated with  $\text{IrH}$  trans to chloride. The resonance was not strong enough to allow heteronuclear spin decoupling (H.N.S.D.) experiments and so it was not possible to assign the corresponding phosphorus resonance; it was possible to assign it to a peak near the main peak, which, off-resonance decoupling indicates, is also due to an Ir(III) species containing a metal hydride. This species is tentatively identified as a B-type isomer (see fig. 2c) formed in trace amounts. It is not possible to say what is on the silicon as the  $\text{SiH}$  resonance is not observed, presumably because it is obscured by another resonance.

As with the previous reaction, the reaction between  $\text{Ir}(\text{CO})\text{Cl}(\text{PEt}_3)_2$  and  $\text{GeH}_3\text{Cl}$  was carried out at low temperatures using toluene as solvent. Addition of  $\text{GeH}_3\text{Cl}$  to  $\text{Ir}(\text{CO})\text{Cl}(\text{PEt}_3)_2$  was the only reaction to occur and this reaction was complete within minutes at room temperature to give a pale yellow solution. The phosphorus n.m.r. spectrum of the solution contains one main peak in the region of the spectrum associated with triethyl-

phosphine bound to Ir(III). This peak was a singlet when proton decoupled and a doublet when observed under off-resonance conditions. The absence of the triplet splitting in the off-resonance experiment was presumably because the decoupling radiation and power used still decoupled the germyl protons. The proton n.m.r. spectrum contains a triplet in the  $\text{GeH}$  region and a triplet in the  $\text{IrH}$  region for a hydride trans to chloride. The species giving rise to these resonances was assigned as a B-type isomer (see fig 2c).

The proton n.m.r. spectrum also contains a triplet of triplets in the  $\text{IrH}$  region. The resonance was too weak to allow H.N.S.D. experiments and it was not possible to assign an associated peak in the phosphorus spectrum, but a small peak close to the main peak is possibly the corresponding phosphorus resonance as off-resonance decoupling shows this peak to be due to a species having a hydride on the metal. These additional resonances are assigned tentatively to an A-type isomer (see fig. 2a). As it was not possible to observe the  $\text{GeH}$  resonance due to the A-type isomer (it is probably obscured by another resonance), it is not possible to be sure of what is on the germanium, but the smaller triplet splitting on the  $\text{IrH}$  resonance indicates that there are only two protons on the germanium. The third substituent on the germanium is probably a halide and, in this case, can be no other than chloride.

Halide exchange reactions usually involve migration of a heavier halide (e.g. I) from silicon or germanium onto the metal and a lighter halide (e.g. Cl) from the metal to the silicon or germanium. One way to prevent such a reaction would be to

start with the heavier halide on the metal: in place of  $\text{Ir}(\text{CO})\text{Cl}(\text{PEt}_3)_2$ ,  $\text{Ir}(\text{CO})\text{Br}(\text{PEt}_3)_2$  or  $\text{Ir}(\text{CO})\text{I}(\text{PEt}_3)_2$  could be used. With  $\text{Ir}(\text{CO})\text{Br}(\text{PEt}_3)_2$  there is still the possibility of migration of iodide onto the metal and for this reason it was decided also to use  $\text{Ir}(\text{CO})\text{I}(\text{PEt}_3)_2$  in the study of addition reactions.

The reactions of  $\text{SiH}_4$  and  $\text{GeH}_4$  with  $\text{Ir}(\text{CO})\text{I}(\text{PEt}_3)_2$  gave very similar results to those for the analogous reactions with  $\text{Ir}(\text{CO})\text{Cl}(\text{PEt}_3)_2$ . Both reactions were complete within a minute at room temperature in benzene. The orange colour of  $\text{Ir}(\text{CO})\text{I}(\text{PEt}_3)_2$  was discharged to give a clear colourless solution in the case of  $\text{SiH}_4$  and a clear pale yellow solution in the  $\text{GeH}_4$  case. The n.m.r. spectra contained similar resonances to those of the analogous reactions with  $\text{Ir}(\text{CO})\text{Cl}(\text{PEt}_3)_2$ , but with some changes in the chemical shifts of the resonances. Trends in chemical shift etc. on changes of halide etc. are discussed at a later stage. The phosphorus n.m.r. spectra contained singlets, when proton decoupled, in a region associated with triethylphosphine bound to Ir(III). Off-resonance decoupling gave a doublet splitting on these peaks indicating the presence of a metal hydride. The proton n.m.r. spectra showed A-type isomers to be present in both cases (triplet of doublets in  $\text{SiH}$  or  $\text{GeH}$  region and triplet of quartets in  $\text{IrH}$  region - see fig.2a). Resonances due to the ethyl protons of bound triethylphosphine were also present in both cases. In the case of the  $\text{GeH}_4$  reaction, the proton n.m.r. spectrum also showed the presence of a B-type isomer (simple triplet in  $\text{GeH}$  region and in region associated with  $\text{IrH}$  trans to iodide 39 -

see fig. 2c). From the phosphorus n.m.r. spectrum, the ratio of A-type isomer to B-type isomer is 1:2.

The reaction of  $\text{SiH}_3\text{Cl}$ ,  $\text{SiH}_3\text{Br}$  and  $\text{SiH}_3\text{I}$  with  $\text{Ir}(\text{CO})\text{I}(\text{PEt}_3)_2$  were allowed to occur at low temperatures in toluene. The reactions went rapidly to completion at  $-40^\circ\text{C}$  to give clear colourless solutions. The products of the reactions of  $\text{SiH}_3\text{Cl}$  and  $\text{SiH}_3\text{Br}$  give n.m.r. spectra of the type outlined in figure 2a and were assigned as A-type isomers with the silyl halide group trans to  $\text{IrH}$ . The  $\text{SiH}_3\text{I}$  reaction gives an unusual result. The phosphorus n.m.r. spectrum contains a single line, when proton decoupled, in the region associated with triethylphosphine bound to  $\text{Ir}(\text{III})$ . The chemical shift of the resonance varies only marginally with temperature. The proton n.m.r. spectrum contains a triplet of triplets in the  $\text{IrH}$  region, which does not vary with temperature. The larger triplet coupling is collapsed by irradiating in the region of the phosphorus resonance outlined above. The smaller triplet splitting is presumably due to two equivalent, or nearly equivalent, protons on the silicon which must therefore be trans to the hydride (A-type isomer). The  $\text{SiH}$  region contains a complex multiplet with an overall triplet envelope. The triplet envelope is collapsed by irradiating in the region of the phosphorus resonance mentioned above (see fig. 2e). On warming to  $80^\circ\text{C}$  the  $\text{SiH}$  resonance sharpens, gradually with increasing temperature, to the more familiar triplet of doublets. However, on cooling to  $-30^\circ\text{C}$ , an equally familiar triplet of doublets of the same magnitude of couplings and chemical shift as that obtained at  $80^\circ\text{C}$  appears. The lack of

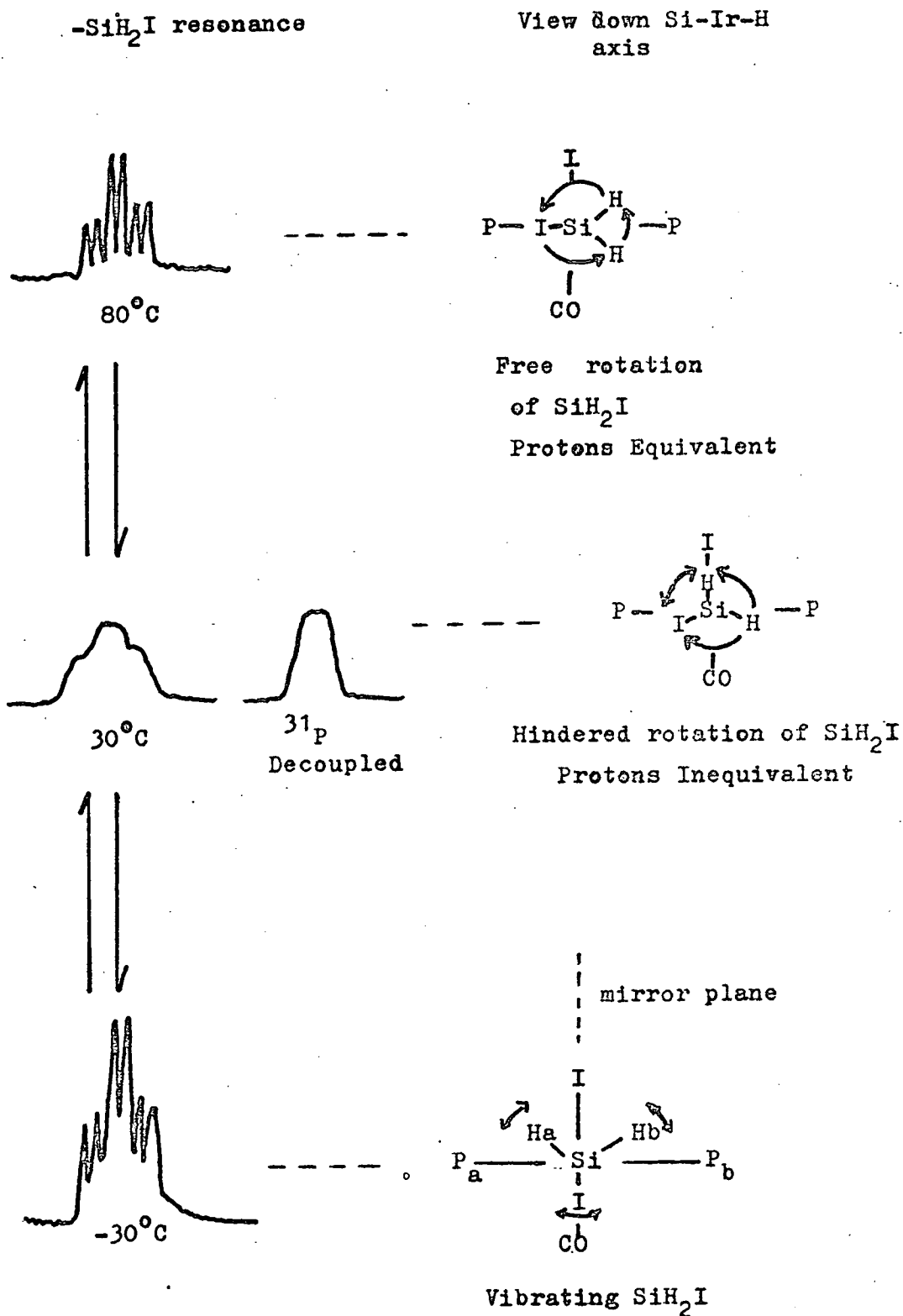


**Figure 2e** Hindered Rotation in IrH(CO)I(PtEt<sub>3</sub>)<sub>2</sub>SiH<sub>2</sub>I

appreciable change in the phosphorus chemical shift and the  $\text{IrH}$  resonance ( $J_{\text{HrSiH}}$  is maintained throughout) suggests that an intra-molecular process is taking place.

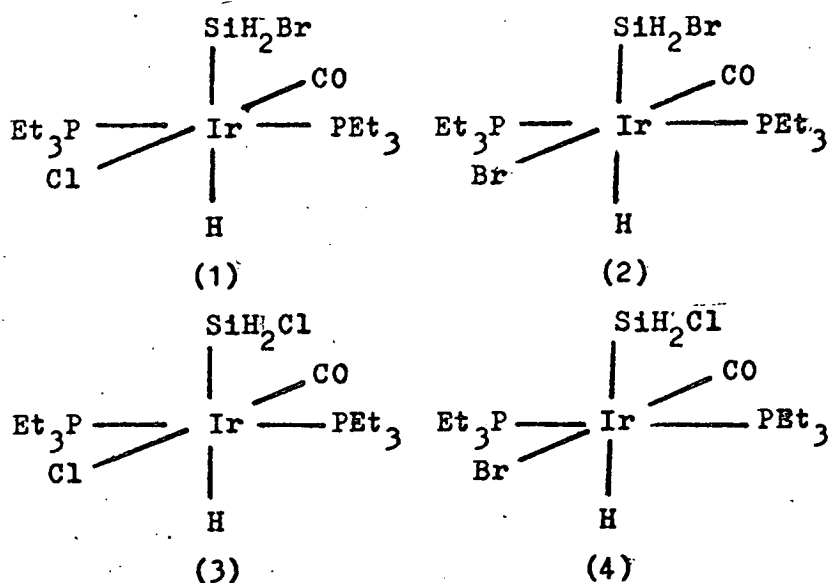
It is difficult to explain what this intra-molecular process could be. One possible explanation is that the variation in the  $\text{SiH}$  resonance is due to some form of hindered rotation. At  $80^\circ\text{C}$ , the  $-\text{SiH}_2\text{I}$  might rotate freely and quickly enough (on an n.m.r. time-scale) to make the silyl protons equivalent, both magnetically and chemically. At room temperature this rotation may well be somewhat hindered, probably because of the bulky iodides on the silicon and iridium atoms, and the  $-\text{SiH}_2\text{I}$  group would spend the majority of its time in a position in which the two silyl protons are chemically inequivalent. This would give rise to the observation of geminal coupling of the silyl protons and lead to the complex multiplet resonance. At low temperatures ( $\approx 30^\circ\text{C}$ ) movement of the  $-\text{SiH}_2\text{I}$  group could cease to such an extent that the  $-\text{SiH}_2\text{I}$  group was held in a position in which the silyl protons were again chemically equivalent. Such a position would be when the mirror plane of the  $-\text{SiH}_2\text{I}$  group was aligned with the mirror plane of the whole molecule (fig. 2e). Such a position would give chemical equivalence to the silyl protons, but not necessarily magnetic equivalence. In figure 2e,  $\text{H}_a$  could couple differently to  $\text{P}_a$  than could  $\text{H}_b$ . These couplings are, however, long range couplings and such couplings are not greatly influenced by orientation, particularly when cross-space coupling is unlikely. It would quite possible that both silyl protons would couple equally to both phosphorus atoms and would be magnetically equivalent.

Be that as it may, the main result of this reaction is that  $\text{SiH}_3\text{I}$  gives an A-type isomer. In none of the reactions of the silyl halides is there a trace of a second isomer.

The reactions of  $\text{GeH}_3\text{Cl}$ ,  $\text{GeH}_3\text{Br}$  and  $\text{GeH}_3\text{I}$  with  $\text{Ir}(\text{CO})\text{I}(\text{PET}_3)_2$  were allowed to occur at low temperatures in toluene. Reaction occurred at  $-60^\circ\text{C}$ , but was slow. At  $-40^\circ\text{C}$  the reactions went rapidly to completion to give yellow solutions. The products give n.m.r. spectra of the type outlined in figure 2c and are therefore thought to have the germyl halide group cis to IrH as with B-type isomers. In none of the reactions of the halides is a trace of second isomer apparent from the proton n.m.r. spectra.

### 2.1.2 Oxidative addition reactions involving halide exchange.

In reactions of  $\text{MH}_3\text{X}$  with  $\text{Ir}(\text{CO})\text{Cl}(\text{PET}_3)_2$  when X is Br or I, in addition to an oxidative addition reaction, there is the possibility of halide exchange. For example in the  $\text{SiH}_3\text{Br}$  reaction four species could be produced.





The relative rates of both types of reaction dictate the distribution of products. If exchange is faster than addition, (4) will predominate, but if addition is faster than exchange, (1) will predominate. This is because exchange primarily involves the square planar iridium complex and is halted when the six co-ordinate species is formed <sup>16</sup>. With  $\text{Ir}(\text{CO})\text{Cl}(\text{PET}_3)_2$ , at low temperatures, addition is the predominant reaction.

The reaction between  $\text{SiH}_3\text{Br}$  and  $\text{Ir}(\text{CO})\text{Cl}(\text{PET}_3)_2$  was allowed to occur at low temperature in toluene. The phosphorus n.m.r. spectrum at  $-80^\circ\text{C}$  shows no reaction taking place. At  $-50^\circ\text{C}$  peaks appear for  $\text{Ir}(\text{CO})\text{Br}(\text{PET}_3)_2$ , one predominant Ir(III) species and traces of five other Ir(III) species. On warming to room temperature, the Ir(I) species disappear, the trace species increase with respect to the predominant species, but remain minor in comparison, and no further exchange is apparent. Off-resonance decoupling shows that all the Ir(III) species contain a metal hydride, but only the major product is present in sufficient concentration for the triplet coupling due to  $-\text{SiH}_2-$  to be resolved (see fig. 2a). The production of secondary isomers in these reactions makes it difficult to assign minor peaks in the phosphorus n.m.r. spectra (c/f the reaction between  $\text{SiH}_3\text{Cl}$  and  $\text{Ir}(\text{CO})\text{Cl}(\text{PET}_3)_2$ ) and it is not possible to be sure which of the likely products (1) to (4) above are present. However from work described earlier, it is possible to establish the presence of  $\text{IrH}(\text{CO})\text{Cl}(\text{PET}_3)_2\text{SiH}_2\text{Cl}$ . The proton n.m.r. spectrum contains resonances of the type outlined in figure 2a. The major product is an A-type isomer with the  $\text{SiH}_2\text{Br}$  group trans to  $\text{IrH}$ . Directly to low frequency

of the triplet of doublets resonance in the  $\text{SiH}$  region of the proton spectrum and partly obscured by this resonance, are small peaks associated with protons on a silicon atom to which chlorine is also bound. In the region of the triplet of triplets due to  $\text{IrH}$  there are also minor resonances. Because these minor resonances come in this region rather than to lower frequency, it could be concluded that the isomers produced by exchange are also of A-type. There is also a small triplet in the region for  $\text{IrH}$  trans to halide, suggesting the presence of a trace of B-type isomer (see fig. 2c). It is not possible to characterise such an isomer further, in this case, due to the complexity introduced by halide exchange.

Work with  $\text{Ir}(\text{CO})\text{I}(\text{PET}_3)_2$  and  $\text{SiH}_3\text{I}$  has made it possible to characterise the products of the reaction between  $\text{Ir}(\text{CO})\text{Cl}(\text{PET}_3)_2$  and  $\text{SiH}_3\text{I}$  more fully. The reaction between  $\text{Ir}(\text{CO})\text{Cl}(\text{PET}_3)_2$  and  $\text{SiH}_3\text{I}$  was allowed to occur at low temperature in toluene.  $\text{Ir}(\text{CO})\text{I}(\text{PET}_3)_2$  was produced as an intermediate and minor Ir(III) species were produced in slightly larger quantity than in the  $\text{Ir}(\text{CO})\text{Cl}(\text{PET}_3)_2/\text{SiH}_3\text{Br}$  case, suggesting slower addition and/or faster exchange. The major resonances in the phosphorus and proton n.m.r. spectra were of the pattern in figure 2a and were compatible with an  $\text{SiH}_2\text{I}$  group trans to  $\text{IrH}$  (A-type isomer). Directly to low frequency of the  $\text{SiH}_2\text{I}$  resonance were resonances probably due to a  $\text{SiH}_2\text{Cl}$  species and there were several minor resonances in the region for  $\text{IrH}$  trans to silyl, suggesting that the exchange products were also A-type isomers. There was also a resonance due to a B-type isomer (triplet to low frequency), but, due to its low concentration and the exchange reactions, it

was not possible to characterise this product further. Using data from work described earlier (see 2.1.1), it was possible, from the phosphorus n.m.r. data, to identify  $\text{IrH}(\text{CO})\text{Cl}(\text{PET}_3)_2\text{SiH}_2\text{Cl}$ ,  $\text{IrH}(\text{CO})\text{I}(\text{PET}_3)_2\text{SiH}_2\text{Cl}$  and  $\text{IrH}(\text{CO})\text{I}(\text{PET}_3)_2\text{SiH}_2\text{I}$  to be the more significant minor products.

The reaction of  $\text{GeH}_3\text{Br}$  with  $\text{Ir}(\text{CO})\text{Cl}(\text{PET}_3)_2$ , done in toluene at low temperature, gives one predominant Ir(III) product and five minor Ir(III) products. The proton n.m.r. spectrum shows the major species produced to be a B-type isomer (see fig.2c). The region of the spectrum associated with  $\text{IrH}$  trans to chloride contains a triplet. When the triplet is collapsed, using a frequency corresponding to the phosphorus chemical shift of the major product, it is possible to see that it is obscuring a second very small triplet, which is also due to  $\text{IrH}$  trans to chloride. A similar small triplet is present 1.6 p.p.m. to high frequency of the large triplet and is probably due to a species with  $\text{IrH}$  trans to bromide. The  $\text{GeH}$  region contains four sets of triplets. One pair are very small and are at a chemical shift associated with  $-\text{GeH}_2\text{Cl}$ . The other pair, one of which is very large (due to main product) and the other small, are in the region for  $-\text{GeH}_2\text{Br}$ . There is also a small broad triplet resonance in the region for  $\text{IrH}$  trans to a germyl group. This is probably due to two nearly coincident triplets of triplets which could be due to A-type isomers. All of the minor resonances were too low in amplitude to allow decoupling experiments. The phosphorus n.m.r. spectrum contains six resonances, all due to Ir(III) species. There would probably be four B-type species present which would be

analogous to (1) to (4) and two A-type isomers present (of unknown halide combination). However, with the exception of the major product and the minor product  $\text{IrH}(\text{CO})\text{Cl}(\text{PEt}_3)_2\text{GeH}_2\text{Cl}$ , it was not possible to assign the peaks in the phosphorus n.m.r. spectrum.

The reaction between  $\text{GeH}_3\text{I}$  and  $\text{Ir}(\text{CO})\text{Cl}(\text{PEt}_3)_2$  at low temperature in toluene gives a B-type isomer of  $\text{IrH}(\text{CO})\text{Cl}(\text{PEt}_3)_2\text{GeH}_2\text{I}$ . This is the only Ir(III) species which can be identified in the proton n.m.r. spectrum at  $-30^\circ\text{C}$ . At this temperature the proton spectrum contains a triplet for  $\text{GeH}_2\text{I}$  and for  $\text{IrH}$  trans to chloride. The spectrum also shows the presence of unreacted  $\text{GeH}_3\text{I}$ . At this temperature the phosphorus n.m.r. spectrum shows the presence of  $\text{Ir}(\text{CO})\text{Cl}(\text{PEt}_3)_2$ ,  $\text{IrH}(\text{CO})\text{I}(\text{PEt}_3)_2\text{GeH}_2\text{Cl}$  and  $\text{IrH}(\text{CO})\text{Cl}(\text{PEt}_3)_2\text{GeH}_2\text{I}$ . The last compound was identified by decoupling experiments on the proton n.m.r. spectrum and is the major species present. The absence of  $\text{IrH}(\text{CO})\text{Cl}(\text{PEt}_3)_2\text{GeH}_2\text{Cl}$  and  $\text{IrH}(\text{CO})\text{I}(\text{PEt}_3)_2\text{GeH}_2\text{I}$  suggests that the halide exchange reaction is immediately followed by addition of  $\text{GeH}_3\text{Cl}$  to  $\text{Ir}(\text{CO})\text{I}(\text{PEt}_3)_2$ .

$\text{IrH}(\text{CO})\text{Cl}(\text{PEt}_3)_2\text{GeH}_2\text{I}$  would appear to be thermally unstable, for at room temperature the n.m.r. spectra totally change and the resonances due to this product are lost. The phosphorus n.m.r. spectrum contains several new lines at room temperature most of which cannot be identified. There are three broad resonances which do not respond to changes in temperature. The proton n.m.r. spectrum also contains broad peaks which do not alter with temperature (see table 2/4). The proton and phosphorus n.m.r. spectra showed the presence of

substantial amounts of  $\text{IrH}(\text{CO})\text{I}(\text{PEt}_3)_2\text{GeH}_2\text{Cl}$  and  $\text{IrH}(\text{CO})\text{I}(\text{PEt}_3)_2\text{GeH}_2\text{I}$ .

It is difficult to come to any conclusion on the nature of the thermal decomposition. From the broad peaks in the n.m.r. spectra, it would seem that polymeric species are formed. However, there are many other species present and from off-resonance decoupling experiments, it would seem that every one of these species contains a metal hydride.

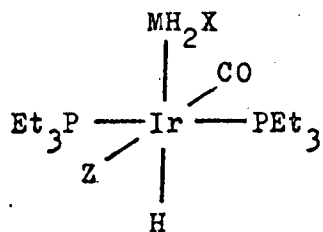
### 2.1.3 Trends in n.m.r. parameters.

The n.m.r. data for the compounds discussed in 2.1.1 and 2.1.2 are tabulated in tables 2/1, 2/2, 2/3 and 2/4.

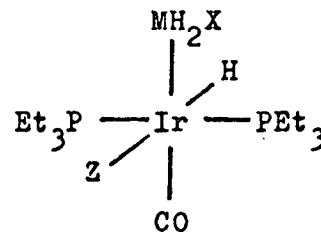
Couplings do not show any regular trend on varying M and X.  $J_{\text{PIrMH}}$  is smaller when X is H than when X is halide, but shows little dependence on the nature of M; Si and Ge transmit couplings to a very similar extent.  $J_{\text{PIrH}}$  is larger in A-type isomers than in B-type isomers which would seem to reflect a difference in the electronic distribution between the two configurations. Couplings are not significantly influenced by the halide on iridium.

The halide on the iridium does influence chemical shifts and trends in chemical shifts.  $\text{MH}$  protons move to low frequency as the halide increases in atomic weight except when there is a chlorine on the iridium, which makes these resonances behave abnormally and shift to a lesser extent to high frequency. Also when there is a silicon atom and a chlorine atom on the iridium, the  $\text{IrH}$  resonance becomes very sensitive (as far as chemical shift is concerned) to the halide on the silicon. If it were





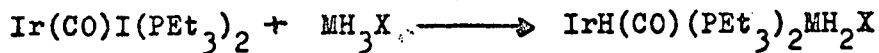
A-type Isomer



B-type Isomer

M	X	Solv.	$\delta_{MH}$	$\delta_{IrH}$	$J_{PIrMH}$	$J_{PIrH}$	$J_{HIrMH}$	$\gamma^{31P}$	$\delta(Et_3P)$	isomer type
Si	H	bz.	3.2t/d	-10.1t/q	5.6	15	3.0	--	-15.7	A
Si	Cl	tol.	5.0t/d	-10.4t/t	8.0	15	4.0	-16	-15.5	A
Si	Br	tol.	4.7t/d	-10.4t/t	8.3	15	3.2	-17	-17.3	A
Si	I	tol.	4.0t/d	-10.2t/t	8.0	15	4.0	-18	-18.5	A
Ge	H	bz.	3.4t/d	-16.3t	6.2	12	0.5*	-23	-23.1	B
Ge	H	bz.	2.7t/d	-10.5t/q	4.4	16	2.6	-17	-17.5	A
Ge	Cl	tol.	5.4t/d	-15.8t	8.0	12	0.8*	-23	-23.3	B
Ge	Br	tol.	4.8t/d	-15.6t	8.0	13	0.9*	-23	-24.1	B
Ge	I	tol.	3.7t/d	-15.4t	8.1	13	0.9*	-24	-25.0	B

Table 2/1



\* These couplings were resolved on expansions of the  $MH$  resonance - expansion of  $IrH$  resonances was not technically possible.

Units and abbreviations:- All chemical shifts in p.p.m.

All coupling constants are in Hz.  $\gamma^{31P}$  - shifts under this heading are from indirect observation. t:triplet t/d:triplet of doublets t/t:triplet of triplets t/q:triplet of quartets

Units and abbreviations:- see Table 2/1 b: broad peak

\* At -20°C

Major Isomers			$\delta_{MH}$	$\delta_{IrH}$	$J_{PIrMH}$	$J_{PIrH}$	$J_{HIRMH}$	$\nu^{31}P$	$\delta(Et_3P)$	Isomer type
M	X	Solv.								
Si	H	bz.	2.9t/d	-8.1t/q	5.2	16.0	3.0	-5	-4.6	A
Si	Cl	tol.	4.8t/d	-8.6t/t	7.0	16.0	3.0	-6	-5.3	A
Si	Br	tol.	4.9t/d	-9.2t/t	7.0	16.0	3.5	-9	-9.2	A
Si	I	tol.	5.1t/d	-10.5t/t	7.8	16.0	4.0	-16	-16.5	A
Ge	H	bz.	3.0t	-18.8t	6.0	10.0	0	--	-13.6	B
2nd. isomer			2.4t/d	-8.5t/q	5.0	16.0	3.0	--	-6.9	A
Ge	Cl	tol.	5.1t	-18.3t	7.5	13.0	0	-14	-14.4	B
Ge	Br	tol.	4.9t	-18.6t	8.0	12.0	0	-15	-14.9	B
Ge	I*	tol.	3.4t	-18.0t	8.6	12.0	0	-13	-13.3	B

Table 2/2

Minor Isomers			$\delta_{IrH}$	$J_{PIrH}$	Associated $\delta(Et_3P)$	Probable Isomer type
M	X					
Si	Cl		-16.0t	12	-3.2	B
Si	Br		-15.1t	12	----	B
Si	I		-14.2t	11	----	B
Ge	Cl		-9.2t/t	18	-13.0	A
Ge	Br		-9.5t/t	16	----	A

Table 2/3

Uniassigned Peaks in R.T. n.m.r. of  $Ir(CO)Cl(PEt_3)_2 + GeH_3I$

$^{31}P$  14.4, -8.1, -13.0, -14.9, -15.0, -15.6, -16.7, -17.6, -18.3, -20.7, -23.8, -25.8, -26.9, -27.5, -27.7b, -41.7, -51.9b.

$^1H$  5.1b, 4.2, 3.8, 3.2b, 3.0 .

Table 2/4



Tables 2/2  
2/3  
2/4

not for the evidence from the phosphorus spectra, these unique occurrences would be attributed to exchange reactions. The chemical shift of  $MH$  is not greatly changed on changing the halide on the iridium, but the phosphorus shifts move about 10 p.p.m. to lower frequency on going from Cl to I and the iridium hydrides trans to the halide move to lower frequency on going from Cl to I, but the hydrides cis to the halide move to higher frequency. The effect on the hydride trans to the halide is easily understood in terms of  $\sigma$  donation, but the cis influence is not understood.

2.2 An n.m.r. Study of the Equimolar Reactions of  
 $IrH(CO)(PPh_3)_3$  with  $MH_3X$  (M: Si, Ge; X: H, F, Cl, Br, I)

These reactions were originally carried out in 1973<sup>43</sup>. At that time, the facilities for pulsed n.m.r. (i.e. F.T.) were not available and it was necessary to attempt to characterise the products of these reactions using continuous wave  $^1H$  n.m.r. and infra-red spectroscopy. The low solubility of the products meant that the quality of the n.m.r. spectra obtained was poor and any assignments of configurations could only be tentative. The aim of this section of the work was to characterise the products of these reactions using  $^{31}P$  n.m.r. and in some

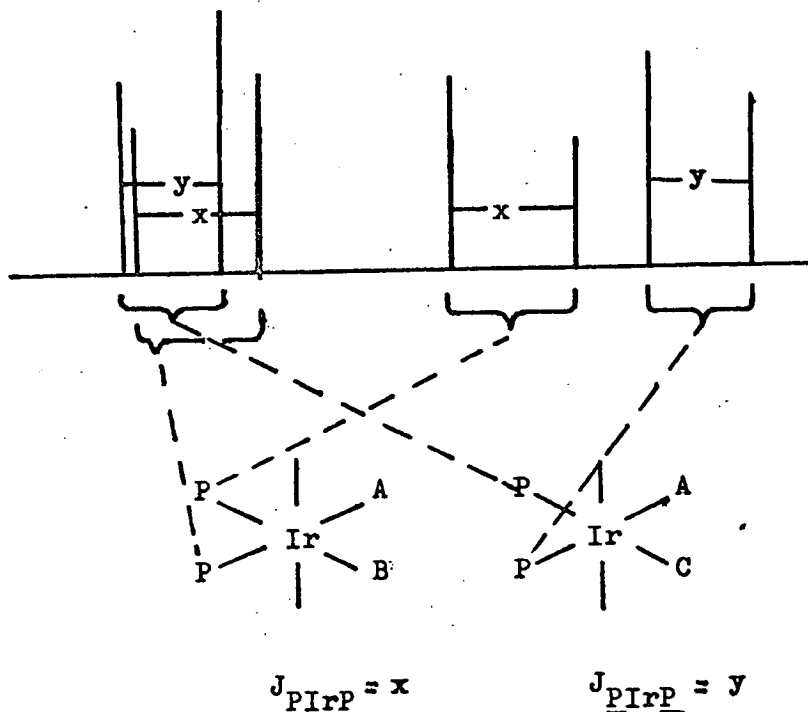


cases  $^{19}\text{F}$  n.m.r.

### 2.2.1 Results of the $^{31}\text{P}$ n.m.r. study

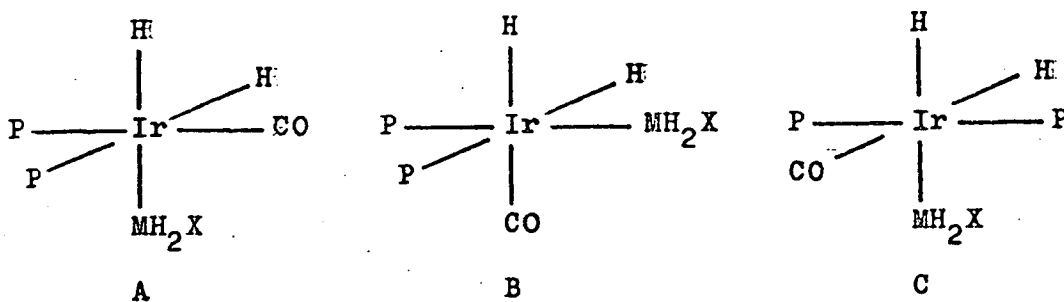
The reactions were repeated under the same conditions as used in the original work. The  $^{31}\text{P}$  n.m.r. spectra of the benzene solutions were obtained at room temperature. Similar spectra were obtained from all the solutions except for the special cases when X is F; these spectra have extra couplings due to the spin of the fluorine nucleus and the consequences of this extra spin active nucleus are discussed in the next section.

The proton decoupled  $^{31}\text{P}$  n.m.r. spectra indicate the presence of free triphenylphosphine ( a peak at -5 p.p.m. common to all of the spectra). The spectra also indicate the presence of an iridium species with mutually cis triphenylphosphines. Each species with mutually cis phosphines gave rise to four peaks (two doublets) which could be identified from internal couplings to be due to inequivalent, but mutually coupled phosphorus nuclei. The inequivalence (giving rise to  $J_{\text{PIrP}}$ ) indicates that the phosphines are both trans to different ligands and the relative chemical shifts, of course, depend on the groups trans to the phosphines (see figure overleaf). Each pair of doublets should be of the same intensity, but peak heights differ slightly because, being trans to different ligands, the proton decoupling is not equally effective on all of the phosphorus atoms and the spectra resemble those for a system which is tending towards AB rather than AX (see 1.4).



The resonances due to species with mutually trans phosphines (which are equivalent when proton decoupled) occur as singlets.

Off-resonance decoupling indicates that in each case the species with mutually cis phosphines have one phosphine trans to IrH. Excluding mutually trans iridium hydrides (this is supported by reliable results from the previous work on this system) the possible products are



N.B. Labels A, B and C bear no relationship to the labels A-type and B-type used in sections 2.1.n .

A, B and C may well be produced in every case, but in some

systems the concentration of a certain product may be too low to be observed. The proportions of products A, B and C depend to a large extent on the nature of M and to a lesser extent on the nature of X.

When M is Si the proportion of species A or B is greater than the proportion of C. The proportion of C rises with increasing atomic weight of X, but in no case, when M is Si, does it exceed the proportion of A or B. When M is Ge the relative concentration of C is greater than that of either A or B. The proportion of C falls, with respect to the other isomers present, as the atomic weight of X increases.

The n.m.r. data for these systems are tabulated in table 2/5 and the spectra are illustrated by stick diagrams in figure 2f. The heights of the lines are proportional, within each stick diagram, to the heights of the peaks in the original spectra. As integration of the peaks is not straightforward, relative concentrations of species are estimated by peak height only and it should be pointed out that this can only be taken as a rough guide to concentration. However, the differences in concentration of the major products with respect to the others present is so large that in most cases this procedure is reasonably satisfactory.

It was hoped that the  $^{31}\text{P}$  shift of triphenylphosphine trans to carbonyl would differ greatly from that of triphenylphosphine trans to silicon or germanium atoms, but as will be seen from figure 2f this is not so. It is therefore possible to distinguish C from A or B, from the phosphorus spectrum alone, but impossible to distinguish A from B and so it is not possible

\* If known, ligand trans to phosphine is given in brackets.

<sup>31</sup> P	M	X	δP(P)*	δP(H)	J <sub>P<sub>1</sub>IrP</sub>	δP(?)	J <sub>P<sub>1</sub>IrP</sub>	δP(?)	J <sub>P<sub>1</sub>IrP</sub>
	Si	H	13.7	6.5	15.8	4.3	15.7		
	Si	F		7.6	16.8	2.6	16.6		
	Si	Cl	12.9	6.6	17.2	4.2	15.4	3.5	17.1
	Si	Br	12.7	6.8	16.9	2.9	16.9	1.8	14.3
	Si	I	12.3	7.3	16.4	2.5	13.7	1.9	16.5
	Ge	H	13.1	5.3	11.3	6.7	12.5		
	Ge	F	12.5	5.2	14.6	6.2	15.2		
	Ge	Cl	12.2	4.9	14.8	6.8	14.6		
	Ge	Br	11.2	5.0	14.5	5.6	18.6	1.2	13.9
	Ge	I	11.9	6.2	14.0	4.8	13.5	1.2	14.6
<sup>19</sup> F			δF	J <sub>P<sub>1</sub>IrMF</sub> <sup>cis</sup>	J <sub>P<sub>1</sub>IrMF</sub> <sup>trans</sup>				
	Si	F	-173.4	13.6	24.1				
	Ge	F	-211.7	12.5	22.5				
			-224.2	2.7					

Table 2/5

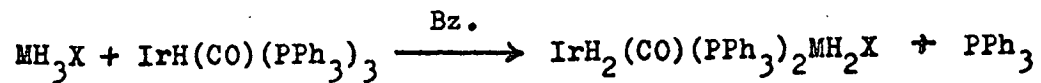


Table 2/5

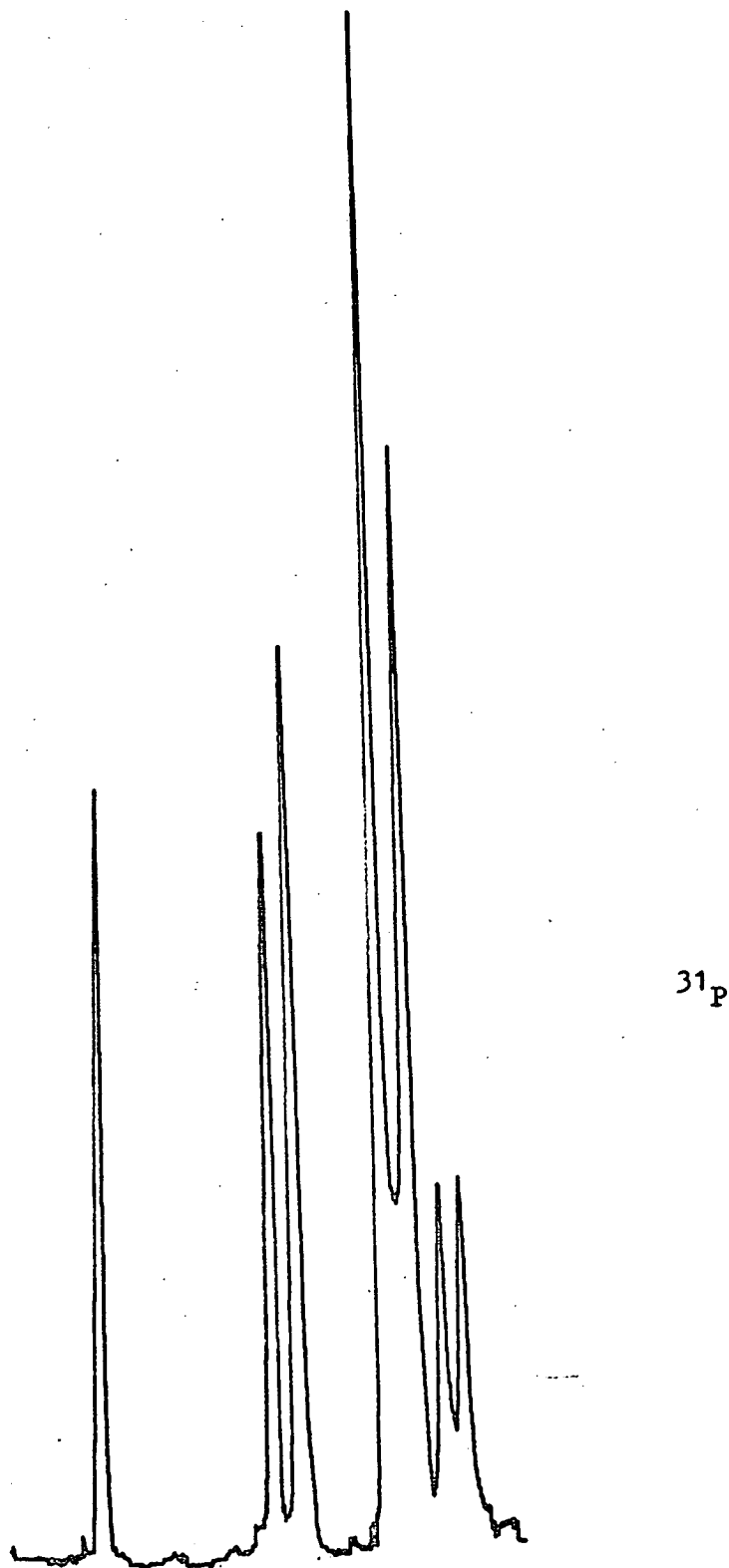


Figure 2e Proton decoupled spectrum of  $\text{IrH}_2(\text{CO})(\text{PPh}_3)_2\text{SiH}_2\text{Br}$  showing  $\text{PPh}_3$  trans to four different ligands. This spectrum is typical.

P = isomer with mutually trans phosphines  
 n.b.  $J_{PIR}$  has been omitted.

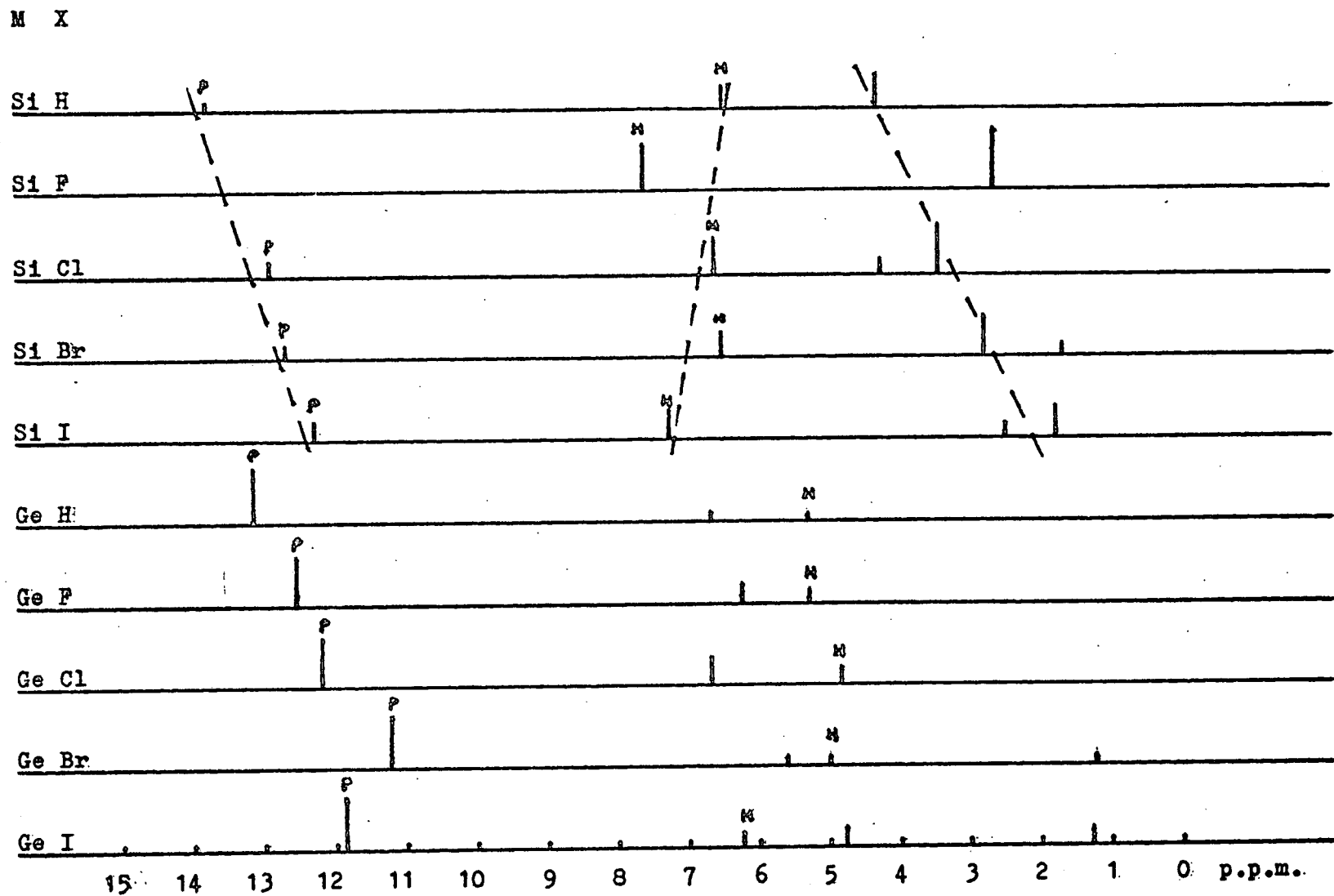


Figure 2f

to identify the major isomer in cases where M is Si apart from narrowing down the choice to A or B.

It is interesting to note that the phosphorus chemical shift of  $\text{PPh}_3$  trans to  $\text{PPh}_3$ , CO,  $\text{SiH}_2\text{X}$  or  $\text{GeH}_2\text{X}$  varies little and that the proton chemical shift for  $\text{IrH}$  trans to  $\text{PPh}_3$ , CO,  $\text{SiH}_2\text{X}$  or  $\text{GeH}_2\text{X}$  (see previous section and next chapter) also varies little.

It might have been reasonable to hope that a distinction between isomers of type A and isomers of type B, in the series of iridium-silyl complexes, could be based on consistent changes in  $^{31}\text{P}$  chemical shift with changes in the substituent at the silicon atoms. It is known that one of the phosphines in A and B is trans to  $\text{IrH}$ , but the problem of finding out what is trans to the other phosphine in the complexes with mutually cis phosphines still remains. It would not be unreasonable to expect that the  $^{31}\text{P}$  chemical shift of a phosphine trans to  $\text{SiH}_2\text{X}$  would behave differently, as X was altered, than that of a phosphine which is cis to  $\text{SiH}_2\text{X}$ . The phosphines in isomer C and the phosphine trans to  $\text{IrH}$  in A and B must all be cis to  $\text{SiH}_2\text{X}$ . It is therefore particularly unfortunate that while the chemical shift of phosphorus trans to phosphine moves to low frequency as the atomic weight of X increases, the chemical shift of phosphorus trans to  $\text{IrH}$  moves to high frequency. It follows that the effect of changing X in  $\text{SiH}_2\text{X}$  upon the  $^{31}\text{P}$  chemical shift of a cis phosphine cannot be predicted even in direction; the observation of an apparent trend in a consistent shift to low frequency of resonances due to an unassigned isomer (drawn in in fig 2f) does not help determine whether these

resonances arise from a phosphine cis or trans to  $\text{SiH}_2\text{X}$ .

It is therefore not possible to make any further assignments of configuration in cases where M is Si. Below is listed a table of assignments made from the previous work. There is little in the phosphorus spectra to contradict these conclusions. However, this recent work has shown that an array of isomers is produced in many cases, which was not apparent from the previous results.

M	X	Major Isomer
Si	H	A
Si	Cl	A
Si	Br	A
Si	I	A
Ge	H	C
Ge	Cl	C
Ge	Br	C
Ge	I	C

### 2.2.2 Results of the $^{19}\text{F}$ n.m.r. study.

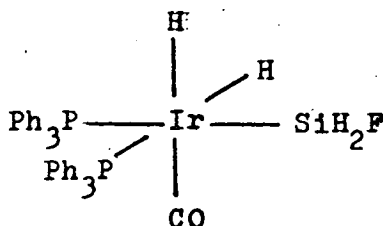
In the previous section, the products where X is F are not discussed. This is because the  $^{31}\text{P}$  spectra obtained from these systems, although essentially the same as the others, are complicated by every line in the spectrum, except that due to free  $\text{PPh}_3$ , receiving an extra doublet splitting from the fluorine atom. Although the presence of fluorine complicates the analysis of  $^{31}\text{P}$  spectra, it allows  $^{19}\text{F}$  n.m.r. to be used ( $^{19}\text{F}$  100% spin $\frac{1}{2}$ ). Using  $^{19}\text{F}$  it was possible to characterise the configurations of the products from the additions of  $\text{SiH}_3\text{F}$  and  $\text{GeH}_3\text{F}$  to  $\text{IrH}(\text{CO})(\text{PPh}_3)_3$ .

The proton decoupled  $^{19}\text{F}$  n.m.r. spectrum of the product from the reaction of  $\text{SiH}_3\text{F}$  and  $\text{IrH}(\text{CO})(\text{PPh}_3)_3$  contains a doublet of



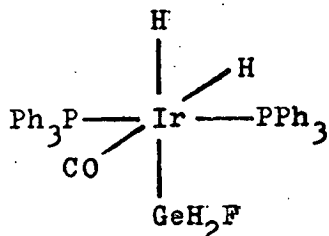
doublets. The smaller doublet coupling was of the same magnitude as a doublet splitting on the resonance due to the phosphine trans to IrH in the  $^{31}\text{P}$  spectrum and this coupling was assigned to a cis phosphorus-fluorine coupling  $J_{\text{PIrSiF}}^{\text{cis}}$ . The larger doublet splitting on the fluorine resonance was of the same magnitude as a doublet splitting on the phosphorus resonance due to the phosphine trans to the unknown ligand and, because this coupling is almost double the value of  $J_{\text{PIrSiF}}^{\text{cis}}$ , it has been assigned to  $J_{\text{PIrSiF}}^{\text{trans}}$ .

Off-resonance decoupling in which only the IrH region of the  $^1\text{H}$  spectrum is irradiated produces a large triplet coupling on the fluorine resonance indicating that there are two protons attached to the silicon atom. When no proton decoupling is used, another small triplet coupling appears due to the two hydrides on the iridium which, although inequivalent, appear sufficiently equivalent with respect to the fluorine atom to produce a triplet. All of this evidence points clearly to a species which in the previous section would have been assigned B viz.



The  $^{19}\text{F}$  n.m.r. of the product from the reaction of  $\text{GeH}_3\text{F}$  with  $\text{IrH}(\text{CO})(\text{PPh}_3)_3$  contains resonances due to two species. One species gave resonances similar to those described for the  $\text{SiH}_3\text{F}$  adduct above and was assigned as having structure B. The other resonance has a triplet coupling which is of the same

magnitude as a doublet splitting on the phosphorus resonance due to the species with mutually trans phosphines. The triplet coupling on the fluorine resonance is assigned as  $J_{\text{P Ir Ge F}}^{\text{cis}}$  and the species producing this resonance is assigned a structure similar to the structure designated C in the last section viz.



### 2.3 Conclusions on Additions of $\text{MH}_3\text{X}$

The most basic and general conclusion which can be made is that both silyl and germyl halides prefer to add Si-H and Ge-H rather than across the group IV-halide bond. This has also been found to be the case in additions of silyl and germyl halides to platinum compounds and is not due to a particular property of iridium, but is a quality of the Si-H and Ge-H bonds.

The products of reaction between  $\text{SiH}_3\text{X}$  and  $\text{Ir}(\text{CO})\text{X}(\text{PEt}_3)_2$  are all those to be expected from trans addition. In the introduction it was pointed out that apparent trans addition could be due to a rearrangement of the product due to an initial cis addition and that formation of trans isomers was influenced by solvent polarity. The reaction between  $\text{SiH}_4$  and  $\text{Ir}(\text{CO})\text{Cl}(\text{PEt}_3)_2$  was attempted in the absence of solvent, but no reaction was observed. The reaction was successfully repeated

using tetramethylsilane as solvent. Reaction was slightly faster than when benzene was used as solvent (2.1.1) and resulted in immediate precipitation of  $\text{IrH}(\text{CO})\text{Cl}(\text{PET}_3)_2\text{SiH}_3$  which proved to be totally insoluble in tetramethylsilane. The products from both solvents, when isolated, gave infra-red spectra which were identical in all respects (see experimental chapter). Tetramethylsilane and benzene differ greatly in polarity, yet they give rise to the same product. It would seem that there is not a clear parallel between the reactions outlined in the introduction and those outlined in this chapter. Not only is there a clear difference in the mode of addition of methyl halides and of silyl or germlyl halides, there is also a clear difference between the mode of addition of silyl and of germlyl halides. In the reactions of  $\text{Ir}(\text{CO})\text{X}(\text{PET}_3)_2$ , silyl species tend to add in a predominantly trans fashion to give A-type isomers, but germlyl compounds tend to add predominantly in a cis fashion to give B-type isomers. It is interesting to recall that in the reactions of silyl and germlyl halides with Vaska's compound,  $\text{SiH}_4$ ,  $\text{SiH}_3\text{Cl}$ ,  $\text{SiH}_3\text{Br}$ ,  $\text{SiH}_3\text{I}$  and  $\text{GeH}_4$  gave insoluble products; these are the group IV species that have been found to give A-type isomers with  $\text{Ir}(\text{CO})\text{X}(\text{PET}_3)_2$ . It may be that the gradual precipitation of the germlyl compounds outlined in the introduction was not due to a change in the mutual arrangement of the phosphines, but to a gradual isomerisation from a B-type isomer to an A-type isomer, driven by the insolubility of the A-type isomer. This is of course highly speculative as the change in phosphine from  $\text{PPh}_3$  to  $\text{PEt}_3$  will no doubt have an influence on the reactions.

The effects of changing a halide for a hydride on the iridium are very evident from the results of the work with  $\text{IrH}(\text{CO})(\text{PPh}_3)_3$ . In the introduction it was shown that this compound dissociated to a slight extent in solution and that addition was to the species  $\text{IrH}(\text{CO})(\text{PPh}_3)_2$  (c/f  $\text{Ir}(\text{CO})\text{Cl}(\text{PPh}_3)_2$ ). The difference in the type of product produced by the reaction with silyl and germyl species manifested itself most clearly in the arrangement of the phosphines. Germyl compounds produce products in which the predominant isomer is of a type with mutually trans phosphines. Silyl compounds produce products in which the predominant isomer has the phosphines mutually cis. This type of behaviour is not seen in any of the reactions with Vaska's compound or any of its analogues and the cis phosphines must be attributed to the presence of the iridium hydride in the starting material. It is plain that the unusual trans influence or effects of the hydride ligand are operating here and it would seem that the effects may be due to a thermodynamically controlled distribution of isomers, those isomers with the most favoured arrangement of ligands being the most abundant. It is also possible that these isomer distributions are due to kinetic factors and that the most abundant isomers are those produced by the most kinetically favoured mechanism and that once formed the isomers cannot rearrange further to reach a thermodynamic distribution. Work on the catalytic properties of similar six co-ordinate species produced from  $\text{Ir}(\text{CO})\text{Cl}(\text{PPh}_3)_2$  and  $\text{IrH}(\text{CO})(\text{PPh}_3)_3$ , outlined in the introduction, suggests that the six co-ordinate products must be capable of some degree of dissociation in order to be catalytically active. The five

co-ordinate species produced by dissociation would be capable of pseudo-rotation to give a more thermodynamically stable product. It is not certain, however, that the species produced here show catalytic activity.

It is not possible to make generalised observations on the thermodynamic suitability of trans arrangements of ligands. In additions to  $\text{Ir}(\text{CO})\text{Cl}(\text{PEt}_3)_2$ , the isomer distributions suggest that silyl groups have a higher tendency to go trans to  $\text{IrH}$  than have germyl groups. However, from the product distributions in the reactions with  $\text{IrH}(\text{CO})(\text{PPh}_3)_3$  the reverse seems to be true and silyl groups seem to have become more attractive as trans ligands to triphenylphosphine. It seems that it is necessary to consider the system as a whole and that little useful information can be gained from looking at isolated pairs of ligands.

CHAPTER 3

Additions of  $\text{H}_3\text{SiCH}_3$  and  $\text{Si}_2\text{H}_6$   
to  $\text{Ir}(\text{CO})\text{Cl}(\text{PEt}_3)_2$  and  
 $\text{IrH}(\text{CO})(\text{PPh}_3)_3$

### 3.1 Reactions of $\text{H}_3\text{CSiH}_3$ and $\text{Si}_2\text{H}_6$ with $\text{Ir}(\text{CO})\text{Cl}(\text{PET}_3)_2$

Reactions of  $\text{H}_3\text{CSiH}_3$  and  $\text{Si}_2\text{H}_6$  with  $\text{Ir}(\text{CO})\text{Cl}(\text{PET}_3)_2$  in benzene were rapid and complete within two minutes at room temperature. The products gave clear colourless solutions in benzene.

#### 3.1.1 1:1 Reaction of $\text{Si}_2\text{H}_6$ with $\text{Ir}(\text{CO})\text{Cl}(\text{PET}_3)_2$

The proton decoupled phosphorus n.m.r. spectrum of the benzene solution of this reaction contains a singlet in the region associated with triethylphosphine bound to Ir(III); therefore the compound has mutually trans phosphines.

The proton n.m.r. spectrum of the benzenic solution contains four sets of resonances due to the product. The pattern of the set due to the ethyl protons of the triethylphosphine groups shows them to be bound to a metal. The peak in the region associated with a metal hydride trans to carbonyl or silyl (see chapter 2) is a triplet of triplets. The larger triplet coupling is collapsed by irradiating at a frequency corresponding to the chemical shift of the singlet in the phosphorus spectrum. It would appear that the disilane has added Si-H rather than Si-Si and that the metal hydride is cis to two mutually trans phosphines.

The two remaining resonances are in the region associated with Si-H. Of these two, the resonance to higher frequency is a complex multiplet, whereas the one to lower frequency is a simple triplet. The triplet coupling is of the same magnitude as the quartet coupling on the resonance to higher frequency and is probably due to coupling with the protons of an adjacent  $-\text{SiH}_2-$

group (which gives rise to the resonance to higher frequency). The resonance is therefore assigned to an  $-\text{SiH}_3$  group. The other resonance, due to the  $-\text{SiH}_2-$  group, is complicated by similarity in the values of  $J_{\text{HSiSiH}}$  (gives rise to the quartet coupling mentioned above) and  $J_{\text{PIrSiH}}$  (gives rise to a triplet coupling on the resonance). Irradiating in the phosphorus region of the spectrum simplifies the complex multiplet to a quartet of doublets, in which the quartet coupling is of the same magnitude as the triplet coupling in the  $-\text{SiH}_3$  resonance and the doublet coupling is of the same magnitude as the smaller triplet coupling on the  $\text{IrH}$  resonance and is probably due to  $J_{\text{HIrSiH}}$ ; the observation of this coupling suggests that the metal hydride is trans to the  $-\text{SiH}_2\text{SiH}_3$  group. The species produced by the reaction would then have  $-\text{SiH}_2\text{SiH}_3$  trans to  $\text{IrH}$ , carbonyl trans to chloride and mutually trans triethylphosphines.

### 3.1.2 1:1 Reaction of $\text{H}_3\text{CSiH}_3$ with $\text{Ir}(\text{CO})\text{Cl}(\text{PEt}_3)_2$

The proton decoupled n.m.r. spectrum of the benzenic solution of the product of this reaction contains a singlet in the region associated with triethylphosphine bound to Ir(III) indicating that the phosphines are mutually trans.

The proton n.m.r. spectrum contains four sets of resonances. The resonances due to the triethylphosphine groups indicate that they are bound to a metal. The resonance due to the metal hydride is in a region associated with  $\text{IrH}$  trans to carbonyl or silyl (see chapter 2) and appears as a triplet of triplets. The larger triplet splitting is collapsed by irradiating in the  $^{31}\text{P}$  region of the spectrum at a frequency corresponding to the



chemical shift of the singlet described above.

Directly to low frequency of the resonances due to triethylphosphine is a simple triplet. The chemical shift corresponds to that associated with  $-\text{CH}_3$  bound to silicon (e.g. tetramethylsilane) and it is likely that the triplet is due to a methyl group bound to a silicon atom which bears two protons. The triplet coupling is collapsed by irradiating in the silyl region. There would appear to be an  $-\text{SiH}_2\text{CH}_3$  group present and methylsilane has added Si-H rather than Si-C or C-H. The resonance due to the  $-\text{SiH}_2-$  protons is complicated because the value of  $J_{\text{PIrSiH}}$  is close to that of  $J_{\text{HCSiH}}$ . When recorded while irradiating in the phosphorus region of the spectrum, the resonance due to  $-\text{SiH}_2-$  appears as a quartet (due to coupling with  $\text{CH}_3$  protons) of doublets. The doublet splitting is of the same magnitude as the smaller triplet splitting on the resonance due to  $\text{IrH}$  and this suggests that the metal hydride is trans to the methylsilyl group. The species produced by the reaction has  $-\text{SiH}_2\text{CH}_3$  trans to  $\text{IrH}$ , carbonyl trans to chloride and mutually trans phosphines.

### 3.2 Reactions of $\text{Si}_2\text{H}_6$ and $\text{H}_3\text{CSiH}_3$ with $\text{IrH}(\text{CO})(\text{PPh}_3)_3$

The reactions of  $\text{Si}_2\text{H}_6$  and  $\text{H}_3\text{CSiH}_3$  with  $\text{IrH}(\text{CO})(\text{PPh}_3)_3$  in benzene at room temperature were rapid and were complete within five minutes to give clear colourless solutions. The n.m.r. spectra of the resulting solutions are discussed in the following sections.

### 3.2.1 1:1 Reaction of $\text{Si}_2\text{H}_6$ with $\text{IrH}(\text{CO})(\text{PPh}_3)_3$

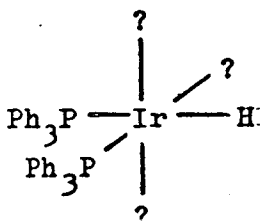
The proton decoupled phosphorus n.m.r. spectrum contains a singlet due to an Ir(III) species with mutually trans triphenylphosphines and two doublets with the same coupling constant due to an Ir(III) species with mutually cis triphenylphosphines. Off-resonance decoupling shows that the doublet to higher frequency is due to a triphenylphosphine trans to a metal hydride. There is also a singlet due to free triphenylphosphine.

The proton n.m.r. spectrum is complicated due to the presence of two isomers. It contains a great deal of information and it is not necessary to use all this information in order to characterise the products. The region of the spectrum due to the silyl protons will be considered first and the conclusions drawn will be used to predict the region of the spectrum due to the metal hydrides. The prediction will then be compared with the actual n.m.r. spectrum observed.

The silyl-proton region contains a weak triplet and a weak complex multiplet. The triplet is unaffected by phosphorus decoupling, but the multiplet is reduced to a quartet structure with a doublet coupling resolved on some of the peaks. By comparison of these resonances with similar resonances outlined in 3.1.1 it is clear that these resonances are due to a species with mutually trans phosphines ( $\text{PPh}_3$  in this case) and  $-\text{SiH}_2\text{SiH}_3$  trans to a metal hydride. The phosphorus n.m.r. spectrum indicates that triphenylphosphine is eliminated during the reaction and so the remaining pair of trans ligands would be carbonyl and metal hydride. The small doublet splitting observed on the  $-\text{SiH}_2-$  resonance, when phosphorus

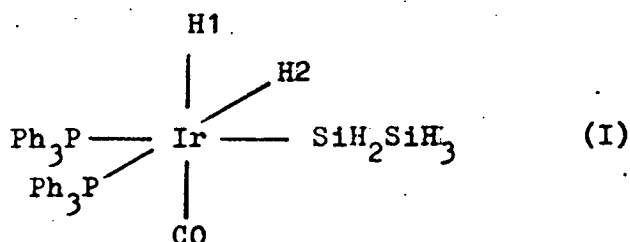
decoupled, probably arises out of coupling to the metal hydride trans to the  $-\text{SiH}_2\text{SiH}_3$  group, the coupling to the cis hydride (that trans to carbonyl) being too small to be resolved. It is unfortunate that the  $-\text{SiH}_2-$  resonance cannot be resolved into its component peaks. This is due to two factors: first,  $J_{\text{PIrSiH}}$  differs in value from  $J_{\text{HSiSiH}}$  which results in many more peaks than in 3.1.1 and this proliferation of peaks results in an unresolvable "hedgehog"; second, this product is only present in very low concentrations compared with that described in 3.1.1.

The remaining peaks in the silyl-proton region of the spectrum are a complex multiplet and a simple quartet. These resonances are a great deal stronger than those just described and are probably due to the major product which, it is known from the  $^{31}\text{P}$  spectrum, contains



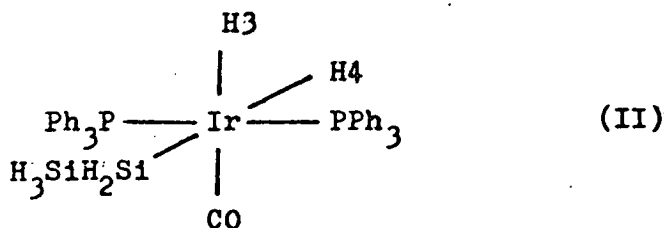
The multiplet is unlike that for the minor product as, rather than coming to a central peak, it comes to a plateau in the centre. This suggests that this resonance has a basic doublet of doublets structure, unlike the complex multiplet outlined above which has a basic triplet structure due to the mutually trans phosphines. The doublet of doublets would result from a silyl group trans to one phosphine, which would give a large doublet coupling, and cis to the other, which would give a smaller doublet coupling. If this analysis of the spectrum is

correct, the use of phosphorus decoupling would give a greater narrowing effect on this complex multiplet compared to its effect on the  $-\text{SiH}_2-$  resonance of the less abundant product and this is seen to be the case, although there is no real improvement in resolution. The quartet is reduced to a triplet when phosphorus decoupling is used, which would also suggest that the disilylanyl group is trans to a phosphine and that it is this unique phosphine which is responsible for the doublet coupling of the same magnitude as the triplet coupling, giving a quartet. By analogy with 3.1.1, it would seem that quartet resonance is due to an  $-\text{SiH}_3$  group and that the triplet coupling is due to two protons on an adjacent  $-\text{SiH}_2-$  group. Although the complex multiplet does not give sufficient information on which to base a definite structure, the quartet resonance indicates a product of the type



Knowing the two species present it is now possible to predict the spectrum due to the metal hydrides and, by comparing predicted with what is observed, to test the above conclusions.

The species present are (I) and (II).

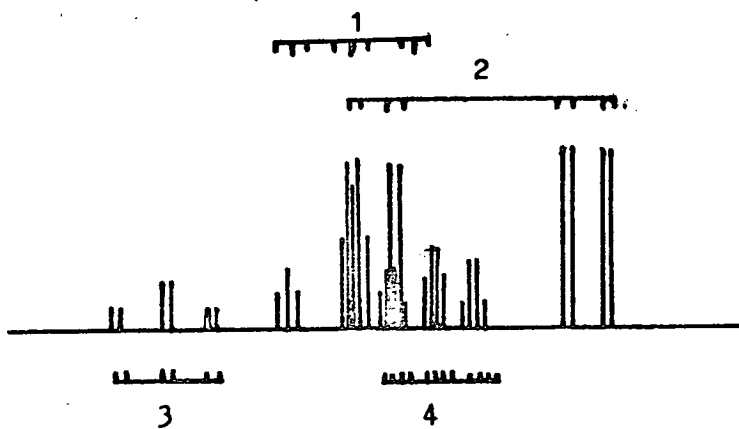


(II) will give rise to two hydride resonances, both with similar chemical shifts ( $\text{IrH}$  trans to carbonyl has a similar shift to  $\text{IrH}$  trans to  $-\text{SiH}_2-$ ). The hydride trans to carbonyl will have a triplet coupling due to the phosphines which are equivalent with respect to both hydrides. The hydride trans to  $-\text{SiH}_2-$  will have a triplet coupling from the phosphines, but, as the trans coupling  $J_{\text{H}\text{Ir}\text{SiH}}$  is observed on the  $-\text{SiH}_2-$  resonance, this hydride resonance will also have a triplet coupling from the  $-\text{SiH}_2-$  protons. There is also the possibility of coupling between the hydrides themselves to give a doublet coupling on both hydride resonances. (II) would therefore give rise to a triplet of doublets ( $\text{IrH}$  trans to carbonyl) and a triplet of doublets of triplets ( $\text{IrH}$  trans to disilylanyl).

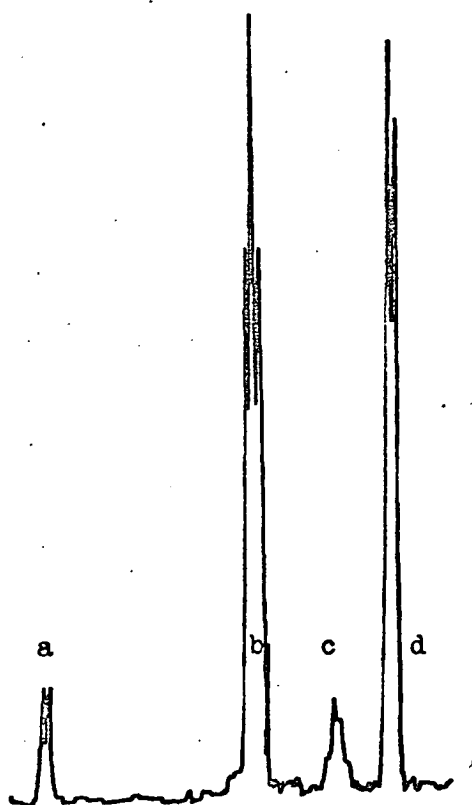
(I) would also give rise to two hydride resonances in the same region as those from (II). As with (II), the hydride trans to carbonyl will give a triplet of doublets, since the coupling from the two cis phosphorus atoms is likely to be almost equal. The hydride trans to phosphine will have a large doublet coupling due to the trans phosphorus atom and a smaller doublet coupling from the cis phosphorus atom. A cis  $J_{\text{H}\text{Ir}\text{SiH}}$  coupling was not observed in the silyl region of the spectrum of isomer (I) and it is thought to be unlikely to be observed in the resonances of isomer (II). The hydrides themselves may couple and give rise to a small doublet splitting on both resonances. (I) would give rise to a triplet of doublets ( $\text{IrH}$  trans to carbonyl) and a doublet of doublets of doublets ( $\text{IrH}$  trans to  $\text{PPh}_3$ ).

The actual spectrum contains a great number of overlapping

peaks



This is simplified by phosphorus decoupling



$^{31}\text{P}$  decoupled

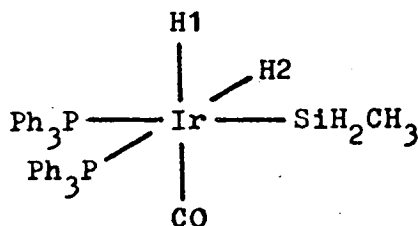
a is due to the hydride trans to carbonyl in (II). c is due to the hydride trans to  $-\text{SiH}_2\text{SiH}_3$  in (II);  $J_{\text{H}\text{Ir}\text{SiH}}$  is approximately equal to  $J_{\text{H}\text{Ir}\text{H}}$  giving rise to a quartet. d is due to the hydride trans to phosphine in (I). The doublet couplings due to the phosphines have been removed to leave the doublet coupling due to the hydride-hydride coupling. b is due to the hydride trans to the carbonyl in (I). As expected it has a doublet coupling of the same magnitude as that in d, but it also has a further doublet coupling of the same magnitude to give a triplet. The origin of this further doublet coupling will be discussed in 3.3

### 3.2.2 1:1 Reaction of $\text{H}_3\text{CSiH}_3$ with $\text{IrH}(\text{CO})(\text{PPh}_3)_3$

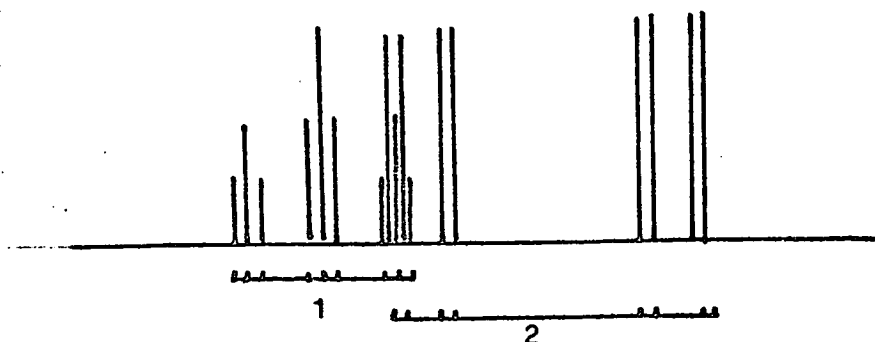
The proton decoupled  $^{31}\text{P}$  n.m.r. spectrum of the product contains peaks due to free triphenylphosphine (singlet) and a species with mutually cis triphenylphosphines bound to Ir(III) (two doublets with the same coupling:  $J_{\text{P}\text{Ir}\text{P}}$ ). Off-resonance decoupling shows the doublet to high frequency to be due to phosphine trans to  $\text{IrH}$ .

The proton n.m.r. spectrum is complex and is best treated in a similar manner to 3.2.1, i.e. to consider the metal hydrides last. The region associated with  $\text{H}_3\text{C-Si}$  contains a quartet, which is reduced to a triplet when phosphorus decoupled, indicating that the methyl is attached to the  $-\text{SiH}_2-$  (c/f 3.1.2) and that the  $\text{H}_3\text{CSiH}_2-$  group is trans to a triphenylphosphine (doublet coupling is due to a unique trans phosphine). The  $-\text{SiH}_2-$  resonance is a complex multiplet and gives little information, but when this resonance is irradiated the triplet

coupling to the  $-\text{CH}_3$  is removed, confirming that the triplet is due to  $J_{\text{HCSiH}}$ . It is possible, from the information given by the  $-\text{CH}_3$  resonance to say that the species formed is

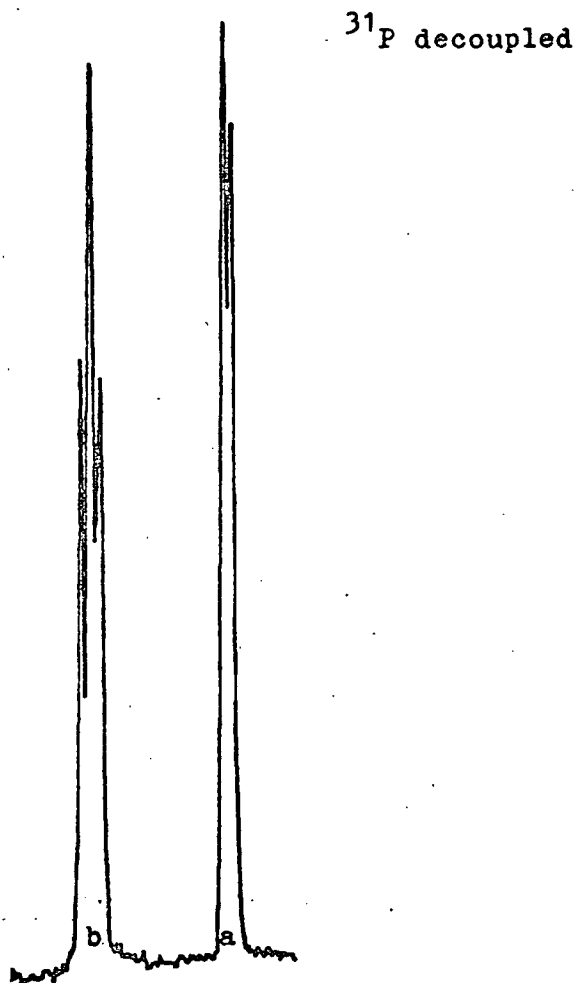


The resonances due to the metal hydrides would all be found in the same general region of the n.m.r. spectrum. The hydride trans to carbonyl is cis to two triphenylphosphines. These phosphines are trans to two different ligands, but may well appear equivalent to the cis hydride and give a triplet coupling rather than a doublet of doublets. The hydride trans to the triphenylphosphine will receive a large doublet coupling from the trans phosphorus atom and a smaller doublet coupling from the cis phosphorus atom. (comparable to the triplet coupling on the other hydride) and will give a doublet of doublets. It is likely that both hydrides will couple to each other and so the triplet may be a triplet of doublets and the doublet of doublets may be a doublet of doublet of doublets. What in fact is seen is like this



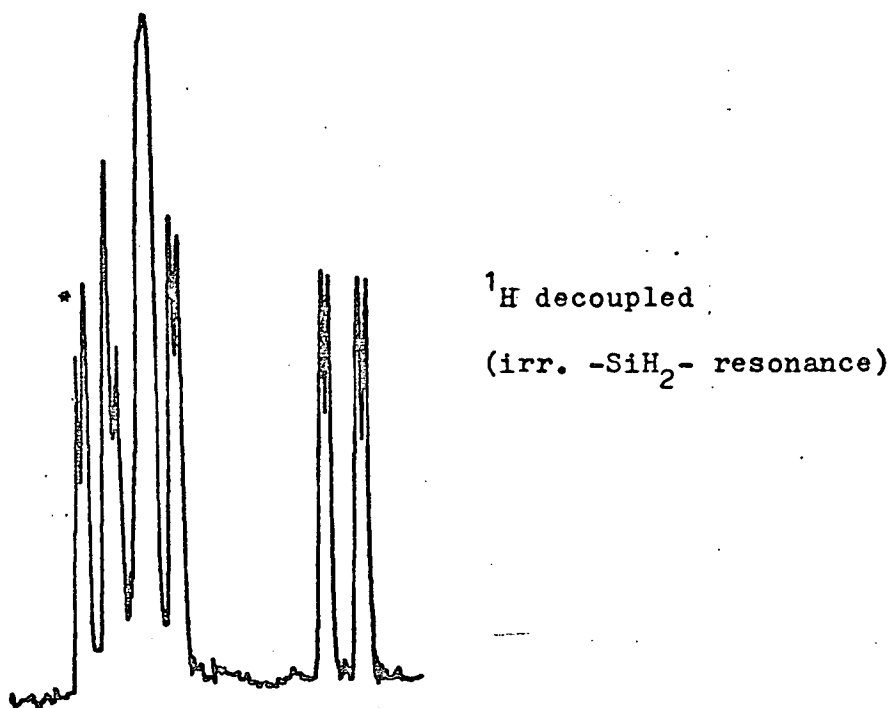


The high frequency part of the doublet coincides with the low frequency part of the triplet. This can be simplified by phosphorus decoupling.



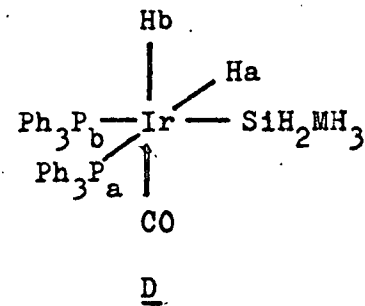
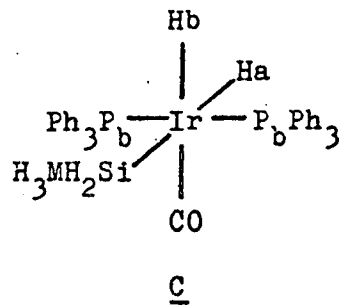
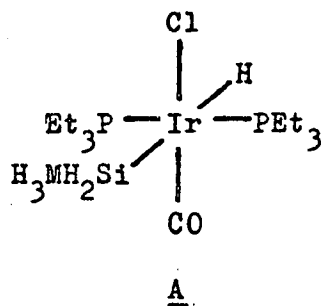
a is due to the hydride trans to the phosphine. The doublet coupling on a is due to the hydride-hydride coupling and the resonance due to the other hydride (i.e. b) also has the same doublet coupling. However, b does not appear as a doublet, but as a triplet, due to a second doublet coupling of the same

magnitude. It was found during the homonuclear decoupling experiment intended to verify  $J_{\text{HCSiH}}$ , that not only did irradiation of the  $-\text{SiH}_2-$  resonance collapse the triplet coupling to the  $-\text{CH}_3$ , it also decoupled the extra doublet coupling to the metal hydride trans to carbonyl. The extra doublet coupling must therefore be due to one of the protons of the  $-\text{SiH}_2-$  group.



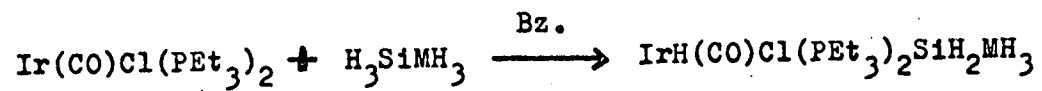
\* this peak is a triplet when no decoupling is used

Units and abbreviations: see table 1/1



M	$\delta_{\text{MH}}$	$\delta_{\text{SiH}}$	$\delta_{\text{IrH}}$	$J_{\text{PIrSiH}}$	$J_{\text{PIrH}}$	$J_{\text{HirSiH}}$	$J_{\text{HSiMH}}$	$\delta^{31}\text{P}$	isomer
Si	2.6t	2.7q/t/d	-8.0t/t	5.0	16.0	2.3	5.0	-5.9	A
C	0.6t	3.6q/t/d	-7.7t/t	4.0	16.0	2.2	4.0	-4.4	A

Table 3/1



\* see Table 3/1

multiplet

Units and abbreviations: see Table 1/1, c.m.:complex

M	$\delta$ SiH	$\delta$ MH	$\delta$ IrHa	$\delta$ IrHb	$\delta$ P <sub>a</sub>	$\delta$ P <sub>b</sub>	isomer*
Si	2.5c.m.	3.4d/t	-11.5d/d/d	-10.6t/t	6.2	4.2	D
Si	2.0q/t/d	2.7t	-10.9t/d/t	-9.1t/d	-	13.2	C
C	4.3c.m.	0.7d/t	-10.3d/d/d	-9.6d/d/t	7.9	3.7	D

M	$J_{P_a IrSiMH}$	$J_{P_b IrSiMH}$	$J_{Ha IrSiH}$	$J_{Hb IrSiH}$	$J_{HSiSH}$	$J_{P_a IrHa}$	$J_{P_b IrHa}$	$J_{PIrHb}$	$J_{Ha IrHb}$	$J_{P_a IrP_b}$
Si	0	2.7	0	3.9	2.7	114.0	14.0	19.0	3.5	15.1
Si	0	-	2.2	0	3.5	-	17.0	17.0	4.0	-
C	0	4.2	0	4.0	4.2	115.5	18.6	16.0, 22.0	3.5	16.2

Table 3/2

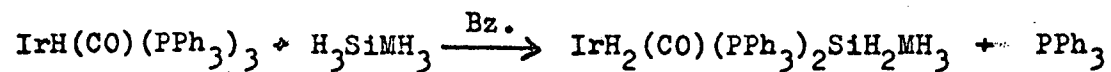


Table 3/2

### 3.3 Conclusions from $H_3MSiH_3$ Addition Reactions

The results for the addition of methylsilane and disilane to  $Ir(CO)Cl(PEt_3)_2$  and  $IrH(CO)(PPh_3)_3$  are similar to those in chapter 2. The addition is always Si-H to give silyl and hydride ligands and as with the addition of silyl halides, the product formed with  $Ir(CO)Cl(PEt_3)_2$  has mutually trans phosphines and silyl trans to hydride. This conforms to the pattern that silyl additions tend to give A-type isomers (see 2.1.1). As with the additions of silyl halides to  $IrH(CO)(PPh_3)_3$ , the major product has mutually cis phosphines and a small amount of an isomer with mutually trans phosphines is also produced, although this is not observed in the  $H_3CSiH_3$  case.

The most intriguing result obtained in these reactions is the observation of coupling between one proton of the  $-SiH_2-$  group to the hydride trans to carbonyl in  $IrH_2(CO)(PPh_3)_2SiH_2CH_3$ . On discovering this result, the spectrum of  $IrH_2(CO)(PPh_3)_2-SiH_2SiH_3$  was re-examined and the same phenomenon observed in the isomer with mutually cis phosphines. The triplet coupling on the  $-CH_3$  and  $-SiH_3$  resonances indicate that there are definitely two protons on the silicon atom attached to the metal. Why they should couple differently to a metal hydride is difficult to explain. The protons of the  $-SiH_2-$  are equivalent with respect to  $-CH_3$  or  $-SiH_3$  and as  $J_{HSiSiH}$  and  $J_{HCSiH}$  would be very sensitive to a difference between the two  $-SiH_2-$  protons in  $HSiC$  or  $HSiSi$  angles, it is fairly certain that the local mirror plane of the  $-SiH_2SiH_3$  and  $-SiH_2CH_3$  groups is retained. The inequivalence of the  $-SiH_2-$  protons must therefore result

from a property of the Si-Ir bond such as restricted rotation about this bond. Such restricted rotation is unlikely to be caused by steric hindrance as isomer (II) exhibits free rotation about the Si-Ir bond. In isomer (II) the groups cis to the  $-\text{SiH}_2\text{SiH}_3$  group are  $\text{PPh}_3, \text{H}, \text{PPh}_3$  and CO. In isomer (I) the  $-\text{SiH}_2\text{SiH}_3$  group is cis to  $\text{PPh}_3, \text{H}, \text{H}$  and CO i.e. a bulky phosphine<sup>37</sup> has been replaced by a less bulky hydride and therefore rotation about the Si-Ir bond should be less sterically hindered in (I) than in (II).

One of the most obvious differences in the situation of the  $-\text{SiH}_2\text{SiH}_3$  group in (I) as opposed to (II) is the trans ligand: in (I) it is trans to a phosphine and in (II) it is trans to a hydride. This difference suggests the possibility of some form of electronic effect exerted by the trans ligand, such as an electronic barrier to rotation, which is stronger in the case where a phosphine ligand is trans to  $-\text{SiH}_2\text{SiH}_3$  than when the trans ligand is  $\text{IrH}$ .

Inequivalence of the  $-\text{SiH}_2-$  protons would explain many of the observations, or lack of them, about the  $-\text{SiH}_2-$  resonances. The protons would differ slightly from each other in chemical shift and this would contribute to the plateau shaped envelope, mentioned earlier, which these resonances have. Also, if only one of the protons is coupled to a hydride, the plateau will be asymmetric as is seen to be the case. Finally, inequivalence would lead to geminal coupling between the  $-\text{SiH}_2-$  protons and further complicate an already complex resonance with second order effects.

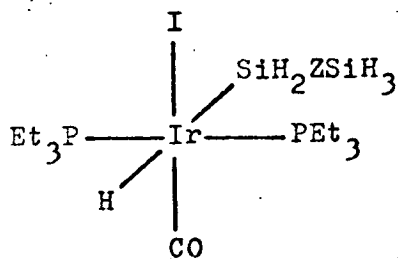
CHAPTER 4

Reactions of  $\text{Ir}(\text{CO})\text{I}(\text{PEt}_3)_2$

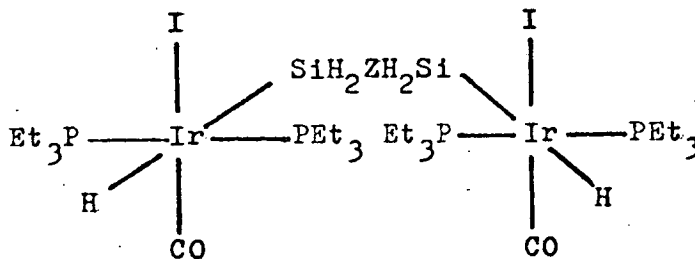
with  $(\text{SiH}_3)_2\text{Z}$  ( $\text{Z}:\text{O},\text{S},\text{Se}$ )

#### 4 Reactions of $\text{Ir}(\text{CO})\text{I}(\text{PEt}_3)_2$ with $(\text{SiH}_3)_2\text{Z}$ ( $\text{Z}:\text{O},\text{S},\text{Se}$ )

Molecules of the type  $\text{Z}(\text{SiH}_3)_2$  ( $\text{Z}:\text{O},\text{S},\text{Se}$ ) have a great variety of bonds which might be broken during oxidative addition. However, from the results of the previous chapters, it appears that the most likely bond to be broken during reaction is the Si-H bond. If only Si-H bonds are broken during reaction, there are two possible modes of addition: firstly, there is mono-addition, in which  $\text{Z}(\text{SiH}_3)_2$  acts like  $\text{SiH}_3\text{X}$  ( $\text{X}=\text{Z}(\text{SiH}_3)$ ) and only one of the silyl groups reacts; secondly, there is bis-addition, in which both silyl groups react to give products containing two iridium atoms joined by an  $-\text{SiH}_2\text{ZSiH}_2-$  bridge.

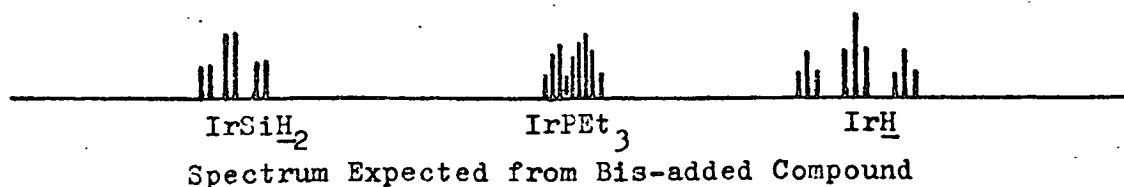


Mono-added Compound



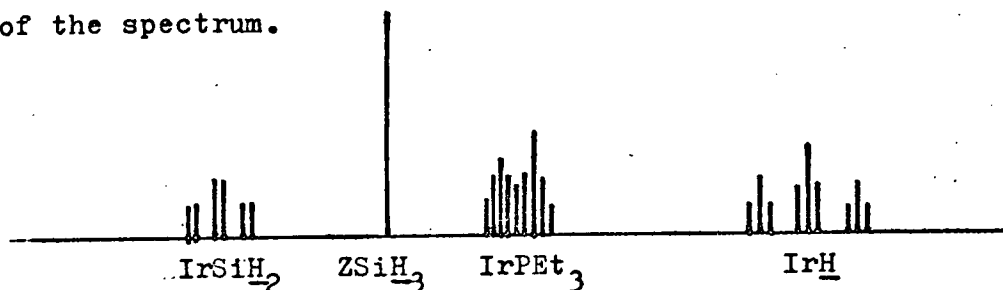
Bis-added Compound

The mono-added compound and the bis-added compound both contain  $\text{IrH}(\text{CO})\text{I}(\text{PEt}_3)_2\text{SiH}_2-$  units and from chapter 2 (Fig. 2a) it is known that such a unit gives a proton n.m.r. spectrum containing an  $\text{SiH}_2$  resonance (triplet (due to  $J_{\text{PIrSiH}}$ ) of doublets (due to  $J_{\text{HIrSiH}}$ )), an  $\text{IrH}$  resonance (triplet (due to  $J_{\text{PIrH}}$ ) of triplets (due to  $J_{\text{HIrSiH}}$ )) and a set of resonances which are characteristic of the ethyl groups of bound triethylphosphine.





The mono-added compound should contain one additional resonance, due to the protons of the  $\text{SiH}_3$  group attached to Z. It is unlikely that the nuclei on either side of Z will couple and  $\text{ZSiH}_3$  should therefore give rise to a singlet in the silyl region of the spectrum.



Spectrum Expected from Mono-added Product

#### 4.1 Reactions of $(\text{SiH}_3)_2\text{O}$ with $\text{Ir}(\text{CO})\text{I}(\text{PET}_3)_2$

The proton n.m.r. spectrum of the benzene solution of the product from the reaction of  $(\text{SiH}_3)_2\text{O}$  with  $\text{Ir}(\text{CO})\text{I}(\text{PET}_3)_2$ , in 1:2 molar ratio, in benzene at room temperature, is of the first type outlined above (i.e. it contains resonances similar to those in figure 2a) and therefore this product is a bis-added or bridged type with two iridium centres joined by an  $-\text{SiH}_2\text{OSiH}_2-$  bridge.

The proton n.m.r. spectrum of the benzene solution of the product from the reaction of excess  $(\text{SiH}_3)_2\text{O}$  with  $\text{Ir}(\text{CO})\text{I}(\text{PET}_3)_2$  is of the second type outlined at the beginning of this chapter. This extra singlet resonance is at a chemical shift which is very close to that of  $(\text{SiH}_3)_2\text{O}$  and is thought to arise from an  $\text{O-SiH}_3$  group. The product of this reaction is therefore presumed to be of the mono-added type, containing an  $-\text{SiH}_2\text{OSiH}_3-$  ligand.

In both reactions, there is evidence for the production of appreciable amounts of  $\text{SiH}_4$ . As the gaseous products and

starting materials in the mixture are removed after the reaction is complete, the evidence for the production of silane is the presence of a triplet of doublets in the proton spectrum at the usual position associated with  $-\text{SiH}_3$  bound to iridium, with a peak in the phosphorus n.m.r. spectrum at  $-15.4$  p.p.m. consistent with the presence in the reaction mixture of the compound  $\text{IrH}(\text{CO})\text{I}(\text{PEt}_3)_2\text{SiH}_3$ . In addition to the products obtained from the reactions of  $(\text{SiH}_3)_2\text{O}$  and  $\text{SiH}_4$  with  $\text{Ir}(\text{CO})\text{I}(\text{PEt}_3)_2$  the phosphorus spectrum also indicated the presence of two other unidentified products (giving rise to peaks at  $-13.7$  and  $-21.6$  p.p.m.) which are probably associated with the reaction which produces silane. The nature of this side-reaction is not understood. As the amount of silane does not increase after the  $\text{Ir}(\text{CO})\text{I}(\text{PEt}_3)_2$  has been consumed, it seems unlikely that the silane is the result of a decomposition of the mono- or bis-added species. It would need to be an alternative reaction to oxidative addition of Si-H across Ir and may involve an unstable species resulting from addition of O-Si, but there is no evidence to confirm this.

#### 4.2 Reactions of $(\text{SiH}_3)_2\text{S}$ and $(\text{SiH}_3)_2\text{Se}$ with $\text{Ir}(\text{CO})\text{I}(\text{PEt}_3)_2$

Analysis of the spectra obtained from the products of these reactions is not as straightforward as those obtained from the analogous reactions with  $(\text{SiH}_3)_2\text{O}$ . It is apparent from the proton and phosphorus n.m.r. spectra that a mixture of products is obtained in each case. As with the reaction of  $(\text{SiH}_3)_2\text{O}$ ,  $\text{SiH}_4$  is produced to some extent in each reaction.

The proton n.m.r. spectrum of the product obtained from reaction

of  $\text{Ir}(\text{CO})\text{I}(\text{PEt}_3)_2$  with  $(\text{SiH}_3)_2\text{S}$  in 2:1 molar ratio in benzene, contains the expected resonances for bound triethylphosphine groups. Two sets of resonances associated with  $\text{IrH}$  trans to  $-\text{SiH}_2-$  are present; these take the form of triplets of triplets which partly obscure each other when phosphorus coupling is retained. The region associated with  $\text{SiH}$  contains three sets of resonances. The set at highest frequency has a triplet of doublets structure, the doublet coupling of which is of the same magnitude as the smaller triplet coupling on the  $\text{IrH}$  resonance of higher frequency; as the remaining couplings to these resonances are removed by irradiating at the same phosphorus chemical shift, these two resonances must belong to the same compound. The remaining resonances in the region associated with  $\text{SiH}$  are a singlet and another triplet of doublets. The doublet coupling to the triplet of doublets, which is partly obscured by the singlet, is of the same magnitude as the smaller triplet coupling to the  $\text{IrH}$  resonance of lower frequency; as the other triplet couplings to these resonances are removed by irradiating at the same  $^{31}\text{P}$  chemical shift, these resonances must belong to the same compound. Therefore, there are two silyl-iridium complexes present. The singlet is assigned to an  $-\text{SSiH}_3$  group. In the phosphorus spectrum there are two major peaks due to  $\text{Ir}(\text{III})$  products. Off-resonance decoupling transforms these two peaks into doublets of triplets (see fig. 2a) indicating that the  $\text{Ir}(\text{III})$  species each contain one  $\text{IrH}$  and one  $\text{IrSiH}_2-$  group. There is therefore the choice of two systems, both of which are giving resonances of the type outlined in figure 2a and one of which is giving the additional  $-\text{SSiH}_3$  resonance. As the proportion of

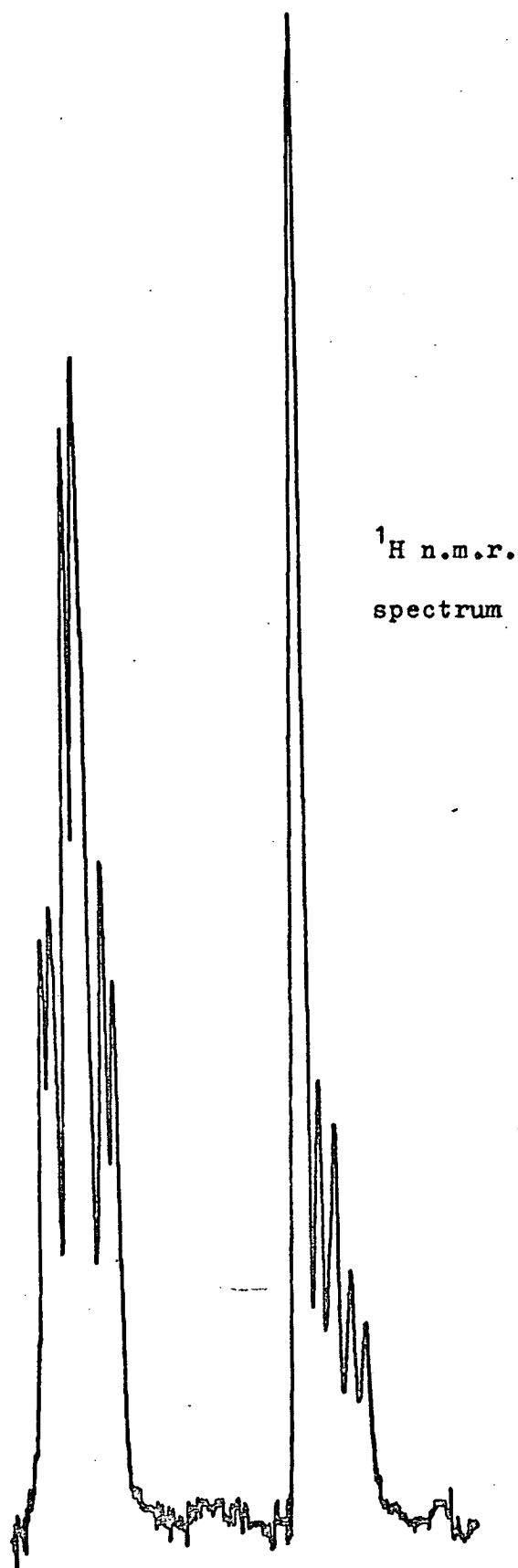


Figure 4 a SiH resonances of  $\text{IrH}(\text{CO})\text{I}(\text{Pet}_3)_2\text{SiH}_2\text{SSiH}_3$   
and  $(\text{IrH}(\text{CO})\text{I}(\text{Pet}_3)_2\text{SiH}_2)_2\text{S}$

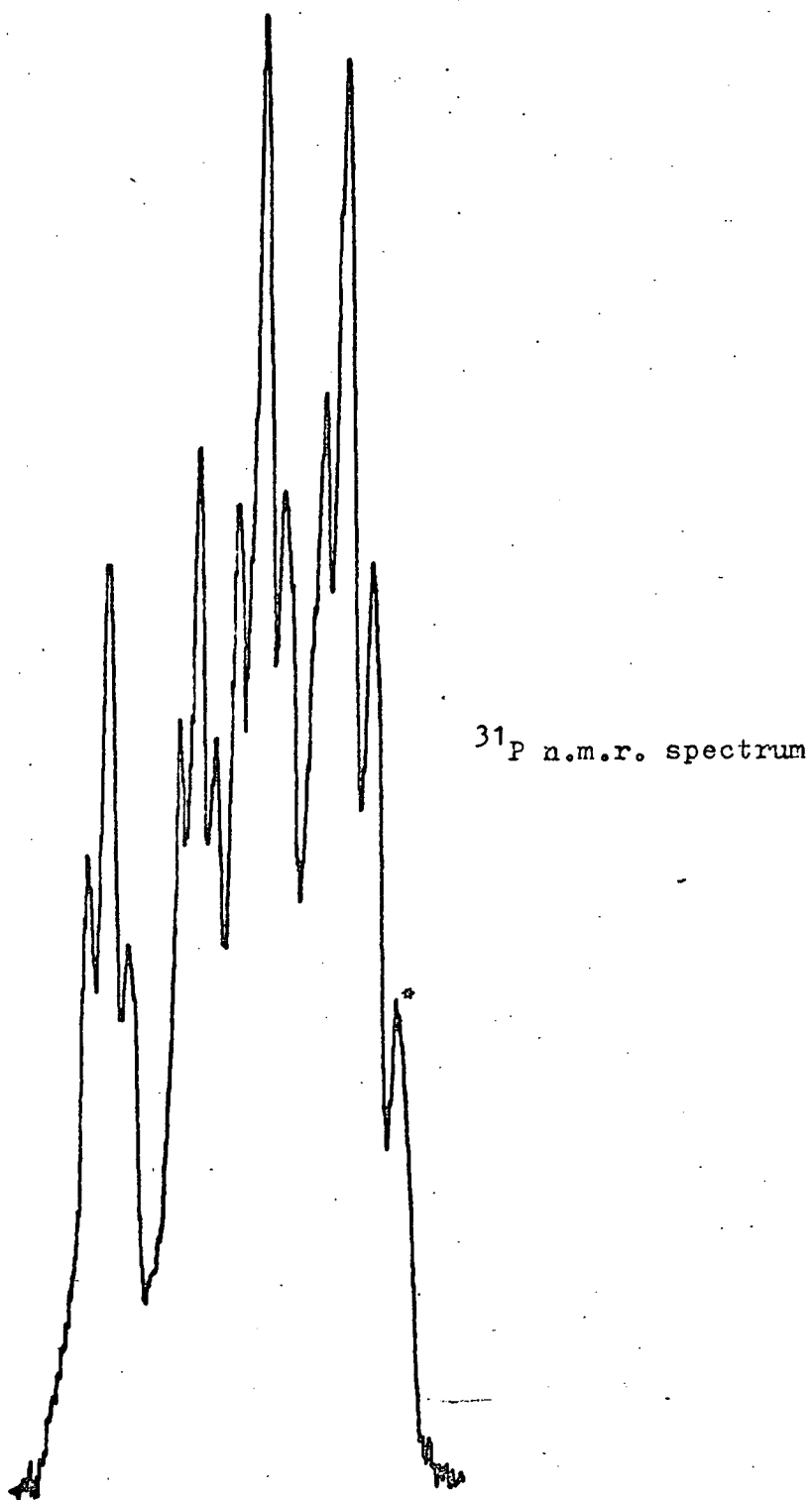


Figure 4b Off-resonance proton decoupled spectrum of  $\text{IrH}(\text{CO})\text{I}(\text{PEt}_3)_2\text{SiH}_2\text{SSiH}_3$  and  $(\text{IrH}(\text{CO})\text{I}(\text{PEt}_3)_2\text{SiH}_2)_2\text{S}$ . Each compound gives rise to a doublet of triplets.

\* unidentified product

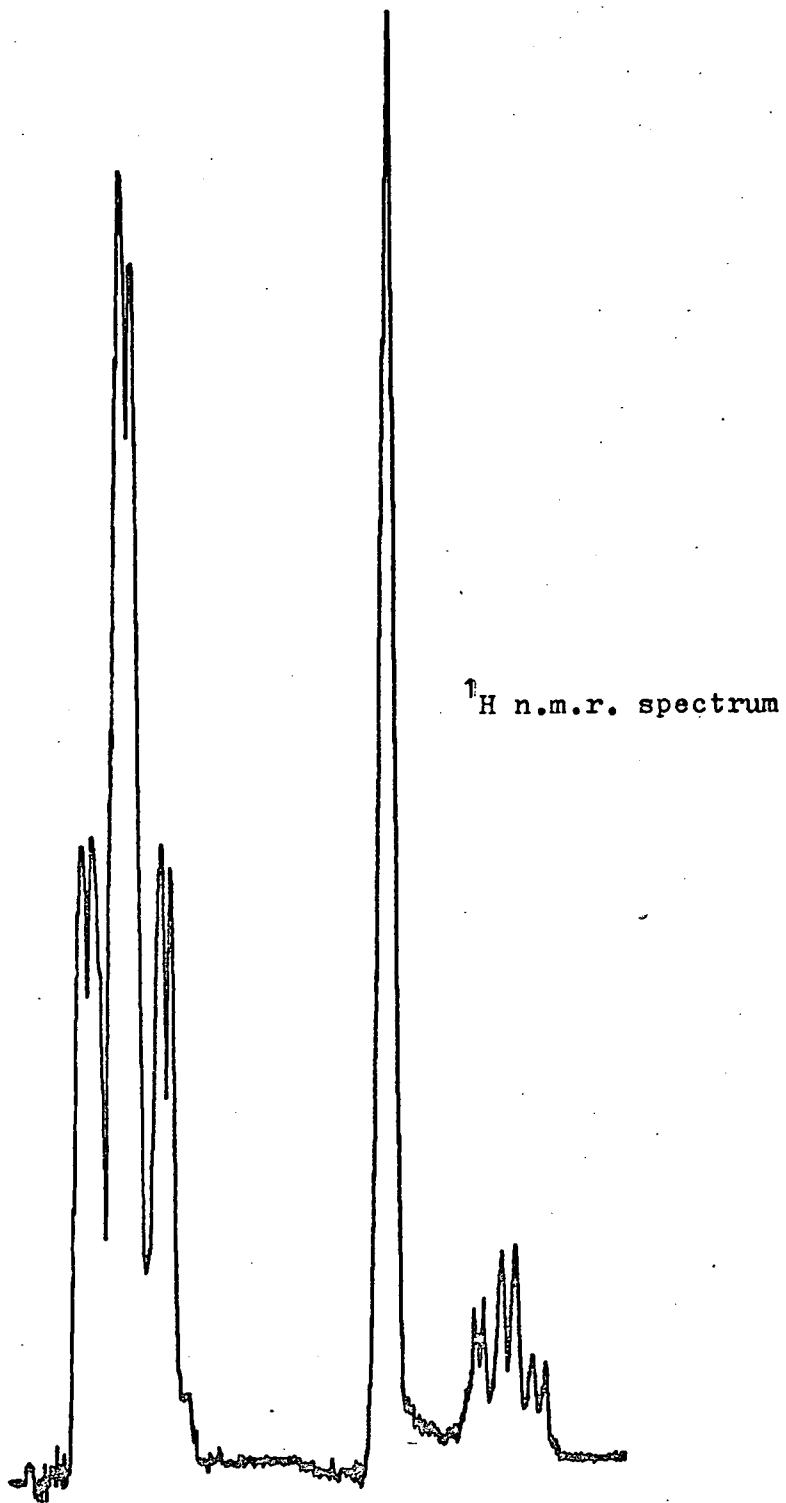


Figure 4c SiH resonances of  $\text{IrH(CO)I(PET}_3)_2\text{SiH}_2\text{SeSiH}_3$   
and  $(\text{IrH(CO)I(PET}_3)_2\text{SiH}_2)_2\text{Se}$

$(\text{SiH}_3)_2\text{S}$  is increased to give a 1:1 molar ratio, the singlet and the triplet of doublets it partly obscures (and resonances associated with this resonance) increase in intensity. It would therefore seem reasonable to assume that these two resonances are those for the  $-\text{SiH}_2\text{SSiH}_3$  ligand and that the high frequency  $\text{SiH}$  and  $\text{IrH}$  resonances and the low frequency phosphorus resonance are due to the bis-added compound.

The spectra obtained of the products from the reactions of  $(\text{SiH}_3)_2\text{Se}$  with  $\text{Ir}(\text{CO})\text{I}(\text{PEt}_3)_2$  contained analogous resonances to those outlined for the reactions of  $(\text{SiH}_3)_2\text{S}$ . As the ratio of  $(\text{SiH}_3)_2\text{Se}$  to  $\text{Ir}(\text{CO})\text{I}(\text{PEt}_3)_2$  is increased, one set of resonances and the singlet (due to  $-\text{SiH}_3$ ) increase in intensity and it is on this criterion that the assignments in table 4/1 are made.

In all of the reactions of  $(\text{SiH}_3)_2\text{S}$  and  $(\text{SiH}_3)_2\text{Se}$  with  $\text{Ir}(\text{CO})\text{I}(\text{PEt}_3)_2$ , the bis-added product is produced in higher concentrations than the mono-added product irrespective of the ratio of the starting compounds.

### 4.3 Conclusions

The n.m.r. parameters for the species outlined in 4.1 and 4.2 are listed in table 4/1. The most apparent difference in the parameters listed for  $(\text{SiH}_3)_2\text{O}$  reactions and those for  $(\text{SiH}_3)_2\text{S}$  and  $(\text{SiH}_3)_2\text{Se}$  is the similarity in the parameters for the mono- and bis-added complexes of  $(\text{SiH}_3)_2\text{O}$  and the difference in parameters, especially those for  $-\text{SiH}_2-$ , in the mono- and bis-added complexes of  $(\text{SiH}_3)_2\text{S}$  and  $(\text{SiH}_3)_2\text{Se}$ . In a compound of the type  $\text{X-Z-Y}$  ( $\text{Z} = \text{O, S, Se}$ ;  $\text{X}$  and  $\text{Y} = \text{H}_3\text{Si}-$  or  $\text{IrH}(\text{CO})\text{I}(\text{PEt}_3)_2\text{SiH}_2-$ ), the n.m.r. parameters of  $\text{X}$  would not be expected to be much

Units and abbreviations:- see table 1/1

Z	SiH <sub>2</sub>	SiH <sub>3</sub>	IrH	J <sub>PIrSiH</sub>	J <sub>PIrH</sub>	J <sub>HIrSiH</sub>	<sup>31</sup> P	(Et <sub>3</sub> P)	Product
O	5.5t/d	--	-10.0t/t	7.3	16.0	2.8	14	-14.1	Bis-added
O	5.5t/d	4.7s	-10.0t/t	7.2	15.8	3.0	14	-14.1	Mono-added
S	5.3t/d	--	-9.95t/t	8.0	15.5	2.3	18	-17.2	Bis-added
S	4.4t/d	4.5s	-10.15t/t	8.0	15.7	3.2	16	-16.6	Mono-added
Se	5.2t/d	---	-9.95t/t	7.8	16.2	2.5	17	-17.3	Bis-added
Se	4.3t/d	4.6s	-10.1t/t	8.0	16.0	3.2	17	-17.1	Mono-added

Table 4/1.

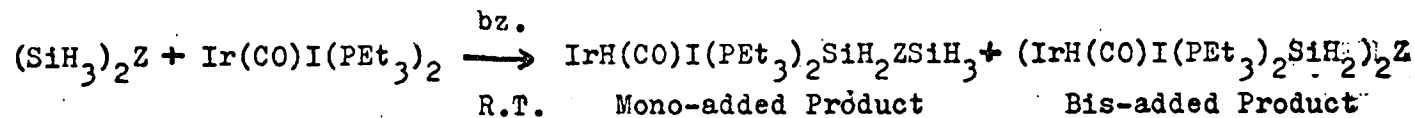


Table 4/1





This compound should give rise to a triplet in the  $\text{SiH}$  region of the proton spectrum due to the  $-\text{SiH}_3$  group on the iridium on the left and should give rise to two singlet resonances in the proton decoupled phosphorus n.m.r. spectrum, only one of which should be transformed into a doublet by off-resonance decoupling. None of these observations has been recorded and there is no evidence for a system of type (I). It is clear from the proton spectra that the unknown product contains  $\text{IrSiH}_2\text{-X}$  where X is not capable of coupling to the silyl protons. In view of the lack of choice in the nature of X, it would seem that the most likely candidate to fill the position of X would be, in fact,  $\text{Z-SiH}_3$ . It is felt that the assignments in table 4/1, although somewhat tentative, are those which best fit the observations.

Analogous reactions to those outlined in 4.1 and 4.2 were carried out using  $\text{trans-PtHI}(\text{PET}_3)_2$ <sup>48</sup> and the relevant n.m.r. parameters are listed below for comparison with table 4/1.

	$\delta_{\text{SiH}_3}$	$\delta_{\text{SiH}_2}$	$\delta_{(\text{PET}_3)}$
$\text{t-PtI}(\text{PET}_3)_2\text{SiH}_2\text{OSiH}_3$	4.7	5.0	13.1
$(\text{t-PtI}(\text{PET}_3)_2\text{SiH}_2)_2\text{O}$		5.1	13.3
$\text{t-PtI}(\text{PET}_3)_2\text{SiH}_2\text{SSiH}_3$	4.5	4.0	9.1
$(\text{t-PtI}(\text{PET}_3)_2\text{SiH}_2)_2\text{S}$		4.2	9.3
$\text{t-PtI}(\text{PET}_3)_2\text{SiH}_2\text{SeSiH}_3$	4.4	4.0	8.4
$(\text{t-PtI}(\text{PET}_3)_2\text{SiH}_2)_2\text{Se}$		4.0	8.6

As with the reactions outlined in 4.1 and 4.2, the tendency to form the bis-added species, rather than the mono-added species, was reported to increase with the atomic weight of Z. This was interpreted in terms of steric hindrance and such

an argument would apply equally well in the reactions of  $\text{Ir}(\text{CO})\text{I}(\text{PET}_3)_2$ . The separation between  $\text{SiH}_3$  groups increases as the atomic weight of Z increases, and the approach of a second molecule of  $\text{Ir}(\text{CO})\text{I}(\text{PET}_3)_2$  would be less hindered on Z going from O to Se<sup>50</sup>.

Appart from the change in the chemical shift of  $-\text{SiH}_2-$  on going from the mono-added species to the bis-added species, the results outlined in this chapter show good agreement with those reported for  $\text{trans-PtHi}(\text{PET}_3)_2$ .

Chapter 5

Addition reactions of  $(\text{SiH}_3)_3\text{P}$

with  $\text{Ir}(\text{CO})\text{I}(\text{PEt}_3)_2$

## 5 Addition Reactions of Trisilylphosphine with $\text{Ir}(\text{CO})\text{I}(\text{PET}_3)_2$

As with  $(\text{SiH}_3)_2\text{O}$ ,  $(\text{SiH}_3)_2\text{S}$  and  $(\text{SiH}_3)_2\text{Se}$ ,  $(\text{SiH}_3)_3\text{P}$  has two types of bond which can be broken during oxidative addition (i.e. Si-P and Si-H). Like the group VIb silyl compounds  $(\text{SiH}_3)_3\text{P}$  can undergo more than one oxidative addition to form bridged compounds (see chapter 4). In the case of the group VIb silyl compounds it was possible to distinguish the mono-added compound (formed by a single oxidative addition) from the bis-added compound (each group VIb molecule undergoing two oxidative additions to give a bridged compound) using proton n.m.r.. This was possible because the mono-added compound contained an  $-\text{SiH}_3$  group with a characteristic proton resonance, whereas the bis-added compound contained no  $-\text{SiH}_3$  group. With oxidative addition involving  $(\text{SiH}_3)_3\text{P}$ , there are three possible products. These are the mono-added compound, the bis-added compound and the tris-added compound. The tris-added compound would not contain a P-SiH<sub>3</sub> group and could be distinguished from the mono- and bis-added compounds by the absence of a P-SiH<sub>3</sub> proton resonance. The mono-added compound would contain two P-SiH<sub>3</sub> groups and the bis-added compound would contain only one. As the mono- and bis-added compounds would both give a P-SiH<sub>3</sub> proton resonance, it would not be possible to distinguish one from the other using proton n.m.r. except by using peak intensities which are not always reliable.

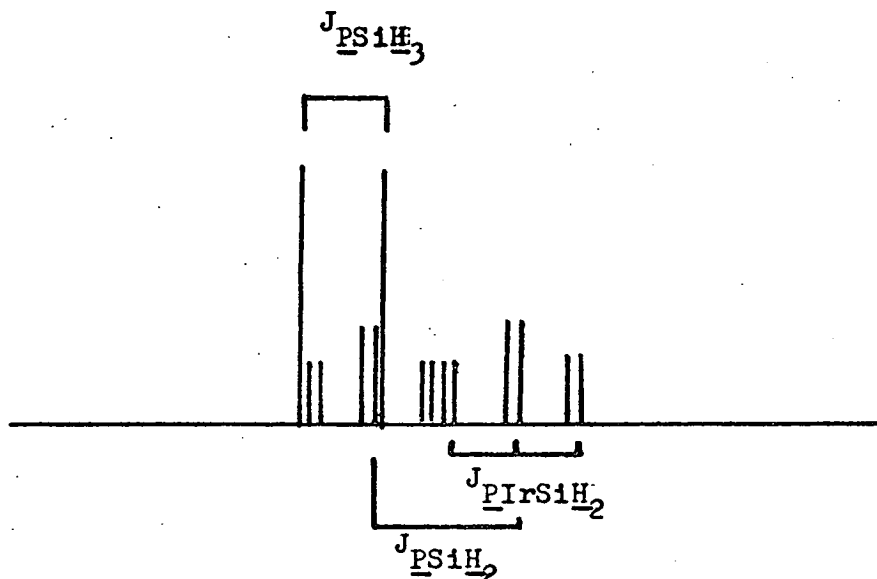
In reactions of  $(\text{SiH}_3)_3\text{P}$  with  $\text{Ir}(\text{CO})\text{I}(\text{PET}_3)_2$ , the products should give phosphorus n.m.r. spectra containing resonances in triethylphosphine and trisilylphosphine regions. A resonance in the triethylphosphine region, when proton decoupled, would

normally be a singlet (see previous chapters), but it is possible that the phosphorus atom of the silylphosphine would couple to the phosphorus atoms of the triethylphosphines to give a doublet splitting on the triethylphosphine resonance. The proton decoupled phosphorus spectrum of  $(\text{SiH}_3)_3\text{P}$  is a singlet. The oxidatively added silylphosphine has the possibility of phosphorus-phosphorus coupling to the phosphorus atoms of the triethylphosphines and, if this occurs, the phosphorus atom of the silylphosphine will give rise to a multiplet in the proton decoupled n.m.r. spectrum. The nature of the multiplet structure would depend on the number of triethylphosphine phosphorus atoms to which the silylphosphine atom was coupled; in the tri-added species, for instance, the silylphosphine phosphorus atom would be coupled to six equivalent phosphorus atoms and would appear as a septet in the proton decoupled phosphorus n.m.r. spectrum.

### 5.1 Reaction of excess $(\text{SiH}_3)_3\text{P}$ with $\text{Ir}(\text{CO})\text{I}(\text{PET}_3)_2$

$\text{Ir}(\text{CO})\text{I}(\text{PET}_3)_2$  was allowed to react with a large excess of  $(\text{SiH}_3)_3\text{P}$  at room temperature using benzene as solvent. The reaction was complete within one minute. The proton n.m.r. spectrum of the benzene solution of the product contained resonances due to four types of protons: those in ethyl groups of a bound triethylphosphine, those bound to silicon atoms which are bound to phosphorus alone ( $\text{P-SiH}_3$ ), those protons which are attached to silicon atoms which are bound to phosphorus and iridium ( $\text{P-SiH}_2\text{-Ir}$ ) and those bound to iridium ( $\text{IrH}$ ). The resonances due to the silyl protons form two sets.

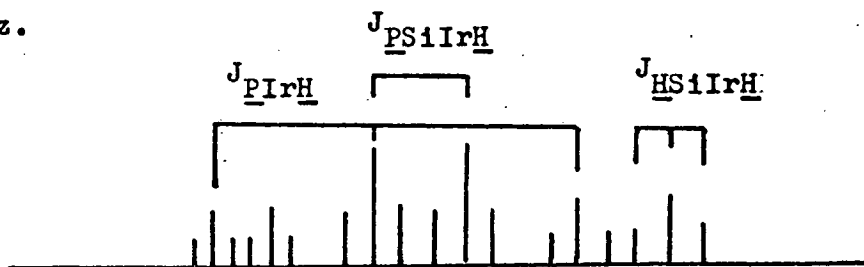
One set is a doublet similar to that for trisilylphosphine itself; the other set is a doublet of triplets of doublets, one half of which is obscured to some extent by one half of the simple doublet.



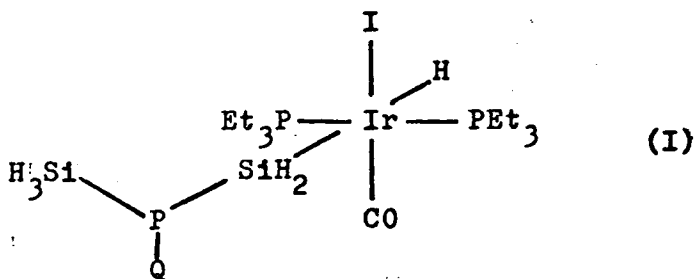
The simple doublet is due to  $-\text{SiH}_3$  bound to a phosphorus atom. The doublet coupling is due to  $J_{\underline{P}\underline{S}i\underline{H}}$ . The doublet of triplets of doublets is due to  $-\text{SiH}_2-$  bound to a metal and a phosphorus atom. The large doublet coupling is due to the phosphorus atom directly bound to the silicon and is collapsed by the same phosphorus frequency as collapses the simple doublet, indicating that the  $-\text{SiH}_3$  and the  $-\text{SiH}_2-$  are bound to the same phosphorus atom, i.e.  $-\text{SiH}_2\text{P}(\text{SiH}_3)_2$  or  $-\text{SiH}_2-\text{P}(\text{SiH}_3)-\text{SiH}_2-$ . The triplet of doublets pattern is similar to those produced by the silyl halides in chapter 2 (see fig. 2a) and is due to an  $-\text{SiH}_2-$  group bound to a metal, trans to a hydride (causing the small doublet splitting) and cis to two mutually trans triethylphosphines (causing the triplet coupling).

The metal hydride resonance is a triplet of doublets of triplets.

viz.



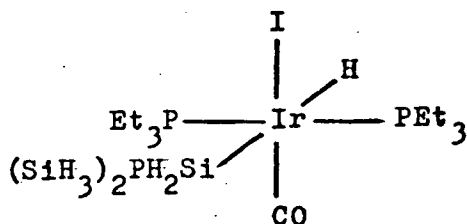
The doublet coupling is due to the silylphosphine phosphorus atom and is decoupled by irradiating at the same chemical shift as that used to decouple the doublet phosphorus couplings to the silyl protons. The much larger triplet coupling is due to the mutually trans triethylphosphines and is collapsed by irradiating at the same chemical shift as that used to decouple the triplet coupling on the silyl proton resonance. The smaller triplet coupling is of the same magnitude as the smaller doublet coupling on the silyl resonance and is probably due to two equivalent silyl protons.  $J_{\text{PSiIrH}}$  is comparable to  $J_{\text{PIrH}}$  despite the fact that it is one bond further from the silylphosphine phosphorus atom to the metal hydride than from the triethylphosphine phosphorus atoms to the metal hydride. This, plus the presence of  $J_{\text{HSiIrH}}$ , suggests that the metal hydride is trans to the  $\text{P-SiH}_2$ - group. To sum up: the evidence from the proton n.m.r. indicates the presence of a compound of the type



Q may be an  $-\text{SiH}_3$  group or an  $-\text{SiH}_2-\text{IrH}(\text{CO})\text{I}(\text{PEt}_3)_2$  group.



The phosphorus n.m.r. spectrum shows a doublet, as predicted, in the triethylphosphine region, when proton decoupled. The trisilylphosphine region contains a triplet, when proton decoupled. The triplet and doublet couplings are of the same magnitude and the triplet coupling on the silylphosphine resonance is probably due to two equivalent triethylphosphine phosphorus atoms. If the molecule contains only two triethylphosphine groups, then the product of the reaction must be



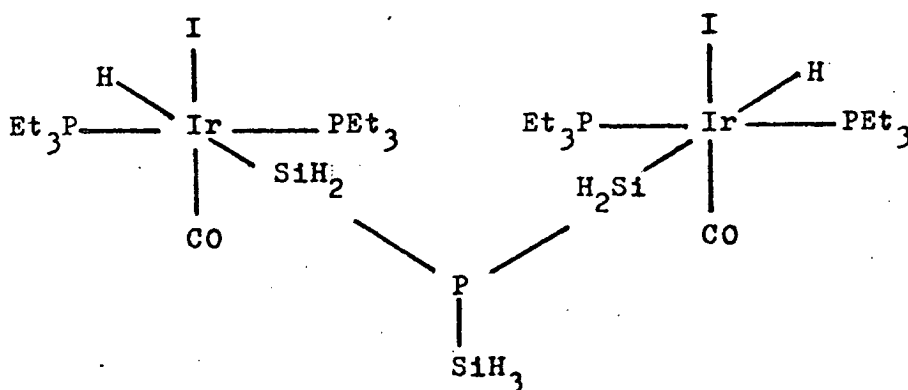
### 5.2 1:2 Reaction of $(\text{SiH}_3)_3\text{P}$ with $\text{Ir}(\text{CO})\text{I}(\text{PEt}_3)_2$

The reaction of  $(\text{SiH}_3)_3\text{P}$  with  $\text{Ir}(\text{CO})\text{I}(\text{PEt}_3)_2$  was also carried out at room temperature in benzene with a two fold excess of  $\text{Ir}(\text{CO})\text{I}(\text{PEt}_3)_2$  in an attempt to prepare a compound with two iridium atoms joined by a silylphosphine bridge.

The proton n.m.r. spectrum of the benzene solution of the product resembled the proton n.m.r. spectrum described in 5.1. It contained resonances of a similar pattern to those described previously, but the chemical shifts of some of the resonances were marginally different and some of the coupling constants varied slightly from the previous n.m.r. spectrum (1st. column c/f 2nd column in table 5/1). It may therefore be assumed that a species of type (I) is also present in this case. The resonance due to  $-\text{SiH}_3$  was less intense with respect to that of the  $-\text{SiH}_2-$  group in this proton n.m.r. spectrum than in the

spectrum outlined in 5.1.

The proton decoupled phosphorus n.m.r. spectrum of the product contains two sets of resonances. The resonance in the triethylphosphine region of the spectrum has a doublet structure, as predicted, due to coupling to the phosphorus atom of the silylphosphine. The resonance due to the phosphorus atom of the silylphosphine has a quintet coupling of the same magnitude as the doublet coupling on the triethylphosphine resonance. The quintet structure is probably due to coupling to four equivalent triethylphosphine phosphorus atoms and this would imply that the molecule contains two  $-\text{SiH}_2-\text{IrH}(\text{CO})\text{I}(\text{PEt}_3)_2$  units and is therefore



### 5.3 1:3 Reaction of $(\text{SiH}_3)_3\text{P}$ with $\text{Ir}(\text{CO})\text{I}(\text{PEt}_3)_2$

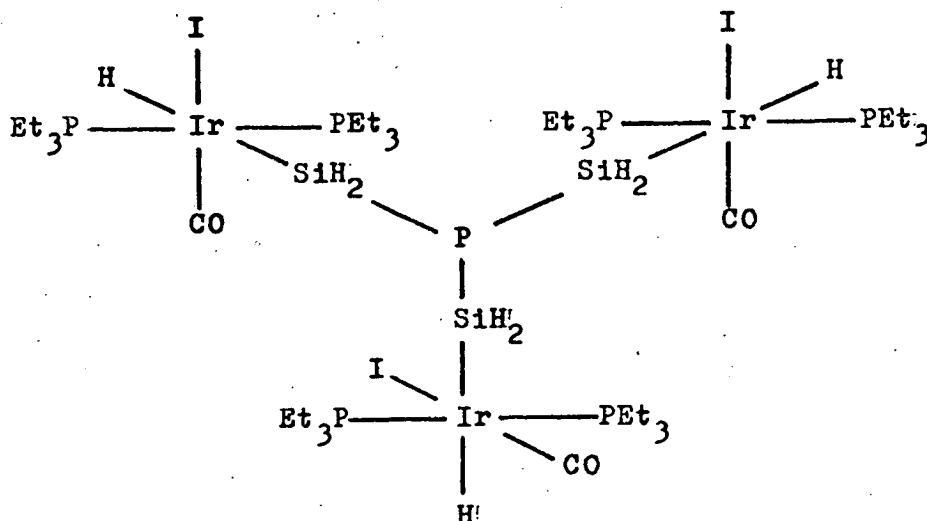
The reaction of  $(\text{SiH}_3)_3\text{P}$  with  $\text{Ir}(\text{CO})\text{I}(\text{PEt}_3)_2$  was also carried out at room temperature in benzene with a three fold excess of  $\text{Ir}(\text{CO})\text{I}(\text{PEt}_3)_2$  in an attempt to prepare a compound with three iridium atoms joined by a common silylphosphine bridge.

The phosphorus n.m.r. spectrum of the product, when proton decoupled, contains a singlet in the triethylphosphine region and a singlet in the silylphosphine region. It would appear

that the phosphorus-phosphorus coupling is too small to be resolved.

The proton n.m.r. spectrum of the product contains three sets of resonances. The resonances in the ethyl region are due to bound triethylphosphine. The resonances in the metal hydride region have a doublet of triplets structure. The doublet coupling is removed by irradiating at the frequency of the singlet in the silylphosphine region of the phosphorus spectrum and the triplet coupling is collapsed by irradiating in the triethylphosphine region of the phosphorus spectrum (both peaks in the phosphorus spectrum belong to the same compound). The absence of  $J_{\text{H}^{\text{Ir}}\text{SiH}}$  (smaller triplet coupling is absent - c/f corresponding peak in 5.1) would suggest that the hydride is not trans to a silyl group, but as  $J_{\text{P}\text{Si}^{\text{Ir}}\text{H}}$  is larger than would be expected for a silylphosphine group cis to a metal hydride and comparable to the analogous couplings in the products described in 5.1 and 5.2, it would therefore be reasonable to assume that, like the products in 5.1 and 5.2, the metal hydrides are trans to the silylphosphine group.

The silyl resonances have a 1:2:2:2:1 quintet structure. Irradiating in the triethylphosphine and silylphosphine regions of the phosphorus spectrum shows this not to be a quintet, but a doublet of triplets. These resonances are due to an  $-\text{SiH}_2-$  group attached to a phosphorus atom (doublet coupling) and to an iridium atom containing two mutually trans triethylphosphines (triplet coupling). The absence of any resonance due to  $-\text{SiH}_3$  indicates that the compound is (next page)



#### 5.4 Conclusions

The data for the spectra outlined in this chapter are tabulated in table 5/1. There are several trends apparent in the data and there are several notable absences of any trend. One such absence is in the chemical shifts which seem to be little influenced by the degree to which the compound is bridged. It would appear that each substituent on the central phosphorus atom is independent of the others and that shifts within a group are essentially the same whether the other groups are silyl or iridium groups. One shift which cannot be independent of the bridging nature of the compound is the phosphorus chemical shift of the central phosphorus atom. This increases by about 40 p.p.m. as the number of iridium groups on the central atom increases. The phosphorus-phosphorus coupling shows no trend, increasing on going from mono-added compound to bis-added compound, but then decreasing on going to the tris-added compound. Other couplings do show a trend, either increasing or decreasing, with increasing number of iridium groups on the central atom, but not always regularly; the largest change generally occurs

between bis-added and tris-added species' values. This is most readily seen when considering  $J_{\text{H}|\text{IrSiH}}$ , which shows a small decrease on going from the mono-added compound to the bis-added compound and a much larger decrease on going to the tris-added compound.

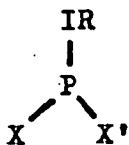
The phosphorus coupling to the  $-\text{SiH}_3$  group ( $J_{\text{PSiH}}$ ) shows only a minor decrease on going from  $(\text{SiH}_3)_3\text{P}$  to  $(\text{SiH}_3)_{3-n}\text{P}(\text{SiH}_2-)_n$  ( $n \neq 3$ ), but in coupling to  $-\text{SiH}_2-$ ,  $J_{\text{PSiH}}$  falls by about 30% ( $J_{\text{PSiH}} = 17.0$  Hz. in  $(\text{SiH}_3)_3\text{P}$ <sup>46</sup>). The addition of a silyl group to the iridium seems to have a large influence on the P-Si bond to the added silyl, but this influence is not apparently transmitted to other P-Si bonds in the molecule.

It is interesting to note that the addition of  $(\text{SiH}_3)_3\text{P}$  to one molecule of  $\text{Ir}(\text{CO})\text{I}(\text{PET}_3)_2$  results in a change of  $^{31}\text{P}$  chemical shift of the silylphosphine phosphorus atom of about 35 p.p.m. ( $^{31}\text{P}$  chemical shift of  $(\text{SiH}_3)_3\text{P}$  is  $-378$  p.p.m.<sup>48</sup>) and that each successive addition of the species to  $\text{Ir}(\text{CO})\text{I}(\text{PET}_3)_2$  results in a further change in shift of about 35 p.p.m. Compare this to the change in  $^{31}\text{P}$  chemical shift of free triethylphosphine ( $-20$  p.p.m.) on co-ordinating to iridium to form  $\text{Ir}(\text{CO})\text{I}(\text{PET}_3)_2$  ( $20$  p.p.m.), which is  $40$  p.p.m. The similarity, in magnitude and in direction (both shift to high frequency), of these chemical shifts is surprising as the phosphorus atom is associating with the metal in two quite different ways. When triethylphosphine binds to a metal, it does so by contributing its lone pair of electrons into the molecular orbitals of the metal system. Its co-ordination number changes and so a large change in chemical shift is

expected. For  $(\text{SiH}_3)_3\text{P}$ , association with  $\text{Ir}(\text{CO})\text{I}(\text{PEt}_3)_2$  entails a change in the molecule which is remote, by comparison with the triethylphosphine case, from the phosphorus atom and does not obviously influence the lone pair on the phosphorus atom. Yet association of  $(\text{SiH}_3)_3\text{P}$  with iridium affects the chemical shift of the phosphorus atom of the silylphosphine as much as it affects the phosphorus atom of triethylphosphine.

In a reaction where  $(\text{SiH}_3)_3\text{P}$  was treated with a vast excess of  $\text{Ir}(\text{CO})\text{I}(\text{PEt}_3)_2$ ,  $\text{Ir}(\text{CO})\text{I}(\text{PEt}_3)_2$  co-existed in solution with  $(\text{IrH}(\text{CO})\text{I}(\text{PEt}_3)_2\text{SiH}_2)_3\text{P}$  and no other species were formed. It is clear that oxidative addition to iridium does not increase the basicity of trisilylphosphine to the level where it is capable of displacing triethylphosphine and co-ordinating to iridium via its lone pair of electrons.

The reactions outlined above contrast with those of  $(\text{SiH}_3)_3\text{P}$  with  $\text{trans-PtHI}(\text{PEt}_3)_2$ <sup>48</sup>. The absence of the metal hydride in  $\text{Ir}(\text{CO})\text{I}(\text{PEt}_3)_2$  avoids an alternative reaction found in the  $\text{trans-PtHI}(\text{PEt}_3)_2$  case in which exchange between  $-\text{SiH}_3$  on phosphorus and  $\text{PtH}$  gives  $\text{PtI}(\text{PEt}_3)_2\text{SiH}_3$ ,  $(\text{SiH}_3)_2\text{PH}$ ,  $(\text{SiH}_3)\text{PH}_2$  and  $\text{PH}_3$ .  $(\text{PtI}(\text{PEt}_3)_2\text{SiH}_2)\text{P}(\text{SiH}_3)_2$  and  $(\text{PtI}(\text{PEt}_3)_2\text{SiH}_2)_2\text{PSiH}_3$  were formed but not  $(\text{PtI}(\text{PEt}_3)_2\text{SiH}_2)_3\text{P}$ . The absence of the last named species was explained in terms of steric hindrance: three  $(\text{PtI}(\text{PEt}_3)_2\text{SiH}_2)-$  could not fit onto one phosphorus atom as they were too bulky. However, there is no reason to believe that  $(\text{IrH}(\text{CO})\text{I}(\text{PEt}_3)_2\text{SiH}_2)-$  is any less bulky than  $(\text{PtI}(\text{PEt}_3)_2\text{SiH}_2)-$  and it is likely that there may be other factors influencing the Pt case.

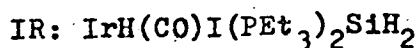


X	SiH <sub>3</sub>	IR	IR
X'	SiH <sub>3</sub>	SiH <sub>3</sub>	IR
a:b	>1:1	1:2	1:3
SiH <sub>2</sub>	3.9d/t/d	4.1t/d/t	4.2d/t
SiH <sub>3</sub>	4.1 d	4.2 d	-
IrH	-10.0t/d/t	-9.8t/d/t	-9.7t/d
J <sub>HSiPSiH</sub>	0	0	-
J <sub>PSiH<sub>3</sub></sub>	16.0	15.7	-
J <sub>PSiH<sub>2</sub></sub>	not obs. see text	10.4	12.0
J <sub>PSiIrH</sub>	7.5	7.9	10
J <sub>PIrSiPSiH</sub>	0	0	-
J <sub>PIrSiH</sub>	7.0	6.3	6.0
J <sub>PIrH</sub>	15.5	15.6	17
J <sub>HIrSiPSiH</sub>	0	0	-
J <sub>HIrSiH</sub>	2.8	1.8	0.0
PEt <sub>3</sub>	-16	-17	-18
PEt <sub>3</sub>	-16.9 d	-17.6 d	-19.0 s
P(SiH <sub>3</sub> ) <sub>n</sub> (SiH <sub>2</sub> ) <sub>3-n</sub>	-342	-298	-257
P(SiH <sub>3</sub> ) <sub>n</sub> (SiH <sub>2</sub> ) <sub>3-n</sub>	-343.7 t	-299.1quin	+259.0 s
J <sub>PSiIrP</sub>	0.6	1.2	0

Table 5/1



Units and abbreviations: (see table 1/1) quin:quintet



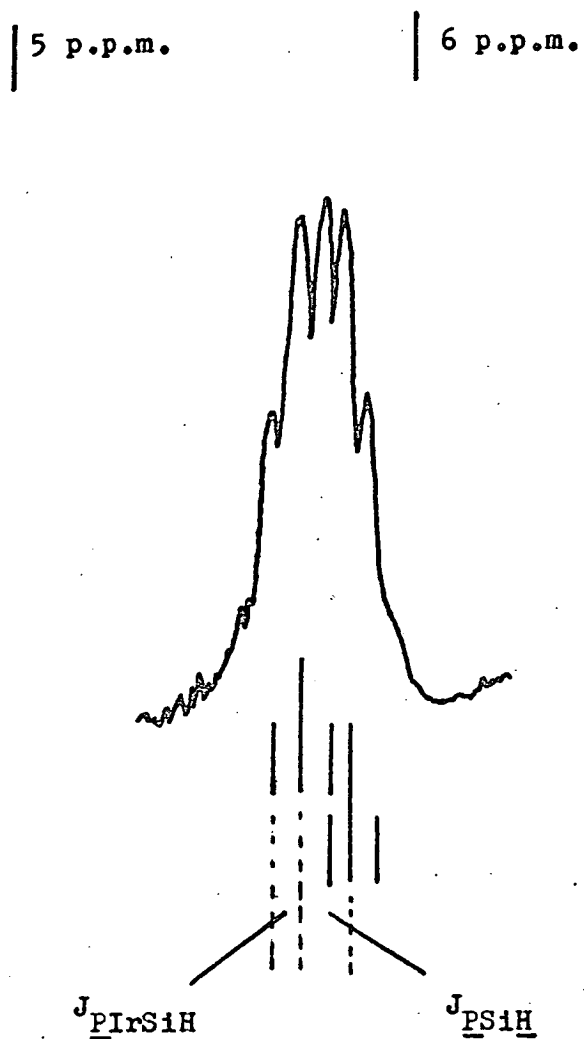


Figure 5a. Quintet due to silyl protons occurs  
because  $J_{\text{P}SiH}$  is twice  $J_{\text{P}i\text{R}SiH}$ .



**Appendices to Part One**

Apendices to Part One(a) Reactions of  $\text{Ir}(\text{CO})\text{Cl}(\text{PEt}_3)_2$  with  $\text{H}_2\text{Z}$  Z:S,Se

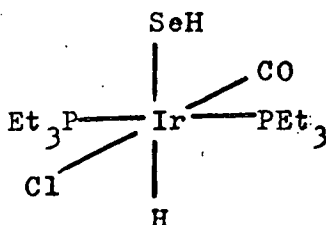
The reaction between  $\text{Ir}(\text{CO})\text{Cl}(\text{PEt}_3)_2$  and  $\text{H}_2\text{S}$  was carried out at room temperature in benzene. Reaction was immediate, giving an emerald green solution. The proton n.m.r. spectrum of the green solution contained only resonances due to bound triethylphosphine and it must be supposed that any protons originating from  $\text{H}_2\text{S}$  must give rise to resonances which are obscured by the triethylphosphine resonances. There are no resonances which could be assigned to a hydride bound to iridium. The phosphorus n.m.r. spectrum indicates that there are five species present in the solution, with mutually trans phosphines. When proton decoupled these give rise to singlet resonances at, in order of highest concentration first, 10.5 p.p.m., 6.3 p.p.m., -6.5 p.p.m., -9.5 p.p.m. and -10.6 p.p.m.. The reaction is obviously not a simple oxidative addition. From the phosphorus chemical shifts in the spectrum, it would seem that both Ir(I) and Ir(III) species are formed during the reaction and two species (those giving rise to resonances at 6.3 p.p.m. and -6.5 p.p.m.) which cannot be defined, with any confidence, to be Ir(I) or Ir(III).

It would appear that the influence of the triethylphosphine is significant in this reaction as in the analogous reaction with  $\text{Ir}(\text{CO})\text{Cl}(\text{PPh}_3)_2$ , the product is reported to be  $\text{IrH}(\text{CO})\text{Cl}(\text{PPh}_3)_2\text{SH}$  resulting from a simple oxidative addition.<sup>51</sup>

The room temperature reaction of  $\text{Ir}(\text{CO})\text{Cl}(\text{PEt}_3)_2$  with  $\text{H}_2\text{Se}$  in benzene yielded a pale amber solution. The phosphorus n.m.r. spectrum of the amber solution contained a singlet, when proton decoupled, with selenium satellites (-12.9 p.p.m.,  $J_{\text{SeIrP}}:8.2 \text{ Hz.}$ ),

indicating that the phosphines are mutually trans and that the selenium is part of the metal complex. The proton n.m.r. spectrum contained three sets of resonances: a complex multiplet due to triethylphosphine bound to a metal, a quartet at -4.1 p.p.m. (an area associated with a proton bound to selenium, although the resonance was not sufficiently strong to observe selenium satellites) and a triplet of doublets at -17.0 p.p.m. (a region associated with a hydride bound to iridium). Phosphorus decoupling changed both the quartet and triplet of doublets to doublets with splittings of the same magnitude and this splitting is thought to arise from a single proton on the selenium and a single hydride on the iridium coupling with each other ( $J_{\text{HIrSeH}}$  is 1.4 Hz.). The triplet coupling to the  $\text{IrH}$  comes from the two phosphorus atoms of the phosphines ( $J_{\text{PIrH}}$ : 12.2 Hz.) and it would appear that the quartet is, in fact, a triplet (due to phosphorus couplings) of doublets (due to a hydride coupling) with both couplings of the same magnitude ( $J_{\text{PIrSeH}}$ : 1.4 Hz.).

By comparison with  $\text{IrH}$  and phosphorus couplings to  $\text{SiH}$  and  $\text{GeH}$  outlined in chapter 2,  $J_{\text{HIrSeH}}$  is extremely large when compared to  $J_{\text{PIrSeH}}$  and this would lead to the conclusion that  $\text{IrH}$  is trans to  $\text{HSe-}$  and that the isomer produced has mutually trans phosphines, carbonyl trans to chloride and hydride trans to  $-\text{SeH}$ : viz.

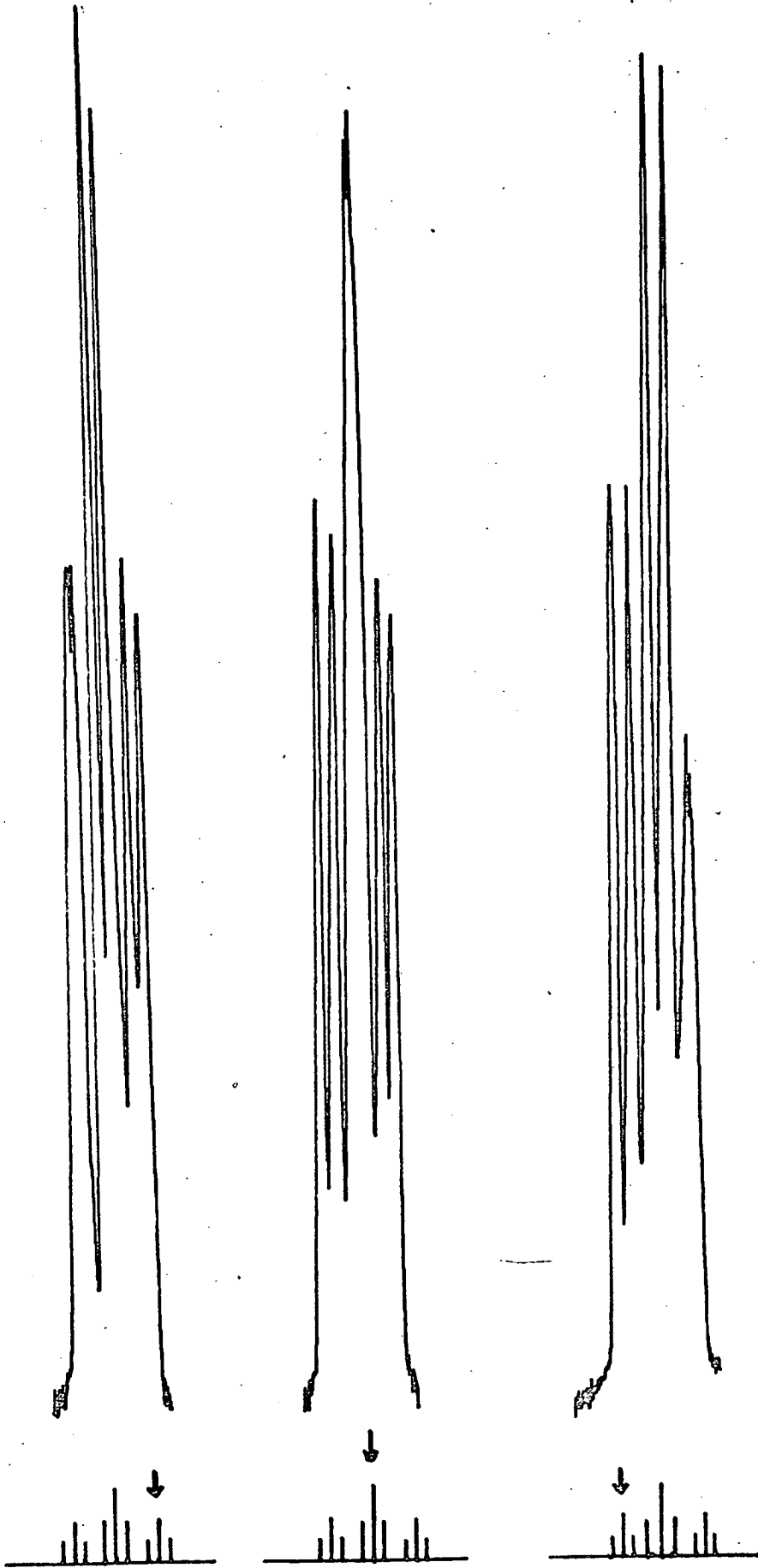


However, in the absence of comparable data from known isomers of this type containing selenium, or an element known to conduct couplings in a similar manner to selenium, such an assignment can only be tentative.

(b) Homonuclear Decoupling Experiment on  $\text{IrH}(\text{CO})\text{I}(\text{PEt}_3)_2\text{SiH}_2\text{Br}$

At a late stage in the work the HA100 n.m.r. spectrometer was modified to allow homonuclear spin decoupling, of  $\text{IrH}$  from  $\text{SiH}$ , to be achieved and several  $J_{\text{HirSiH}}$  couplings were confirmed. Illustrated overleaf is a particularly successful experiment carried out on the compound  $\text{IrH}(\text{CO})\text{I}(\text{PEt}_3)_2\text{SiH}_2\text{Br}$ . Three copies of the  $\text{SiH}$  resonance of this compound (normally triplet of doublets) are shown overleaf and under each resonance is a schematic representation of the  $\text{IrH}$  resonance. Each representation includes an arrow which marks the centre of the irradiating frequency when the resonance above it was recorded.

Not only is  $J_{\text{HirSiH}}$  confirmed, but also it is clear that  $J_{\text{PirH}}$  is, as expected, of opposite in sign to  $J_{\text{PirSiH}}$ .



(c) 2:1 Molar Reaction of  $\text{SiH}_4$  with  $\text{Ir}(\text{CO})\text{Cl}(\text{PEt}_3)_2$

The introduction included a report that the reaction of two moles of  $\text{R}_3\text{SiH}$  with one mole of  $\text{Ir}(\text{CO})\text{Cl}(\text{PPh}_3)_2$  resulted in the formation of the dihydride  $\text{IrH}_2(\text{CO})(\text{PPh}_3)_2\text{SiR}_3$ . An analogous reaction was attempted with  $\text{SiH}_4$  and  $\text{Ir}(\text{CO})\text{Cl}(\text{PEt}_3)_2$  in benzene at room temperature. The proton n.m.r. spectrum contained evidence of excess  $\text{SiH}_4$  and  $\text{IrH}(\text{CO})\text{Cl}(\text{PEt}_3)_2\text{SiH}_3$  in the reacted mixture, but even on standing at room temperature for several days, no evidence was found for a dihydride iridium species.

PART TWO

CHAPTER 6

Reactions of  $\text{SiH}_3\text{X}$  and  $\text{GeH}_4$  (X:H,Cl,I, $\text{CH}_3$ , $\text{SiH}_3$ )

as well as with  $\text{Et}_3\text{PAuX}$  (X:Cl,I, $\text{CH}_3$ ) and

$(\text{Et}_2\text{P}(\text{CH}_2)_2)_2\text{Au}_2$

## 6 Introduction to Gold Work

At the beginning of 1.1 it was stated that for simple oxidative addition to occur, a system must be capable of undergoing a decrease in d electron configuration of two and supporting an increase of two in co-ordination number. Inspection of the table of d electron configurations and associated co-ordination numbers, given in 1.1, will reveal that another possible candidate for simple oxidative addition is the two co-ordinate  $d^{10}$  system, which, on oxidative addition would go to a four co-ordinate  $d^8$  system.

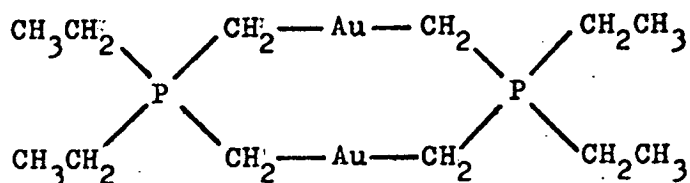
The aim of this section of the work was to extend the oxidative addition reactions of silyl compounds beyond the platinum metals. For this reason the coinage metals (Cu, Ag, Au) and in particular, gold was thought to be the most promising as it has a stable oxidation state of three, but has many compounds in which it has the formal oxidation state Au(I).

The compound  $\text{Et}_3\text{PAuCl}$  was chosen because the formal oxidation state of the metal is Au(I) and it contained a phosphine. It is generally accepted that, in the case of platinum metals, phosphines tend to stabilise higher oxidation states and it was hoped that triethylphosphine would act in a similar manner with gold compounds.  $\text{Et}_3\text{PAuCl}$  has been reported to add halogens  $\text{X}_2$  and  $\text{XY}$  (X and Y : Cl, Br, I) oxidatively to form square planar compounds  $\text{Et}_3\text{PAuXYCl}$ <sup>49</sup>, but has not been reported to add  $\text{CH}_3\text{I}$ . Platinum metal complexes which are capable of adding silyl compounds are generally capable of adding  $\text{CH}_3\text{I}$ .

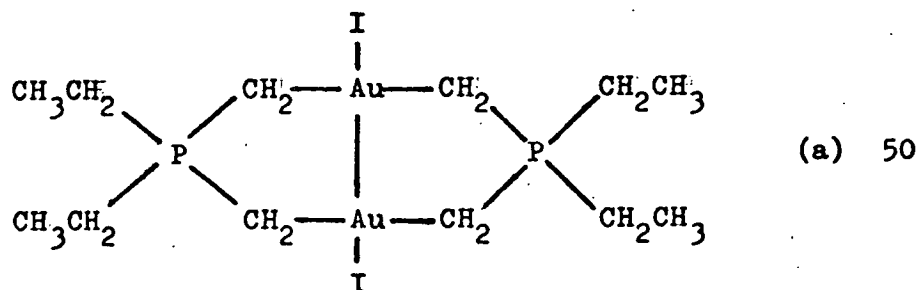
The other compound which was tested for its ability to participate in oxidative addition reactions with silyl compounds



was  $(\text{Et}_2\text{P}(\text{CH}_2)_2)_2\text{Au}_2$  viz.



which is prepared from  $\text{Et}_3\text{PAuCl}$  and a compound of the type discussed in chapter 8 (see chapter 8).  $(\text{Et}_2\text{P}(\text{CH}_2)_2)_2\text{Au}_2$  has been reported to add  $\text{I}_2$  to form



$(\text{Et}_2\text{P}(\text{CH}_2)_2)_2\text{Au}_2$  also passes the shibboleth of  $\text{CH}_3\text{I}$  addition, being able to add  $\text{CH}_3\text{I}$  across one or both Au atoms, culminating, in the case where two molecules of  $\text{CH}_3\text{I}$  have been added, in the elimination of ethane to give compound (a) <sup>51</sup>.  $(\text{Et}_2\text{P}(\text{CH}_2)_2)_2\text{Au}_2$  was thought to be a very promising candidate for similar reactions involving analogous silicon compounds.

The results of reactions involving  $\text{Et}_3\text{PAuCl}$  and  $(\text{Et}_2\text{P}(\text{CH}_2)_2)_2\text{Au}_2$  are contained in the following sections.

### 6.1 Reactions between $\text{Et}_3\text{PAuCl}$ and Group IVb hydrides and halides.

Equimolar amounts of  $\text{Et}_3\text{PAuCl}$  and  $\text{CH}_3\text{I}$  or  $\text{SiH}_4$  or  $\text{GeH}_4$  were dissolved in toluene or dichloromethane and the proton n.m.r. spectrum was observed over the range  $-60$  to  $50^\circ\text{C}$ , but no reaction occurred and the presence of starting materials was verified by proton n.m.r. and by infra-red spectroscopy.

The equimolar combination of  $\text{Et}_3\text{PAuCl}$  and  $\text{SiH}_3\text{Cl}$  in toluene at room temperature resulted in the production of equimolar amounts of  $\text{SiH}_4$  and  $\text{SiH}_2\text{Cl}_2$ . The phosphorus n.m.r. spectrum indicated that  $\text{Et}_3\text{PAuCl}$  was not consumed during the reaction and could only be acting as a catalyst for the reaction. However, further experiments with  $\text{Et}_3\text{P}$  alone gave a similar result with  $\text{SiH}_3\text{Cl}$ , proving that the gold is not significantly involved in the reaction, which appears to be a base catalysed disproportionation due to trace amounts of  $\text{Et}_3\text{P}$  produced by slight dissociation of  $\text{Et}_3\text{PAuCl}$  or present as a trace impurity.  $\text{SiH}_4$  and  $\text{SiH}_2\text{Cl}_2$  were identified by n.m.r. and infra-red spectroscopy.

Equimolar combination of  $\text{Et}_3\text{PAuCl}$  and  $\text{SiH}_3\text{I}$  in toluene at  $-30^\circ\text{C}$  yielded equimolar amounts of  $\text{Et}_3\text{PAuI}$  and  $\text{SiH}_3\text{Cl}$ . By means of this simple exchange reaction, it was hoped to facilitate oxidative addition of  $\text{SiH}_3\text{Cl}$  by placing a more electron releasing halide on the gold. However, the only subsequent reaction on warming to higher temperatures was a base catalysed disproportionation of the type outlined above.

The chloride in  $\text{Et}_3\text{PAuCl}$  was replaced to give  $\text{Et}_3\text{PAuCH}_3$ , using  $\text{MeLi}^{52}$ , in the hope that the more electron releasing methyl group would permit oxidative addition to occur, but no reaction was observed with  $\text{SiH}_4$  in toluene over the range  $-50 - 50^\circ\text{C}$ .

The first reaction to the lack of oxidative additions by these group IVb species is to conclude that they do not have sufficient oxidising properties to convert  $\text{Au(I)}$  to  $\text{Au(III)}$ , but further evidence produced in the following sections suggests that the reason for the lack of reactivity may be also due to other factors and the results of this section are discussed in the next section.

## 6.2 Reactions between $\text{Et}_3\text{PAuX}$ ( $\text{X:Cl,I}$ ) and $\text{SiH}_3\text{MH}_3$ ( $\text{M:C,Si}$ )

No reaction was observed between  $\text{Et}_3\text{PAuCl}$  and  $\text{SiH}_3\text{CH}_3$  in toluene over the range  $-60$  to  $70^\circ\text{C}$ .

The reaction between  $\text{Et}_3\text{PAuCl}$  and  $\text{Si}_2\text{H}_6$  in toluene is rapid at room temperature and complete within five minutes. The reaction produces  $\text{H}_2$ ,  $\text{SiH}_4$ , some elemental gold, a black oil and several other unidentified products. However, at  $-10^\circ\text{C}$ , the equimolar reaction between  $\text{Et}_3\text{PAuCl}$  and  $\text{Si}_2\text{H}_6$  occurs much more slowly and requires over 30 minutes to go to completion in toluene. Over the period of half an hour the peak, in the proton n.m.r., due to  $\text{Si}_2\text{H}_6$  (distinctive because of its silicon satellites which take the form of quartets) decreases and is replaced by a peak due to  $\text{SiH}_4$  (silicon satellites for this compound are singlets).  $\text{SiH}_4$  was confirmed, by infra-red spectroscopy, to be the only volatile product and was produced in the same quantity as the  $\text{Si}_2\text{H}_6$  reacted. There were no non-condensable products produced. The phosphorus n.m.r. indicates that  $\text{Et}_3\text{PAuCl}$  is consumed during the reaction and no peak appears to replace the  $\text{Et}_3\text{PAuCl}$  peak. The reaction produces a two phase system in which the heavier phase is composed of a black oil and the lighter phase consists of  $\text{SiH}_4$  dissolved in toluene.

When combined under the same conditions,  $\text{Et}_3\text{P}$  and  $\text{Si}_2\text{H}_6$  show no reaction, therefore any effect due to the basic character of  $\text{Et}_3\text{P}$  may be ruled out.

On removing the solvent and  $\text{SiH}_4$ , the lower phase proved to be an intractable gum. If the lighter phase contains only  $\text{SiH}_4$ , the remainder of the reaction mixture must be contained in the gum, but the manner in which the components of the gum are

combined is not known.

The production of silane must involve the breaking of the silicon-silicon bond in disilane and this could occur in several ways. An oxidative addition to  $\text{Et}_3\text{PAuCl}$  may occur, breaking an Si-H bond and producing a Au(III) hydride compound. The hydride compound could be unstable and react with disilane in solution to form silane and  $\text{Et}_3\text{PAu}(\text{SiH}_2\text{SiH}_3)(\text{SiH}_3)\text{Cl}$ , but this would not produce one mole of silane for every mole of  $\text{Si}_2\text{H}_6$ . Also addition across Si-H bonds in the previous section, even with compounds which would be expected to have better oxidising properties than  $\text{Si}_2\text{H}_6$ , do not occur. The most fundamental difference between  $\text{Si}_2\text{H}_6$  and the other molecules is the Si-Si bond and it is likely that this plays a role in the reaction. Oxidative addition to  $\text{Et}_3\text{PAuCl}$  could involve breaking the Si-Si bond to produce  $\text{Et}_3\text{PAu}(\text{SiH}_3)_2\text{Cl}$ . Although compounds of the type  $\text{Et}_3\text{PAuSiR}_3$  ( $\text{R} \neq \text{H}$ ) are well known, silyl-Au(III) bonds are not well documented and may well be unstable.  $\text{Et}_3\text{PAu}(\text{SiH}_3)_2\text{Cl}$  may react with other molecules of the same type or with disilane to produce silane and silyl polymer. Such a reaction would not consume  $\text{Et}_3\text{PAuCl}$  which must therefore be somehow incorporated into the silyl polymer to form the black gum.

If  $\text{Si}_2\text{H}_6$  is capable of oxidising Au(I) to Au(III), it cannot be a simple lack of oxidising power which prevents  $\text{SiH}_3\text{X}$  from doing likewise. It would seem that other factors may well operate such as a kinetic block for oxidation across Si-H bonds.

### 6.3 Reaction between $(Et_2P(CH_2)_2)_2Au_2$ and $SiH_3I$

In the light of reported reactions between  $(Et_2P(CH_2)_2)_2Au_2$  and  $CH_3I$ , analogous reactions were attempted with  $SiH_3I$ . The reactions were allowed to happen at low temperatures in toluene with 2:1 and 1:1 molar ratios of  $(Et_2P(CH_2)_2)_2Au_2$  and  $SiH_3I$  and the resulting reactions were observed by n.m.r. over the range of  $-80^\circ C$  to  $30^\circ C$ .

With the 2:1 molar ratio, the proton n.m.r. at  $-80^\circ C$  contained two peaks which could be attributed to protons on a silicon atom. One of the peaks was due to protons in the compound  $SiH_3I$  and the other peak (4.1 p.p.m.) was due to an unknown species. On raising the temperature, both peaks broadened and coalesced to give a broad peak (3.1 p.p.m.) at  $-20^\circ C$ . At this temperature peaks due to  $SiH_4$  and  $H_2$  became apparent. Cooling the system at this stage gave the initial two  $SiH$  peaks at  $-80^\circ C$ , but on warming above  $20^\circ C$ , the peak at 3.2 p.p.m. rapidly diminished, the peaks due to  $SiH_4$  and  $H_2$  grew in relative intensity and the reaction could not be reversed by cooling.

The reaction with a 1:1 molar ratio gave a similar result except that the peak due to  $SiH_3I$  was absent at low temperatures. The peak at 4.1 p.p.m. broadened on raising the temperature and at its broadest (at  $0^\circ C$ ) was centred about 3.4 p.p.m.. At  $0^\circ C$  a peak due to  $H_2$  was evident, but there was no peak due to  $SiH_4$  visible. On warming to  $20^\circ C$ , the broad peak sharpened to some extent at 3.2 p.p.m., but not to the extent observed in the 2:1 case and the reaction could be reversed to give the original peak at  $-80^\circ C$ . Above  $20^\circ C$ , the unknown peak disappeared and was replaced by peaks due to  $H_2$  and  $SiH_4$ . the reaction at high

temperatures was irreversible.

Resonances due to the protons in the ligand  $(\text{Et}_2\text{P}(\text{CH}_2)_2)_2$  were apparent throughout the 1:1 reaction, but are lost above  $20^\circ\text{C}$  in the 2:1 reaction and at no time in any reaction were resonances, which could be attributed to a hydride directly bound to gold, observed.

The phosphorus n.m.r. spectrum of the 1:1 reaction contains a sharp peak at 40.5 p.p.m. at  $-80^\circ\text{C}$  which broadens on warming to give, at its broadest, a peak centred at 41.7 p.p.m. at  $0^\circ\text{C}$ . At  $20^\circ\text{C}$  the peak sharpens and is centred about 42.2 p.p.m. On cooling, the original peak at  $-80^\circ\text{C}$  is observed. Above  $20^\circ\text{C}$ , the peak sharpens further and is comparable in line width to the peak observed at  $-80^\circ\text{C}$ . However on cooling the peak does not alter position and remains at 42.8 p.p.m., which is the observed shift for  $(\text{Et}_2\text{P}(\text{CH}_2)_2)_2\text{Au}_2$ .

At  $-80^\circ\text{C}$  the solution in the n.m.r. tube is green. On warming, the colour fades slightly and above  $20^\circ\text{C}$  the solution becomes colourless and a black oil is deposited in globules on the side of the tube.

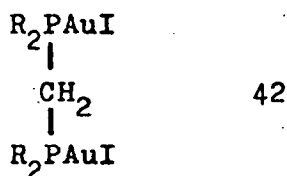
The phenomena outlined above are most readily interpreted in terms of an association between  $\text{SiH}_3\text{I}$  and  $(\text{Et}_2\text{P}(\text{CH}_2)_2)_2\text{Au}_2$  at low temperatures. Comparison of the proton spectra of the 2:1 reaction with those of the 1:1 reaction indicates that only one molecule of  $\text{SiH}_3\text{I}$  associates with each molecule of  $(\text{Et}_2\text{P}(\text{CH}_2)_2)_2\text{Au}_2$ . The exact nature of the association is uncertain, but as only a marginal chemical shift change occurs in the phosphorus spectrum between free  $(\text{Et}_2\text{P}(\text{CH}_2)_2)_2\text{Au}_2$  and the associated species, it is unlikely to involve the phosphorus atoms directly. Also, as



At  $-80^{\circ}\text{C}$ , the equilibrium on the previous page would tend towards (A) or (B), but at  $20^{\circ}\text{C}$  the equilibrium would favour  $\text{SiH}_3\text{I}$  and  $(\text{Et}_2\text{P}(\text{CH}_2)_2)_2\text{Au}_2$ .

At temperatures above  $20^{\circ}\text{C}$ , it is possible that silyl addition as Si-H begins to occur, leading to an unstable gold intermediate which decomposes to give  $\text{H}_2$  and  $\text{SiH}_4$  and the black oil. As all of the gold starting material is lost in the 2:1 reaction, but not in the 1:1 reaction, the reaction at high temperatures must involve two molecules of  $\text{SiH}_3\text{I}$  per gold molecule.

Recent work <sup>53</sup> has shown that compounds of the type



are capable of oxidatively adding  $\text{I}_2$  and  $\text{CH}_3\text{I}$ . These compounds are closely related to the compounds studied in 6.1 and 6.2 and it is strange that these binuclear compounds should be capable of adding  $\text{CH}_3\text{I}$ , but the mono-nuclear compounds should not.

It is clear that the ability of gold compounds to undergo oxidative addition is not only influenced by the nature of the ylide ligand, but is also promoted, in some mysterious way, by the presence of two gold atoms in the same molecule. It is likely that these binuclear compounds will also react with silyl compounds and such reactions may be worth investigating in the future.



PART THREE

CHAPTER 7

Introduction to Methods and Terms  
used in the Electron Diffraction  
Structure Determinations

## 7 Introduction to Electron Diffraction Methods

An electron diffraction apparatus consists essentially of three components: an electron beam source; a photographic plate, which can be placed at various distances from the electron source, in order to collect the electrons, each of which registers as a dark spot on the plate, and a nozzle, which allows gaseous compounds to be passed directly in front of the electron beam source. The pattern produced on the plate is circular, centred at the point on the plate at which the electrons strike the plate at right angles to the plate itself. The intensity data are recorded as a function of  $s$ , where  $s$  is  $(4\pi\sin\theta)/\lambda$  ( $\lambda$  is the wavelength of the electrons and  $\theta$  is the angle subtended at the beam source by the point on the plate and the centre of the plate).

The pattern produced on the plate arises from several factors: atomic scattering (coherent and incoherent) from atoms in the compound being passed in front of the beam, extraneous scattering due to the apparatus and molecular scattering, arising from the pairs of atoms within the molecules of the compound. Each pair of atoms gives a sine wave intensity pattern, the frequency of which depends on the interatomic distance.

Patterns are recorded on plates at usually two or three distances from the beam source (these are referred to as "camera heights") and sets of data are collected by scanning diameters of the circular patterns produced with a microdensitometer, which converts the variation in intensity into numerical form for use on a computer. More than one plate is often exposed at a particular camera height and several sets of data may be collected from a single plate.

On the computer, programs are used which centre and combine sets of data collected at the same camera height, make corrections for emulsion response and planarity of plates and make an adjustment for the shape of the sector which is a device used, during the exposure, to ensure a more uniform exposure of the plate. After subtraction of atomic scattering, the general form of the contribution from extraneous scattering can often be subtracted from the data (the apparatus used in the following structure determinations produces extraneous scattering of an overall form which approximates to a cubic function) leaving the molecular diffraction pattern, incoherent atomic scattering and remaining extraneous scattering. A visual display of the data collected at each camera height enables the background scattering, which is superimposed on the molecular diffraction pattern, to be assessed and subtracted. This process is known as "subtracting a background". At this stage, the data has been processed to the point where comparisons can be made with predicted data.

The programs which predict data from each camera height use a mathematical model in their calculations. The model uses a limited number of refineable parameters, usually bond lengths and angles, to define the positions of all atoms within the molecule and, from these, all, or as many as the programs can cope with, of the inter-atomic distances are calculated and used to produce the predicted data by means of the equation

$$I_{\text{calc}}(s) = k_m \sum_{i,j} G_{ij} \text{Sin} \left[ s(r_{ij} - K_{ij}s^2) \right] \exp(-u_{ij}^2 s^2 / 2) / sr_{ij}$$

where  $k_m$  is a refineable scale factor operating on data set  $m$  (data collected at a particular camera height),  $G_{ij}$  is a term derived from the scattering amplitudes and phase shift parameters for atoms  $i$  and  $j$ ;  $r_{ij}$ ,  $u_{ij}$  and  $K_{ij}$  are the inter-atomic distance, amplitude of vibration and anharmonicity for atoms  $i$  and  $j$  ( $K = (a_{ij}u_{ij}^4)/6$ ;  $a_{ij}$  is an asymmetry parameter which is set at  $2 \text{ \AA}^{-1}$  for bonded distances and zero for non-bonded distances). Usually one or two parameters are refined initially and then the number of parameters simultaneously refined is increased. The number of parameters with which a program can cope at the same time depends on the design of the program itself and ultimately on the computer as a point is reached where computing time becomes excessive. If changes in a particular parameter do not make a significant impact on the comparison between predicted and observed data, the parameter will not refine satisfactorily and it must be varied periodically over a range of values and the effect on the match between observed and predicted data monitored (this process is referred to in the text as an R-factor loop). Backgrounds are subtracted throughout the refinement, when they become apparent.

Data comparison is quantified by the R-factor. The observed and predicted data for each camera height are composed of  $n$  intensities distributed at regular  $s$ -unit intervals. The difference in observed and predicted intensity at  $s$ -unit  $s_1$  is  $d_1$  and the vector of these differences is labelled  $\underline{D}$ .

To calculate the R-factor, another matrix is required; the  $\underline{W}$  matrix. This makes use of the weighting points  $s_1$  and  $s_2$  which are particular values of  $s_1$  and are usually chosen to be

towards the maximum and minimum values of  $s$ . Selection of  $s_1$  and  $s_2$  depends on the quality of the data.  $s_1$  and  $s_2$  operate with  $s_0$  and  $s_n$  (which may also be chosen on the basis of data quality) to make up the elements of the two dimensional  $\underline{W}$  matrix in the following way.

- (a)  $w_{ii} = (s_i - s_0)/(s_1 - s_0)$  if  $s_0 \leq s_i \leq s_1$
- (b)  $w_{ii} = 1$  if  $s_1 \leq s_i \leq s_2$
- (c)  $w_{ii} = (s_n - s_i)/(s_n - s_2)$  if  $s_2 \leq s_i \leq s_n$
- (d)  $w_{ij} = 0$
- (e)  $w_{ij} = -0.5(w_{ii} - w_{jj})p/h$  if  $i = j \pm 1$

The R-factor is defined as  $(\underline{D}'\underline{W}\underline{D}/\underline{I}'\underline{W}\underline{I})^{1/2}$ , where  $\underline{I}$  is the intensity vector similar to the difference vector  $\underline{D}$  except that it is made up of elements  $i_i$ , where  $i_i$  is the intensity observed at s-unit  $s_i$ .

If only conditions (a) to (d) above are included in the calculation of the R-factor,  $R_D$  is calculated.  $R_D$  is the diagonal R-factor and it is so named because it uses only the diagonal terms of the weight matrix  $\underline{W}$  and can be defined as

$$R_D \equiv \sqrt{\frac{\sum w_{ii} d_i^2}{\sum w_{ii} i_i^2}}$$

If condition (e) is included and over-rides condition (d), the quantity calculated is  $R_G$  (the general R-factor) which takes data correlation into account by including the off-diagonal elements of  $\underline{W}$  in the calculation.  $R_G$  treats individual data points as if they were independent observations. This is not

strictly valid as the points lie on a curve and the position of any point will be determined to a large extent by its neighbouring points. The dependence of the position of a point on its neighbours is taken into account by  $R_G$ .

The e.s.d. (estimated standard deviations) quoted in the tables of parameters at the end of each structure determination are random errors obtained in the least squares analysis, increased to allow for systematic errors. As off-diagonal weight matrices are used, the e.s.d. include allowances for data correlation.

The final set of parameters, which are taken to be the best description of the molecule, is that which gives the lowest R-factors. For each of the refinements described in the following chapters the list of parameters giving the lowest R-factors is given along with a table containing  $s_0$  (listed under  $s_{\min}$ ),  $s_1$  (listed under  $sw_1$ ),  $s_2$  (listed under  $sw_2$ ),  $s_n$  (listed under  $s_{\max}$ ),  $p/h$  (the correlation parameter used in the  $\underline{W}$  matrix) and the scale factor ( $k_m$ ) for each camera height and the least squares correlation matrix (indicating how strongly values of parameters are correlated with each other). Also at the end of each section a graphic representation of the observed data is supplied, with the difference from calculated data shown underneath, for each camera height and a combined set of data incorporating the curves for each camera height is also given. Finally the inter-atomic distances in the molecule are given in the form of radial distribution curves  $P(r)/r$  (which is a Fourier transformation of the combined data from the frequency domain into the distance domain) and  $P(r)$ , which is calculated from  $P(r)/r$  by multiplying by  $r$ .

**Chapter 8**

**Gas Phase Molecular Structure of**

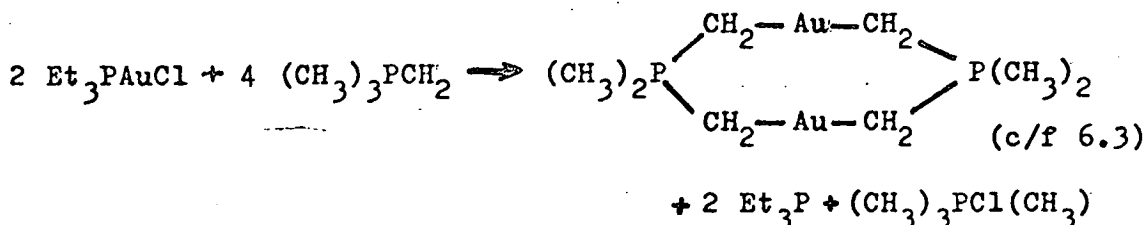
**Trimethyl(methylene)phosphorane**

**as Determined by Electron Diffraction**

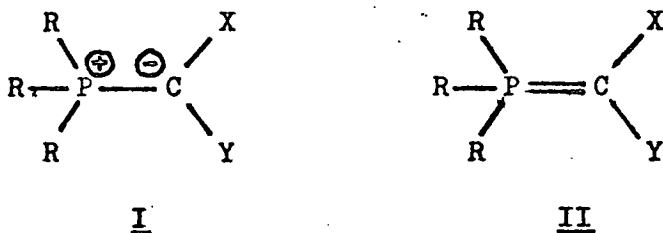
8 Gas Phase Molecular Structure of Trimethyl(methylene)Phosphorane as Determined by Electron Diffraction

The compound  $(\text{CH}_3)_3\text{PCH}_2$  has proved very useful in the preparation of a large range of metal complexes. These are generally formed by reactions of the type:-

54



However,  $(\text{CH}_3)_3\text{PCH}_2$  is of some interest in its own right. It is one of a set which can be given the general formula  $\text{R}_3\text{PCXY}$ . Interest lies mainly in the question of the exact nature of the bonding between the methylenic carbon and the phosphorus atom. The bonding within the molecule could be described by two formal structures viz.



The current debate centres on which of the two structures describes more fully the actual bonding within the molecule, but it is generally accepted that both I and II will contribute to a greater or lesser extent.

From reactions of the type outlined above, it appears that the methylenic carbon atom is essentially basic and that structure I predominates. This view is also supported by evidence from photoelectron spectroscopy.<sup>55</sup> The photo-



electron spectrum of trimethyl(methylene)phosphorane can best be simulated by assuming the methylenic carbon to be essentially  $sp^3$  hybridised and to contain a lone pair of electrons, giving it its basic properties.

Nuclear magnetic resonance spectroscopy also supports a large contribution from structure I as the methylenic protons resonate to low frequency, suggesting that there is a high electron density on the methylenic carbon which is shielding the protons. However, the carbon-hydrogen coupling within the methylene group ( $J_{CH}$  ca. 150 Hz. <sup>56</sup>) is comparable to systems in which the carbon bearing the proton is  $sp^2$  hybridised and this would seem to support structure II as being the better description of the molecule.

The stretching frequency of the P-C(methylene) bond is  $1006\text{ cm}^{-1}$ , which yields a calculated force constant of  $5.59\text{ mdyne \AA}^{-1}$ . This value of the force constant indicates a bond order of 1.65 <sup>57</sup> which would support a structure which is about midway in the spectrum of which I and II are extremes.

Solid phase structural data has been collected from compounds of the type  $\text{Ph}_3\text{PCXY}$  and P-C(XY) bond lengths of  $166\text{ pm}$  <sup>58</sup> and  $175\text{ pm}$  <sup>59</sup>, corresponding to bond orders of between 1.4 and 2, have been found. Structural data of this type must be considered in terms of crystal packing effects, which may distort the molecules. Unfortunately molecules of the type  $\text{Ph}_3\text{PCXY}$  are not volatile enough to allow structure determinations in the gas phase.

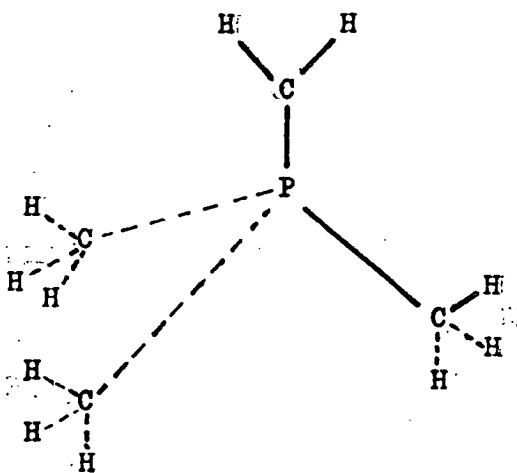
The compound  $(\text{CH}_3)_3\text{PCH}_2$  is more reactive than the phenyl analogue and, due to difficulties in handling, has only been isolated recently <sup>56</sup>. It has two advantages over the phenyl

analogue; firstly it contains fewer atoms per molecule and secondly, it is sufficiently volatile to allow an electron diffraction determination to be done in the gas phase where influences due to crystal packing effects are absent. A gas phase determination of the structure of this compound was seen to be essential in the characterisation of the phosphorus methylenic carbon bond.

### 8.1 Model

During the refinement of the structure of trimethyl(methylene)-phosphorane, a mathematical model was used, in which the following assumptions were made.

The  $\text{PCH}_2$  section of the molecule was assumed to have  $\text{C}_{2v}$  local symmetry and <sup>the</sup>  $\text{CP}(\text{CH}_3)_3$  section was assumed to have overall  $\text{C}_3$  symmetry with the  $\text{PCH}_3$  groups having  $\text{C}_{3v}$  local symmetry. Using these assumptions, it is possible to define the molecule by using two carbon-hydrogen bond lengths, two carbon-phosphorus bond lengths, two phosphorus-carbon-hydrogen bond angles, one carbon-phosphorus-carbon bond angle, a torsion about the P-C(methylene) bond and a torsion about the P-C(methyl) bonds.



Bonds in the plane of of the paper are shown as solid lines.

All torsions are zero if the molecule adopts this conformation.

## 8.2 Refinement and Results

The geometrical parameters associated with the heavier atoms in the molecule, P-C(methyl), P-C(methylene) and angle CPC, all refined satisfactorily as these atoms give rise to the largest peaks in the radial distribution curve (peaks at 180 and 290 pm and a shoulder at 160 pm). Other significant peaks in the radial distribution curve are at 110, 240 and 300 pm and result from distances associated with protons in the methyl groups: this meant that satisfactory refinement of the parameters associated primarily with the methyl groups (C-H(methyl) and angle PCH(methyl)) was possible. Amplitudes of vibration of the heavier atoms were readily refined. It was possible to refine amplitudes of vibration for C-H(methyl) and P....H as well as one group of non-bonded C....H amplitudes of vibration.

The peaks in the radial distribution curve associated with the distances involving the methylenic protons fell close to, or under, the peaks caused by distances involving the methyl protons. Parameters involving the methylenic protons could not, therefore, be satisfactorily refined. Values: C-H(methylene), angle PCH(methylene), the methylenic torsion and the methyl torsion were varied using an R-factor loop and the combination of values which gave the lowest R-factor were used in subsequent refinements. This process was repeated at a later stage in the refinement. The methyl torsion was allowed to refine briefly at several stages during the refinement.

Parameters obtained in the best refinement which converged to give  $R_G$  0.13 and  $R_D$  0.10 are listed with the tables at the end of this chapter.

### 8.3 Conclusions

The parameters associated solely with the methyl groups are as expected; the angle PCH(methyl) is close to tetrahedral and the torsion about the P-C(methyl) bonds minimises the steric interaction between methyl groups.

The P-C(methyl) bonds are short, (181.5(3) pm) in comparison with the corresponding bonds in the trimethylphosphine molecule (184.1(3) pm<sup>60</sup>) and the angle C(methyl)PC(methyl) is large in comparison to that in trimethylphosphine (101.6(5)<sup>o</sup> as compared with 99.1(2)<sup>o</sup>). Such differences between the three and four co-ordinate cases are common: with trimethylphosphine oxide and trimethylphosphine sulphide the corresponding values are 180.9(2) pm and 104.1(8)<sup>o</sup> for the oxide and 181.8(2) pm and 104.5(3)<sup>o</sup> for the sulphide<sup>61</sup>. Values obtained in this work compare favourably with those for the oxide and sulphide.

The C(methylene)PC(methyl) angle is 116.5(6)<sup>o</sup>, indicating a marked distortion, from a tetrahedral arrangement, about the phosphorus. Such a distortion has been reported in the solid phase determinations of the analogous phenyl compounds and the degree of distortion seems to be related to the P-C(methylene) bond length: as the bond shortens the angle increases. The distortion is very apparent in this case as the P-C(methylene) bond is the shortest yet reported (164.9(6) pm) for a phosphorus atom bound to a three co-ordinate carbon atom.

The P-C(methylene) bond length corresponds to a bond order of 2, if single, double and triple bond lengths are taken to be 187, 164 and 153 pm respectively<sup>62</sup>. Such a high bond order would immediately suggest that structure II must predominate.

However, the bond order, or apparent bond order, of the unique carbon-phosphorus bond does not yield as much information as might at first be thought. Structure I shows a P-C(methylene) bond order of one, but a bond length corresponding to a bond order of one would not be expected. The bond in question joins two centres of high and opposite charge and, as a result, some degree of Coulombic attraction would be expected, which would have the effect of shortening the bond and giving an apparent bond order of more than 1. How much greater than 1 the apparent bond order would be is difficult to say as the magnitude of the dipole across the bond is not known, but Coulombic attraction leading to an apparent bond order of more than two cannot be ruled out.

The essential difference between structures I and II is that the methylene group has the C-P and C-H bonds co-planar in structure II, but pyramidal in structure I. This difference arises out of the different hybridisation of the carbon atom in the methylene group ( $sp^3$  in I,  $sp^2$  in II).

Unfortunately it was not possible to characterise the structure about the methylene group in this compound, but if the protons on the methylene groups were replaced by heavier atoms, which would give rise to stronger interference patterns, it should be possible to determine the hybridisation of the methylenic carbon. Atoms heavier than hydrogen on the methylenic carbon atom tend to reduce the volatility of the compound, but  $(CH_3)_3PC(SiH_3)_2$  is sufficiently volatile for examination by electron diffraction and such a study would make a worthwhile contribution to the solution of the problem.

Molecular Parameters for Trimethyl(methylene)phosphorane.

Independent Distances	Distance /pm	Amplitude of Vibration /pm
r1 P=C	164.0(6)	5.3(8)
r2 P-C	181.5(3)	6.2(4)
r3 C-H(methyl)	109.9(5)	7.9(7)
r4 C-H(methylene)	106.0(fixed)*	7.1(tied to u3)
Dependent Distances		
u5 C(methyl)...C(methyl)	281.2(34)	11.5(10)
u6 C(methyl)...C(methylene)	294.0(57)	
u7 P.....H(methyl)	241.3(30)	11.6(6)
u8 P.....H(methylene)	244.9(40)	
u9 C.....H	374 - 396**	17.8(16)
u10 C.....H	277 - 342**	15.0(fixed)
u11 H...H Geminal methylene	165.1(15)	14.0(fixed)
u12 H...H Geminal methyl	179.7(47)	14.0(fixed)
u13 H.....H	266 - 478	20.0(fixed)
Angles/degrees		
<1> (C=P-C)	116.5(6)	
<2> (C-P-H)(methyl)	109.3(4)	R <sub>G</sub> 0.13
<3> (C-P-H)(methylene)	128(fixed)*	R <sub>D</sub> 0.10
<4> (methyl twist)	17(see text)*	
<5> (methylene twist)	0(fixed)*	

\*Value chosen by R-factor loop.

\*\*Values fell into two ranges

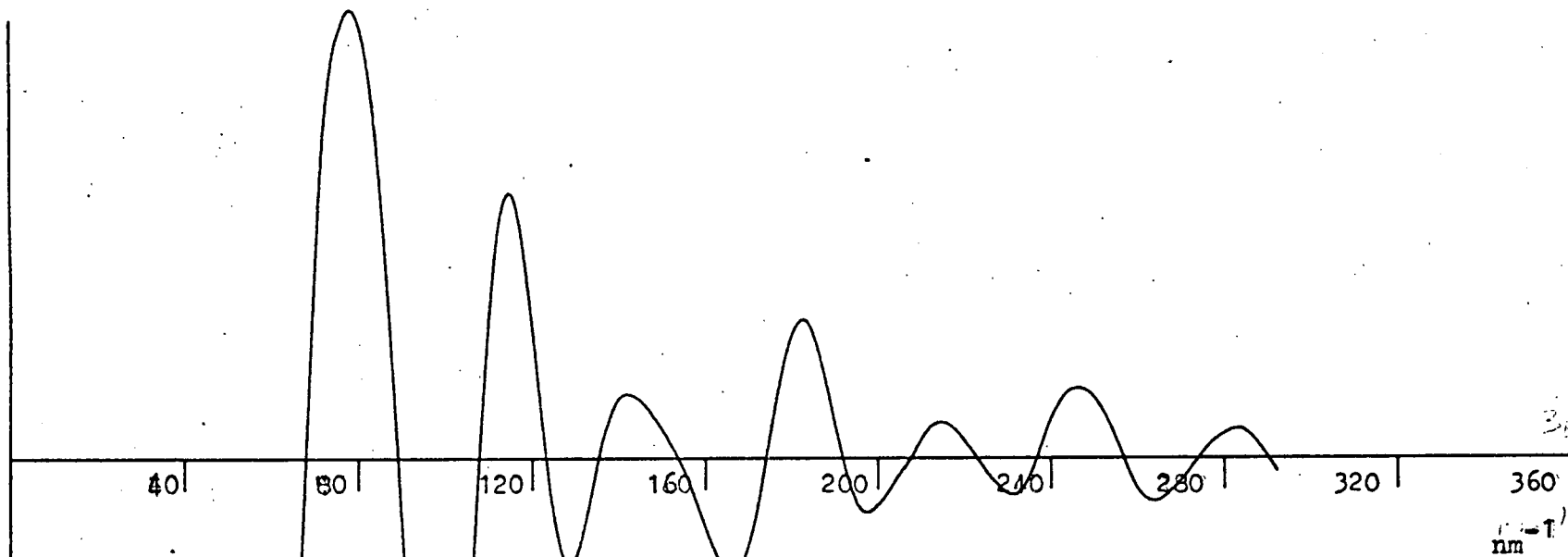
Amplitudes of vibration given for ranges of distances are those for the individual distances within that range.

Camera Height	$\Delta s$	$s_{\min}$	$sw_1$	$sw_2$	$s_{\max}$	p/h	Scale Factor
mm	$\text{nm}^{-1}$	$\text{nm}^{-1}$	$\text{nm}^{-1}$	$\text{nm}^{-1}$	$\text{nm}^{-1}$		
250	4	64	68	286	292	0.4611	0.704(19)
500	2	26	29	144	152	0.4975	0.728(16)
1000	1	15	18.5	72	76	0.4999	0.503(25)

Weighting functions, scale factors and correlation parameters

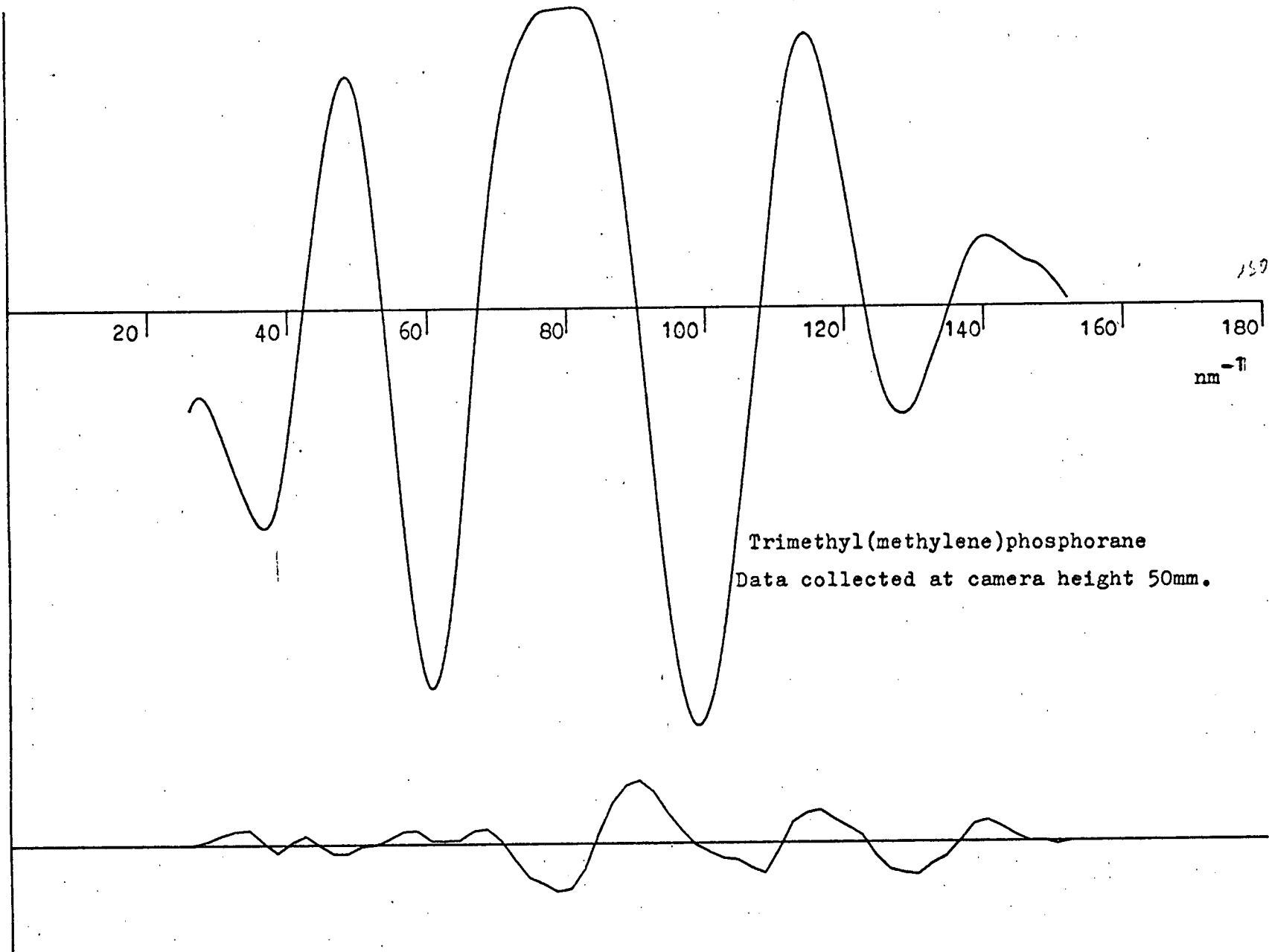
r1	r2	r3	< 1	< 2	u1	u2	u3	u5	u7	u9	k1	k2	k3	
100	31	-10	15	-23	-23	-31	-26	-40	-20	-4	-52	-38	-7	r1
	100	-6	12	-42	-14	1	1	0	1	13	2	12	9	r2
		100	-36	2	4	10	-3	28	-9	4	12	9	3	r3
			100	-72	-11	-10	1	-74	-13	-8	-12	-6	-1	< 1
				100	4	-7	-2	36	24	-11	0	-17	-15	< 2
					100	70	17	27	12	11	42	38	12	u1
						100	35	36	20	16	71	56	16	u2
							100	15	24	2	53	30	34	u3
								100	17	14	42	42	19	u5
									100	2	39	16	-10	u7
										100	14	19	13	u9
											100	53	12	k1
												100	18	k2
													100	k3

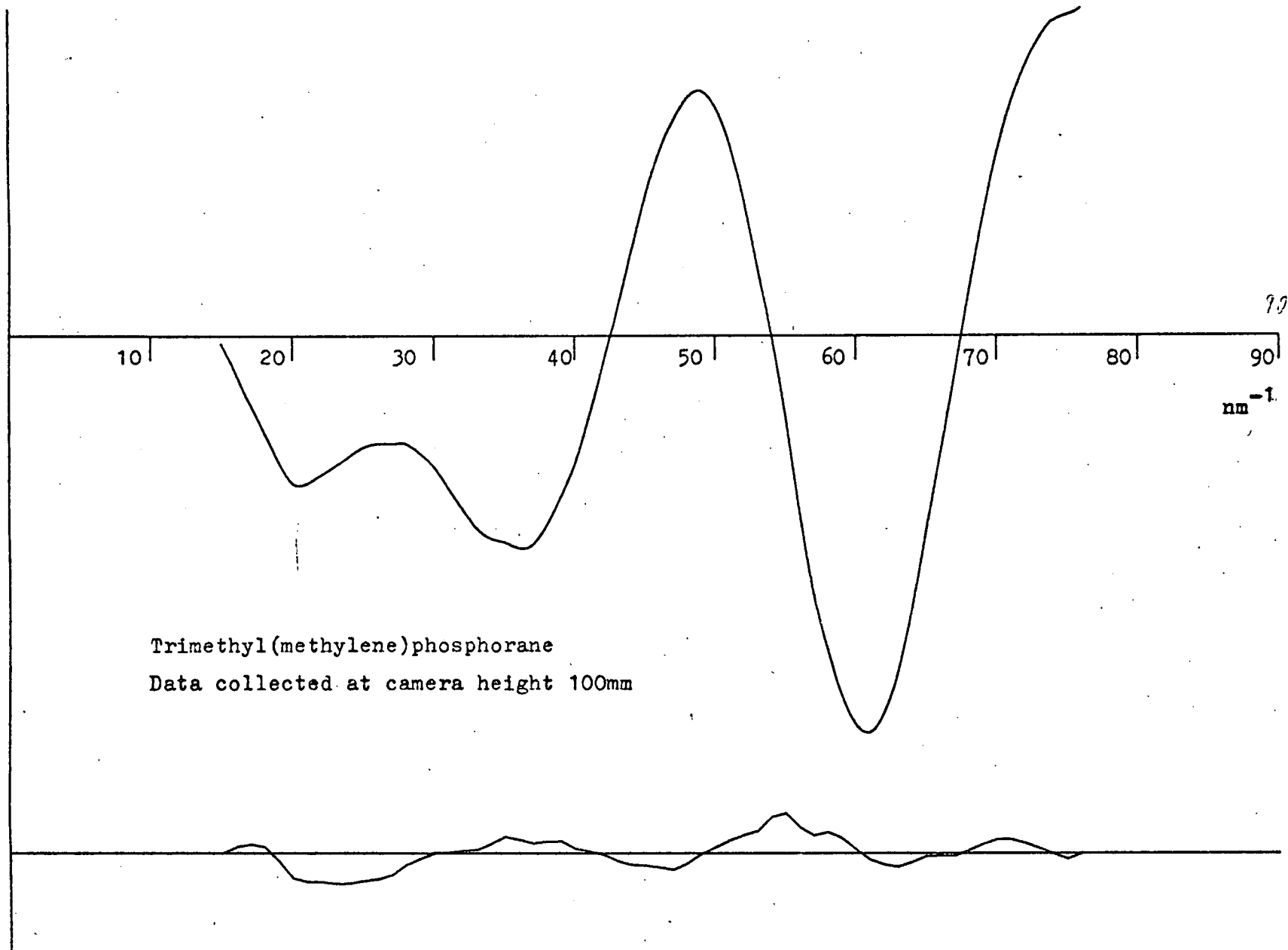
Least squares correlation matrix multiplied by 100



Trimethyl(methylene)phosphorane  
Data collected at camera height 25mm.

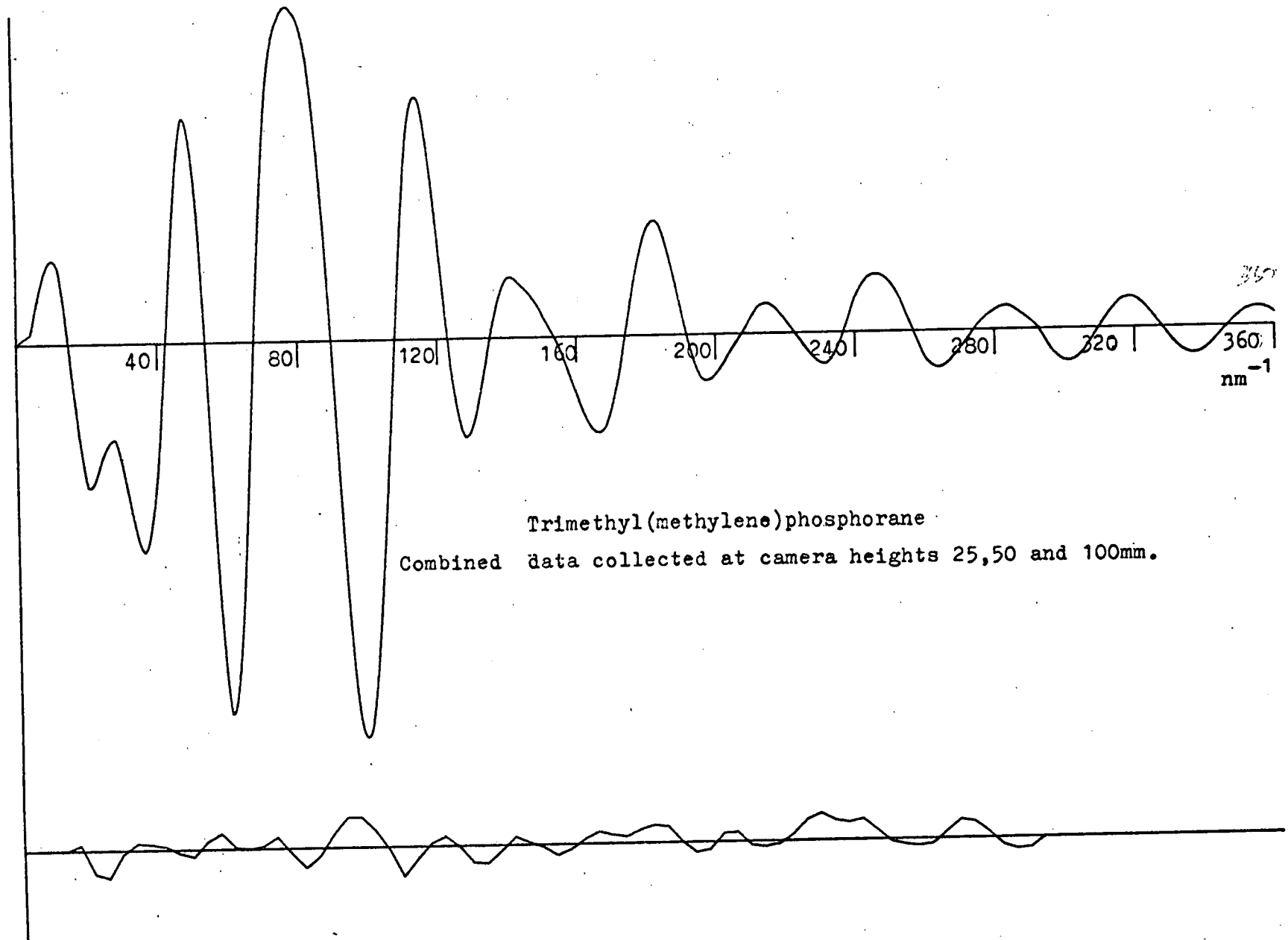


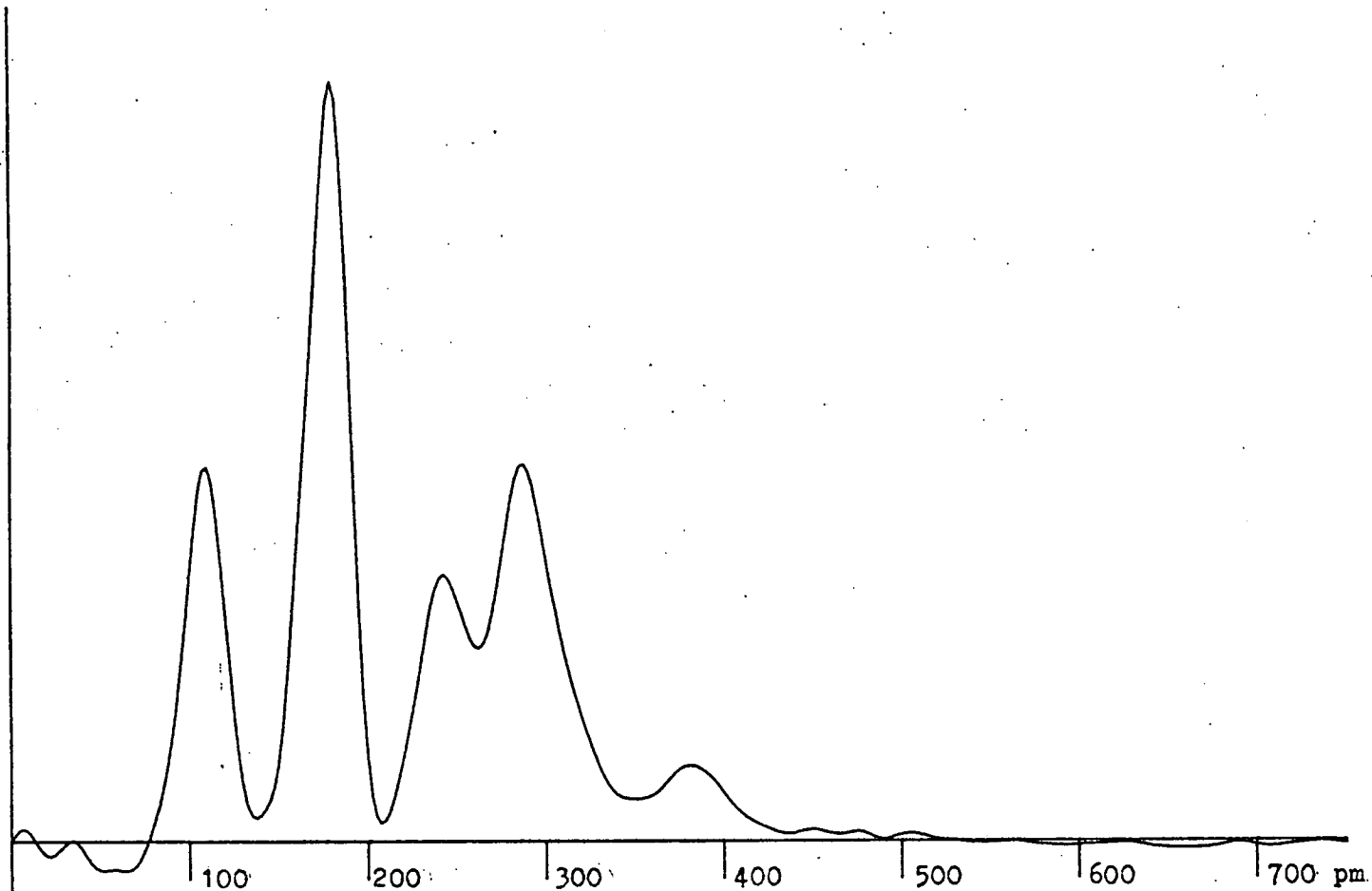




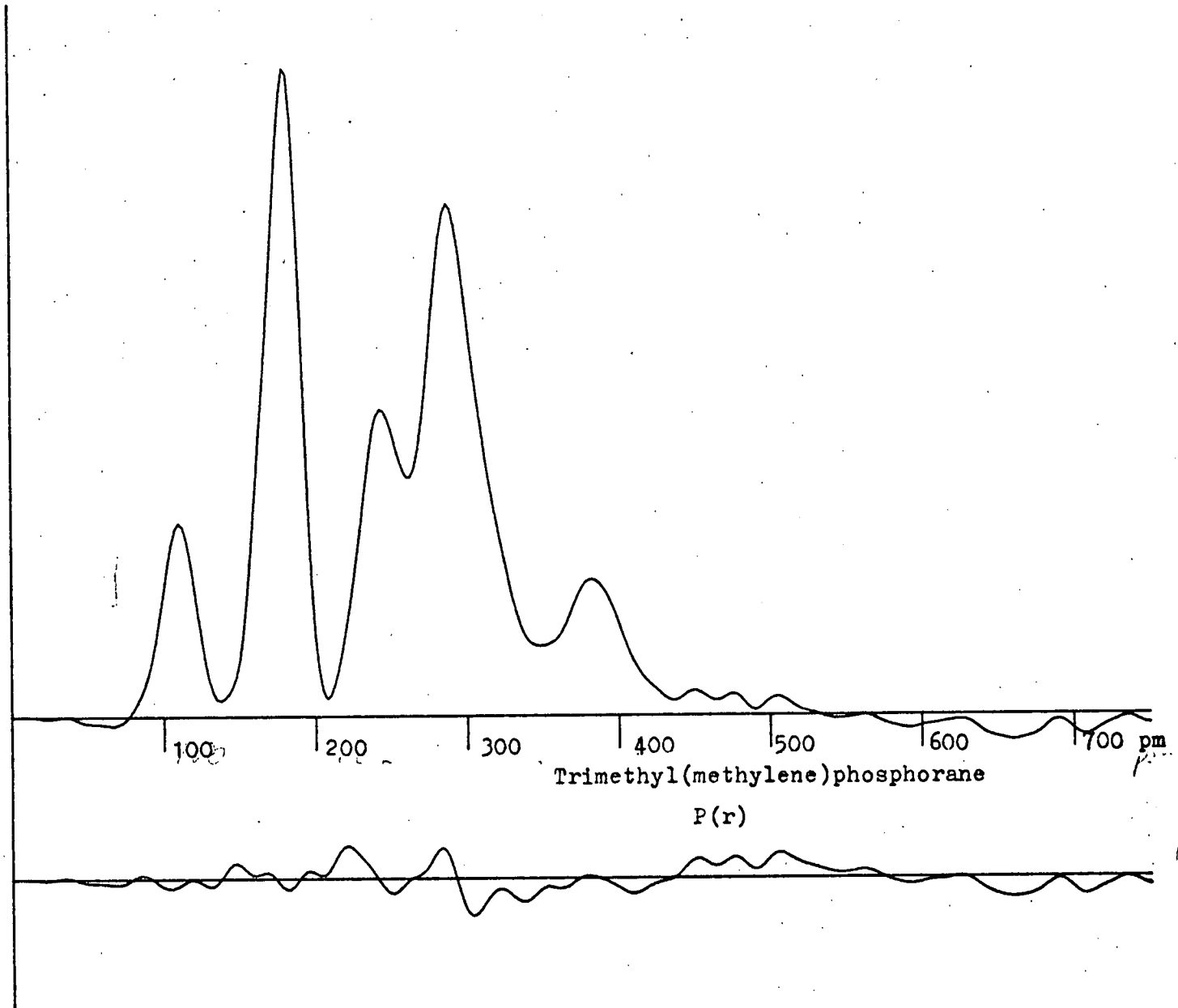
90.

$\text{cm}^{-1}$





Trimethyl(methylene)phosphorane  
P(r)/r



Chapter 9

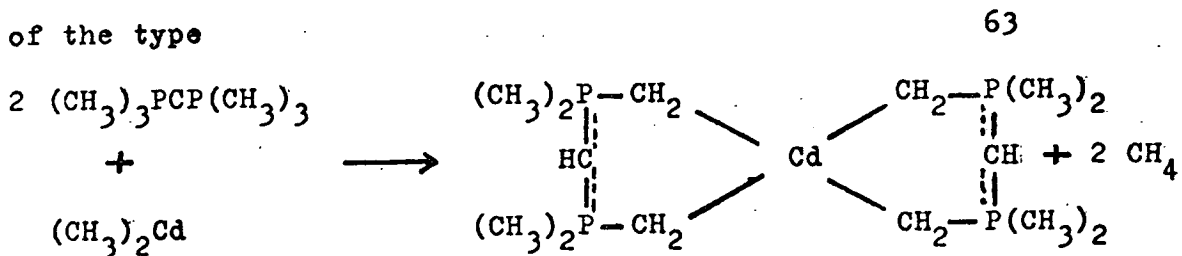
Gas Phase Structure of

Hexamethylcarbodiphosphorane

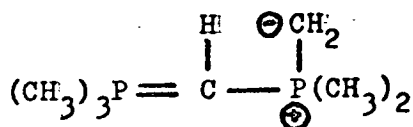
as Determined by Electron Diffraction

9 Gas Phase Structure of Hexamethylcarbodiphosphorane  
as Determined by Electron Diffraction

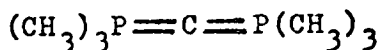
The compound hexamethylcarbodiphosphorane is used in the preparation of several metal complexes, usually by reactions of the type



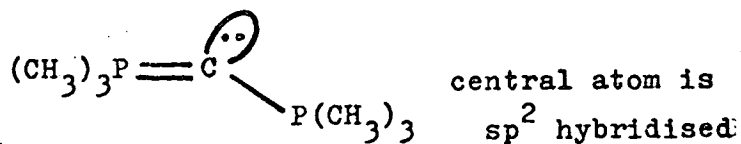
The molecule appears to attack the metal compound as



This would imply that the central carbon atom is basic and may not be  $sp$  hybridised as would be suggested by the formal structure viz.



If the central carbon is  $sp$  hybridised, the molecule should, in the vibrational ground state, be a symmetric top with a linear PCP unit, but, if the central carbon is hybridised in any other way (e.g.  $sp^2$  - see below), the PCP unit cannot be linear.



Structural determinations in the solid phase on related compounds do not clearly resolve this question. Solid  $\text{Rh}_3\text{PCPPh}_3$  contains two molecules per unit cell, both of which have bent PCP units. However, they are bent by different amounts; one molecule has a PCP angle of  $143.8^\circ$  and the other

molecule has a PCP angle of  $130.1^\circ$ <sup>64</sup>, indicating that the PCP angle is, in this instance, more a function of crystal packing constraints than of the electron configuration of the central carbon atom. The isoelectronic cation  $(\text{Ph}_3\text{PNPPh}_3)^+$  is linear when  $(\text{V}(\text{CO})_6)^-$  is the counter ion<sup>65</sup>, but has PNP angles of between  $134.6^\circ$  and  $142.8^\circ$ <sup>66,67</sup> with other counter ions.

Again, this variation in PNP angles must be viewed in terms of crystal packing constraints. Other molecules with a PCX unit,  $\text{Ph}_3\text{CCO}$ <sup>68</sup> and  $\text{Ph}_3\text{PCCS}$ <sup>69</sup>, have PCC angles of  $145.5^\circ$  and  $168.8^\circ$  and the bulk of the available evidence seems to suggest that very little energy is required to distort a linear PCP unit by  $40 - 50^\circ$ .

In the gas phase, the crystal packing effects, which complicate the interpretation of the results given above, would be absent. If, as the above results would indicate, the PCP unit is easily distorted, it is very likely that the molecule  $(\text{CH}_3)_3\text{PCP}(\text{CH}_3)_3$  will undergo a low frequency bending vibration about the central carbon atom, giving rise to problems with shrinkage effects. Shrinkage effects arise because it is the structure which best fits the average inter-atomic distances which is determined by electron diffraction. If the molecule is undergoing a bending vibration, the average structure may be linear, but the P...P distance will be less than the combined P-C-P bond lengths and the molecule will appear to be bent in the final structure. Carbon suboxide is a linear molecule with a low frequency bending mode at  $18 - 19 \text{ cm}^{-1}$ ; it appears to have a CCC angle of  $158^\circ$  in the electron diffraction determination<sup>70</sup>. Silyl isocyanate has an SiNC angle of  $151^\circ$ .



when determined by electron diffraction <sup>71</sup>, but has been shown to have a linear SiMC unit by microwave spectroscopy. <sup>72</sup> Shrinkage effects, which make a linear portion of a molecule appear bent by over 30°, are therefore well established.

In the structure determination of  $(\text{CH}_3)_3\text{PCP}(\text{CH}_3)_3$ , two models were used. The refinement outlined in 9.1 uses a model in which the fixed conformation of the  $\text{P}(\text{CH}_3)_3$  units is assumed. The refinement outlined in 9.2 uses a model in which free rotation of  $\text{P}(\text{CH}_3)_3$  units is assumed.

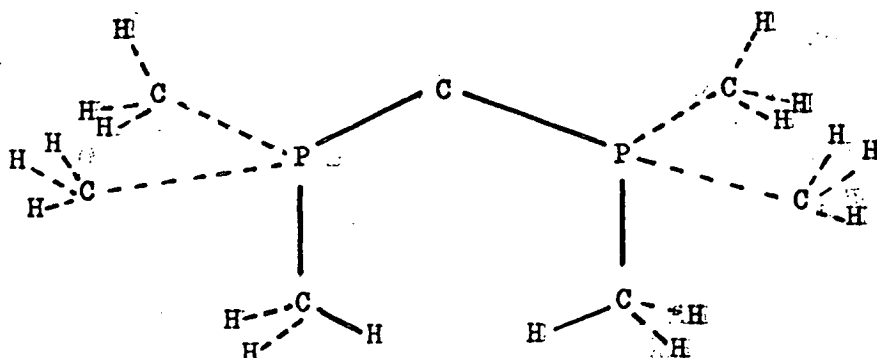
## 9.1 Refinement Assuming Fixed Conformation of $\text{P}(\text{CH}_3)_3$ Units

### 9.1.1 Model A

In model A the  $\text{CP}(\text{CH}_3)_3$  units were assumed to have  $\text{C}_3$  overall symmetry with the  $\text{PCH}_3$  groups having  $\text{C}_{3v}$  local symmetry. The molecule was considered to contain two such units which shared a common central carbon atom. With such a model, it was possible to define the molecule using two phosphorus-carbon bond lengths, one carbon-hydrogen bond length, one PCH bond angle, one CPC bond angle, one PCP bond angle, a methyl torsion about P-C(methyl) (assumed to be the same for all methyl groups) and two torsions about P-C(central) bonds.

A torsion constraint governed the torsions about P-C(central) and could act in three ways: it could allow both torsions to refine independently or it could make both torsions equal (giving the heavy atom skeleton  $\text{C}_6$  symmetry) or it could give both torsions equal magnitude but opposite sign (giving the heavy atom skeleton  $\text{C}_2$  symmetry).

Long range hydrogen-hydrogen distances between  $P(CH_3)_3$  units were too numerous to be all included in the model and, as it was felt that they would make little contribution to the intensity data, they were ignored.



When the molecule adopts this conformation, all torsions are at zero (n.b. Bonds in the plane of the paper are shown by solid lines,)

### 9.1.2 Refinement and Results

Parameters obtained in the best refinement which converged to give  $R_G$  0.13 and  $R_D$  0.07 are listed with the tables at the end of this section. All molecular parameters refined satisfactorily. The results for the  $P(CH_3)_3$  units resembled those for the  $P(CH_3)_3$  unit in trimethyl(methylene)phosphorane (see previous chapter) with the exception of the methyl torsion. In hexamethylcarbodiphosphorane there are twice as many methyl groups per molecule as there are in trimethyl(methylene)phosphorane, leading to a greater sensitivity, in correlation of predicted and observed data, to the methyl torsion. Also there is no methylene group present to influence the results. For these reasons, it is felt that the value for the methyl torsion from this refinement is more reliable than that for trimethyl(methylene)phosphorane.

Molecular Parameters for Hexamethylcarbodiphosphorane -Fixed Conformation $R_G$  0.131 $R_D$  0.077

	Distance /pm	Amplitudes of Vibration /pm
Independent distances		
r1 P=C	161.1(5)	5.6(8)
r2 P-C	181.4(3)	5.5(5)
r3 C-H	109.3(5)	7.6(7)

## Dependent Distances

u4 C....C	289.6(31)	
within $P(CH_3)_3$ units		7.6(9)
u5 C....C	283.8(30)	
u6 P....H	241.9(19)	11.6(7)
C....H	279 - 486	15.0(fixed)
H...H Geminal	177.7(29)	14.0(fixed)
H.....H	272 - 448	20.0(fixed)
between $P(CH_3)_3$ units		
u7 P....P	306.7(25)	8.0(fixed)
u8 P....C	382 - 447	14.1(13)
C....C	406 - 565	20.9(18)
C....,H	374 - 629	20.0(fixed)
P....H	306 - 499	20.0(fixed)

## Angles /degrees

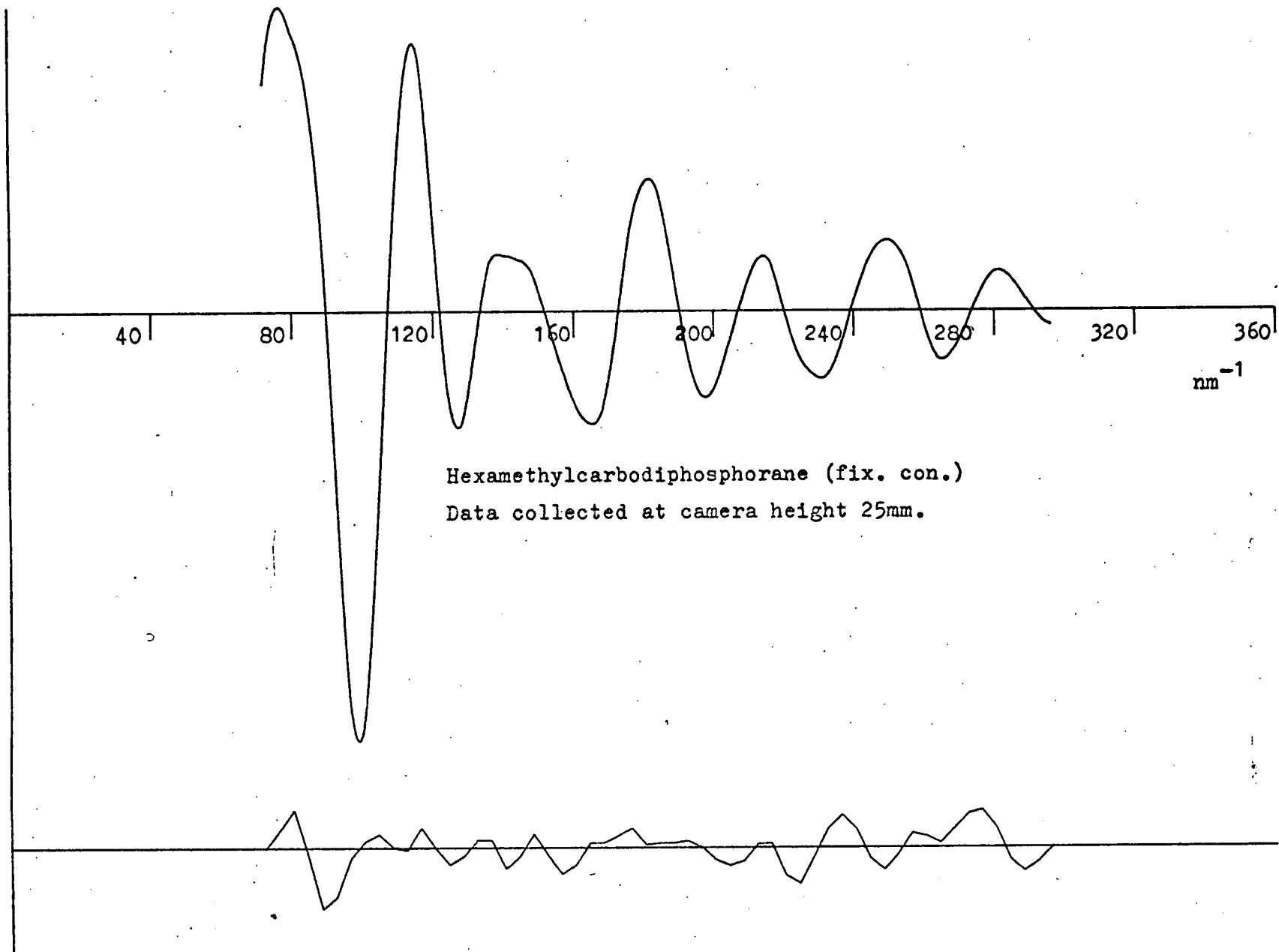
<1 CPC	144.3(6)	<2 CPC	115.4(6)	<3 PCH	110.1(8)
<4 methyl twist	37.7(18)	<5 $PC_3$ twist	31.4(6)		

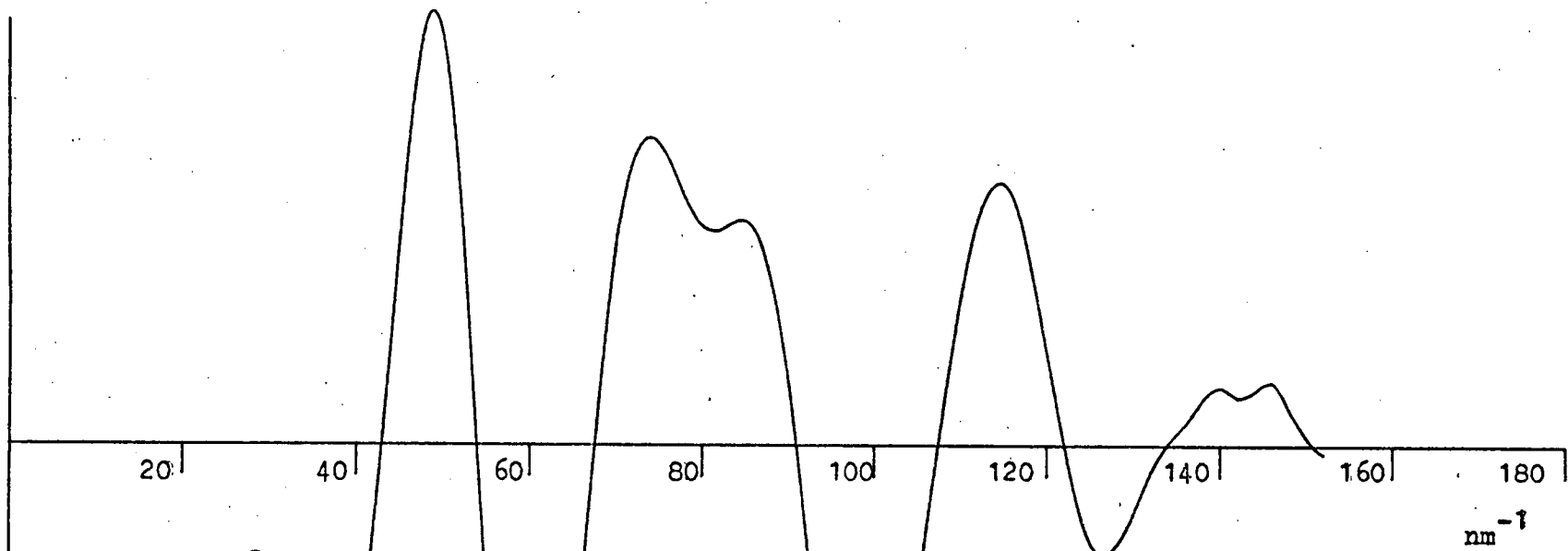
Weighting Functions, Correlation Parameters and Scale Factors.

Camera	$\Delta s$	$s_{\min}$	$sw_1$	$sw_2$	$s_{\max}$	$p/h$	Scale Factor
height	$\text{nm}^{-1}$	$\text{nm}^{-1}$	$\text{nm}^{-1}$	$\text{nm}^{-1}$	$\text{nm}^{-1}$		
mm							
250	4	72	87	282	296	0.4249	0.388(13)
500	2	24	29	142	152	0.4807	0.701(12)
1000	1	10	11.5	76	78	0.4980	0.568(16)

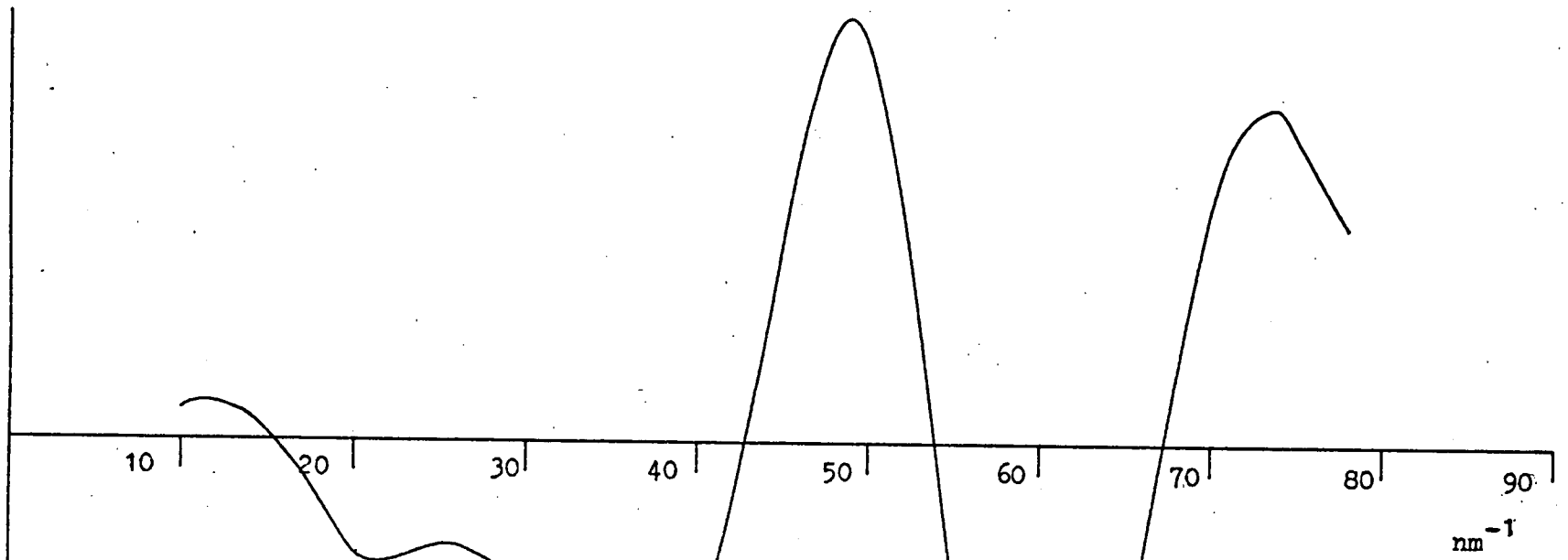
Least Squares Correlation Matrix, Multiplied by 100

r1	r2	r3	<1	<2	<3	<4	<5	u1	u2	u3	u4	u5	u6	u8	k1	k2	k3	
100	30	-9	-60	-58	-25	-61	55	-13	-20	-6	36	-55	5	-16	-24	-44	-25	r1
	100	-3	-6	10	-27	-27	13	-10	9	6	13	8	0	5	13	10	2	r2
		100	16	15	-14	30	-14	-5	9	4	-8	21	2	-1	8	18	12	r3
			100	54	20	68	-72	9	33	15	-46	76	4	14	31	59	40	<1
				100	36	65	-74	10	39	16	-19	54	-19	8	39	64	40	<2
					100	60	-74	7	8	5	-18	6	-13	17	11	16	10	<3
						100	-92	10	27	11	-42	59	-14	16	23	54	40	<4
							100	-10	-32	-15	40	-60	12	-17	-31	-58	-40	<5
								100	43	-7	-3	12	1	8	19	18	9	u1
									100	27	-9	42	2	13	66	58	29	u2
										100	-5	18	2	7	35	27	11	u3
											100	-42	-9	-9	-9	-20	-13	u4
												100	4	12	40	70	45	u5
													100	-1	1	3	3	u6
														100	30	13	-9	u8
															100	49	21	k1
																100	41	k2
																	100	k3

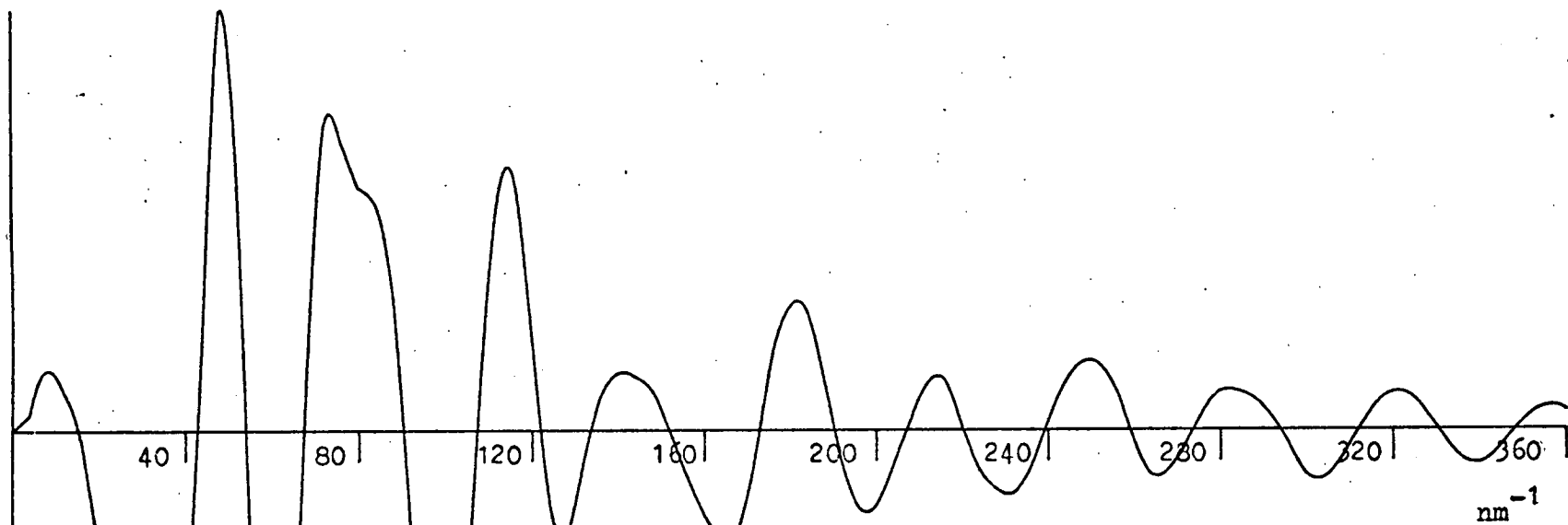




Hexamethylcarbodiphosphorane (fix. con.)  
Data collected at camera height 50mm.

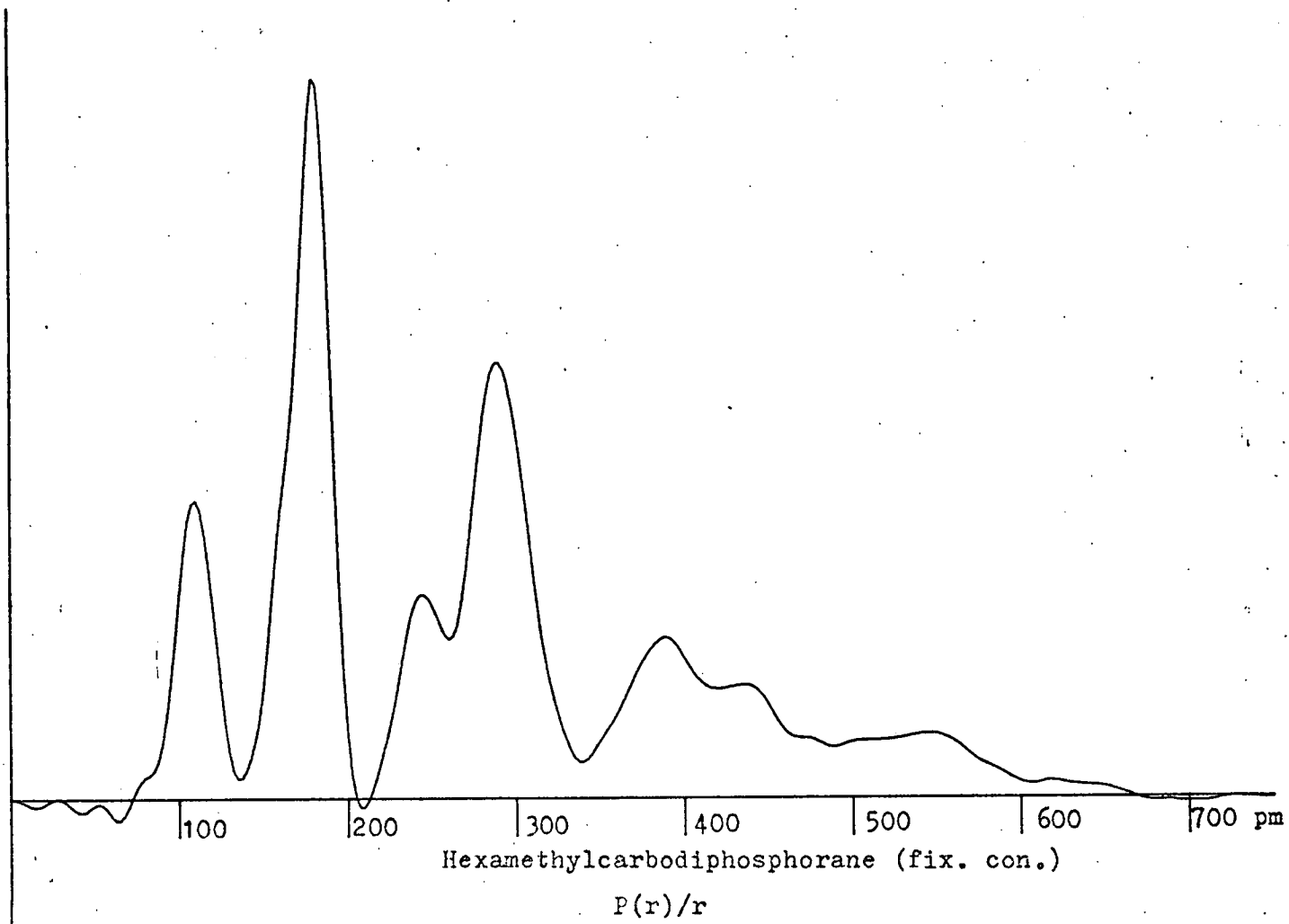


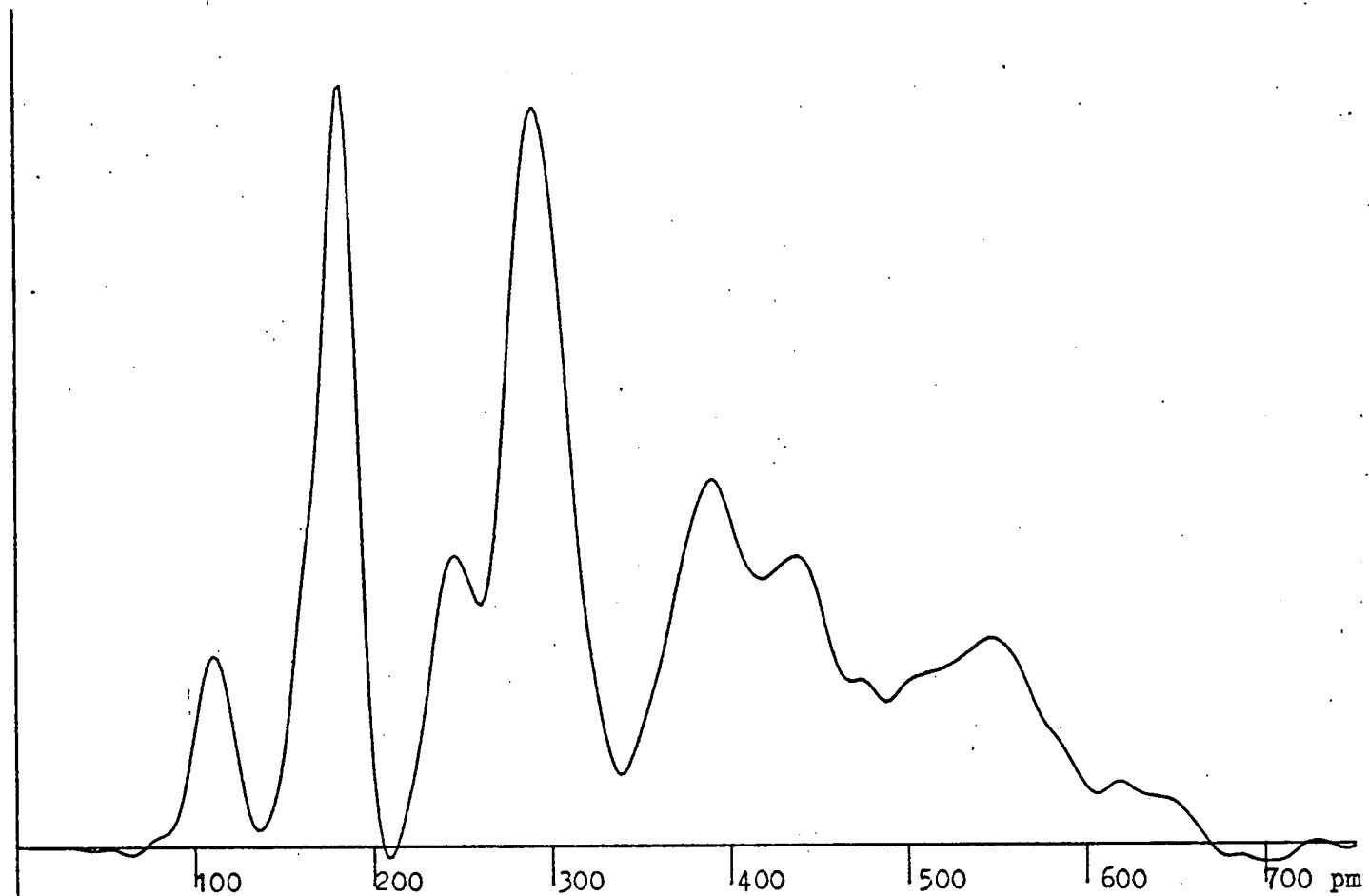
Hexamethylcarbodiphosphorane (fix. con.)  
Data collected at camera height 100mm.



Hexamethylcarbodiphosphorane (fix. con.)  
Combined data collected at camera heights 25, 50 and 100mm.

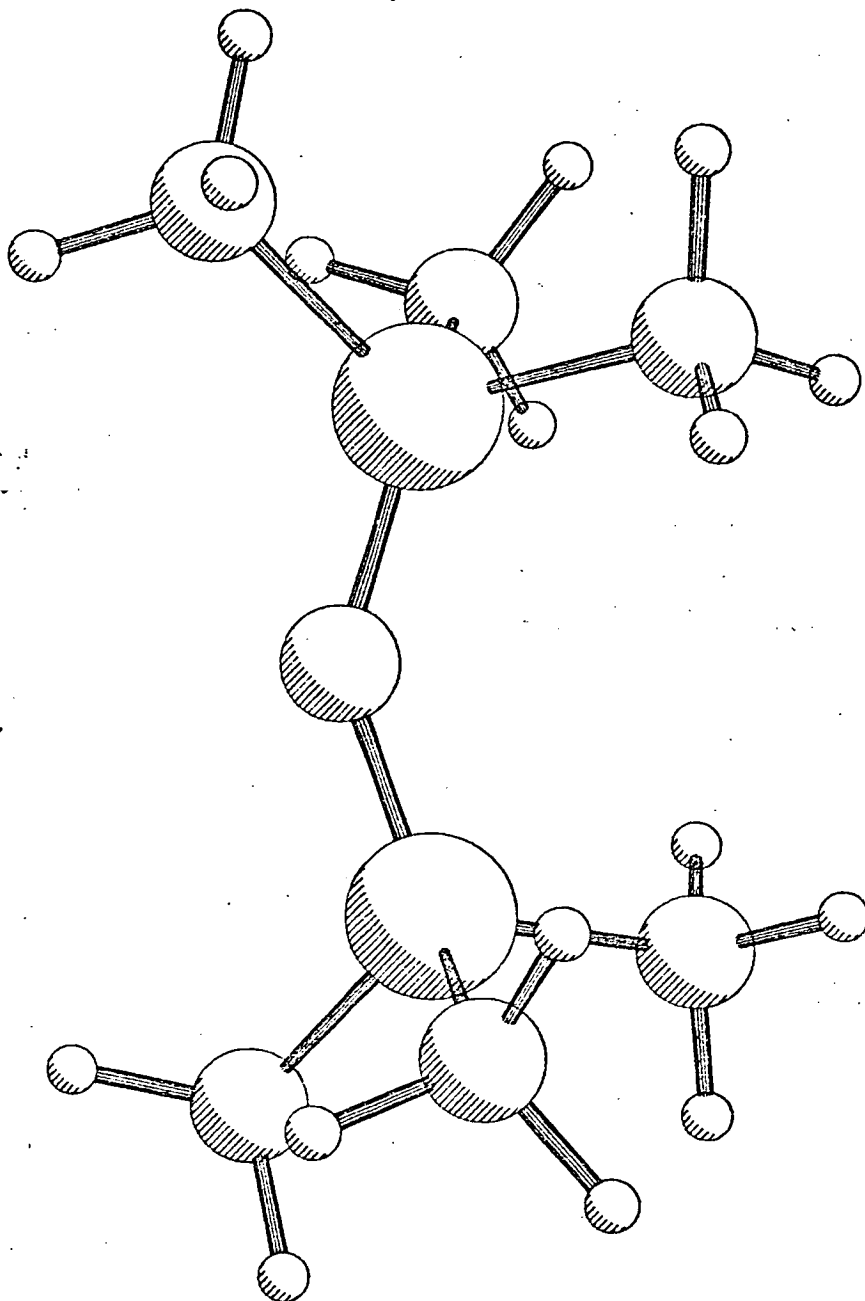






Hexamethylcarbodiphosphorane (fix. con.)

P(r)

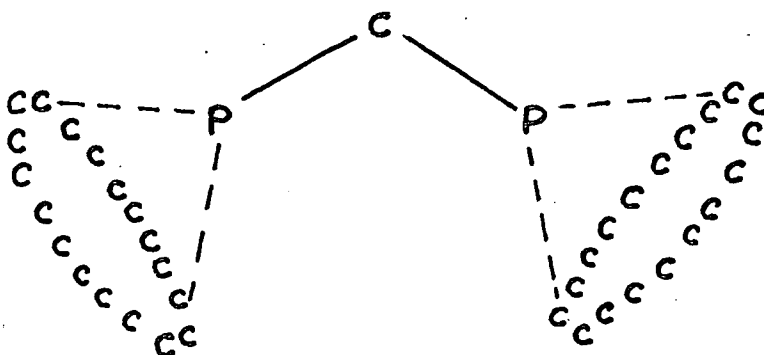


Scale drawing of hexamethylcarbodiphosphorane  
using parameters from the best refinement.

## 9.2 Refinement Assuming Free Rotation of $P(CH_3)_3$ Units

### 9.2.1 Model B

Model B closely resembles model A (see 9.1.1), but with one basic difference: the torsion of the  $PC_3$  units about P-C(central) and the torsion constraint are dispensed with and replaced by a section of the model which simulates free rotation of the  $PC_3$  units about the P-C(central) bond. True free rotation would involve smearing out the carbon atoms in each  $PC_3$  unit to form a "ring of carbon" which would form the circumference of the base of a cone whose apex coincided with the phosphorus atom. This was not possible in the model, but a reasonable approximation, which was used, was to distribute the three carbon atoms in each unit about 18 points on the circumference of the cone, viz.



The number of carbon-carbon distances between two rings of carbon would be infinite, but even with this model the number of carbon-carbon distances is 162 and with extra phosphorus-carbon and existing carbon-hydrogen distances, the numbers involved reach unmanageable proportions. The total number of phosphorus-carbon distances to be calculated was 9 and these were each given a separate distance storage location, within

the computing program, in the usual way. The 162 storage locations, required for the carbon-carbon distances, exceeds more than twice the number of distances which current programs are capable of handling before computing time becomes inordinately long. The distances involved ranged between 360 and 590 pm and the problem was overcome by creating "pigeon holes" to accept carbon-carbon distances within this range. The pigeon holes took the form of distance storage locations which were each programmed to accept carbon-carbon distances within a range of 10 pm. If, for example, a carbon-carbon distance of 483 pm was calculated this would register in the pigeon hole collecting distances in the range 480 - 489 pm. When the distance calculations were complete, the mean distance in each pigeon hole was calculated and this distance, weighted according to the proportion of the total number of carbon-carbon distances contained in a particular pigeon hole, was used in the calculation of intensity data. In this way, 162 distances were reduced to about 24 distances which were good approximations of the originals.

The range of values which would be involved in a pigeon hole treatment of the intra- $\text{P}(\text{CH}_3)_3$  unit carbon-hydrogen distances make such a treatment unworkable. It was felt that, rather than omit these distances, a fixed conformer representation, with respect to the hydrogen atoms, would be a reasonable approximation and the best values of the parameters influencing the long range carbon-hydrogen distances were selected from the fixed conformer refinements (using model A) and used in this refinement.

### 9.2.2 Results

Introducing free rotation of the  $\text{P}(\text{CH}_3)_3$  units does not greatly change the parameters which govern atomic positions within the units themselves: these parameters are very similar to those obtained using model A. The values which change most significantly, on using model B, are P-C(central) and the CPC bond angle. The P-C(central) bond length decreased and the PCP angle widened from the values obtained in 9.1. The list of parameters which were obtained in the best refinement (converged to give  $R_G$  0.11 and  $R_D$  0.06) are listed with the tables at the end of this section.

Molecular Parameters for Hexamethylcarbodiphosphorane-Free Rotation

	Distance /pm	Amplitude of Vibration /pm
<b>Independent Distances</b>		
r1 P=C	159.4(3)	6.9(8)
r2 P-C	181.4(3)	6.1(4)
r3 C-H	108.9(5)	7.4(7)
<b>Dependent Distances</b>		
u4 C....C	290.4(20)	7.9(8)
Within P(CH <sub>3</sub> ) <sub>3</sub> groups		
u5 C....C	280.6(16)	
u6 P....H	240.5(18)	11.3(6)
C....H	272 - 376	15.0(fixed)
H...H Geminal	178.0(96)	14.0(fixed)
H.....H	273 - 414	20.0(fixed)
<b>Between P(CH<sub>3</sub>)<sub>3</sub> groups</b>		
u7 P....P	306.0(22)	7.8(11)
u8 P....C	383 - 449	12.2(11)
C....C	365 - 585	22.5(fixed)*
P....H	371 - 534	20.0(fixed)
C....H	387 - 658	20.0(fixed)
<b>Angles /degrees</b>		
<1 PCP 147.6(5)	<2 CPC 116.7(4)	<3 PCH 109.3(9)
<4 Methyl Twist 36.3(11)		
	R <sub>G</sub> 0.113	R <sub>D</sub> 0.066

\*Value chosen by R-factor loop.

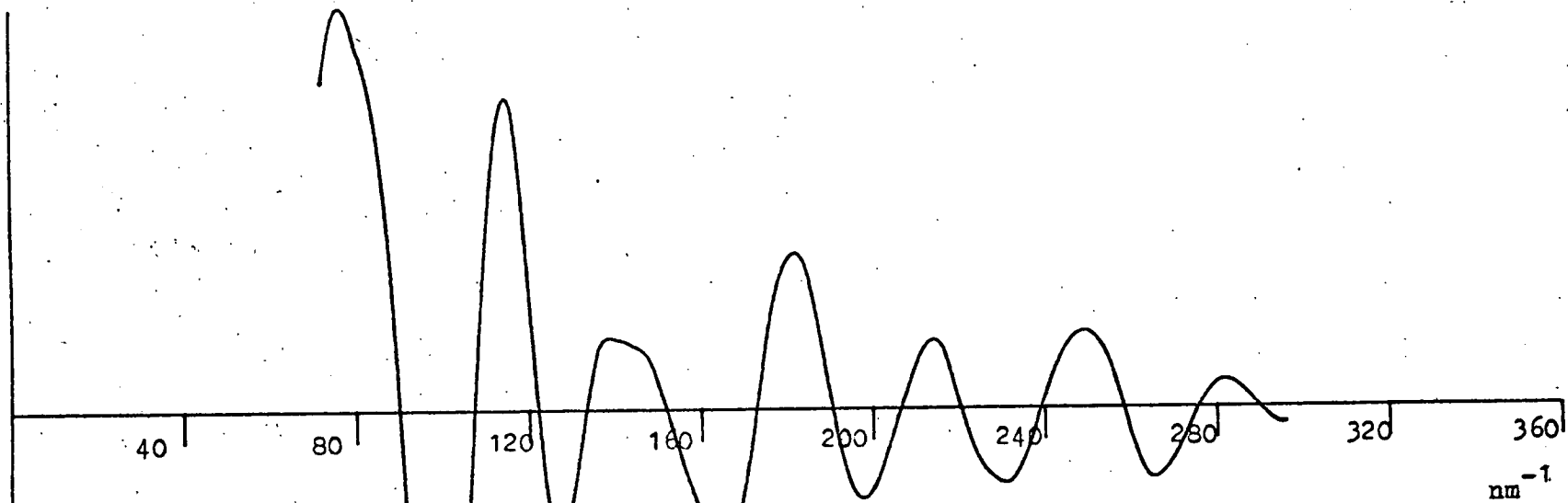
Weighting Functions, Correlation Parameters and Scale Factors

Camera							Scale
height	$\Delta s$	$s_{\min}$	$sw_1$	$sw_2$	$s_{\max}$	$p/h$	Factor
mm	$\text{nm}^{-1}$	$\text{nm}^{-1}$	$\text{nm}^{-1}$	$\text{nm}^{-1}$	$\text{nm}^{-1}$		
250	4	72	87	282	296	0.4193	0.417(14)
500	2	24	29	142	152	0.4687	0.747(12)
1000	1	10	11.5	76	78	0.4978	0.603(15)

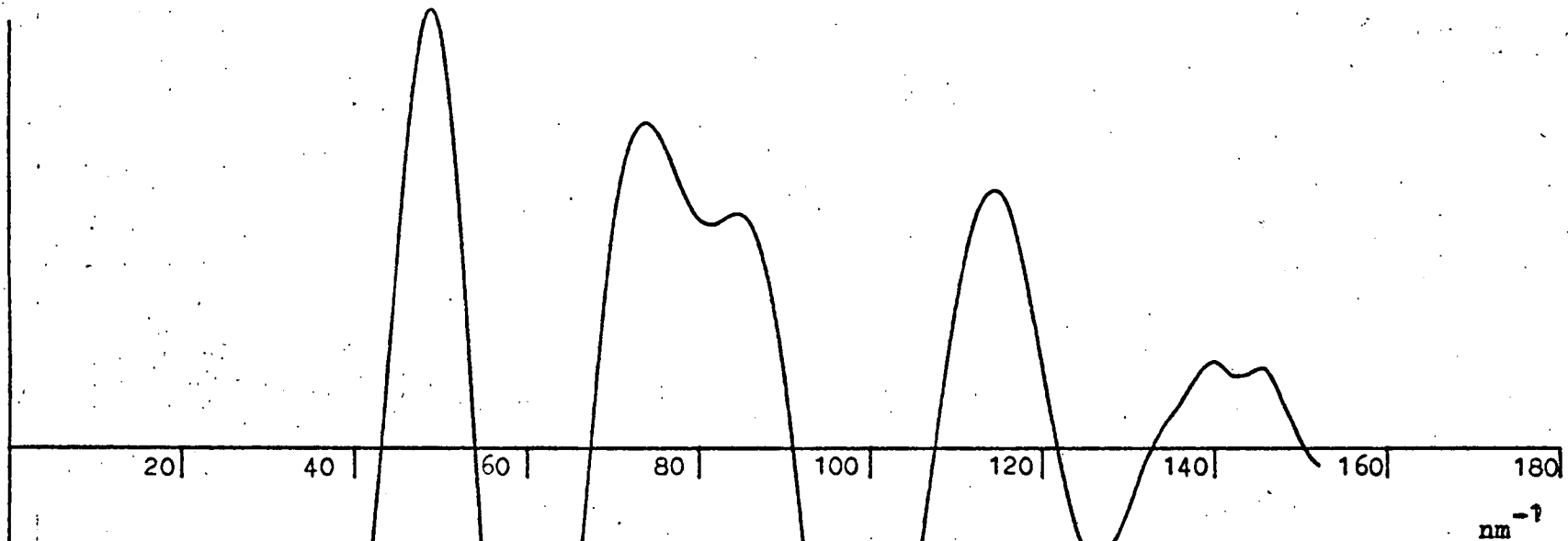
Least Squares Correlation Matrix Multiplied by 100

r1	r2	r3	<1	<2	<3	<4	u1	u2	u3	u4	u5	u7	u8	k1	k2	k3	
100	-54	-5	-62	29	7	15	7	-20	-10	-34	4	1	-4	-25	-42	-21	r1
	100	-7	41	-14	24	-47	-2	19	7	24	-2	5	1	24	33	14	r2
		100	14	-19	-24	22	-19	2	4	5	-13	-5	8	3	8	3	r3
			100	-62	-2	-25	-7	24	10	17	-12	-41	6	24	38	21	<1
				100	-30	-24	-3	-4	4	-51	13	21	12	-1	-5	-6	<2
					100	-90	28	-5	-16	17	-27	-8	-14	-11	-23	-8	<3
						100	-25	-10	8	-16	27	16	10	-5	-1	-4	<4
							100	39	-12	11	-1	5	-4	11	5	4	u1
								100	29	25	4	16	9	65	58	25	u2
									100	10	11	11	8	40	35	11	u3
										100	-5	50	-13	23	38	27	u4
											100	9	0	26	8	-14	u6
												100	-2	17	22	14	u7
													100	10	13	6	u8
														100	51	18	k1
															100	31	k2
																100	k3



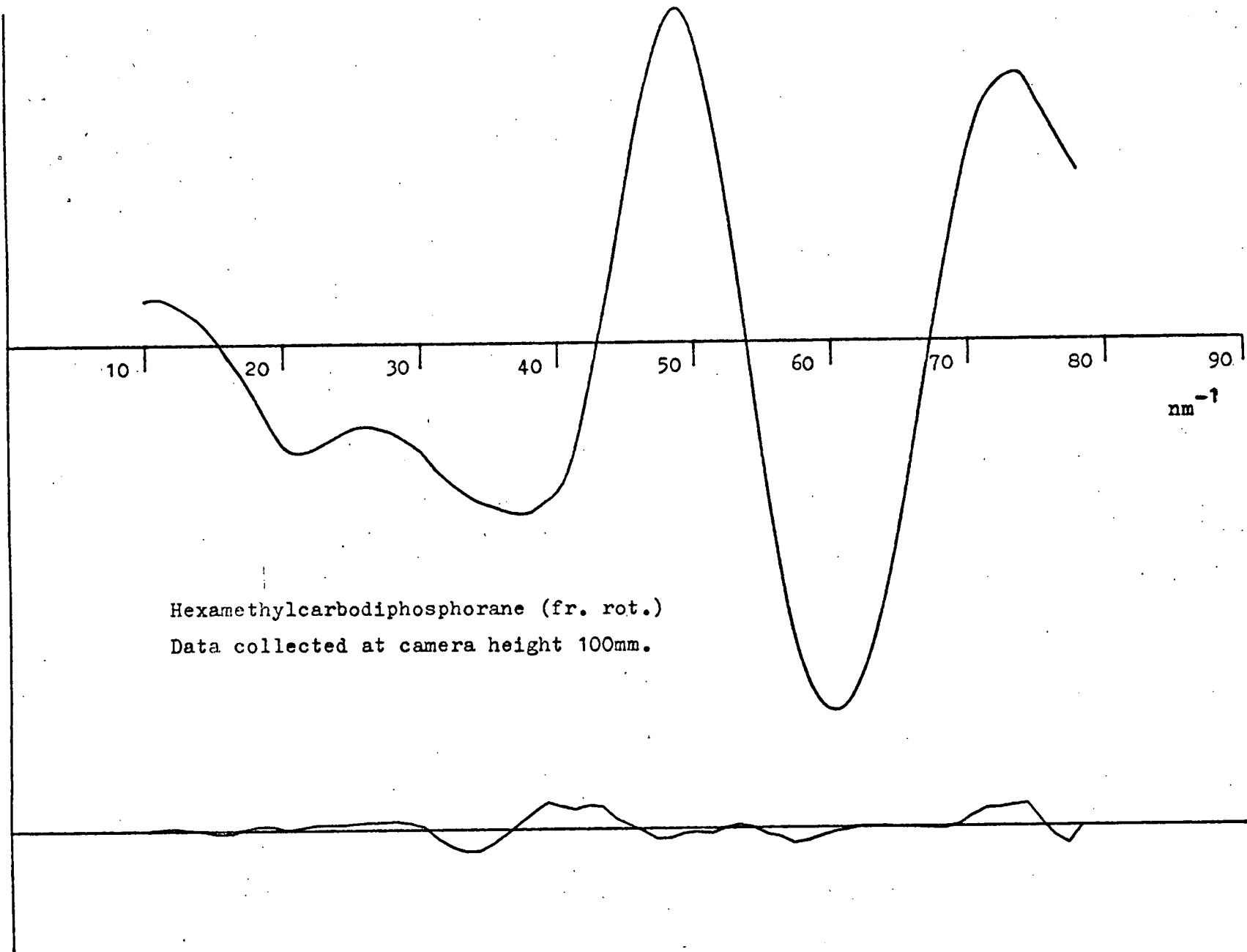


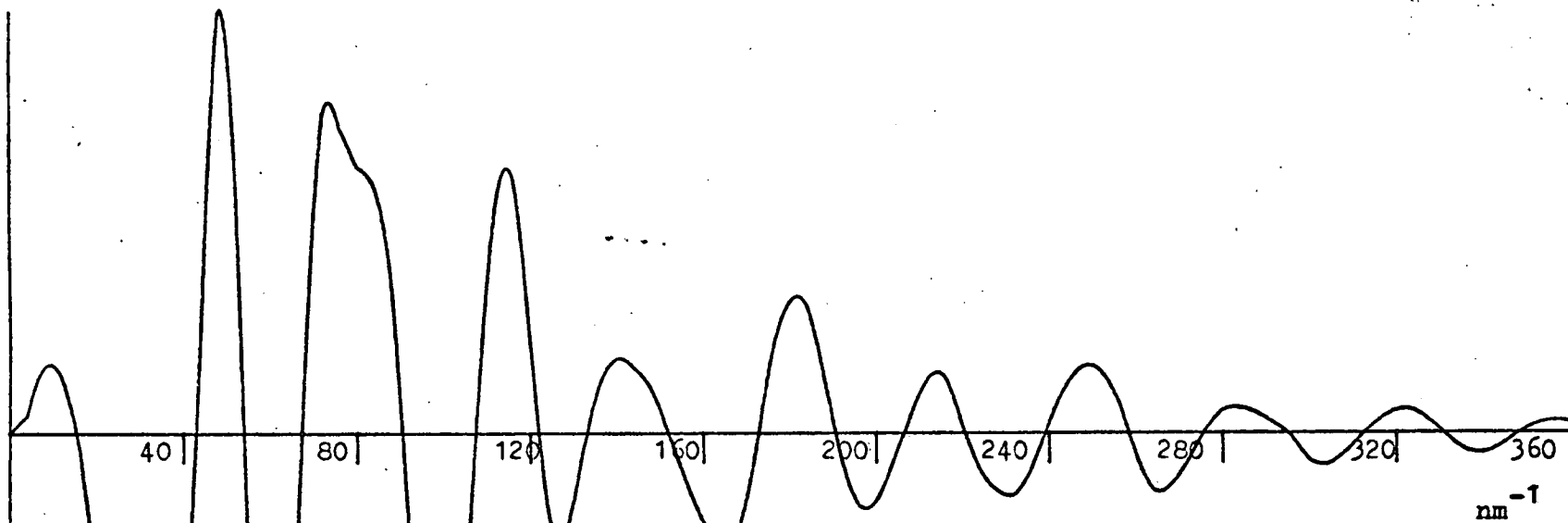
Hexamethylcarbodiphosphorane (fr. rot.)  
Data collected at camera height 25mm.



Hexamethylcarbodiphosphorane (fr. rot.)

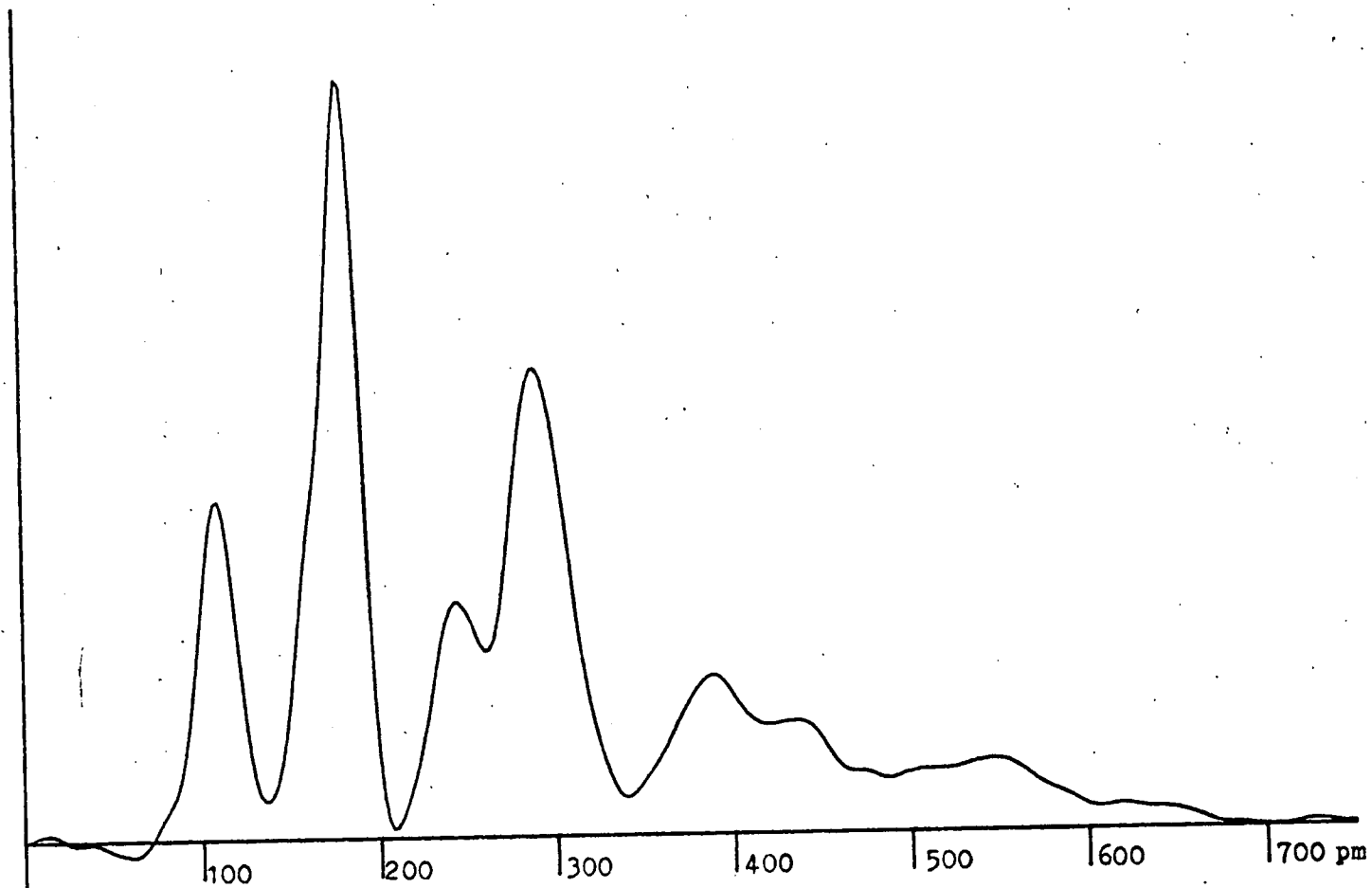
Data collected at camera height 50mm.





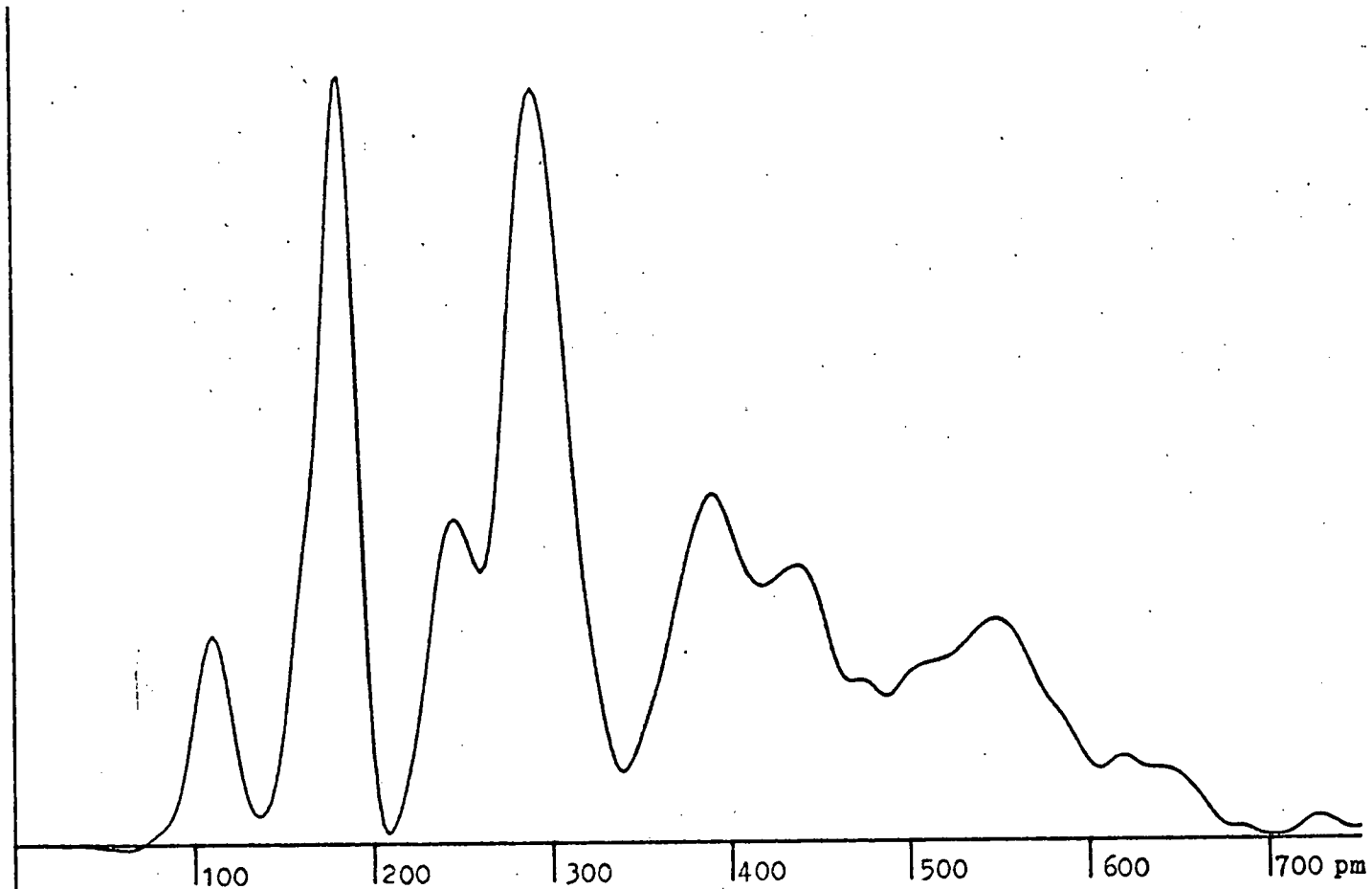
Hexamethylcarbodiphosphorane (fr. rot.)

Combined data collected at camera heights 25, 50 and 100mm.



Hexamethylcarbodiphosphorane (fr. rot.)

$P(r)/r$



Hexamethylcarbodiphosphorane (fr. rot.)

P(r)

### 9.3 Conclusions

In the structure obtained using model A, the P-C(central) bond length is less than that for P-C(methylene) in trimethyl-(methylene)phosphorane (161.1(5) pm as opposed to 164.0(6) pm). This shortening of the bond length suggests that there is more s character in P-C(central) than in P-C(methylene) and is commonly found on going from a triply connected carbon atom to a doubly connected carbon atom.

In the structure obtained using model B, the PCP angle is even wider than that obtained using model A and is now quite readily explained in terms of the shrinkage effects outlined at the beginning of this chapter. The results obtained using model B strongly indicate that the molecule is a symmetric top in the ground state. The P-C(central) bond is shorter than that obtained in refinements using model A suggesting that the central carbon atom is sp hybridised. In the case of linear  $(\text{Ph}_3\text{PNPPH}_3)^+$  the bond of P-N is 153 pm (as opposed to 157 - 158 pm at other PNP angles), if adjustments were made for the different central atom in each case, the substitution of a carbon for nitrogen in the PNP unit would give a P-C bond length of 159 pm, which is almost the value of P-C(central) determined in 9.2.

Establishment of free rotation about the P-C(central) bonds also points strongly to the molecule being a symmetric top. If the molecule has  $D_{3h}$ ,  $D_{3d}$  or  $D_3$  symmetry, the p orbitals on the central carbon atoms fall into two types. The first type is that of the  $p_z$  which falls on the  $C_3$  axis (which is also the PCP bond axis) and is a unique p orbital of the same

symmetry as the s orbital on the central carbon atom, therefore allowing orbital mixing to occur (c/f sp hybridisation). The remaining orbitals,  $p_x$  and  $p_y$ , form a degenerate pair and can undergo an infinite number of linear combinations to form an infinite number of arrangements of pairs of orthogonal p orbitals about the  $C_3$  axis. On the phosphorus atoms, the  $d_{xz}$  and  $d_{yz}$  orbitals form similar degenerate pairs.  $\Pi$ -bonding between  $P(CH_3)_3$  units and the central carbon atom (p-d  $\Pi$ -bonding) is therefore not restricted to specific orientations of the  $P(CH_3)_3$  units.

If the PCP unit is bent,  $D_3$  symmetry is lost and  $C_{2v}$  or  $C_2$  symmetry begins to operate. In  $C_2$  symmetry, the unique p orbital,  $p_z$ , now lies on the  $C_2$  axis (in  $D_3$  symmetry this was one of the orbitals which made up the degenerate pair) and is of the same symmetry as the s orbital on the central carbon atom, allowing orbital mixing to occur and giving  $p_z$  the capacity for  $\sigma$ -bonding. Of the other two orbitals,  $p_x$  points in the general direction of the phosphorus atoms and is also capable of  $\sigma$ -bonding (c/f  $sp^2$  hybridisation). Of the degenerate pairs of d orbitals in  $D_3$  symmetry, one (now  $d_{xz}$ ) is capable of some  $\sigma$ -overlap with  $p_x$  on the central carbon atom. The remaining d orbitals  $d_{yx}$  and  $p_y$  on the central carbon atom are the only orbitals which can now undergo pure  $\Pi$ -bonding and alignment of these orbitals, so as to maximise  $\Pi$ -overlap is required to obtain maximum  $\Pi$ -bonding. An electronic barrier to rotation of  $P(CH_3)_3$  units has been introduced, which will increase as the PCP angle decreases and  $C_2$  symmetry further governs the system.



It is uncertain if the electronic barrier would be large enough to prevent free rotation. It would appear from the refinement using model B that free rotation is occurring and is not stopped by the bending vibration.

In the results for  $(\text{Ph}_3\text{PNPPh}_3)^+$  and  $\text{Ph}_3\text{PCPPPh}_3$ , values for the PXP angle below  $130^\circ$  are not found. This suggests that the potential well for the bending vibration in  $(\text{CH}_3)_3\text{PCP}(\text{CH}_3)_3$  has a fairly flat bottom, but rises as the PCP angle falls below  $130^\circ$ , when interaction between  $\text{P}(\text{CH}_3)_3$  units (also preventing free rotation) begins to occur. The frequency of the bending vibration would be expected to have a very low value ( $80\text{ cm}^{-1}$  or less) and has not, to date, been satisfactorily assigned.

It is difficult to see what further work could, at present, be done on this compound. It appears, from the amplitudes (P...P is less than expected and P-C(central) is more than expected), that, during the PCP bending vibration, the central carbon atom moves a great deal more than the phosphorus atoms and that  $\text{C}_3$  symmetry of  $\text{CP}(\text{CH}_3)_3$  groups may be lost due to the  $\text{P}(\text{CH}_3)_3$  units lagging behind the central carbon atom during the bending vibration. Also, the rotation may not be strictly free and the carbon density at points on the circumference of the carbon phosphorus cone may be related to the PCP angle during the vibration. Mathematical models could be written which could deal with non- $\text{C}_3$   $\text{CP}(\text{CH}_3)_3$  symmetry and non-free rotation as outlined above, but they would require computing programs which could cope with many more parameters than the present programs are capable of doing and a computer which can operate at higher speeds than the present machine.

A similar model to model A was used in the structure determination of hexamethyldisiloxane<sup>73</sup>. The value for the SiOSi angle and the Si(CH<sub>3</sub>)<sub>3</sub> torsion (144° and 30°) agree well with the corresponding parameters in 9.1; PCP angle and P(CH<sub>3</sub>)<sub>3</sub> torsion (148° and 31°). In view of this similarity it may be worthwhile to attempt a structure determination of hexamethyldisiloxane using a model similar to model B.

**Chapter 10**  
**Experimental**

## 10 Experimental

### Equipment

Volatile compounds were handled on a conventional Pyrex vacuum line with ground glass taps and joints. Appropriate grades of Apiezon grease were applied to all ground glass taps and joints. Quantities of volatile compounds were measured in known volumes using a glass spiral gauge to measure pressure. Reactions involving volatile compounds were carried out in Pyrex tap-ampoules fitted with greaseless Soveril taps or in sealed Pyrex n.m.r. tubes. Air sensitive compounds were prepared on a conventional nitrogen line (or Schlenk line). High purity  $N_2$  (B.O.C. White Spot Nitrogen specified less than 0.5%  $H_2O$  and  $O_2$ ) was passed through columns of NaOH pellets and  $CaCO_3$  before going into the line. The facility for removing unwanted gases from reaction vessels by suction was available. The pressure in the line was maintained marginally above atmospheric pressure. Preparations were carried out in Pyrex reaction vessels and agitated with Pyrex or Teflon coated magnetic stirrer bars. Solutions and slurries were transferred between vessels using Pyrex syringes with stainless steel needles. Air sensitive solids were transferred between vessels in a V.A.C. Model HE-493 glove box equipped with a V.A.C. Model HE-493 Dri-Train (sic.). High purity nitrogen was fed directly from a cylinder into the body of the box and then continually circulated through the Dri-Train to remove contaminants. The pressure in the box was maintained marginally above atmospheric pressure by means of a Pedatrol attachment supplied by V.A.C. (California, U.S.A.).

$^{31}\text{P}$ ,  $^{19}\text{F}$  and  $^1\text{H}$  (in section 3.2 only) were obtained, using a Varian XL100 n.m.r. spectrometer, by pulsed (F.T.) methods. Remaining  $^1\text{H}$  n.m.r. spectra were obtained using a Varian HA100 n.m.r. spectrometer operating in the HA mode and varying frequency. The HA100 spectrometer had been modified to allow heteronuclear spin decoupling experiments, the decoupling frequency being generated using a Schlumberger FS 30 frequency synthesiser. Decoupling frequencies collected from the frequency synthesiser were corrected and transformed into chemical shifts by the following procedure.

$$\nu/\text{Hz.} = \text{Frequency} + (Q - \text{Offset} - 100,000,000)(R/100,000,000)$$

$$\delta/\text{p.p.m.} = \frac{\nu - R}{R} \cdot 100,000,000$$

where  $Q$  is the operating frequency of the spectrometer as determined by the synthesiser,

$R$  is the reference frequency for the nucleus being decoupled

and the offset is the difference in Hz. of the sideband from the main locking frequency. (see below)

All proton resonances were measured using a reference frequency which was locked to the resonating frequency of T.M.S. : if this were not the case, a further adjustment would have to be made to the frequency from the synthesiser.

The HA100 spectrometer operated at approximately 100 MHz. and sidebands were generated on either side of the main frequency using a modulating frequency generated by the spectrometer itself.

When scanning the spectrum by varying frequency, it was necessary to use, as a locking frequency, the first upper sideband of the main locking frequency. Using the modulating frequency generated by the spectrometer, it was possible to observe resonances over a range of -1,000 Hz. to 1,000 Hz., although, by locking onto the first lower sideband and observing on frequency sweep, it was possible to extend this range down to -2,000 Hz. One consequence of locking onto the lower sideband, while scanning the spectrum by varying frequency, was that it was extremely difficult to decouple protons resonating in the region -1,000 to 1,000 Hz. from those resonating in the region -1,000 to -2,000 Hz. and vice versa. At a late stage in the work, the spectrometer was modified so that the modulating frequency could be supplied by a Muirhead decade oscillator and this greatly extended the observable range, while locked on the upper sideband, and facilitated homonuclear decoupling experiments. The homonuclear decoupling frequency was supplied by a Muirhead decade oscillator.

All chemical shifts are given in p.p.m. and measured relative to T.M.S. ( $^1\text{H}$ ), phosphoric acid ( $^{31}\text{P}$ ) or Arcton ( $\text{CCl}_3\text{F}$ ) ( $^{19}\text{F}$ ). All coupling constants are given in Hz. All n.m.r. samples were dissolved in deuterated solvents at concentrations of between 0.5 and 0.2 mmoles  $\text{ml}^{-1}$  and, with the exception of those in section 3.2, contained a small amount of T.M.S. All spectra were obtained using 5 mm n.m.r. tubes.

Infra-red spectra were recorded using a Perkin Elmer 457 grating spectrometer calibrated against polystyrene. Gas phase spectra were obtained using a gas cell fitted with KBr

plates and solid phase spectra were recorded from Nujol mulls on CsI plates (held in a sealed container in the cases of air sensitive compounds). The Nujol was dried over molecular sieve and the CsI plates were stored in a desiccator.

Analyses for carbon and hydrogen were carried out using a Perkin Elmer 240 Elemental Analyser. Compounds suspected to be air sensitive were sealed in aluminium pans under nitrogen.

### Solvents

The following solvents were distilled and found to be sufficiently pure without further treatment:- T.M.S.,  $d_6$ -benzene,  $d_2$ -methylene chloride,  $d_8$ -toluene and commercially dried Acetone.

Other solvents were purified as follows:-

Benzene --- analar grade distilled off sodium wire.

Toluene --- analar grade distilled off sodium wire.

Methylene chloride --- distilled off molecular sieve.

Cyclohexane--- distilled off molecular sieve.

Purity was checked using n.m.r. spectroscopy.

### Preparations of Group IVb Compounds

Compound	Method	Reference
$\text{SiH}_4$	$\text{SiCl}_4 + \text{LiAlH}_4$	74
$\text{PhSiH}_3$	$\text{PhSiCl}_3 + \text{LiAlH}_4$	75
$\text{SiH}_3\text{Br}$	$\text{PhSiH}_3 + \text{HBr}$	75
$\text{SiH}_3\text{Cl}$	$\text{SiH}_3\text{Br} + \text{HgCl}_2$	76
$(\text{SiH}_3)_3\text{N}$	$\text{SiH}_3\text{Cl} + \text{NH}_3$	77
$\text{SiH}_3\text{I}$	$(\text{SiH}_3)_3\text{N} + \text{HI}$	77
$\text{SiH}_2\text{F}$	$\text{SiH}_3\text{I} + \text{SbF}_3$	79
$\text{Si}_2\text{H}_6$	$\text{Si}_2\text{H}_6 + \text{LiAlH}_4$	80

Compound	Method	Reference
$\text{H}_3\text{CSiH}_3$	$\text{H}_3\text{CSiCl}_3 + \text{LiAlH}_4$	81
$(\text{SiH}_3)_2\text{O}$	$\text{SiH}_3\text{Br} + \text{N}(\text{CH}_3)_3$ then $\text{H}_2\text{O}$	82
$\text{H}_2\text{S}$	$\text{Fe}_2\text{Se}_3 + \text{H}_2\text{SO}_4$	83
$(\text{SiH}_3)_2\text{S}$	$\text{H}_2\text{S} + (\text{SiH}_3)_3\text{N}$ then $\text{SiH}_3\text{Cl}$	84
$\text{Al}_2\text{Se}_3$	Stoichiometric mixture of powdered Se and Al ignited with Mg ribbon -- violent reaction.	
$\text{H}_2\text{Se}$	$\text{Al}_2\text{Se}_3 + \text{H}_2\text{SO}_4$	83
$(\text{SiH}_3)_2\text{Se}$	$\text{H}_2\text{Se} + (\text{SiH}_3)_3\text{N}$ then $\text{SiH}_3\text{Cl}$	84
$(\text{SiH}_3)_3\text{P}$	$\text{KPH}_2 + \text{SiH}_3\text{Br}$	85
$\text{GeH}_4$	$\text{GeO}_2 + \text{KOH} + \text{KBH}_4 + \text{Glac. Acetic Acid.}$	86
$\text{GeH}_3\text{Cl}$	$\text{GeH}_4 + \text{SnCl}_2$	87
$\text{GeH}_3\text{F}$	$\text{GeH}_3\text{Br} + \text{PbF}_2$	88
$\text{GeH}_3\text{Br}$	$\text{GeH}_3\text{Cl} + \text{HBr}$	89
$\text{GeH}_3\text{I}$	$\text{GeH}_3\text{Cl} + \text{HI}$	90

Purity of group IVb compounds was checked using infra-red spectroscopy.  $(\text{SiH}_3)_3\text{P}$  was kindly provided by Mr D. Hutchison.

### 10.1 Iridium Starting Materials (Ir(I) compounds)

$\text{Ir}(\text{CO})\text{Cl}(\text{PPh}_3)_2$  was produced by refluxing  $\text{IrCl}_3 \cdot 3\text{H}_2\text{O}$  with triphenylphosphine in dimethylformamide under nitrogen <sup>91</sup>.

$\text{IrH}(\text{CO})(\text{PPh}_3)_3$  was produced by reducing  $\text{Ir}(\text{CO})\text{Cl}(\text{PPh}_3)_2$  with  $\text{NaBH}_4$  in ethanol under nitrogen <sup>92</sup>.

$\text{Ir}_2\text{Cl}_2(\text{cyclo-octene})_4$  was produced by refluxing  $\text{IrCl}_3 \cdot 3\text{H}_2\text{O}$  with cyclo-octene in isopropanol and  $\text{H}_2\text{O}$  under nitrogen <sup>93</sup>.



Ir(CO)Cl(PEt<sub>3</sub>)<sub>2</sub>

Ir<sub>2</sub>Cl<sub>2</sub>(cyclo-octene) (0.447g) was stirred to a slurry under N<sub>2</sub> in degassed acetone (5 mls). Triethylphosphine (0.240g) was dissolved in acetone (5 mls), degassed and kept under nitrogen. At room temperature, CO was bubbled at a slow rate through the slurry until the orange colour was replaced by a deep blue (approximately 4 mins). The solution of Et<sub>3</sub>P was added gradually and the reaction stirred rapidly until a yellow solution was obtained. The solvent was evaporated off at reduced pressure and the product maintained at 80°C for 90 minutes. The product sublimed at 120°C in vacuum giving yellow crystals which could be handled for short periods in air, but which deteriorated after about 30 minutes in air. The yield varied, depending on the quality of the IrCl<sub>3</sub>.3H<sub>2</sub>O used in the preparation of the cyclo-octene dimer.

Ir(CO)I(PEt<sub>3</sub>)<sub>2</sub> was prepared by reaction of a 100% excess of NaI with Ir(CO)Cl(PEt<sub>3</sub>)<sub>2</sub>. This could be done at two stages: a (CH<sub>3</sub>)<sub>2</sub>CO solution of NaI could be added to the reaction mixture after the addition of Et<sub>3</sub>P (see above) and the sublimation carried out at 140°C or NaI and Ir(CO)Cl(PEt<sub>3</sub>)<sub>2</sub> could be reacted in degassed acetone, the acetone removed and the sublimation carried out at 140°C. The latter method was found to give the better yield (approx. 80%).

Purity of Ir(I) compounds was checked by infra-red and <sup>31</sup>P n.m.r. spectroscopies.

### 10.2.1 $\text{Ir}(\text{CO})\text{X}(\text{PEt}_3)_2 + \text{MH}_3\text{X}$

In a typical reaction, 0.2 mmoles of  $\text{Ir}(\text{CO})\text{X}(\text{PEt}_3)_2$  was weighed into a dry n.m.r. tube and the tube evacuated. Solvents were condensed into the tube (benzene for reaction with  $\text{SiH}_4$  and  $\text{GeH}_4$ , toluene for all others, and a small amount of T.M.S.) and lastly 0.2 mmoles  $\text{MH}_3\text{X}$ . The tube was sealed under vacuum and stored at  $-196^\circ\text{C}$ . The tubes were allowed to warm up and react in the n.m.r. spectrometer.

After reaction was complete and the n.m.r. recorded the tubes containing products from  $\text{Ir}(\text{CO})\text{Cl}(\text{PEt}_3)_2$  where exchange had not taken place were opened under nitrogen and the contents transferred to greaseless tap-ampoules and the solvent removed, giving gums. Cyclohexane was condensed onto the gums and subsequently evaporated off in an attempt to isolate a solid, but in the majority of cases this was not successful. Despite rigorous precautions, in the handling of  $\text{Ir}(\text{CO})\text{I}(\text{PEt}_3)_2$ , to exclude oxygen, every n.m.r. tube, except one, containing this compound, contained an appreciable amount of apparently inert  $\text{Ir}(\text{CO})\text{I}(\text{PEt}_3)_2 \cdot \text{O}_2$  and no attempt was made to isolate the contaminated products as the solubilities of the group IVb complexes and the oxygen adduct in common solvents were found to be similar and therefore separation of the compounds was complicated.

Solid compounds isolated:-

$\text{IrH}(\text{CO})\text{Cl}(\text{PEt}_3)_2\text{SiH}_3$	m.p. 77-78 $^\circ\text{C}$		
Analysis	Found	27.5 %C	6.1 %H
	Expected	29.8 %C	6.5 %H

I.R. spectrum  $\nu_{\text{CO}}$  1975  $\text{cm}^{-1}$   $\nu_{\text{SiH}}$  2095  $\nu_{\text{IrH}}$  not observed  
 also unassigned peaks at 930, 840, 800, 485, 469  
 and 450  $\text{cm}^{-1}$  possibly due to  $\delta_{\text{SiH}}$   $\tau_{\text{SiH}}$   $\delta_{\text{CO}}$  or  $\delta_{\text{IrH}}$

$\text{IrH}(\text{CO})\text{I}(\text{PET}_3)_2\text{SiH}_2\text{Br}$  m.p. 87-88°C

Analysis Found 22.4 %C 4.5 %H

Expected 22.6 %C 4.7 %H

I.R. spectrum  $\nu_{\text{CO}}$  1977  $\text{cm}^{-1}$   $\nu_{\text{SiH}}$  2066  $\text{cm}^{-1}$   $\nu_{\text{IrH}}$  not observed  
 also unassigned peaks at 980, 830, 613, 570, 480,  
 462, 436, 400 and 335  $\text{cm}^{-1}$  possibly due to  $\delta_{\text{CO}}$   $\delta_{\text{SiH}}$   
 $\tau_{\text{SiH}}$  or  $\nu_{\text{SiBr}}$

### 10.2.2 $\text{IrH}(\text{CO})(\text{PPh}_3)_3 + \text{MH}_3\text{X}$

n.m.r. samples were made up as in 10.2.1, but on a 0.5 mmole  $\text{ml}^{-1}$   
 scale, on account of the low solubility of the products. Also  
 T.M.S. was omitted and  $\text{C}_6\text{D}_6$  was used as solvent in every case.

### 10.3.1 $\text{Ir}(\text{CO})\text{Cl}(\text{PET}_3)_2 + \text{H}_3\text{SiMH}_3$

n.m.r. samples were made up as in 10.2.1. The products were  
 intractable gums which could not be crystallised from cyclohexane.

### 10.3.2 $\text{IrH}(\text{CO})(\text{PPh}_3)_3 + \text{H}_3\text{SiMH}_3$

n.m.r. samples were made up as in 10.2.2. The iridium complex  
 produced by the reaction was contaminated with triphenylphosphine  
 which was produced during the reaction. The iridium product  
 proved to be soluble in all the common solvents in which tri-  
 phenylphosphine is soluble and separation of the products could  
 not be achieved. No further attempt was made to characterise  
 the products other than by n.m.r.

#### 10.4.1 $\text{Ir}(\text{CO})\text{I}(\text{PEt}_3)_2 + (\text{SiH}_3)_2\text{O}$

Reactions were carried out in a greaseless tap-ampoule to the side of which was fitted an n.m.r. tube which was open to the bulk of the ampoule.  $\text{Ir}(\text{CO})\text{I}(\text{PEt}_3)_2$  (approx. 0.2mmoles : due to the presence of varying amounts of  $\text{Ir}(\text{CO})\text{I}(\text{PEt}_3)_2 \cdot \text{O}_2$ , it is difficult to weigh out this compound precisely) was weighed into the ampoule under nitrogen and the ampoule evacuated. Benzene was distilled into the ampoule and the Ir(I) compound allowed to dissolve.  $(\text{SiH}_3)_2\text{O}$  (0.2 mmoles or 0.1 mmoles) was condensed into the ampoule at  $-196^\circ\text{C}$  and the reaction mixture allowed to come to room temperature and shaken vigorously until reaction was complete. The ampoule was evacuated and fresh benzene distilled into the ampoule. This process was repeated twice and finally  $\text{C}_6\text{D}_6$  was used to dissolve the resulting gum. After the addition of a small amount of T.M.S., the solution was transferred to the n.m.r. tube and the tube sealed.

One of the 1:1 molar ratio reactions contained only a small trace of  $\text{Ir}(\text{CO})\text{I}(\text{PEt}_3)_2 \cdot \text{O}_2$  and an unsuccessful attempt was made to isolate a solid product by precipitation from cyclohexane.

#### 10.4.2 $\text{Ir}(\text{CO})\text{I}(\text{PEt}_3)_2 + (\text{SiH}_3)_2\text{Z}$

Reactions were carried out as in 10.4.1. The n.m.r. spectra indicated that a mixture of products was formed (see 4.2) and no attempt was made to characterise these products further.

#### 10.5.1 $\text{Ir}(\text{CO})\text{I}(\text{PEt}_3)_2 + (\text{SiH}_3)_3\text{P}$

This reaction was carried out in an ampoule of the type described in 10.4.1.  $\text{Ir}(\text{CO})\text{I}(\text{PEt}_3)_2$  (0.2 mmoles) was weighed

into the ampoule, under nitrogen and the ampoule was evacuated. The  $\text{Ir}(\text{CO})\text{I}(\text{PEt}_3)_2$  was dissolved in neat  $(\text{SiH}_3)_3\text{P}$  (approx. 1 ml). Reaction was slow, but was greatly accelerated by the addition of benzene (approx. 1 ml). When reaction was complete the ampoule was evacuated and fresh benzene was distilled into the ampoule. This procedure was repeated twice and  $\text{C}_6\text{D}_6$  plus a small amount of T.M.S. was used to dissolve the product. The solution was tipped into the n.m.r. tube and the tube sealed. Although the major product was the mono-added species, some of the bis-species was also present and no attempt was made to characterise the product further.

#### 10.5.2 $2\text{Ir}(\text{CO})\text{I}(\text{PEt}_3)_2 + (\text{SiH}_3)_3\text{P}$

The n.m.r sample was made up as in 10.2.1 using  $\text{Ir}(\text{CO})\text{I}(\text{PEt}_3)_2$  (0.2 mmoles),  $\text{C}_6\text{D}_6$ , T.M.S. and  $(\text{SiH}_3)_3\text{P}$  (0.1 mmoles). The reaction mixture was warmed gradually to room temperature and shaken vigorously until the reaction was complete. The n.m.r. spectrum confirmed that the major product was the bis-added species but also indicated the presence of small amounts of the mono- and tris-added species. No further characterisation of the product was attempted.

#### 10.5.3 $3\text{Ir}(\text{CO})\text{I}(\text{PEt}_3)_2 + (\text{SiH}_3)_3\text{P}$

The n.m.r. sample was made up as in 10.5.2 using  $\text{Ir}(\text{CO})\text{I}(\text{PEt}_3)_2$  (0.3 mmoles) and  $(\text{SiH}_3)_3\text{P}$  (0.08 mmoles). A solid product was precipitated out of the benzene solution of the tris-added species on the addition of cyclohexane and collected, under nitrogen, on a frit. The excess  $\text{Ir}(\text{CO})\text{I}(\text{PEt}_3)_2$  was removed by washing with T.M.S., but the impurity of  $\text{Ir}(\text{CO})\text{I}(\text{PEt}_3)_2 \cdot \text{O}_2$  could not be removed. However attempts were made to characterise the

product further. m.p. 103-107°C

Analysis Found 25.2 %C 4.9 %H

Expected: 22.1 %C 5.3 %H

I.R. spectrum  $\nu_{\text{CO}}$  1970  $\text{cm}^{-1}$   $\nu_{\text{SiH}}$  2070  $\text{cm}^{-1}$   $\nu_{\text{IrH}}$  not observed.  
also an unassigned peak at 440  $\text{cm}^{-1}$  possibly  
due to  $\nu_{\text{PSi}}$

The spectrum also contained a peak at 2010  $\text{cm}^{-1}$   
( $\nu_{\text{CO}}$  of  $\text{Ir}(\text{CO})\text{I}(\text{PEt}_3)_2 \cdot \text{O}_2$ )

10-appendix  $\text{Ir}(\text{CO})\text{Cl}(\text{PEt}_3)_2 + \text{H}_2\text{Se}$

The n.m.r. sample was made up as in 10.2.1 in equimolar ratio  
and using  $\text{C}_6\text{D}_6$  (70%)/ $\text{C}_6\text{H}_6$  (30%) as solvent (T.M.S. was omitted and  
 $\text{C}_6\text{H}_6$  used as a lock solvent because it was felt that there was  
a possibility of the  $\text{SeH}$  resonance arising about 0 p.p.m.).

A solid product was obtained directly on removing the solvent  
from the solution after the product had been characterised by  
n.m.r.

m.p. 109-110°C

Analysis Found 27.2 %C 5.5 %H

Expected 27.2 %C 5.6 %H

I.R. spectrum  $\nu_{\text{CO}}$  2000  $\text{cm}^{-1}$   $\nu_{\text{IrH}}$  and  $\nu_{\text{SeH}}$  2180 and 2190  
 $\text{cm}^{-1}$  also unidentified peak at 840  $\text{cm}^{-1}$  probably

$\delta_{\text{CO}}$

The compounds analysed for C and H in 10.2-10-appendix (i.e.  
part one of the thesis) were sealed in aluminum pans. They  
were all found to decompose in air over a matter of days.

## 10.6 Gold Work

$\text{Et}_3\text{PAuCl}$  was made by the reduction of chloroauric acid by triethylphosphine and water in ethanol.<sup>78</sup>

### 10.6.1 $\text{Et}_3\text{PAuX} + \text{MH}_3\text{X}$

n.m.r. samples were made up as in 10.2.1.

### 10.6.2 $\text{Et}_3\text{PAuCl} + \text{H}_3\text{SiMH}_3$

n.m.r. samples were made up as in 10.2.1. The pressures of the silyl reactant and product were measured in the same volume and found to be the same. The production of  $\text{SiH}_4$  was verified by infra-red spectroscopy. The black tar (see text) proved to be intractable and no further characterisation was possible.

### 10.6.3 $(\text{Et}_2\text{P}(\text{CH}_2)_2)_2\text{Au}_2 + \text{SiH}_3\text{I}$

$(\text{Et}_2\text{P}(\text{CH}_2)_2)_2\text{Au}_2$  was kindly supplied by Professor H. Schmidbaur.<sup>54</sup>

An analogous preparation is outlined at the beginning of 8.1.

No attempt was made to isolate the low temperature product.

## 10.7 Electron Diffraction

Electron diffraction patterns were recorded on Kodak Electron Image Plates using a Balzers' MKD.G2 diffraction apparatus. The photographically recorded data were converted into digital form using a Joyce-Loebl automatic microdensitometer.

All calculations were carried out on a ICL 4-75 computer at the Edinburgh Regional Computing Centre using data reduction and least squares refinement programs, which have been described previously<sup>94</sup>. Scattering factors of Schäfer, Yates and Bonham were used in all calculations.<sup>95</sup>

## 10.8 Structure of $(\text{CH}_3)_3\text{PCH}_2$

## 10.8

The sample of trimethyl(methylene)phosphorane was supplied by Prof. H. Schmidbaur and was prepared by a route described earlier<sup>96</sup>. The sample was purified by fractional distillation and its purity was checked spectroscopically.

The sample was maintained at 325K and the nozzle at 347K during exposures at three camera heights, 250 (3 plates), 500 (3 plates) and 1000 mm (1 plate), giving data over a range of 15 to 292 nm<sup>-1</sup> in the scattering variable, s. The electron wavelength used (5.672 ± 0.002 pm) was determined from the diffraction pattern of gaseous benzene.

## 10.9 Structure of (CH<sub>3</sub>)<sub>3</sub>PCP(CH<sub>3</sub>)<sub>3</sub>

The sample of hexamethylcarbodiphosphorane was supplied by Dr C.O. Gasser and was prepared by a method described earlier<sup>97</sup>. The sample was purified by fractional distillation and its purity was checked spectroscopically.

The sample and the inlet nozzle were maintained at 350K during exposures at three camera heights, 250 (3 plates), 500 (3 plates) and 1000 mm (3 plates), giving data over a range of 10 to 296 nm<sup>-1</sup> in the scattering variable, s. The electron wavelength used (5.661(5) pm) was determined from the diffraction pattern of gaseous benzene.



References

1. G.L.Geoffroy & R.Pierantozzi, J. Amer. Chem. Soc. 98(1976)8054.
2. L.Vaska & J.W.Di Luzio, J. Amer. Chem. Soc. 83(1961)2784.
3. M.Anoletta, Gazz. Chim. Ital. 89(1959)2539.
4. L.Vaska & J.W.Di Luzio, J. Amer. Chem. Soc. 84(1962)679.
5. Transition Metal Complexes of Phosphorus, Arsenic and Antimony Ligands. Editor: C.A.McAuliffe (1973) Macmillan Press Ltd. London.....page 116.
6. L.Vaska & S.S.Bath, J. Amer. Chem. Soc. 85(1963)3500.
7. L.Vaska, Science 140(1963)809.
8. J.LaPlaca & J.A.Ibers, J. Amer. Chem. Soc. 87(1965)2581
9. P.B.Chalk & J.Halpern, J. Amer. Chem. Soc. 88(1966)3511.
10. M.A.Bennet, R.J.H.Clark & D.L.Milner, Inorg. Chem. 6(1967)1647.
11. J.M.Jenkins & B.L.Shaw, J. Chem. Soc. (1965)6789.
12. L.Vaska, Acc. Chem. Res. 1(1968)335.
13. A.J.Deeming & B.L.Shaw, J. Chem. Soc. (A)(1969)1128.
14. J.P.Collman & C.T.Seers Jr., Inorg. Chem. 7(1968)27.
15. A.J. Deeming & B.L.Shaw, Chem. Comm. (1968)751.  
A.J. Deeming & B.L.Shaw, J. Chem. Soc. (A)(1969)1562.
16. D.M.Blake & M.Kubota, Inorg. Chem. 9(1970)989.
17. M.C.Ball & J.M.Pope, J. Chem. Soc. Dalton (1973)1802.
18. R.W.Johnson & R.G.Pearson, Chem. Comm. (1970)986.  
R.G.Pearson & W.R.Muir, J. Amer. Chem. Soc. 92(1970)5519.
19. F.R.Jenson & B.Knickel, J. Amer. Chem. Soc. 93(1971)6339.  
G.M.Whitesides & D.J.Baschetto, J. Amer. Chem. Soc. 93(1971)1529.  
F.R.Jenson & D.D.Davis, J. Amer. Chem. Soc. 93(1971)4048.
20. J.A.Labinger, A.U.Kramer & J.A.Osborn, J. Amer. Chem. Soc. 95(1973)7908.

21. J.S.Bradley, D.E.Connor, D.Dolphin, J.A.Labinger & J.A.Osbarn, *J. Amer. Chem. Soc.* 94(1972)4043.
22. A.J.Chalk, *Chem. Comm.* (1969)1207.
23. L.H.Sommer, J.E.Lyons & H.Fujimoto, *J. Amer. Chem. Soc.* 91(1969)7051.
24. J.F.Harrodd, D.F.R.Gibson & R.Charles, *Canad. J. Chem.* 47(1969)2205.
25. F.Glockling & M.O.Wilbey, *Chem. Comm.* (1969)286.  
F.Glockling & M.O.Wilbey, *J. Chem. Soc. (A)*(1970)1657.
26. L.Vaska & R.E.Rhodes, *J. Amer. Chem. Soc.* 87(1965)4970.
27. G.G.Eberhardt & L.Vaska, *J. Catalysis* 8(1967)183.
28. J.K.Nicholson & B.L.Shaw, *Tet. Letters* (1965)3533.
29. B.R.James & N.A.Memon, *Canad. J. Chem.* 46(1968)217.
30. J.Powell & B.L.Shaw, *J. Chem. Soc. (A)*(1968)617.
31. W.Strohmeir & G.Osantos, *J. Organomet. Chem.* 72(1974)277.
32. C.U.Pittman Jr., S.E.Jacobson & H.Hiramoto, *J. Amer. Chem. Soc.* 97(1965)4774.
33. L.Vaska, *Inorg. & Nucl. Chem. Letters* 1(1965)89.
34. M.G.Burnett, R.J.Morrison & G.J.Strugnell, *J. Chem. Soc. Dalton* (1974)1663.
35. E.M.Hyde & B.L.Shaw, *J. Chem. Soc. Dalton* (1975)765.
36. E.M.Miller & B.L.Shaw, *J. Chem. Soc. Dalton* (1974)480.
37. C.A.Tolman, *J. Amer. Chem. Soc.* 92(1970)2956.
38. F.Glockling & M.D.Wilbey, *J. Chem. Soc. (A)*(1970)1675.
39. J.Chatt, N.P.Johnson & B.L.Shaw, *J. Chem. Soc.* (1964)1625.
40. G.Yagupsky, C.K.Brown & G.Wilkinson, *J. Chem. Soc. (A)*(1970)1392.
41. A.J.Chalk & J.F.Harrodd, *J. Amer. Chem. Soc.* 87(1965)16

42. H.Schmidbaur et al. Chem. Ber. in print.
43. Diana M. Leitch (Nee Bridges) Ph.D. Thesis 1973 Edinburgh.
44. Dr F. Reed to be published.
45. E.A.V.Ebsworth & D.M.Leitch, J. Chem. Soc. Dalton (1973)1287.
46. Inorganic Synthesis 15 82
47. S.O.Grim, R.L.Keiter & W. McFarlane, Inorg. Chem. 6(1967)1287.
48. J.M.Edwards Ph.D. Thesis 1976 Edinburgh.
49. F.G.Mann & Purdie, J. Chem. Soc. (1940)1235.
50. A. Almenningen, K.Hedburg & R.Seip, Acta. Chem. Scan.  
17(1963)2264, 2455.  
A.Almenningen, L.Fernholt & R.Seip, Acta. Chem. Scan.  
22(1968)51.
51. H.Singer & G.Wilkenson, J. Chem. Soc. (A)(1968)2516.
52. G.G.Coates & C.Parkin, J. Chem. Soc. (1962)3220.
53. Private Communication Prof.H.Schmidbaur et al.
54. H.Schmidbaur & R.Franke, Inorg, Chim. Acta. 13(1975)79.
55. H.Bock, Private Communication
56. H.Schmidbaur & W.Tronich, Chem. Ber. 101(1968)595.
57. W.Lüttke & K.Wilhelm, Angew. Chem. Internat. Ed. 4(1965)875.  
W.Sawody, Z. Anorg. Allg. Chem. 368(1969)284.
58. J.C.J.Bart, J. Chem. Soc. (B)(1969)350.
59. J.Buckle, P.G.Harrison, T.J.King & J.A.Richards, Chem. Comm.  
(1972)1104.
60. D.R.Lide, & D.E.Mann, J. Chem. Phys. 29(1958)94.
61. C.J.Wilkins, K.Hagen, L.Hedburg, Q.Sben & K.Hedburg,  
J. Amer. Chem. Soc. 97(1975)6352.
62. L.Pauling, The Nature of the Chemical Bond, 3rd. Edn.  
Cornell University Press, Ithica, New York, U.S.A. 1960.

63. C.O.Gasser Ph.D. Thesis 1977 T.U. Munich.
64. A.T.Vincent & P.J.Wheatly, J. Chem. Soc. (A)(1966)1703.
65. R.D.Wilson & R.Bau, J. Amer. Chem. Soc. 96(1974)7601.
66. J.K.Ruff, J.P.White & L.F.Dahl, J. Amer. Chem. Soc.  
93(1971)2159 and refs. therein.
67. H.B.Chin, M.B.Smith, R.D.Wilson & R. Bau.  
J. Amer. Chem. Soc. 96(1974)5285.
68. J.J.Daly & P.J.Wheatly, J. Chem. Soc. (A)(1966)1703.
69. J.J.Daly, J. Chem. Soc. (A)(1967)1913.
70. W.H.Weber & P.D.Maker, J. Mol. Spec. 66(1977)133.  
W.H.Weber & P.D.Maker, J. Chem. Phys. 64(1976)2149.
71. C.Glidewell, A.G.Robiette & G.M.Sheldrick,  
Chem. Phys. letters 16(1972)526.
72. J.A.Duckett, A.G.Robiette & I.M.Mills, J. Mol. Spec.  
62(1976)34.
73. B.Csákvári, Z.S.Wagner, P.Gömöry, F.C.Mijloff, B.Rozsondai  
& I.Hargittai, J. Organomet. Chem. 107(1976)287.
74. G.W.Bithke & M.K.Wilson, J. Organomet. Chem. 26(1957)1107.
75. D.Kummer & J.Fritz, Z. Anorg. Chem. 308(1961)105.  
*J.R.Hall, H.F.McKillop, D.G.McKean, N.Shepard & L.A.Woodward.*
76. E.A.V.Ebsworth et al. Spectrochim Acta 13(1958)202.
77. J.C.Thompson Ph.D. Thesis 1965 Cambridge.
78. F.D.Mann, A.F.Wells & D.Purdie, J. Chem. Soc. (1937)1828.
79. B.Borge, J.Bruhn & J. Rastrup-Anderson, Acta. Chem. Scan.  
8(1954)367.
80. A.E.Finholt, A.C.Bond, K.E.Wilzbach & H.L.Schleimer  
J. Amer. Chem. Soc. (1947)2692.
81. R.W.Shade & G.N.Cooper, J. Phys. Chem. 52(1958)1467.
82. E.A.V.Ebsworth & S.D.G.Henderson Private Communication.

83. G.Brauer, Handbook of Inorganic Chemistry Vol. 1  
Academic Press 1963.
84. H.F.Angus, S.Cradock, E.A.V.Ebsworth & C.Glidewell,  
J. Inorg. & Nucl. Chem. Lets 5(1969)717.
85. E.Amberger & H.Boeters, Angew. Chem. Int. Edn. 1(1962)52.
86. W.C.Jolly, J. Amer. Chem. Soc. 83(1961)335.
87. N.A.Hossmann, Ph.D. Thesis 1974 Edinburgh.
88. S.Cradock Private Communication.
89. S.Cradock & E.A.V.Ebsworth, J. Chem. Soc. (A)(1967)1226.
90. S.Cradock Ph.D. Thesis 1966 Cambridge.
91. Inorganic Synthesis 11 101.
92. Inorganic Synthesis 13 126.
93. Inorganic Synthesis 13 94, 15 18.
94. D.M.Bridges, G.C.Hollywell, D.W.H.Rankin & J.M.Freeman,  
J. Organomet. Chem. 32(1971)87.  
G.C.Hollywell, D.W.H.Rankin, B.Beagley & J.M.Freeman  
J. Chem. Soc. (A)(1971)785.
95. L.Schäfer, A.C.Yates & R.A.Bonham, J. Chem. Phys. 55(1971)3055
96. H.Schmidbaur & L.Trönich, Chem. Ber. 101(1968)595.
97. O.Gasser & H.Schmidbaur, J. Amer. Chem. Soc. 97(1975)6281.

Appendix  
Published Papers

## The Molecular Structure of Trimethyl(methylene)phosphorane in the Gas Phase, Determined by Electron Diffraction

E. A. V. Ebsworth\*, Thomas E. Fraser, and David W. H. Rankin

Department of Chemistry, University of Edinburgh,  
West Mains Road, Edinburgh, EH9 3JJ, Scotland

Received December 30, 1976

The molecular structure of trimethyl(methylene)phosphorane,  $(\text{CH}_3)_3\text{P}=\text{CH}_2$ , in the gas phase has been determined by electron diffraction. Principal distances are  $r_s(\text{P}-\text{C}) = 181.5(3)$ ,  $r_s(\text{P}=\text{C}) = 164.0(6)$  pm; and the angles between the  $\text{P}-\text{C}(\text{methyl})$  bonds are  $101.6(5)^\circ$ . These parameters lead to a value for the order of the highly polar  $\text{P}-\text{C}(\text{methylene})$  bond of about 2.0.

### Die Molekülstruktur von Trimethyl(methylen)phosphoran in der Gasphase aus einer Elektronenbeugungsuntersuchung

Die Molekülstruktur von Trimethyl(methylen)phosphoran,  $(\text{CH}_3)_3\text{P}=\text{CH}_2$ , in der Gasphase wurde durch Elektronenbeugung bestimmt. Wichtigste Atomabstände  $r_s$  sind  $\text{P}-\text{C} = 181.5(3)$  und  $\text{P}=\text{C} = 164.0(6)$  pm. Die Valenzwinkel zwischen den  $\text{P}-\text{C}(\text{Methyl})$ -Bindungen betragen  $101.6(5)^\circ$ . Diese Parameter ergeben für die stark polare  $\text{P}=\text{C}(\text{Methylen})$ -Bindung eine Bindungsordnung von etwa 2.0.

### Introduction

Compounds of the type  $\text{R}_3\text{PCXY}$  have attracted widespread interest, but particular attention has been paid to the nature of the phosphorus-carbon bond. This bond has orders of 1 and 2 in the extreme formal structures, 1 and 2, and evidence from various sources has been used to ascertain how the electronic structures of particular compounds can be



described relative to the extremes. Thus the values of  $^1J(\text{CH}(\text{methylene}))$  in trialkyl(methylene)phosphoranes (ca. 150 Hz)<sup>1)</sup> suggest that the orbital hybridisations of the carbon atoms are close to  $\text{sp}^2$ , and form 2 is appropriate. On the other hand, the low frequency chemical shift of the methylene protons has been interpreted<sup>2)</sup> as indicating that there is a negative charge on the methylene carbon atom, giving increased shielding of the protons. This fits better with the ylide form, 1. The assigned frequency of  $1006\text{ cm}^{-1}$  for the " $\text{P}=\text{C}$  stretching mode" in trimethyl(methylene)phosphorane has been used to

<sup>1)</sup> H. Schmidbaur and W. Tronich, Chem. Ber. 101, 595 (1968). — <sup>2)</sup> H. Schmidbaur, W. Buchner, and D. Scheutzw, ibid. 106, 1651 (1973).

calculate a force constant of  $5.59\text{ mdyne \AA}^{-1}$  for the stretching of the bond, and from this a bond order of 1.65 was derived<sup>2)</sup>.

Structural data have been obtained for many compounds of the type  $\text{Ph}_3\text{PCXY}$  in the solid phase. In these, the length of the central bond ranged from 175<sup>3)</sup> to 166<sup>4)</sup> pm for triply connected carbon: these bond lengths indicate  $\text{P}-\text{C}$  bond orders of between 1.4 and 2.0. There is little variation in  $\text{P}-\text{C}(\text{phenyl})$  bond lengths in this series of compounds, but the angles between the three  $\text{P}-\text{C}$  bonds are smallest in the compounds with the shortest  $\text{P}-\text{C}(\text{methylene})$  bonds.

In view of the wide range of crystal structures that has been determined, it is remarkable that no gas phase structures of  $\text{R}_3\text{PCXY}$  compounds have been reported. However, the derivatives in which  $\text{R} = \text{Ph}$  are not very volatile, and the analogous compounds in which  $\text{R} = \text{Me}$  are harder to handle, being highly reactive, and have only been isolated relatively recently<sup>5)</sup>. Consequently, it seemed worthwhile to us to undertake a study of trimethyl(methylene)phosphorane, and to obtain information about its structure in the gas phase free from crystal packing constraints. Such a study is also very important in the light of recent theoretical calculations on ylides, predominantly on the hypothetical molecule  $\text{H}_3\text{P}=\text{CH}_2$ <sup>5-7)</sup>. We present here the results of the study.

### Molecular Model

During refinements of the structure of trimethyl(methylene)phosphorane a model was used in which it was assumed that the three  $\text{P}-\text{CH}_3$  groups had local  $\text{C}_{3v}$  symmetry,

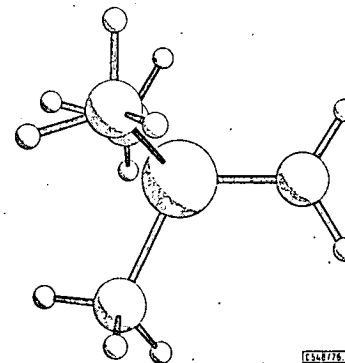


Fig. 1. Molecular Model of  $(\text{CH}_3)_3\text{P}=\text{CH}_2$

<sup>2)</sup> W. Sawodny, Z. Anorg. Allg. Chem. 368, 284 (1969); W. Lütke and K. Wilhelm, Angew. Chem. 77, 867 (1965); Angew. Chem., Int. Ed. Engl. 4, 875 (1965).

<sup>3)</sup> J. Buckle, P. G. Harrison, T. J. King, and J. A. Richards, J. Chem. Soc., Chem. Commun. 1972, 1104.

<sup>4)</sup> J. C. J. Bart, J. Chem. Soc. B 1969, 350.

<sup>5)</sup> R. Hoffmann, D. B. Boyd, and S. Z. Goldberg, J. Am. Chem. Soc. 92, 3929 (1970).

<sup>6)</sup> I. Absar and J. R. van Wazer, J. Am. Chem. Soc. 94, 2382 (1972).

<sup>7)</sup> K. A. Ostoja-Starzewski, H. tom Dieck, and H. Bock, J. Organomet. Chem. 65, 311 (1974). —

<sup>8)</sup> K. A. Ostoja-Starzewski, W. Richter, and H. Schmidbaur, Chem. Ber. 109, 473 (1976).

and that the whole molecule apart from the methylene hydrogen atoms had  $C_3$  symmetry. The P-CH<sub>2</sub> group was assumed to have  $C_{2v}$  local symmetry. With these constraints, the molecular geometry was defined by two P-C and two C-H bond lengths, PCH angles for the methyl and methylene groups, the twist angle of the methyl groups, defined as zero when one CH bond was *trans* to the P-C(methylene) bond, and the twist angle of the methylene group, defined as zero when the CH<sub>2</sub> plane also contained one P-C(methyl) bond (Fig. 1).

### Refinement and Results

The three geometrical parameters defining the skeletal structure, and three of the four amplitudes of vibration involving heavy atoms, all refined satisfactorily. These heavy atom distances account for the large peaks in the radial distribution curve (Fig. 2) at about 180 and 290 pm. The other substantial peaks in the radial distribution curve, at about 110, 240, and 380 pm, are due mainly to distances involving methyl hydrogen atoms. Thus it was possible to refine the C-H distance and PCH angle, and CH and P...H amplitudes of vibration, for the methyl groups. In addition, the twist angle of the groups was found by doing refinements with this angle and the methylene twist angle fixed at different values, and comparing the *R* factors obtained. One group of non-bonded C...H amplitudes of vibration was also refined. No parameters relating to the geometry of the methylene group were refined, as all the relevant peaks in the radial distribution curve coincided with more intense peaks representing distances associated with methyl hydrogen atoms. The refined values for the parameters associated with the methyl groups may therefore be slightly dependent on the assumed parameters for the methylene group: the quoted errors for these parameters have been increased to allow for this.

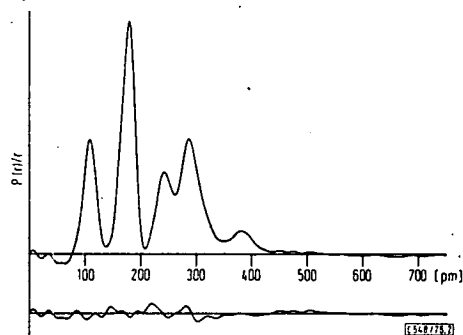


Fig. 2. Radial distribution curve,  $P(r)/r$ , for  $(CH_3)_3P=CH_2$ . Before Fourier inversion the data were multiplied by  $s \cdot \exp[-0.00002 s^2/(z_p - f_p)(z_c - f_c)]$ .

The parameters obtained in the best refinement, which converged to give  $R_C$  0.13 and  $R_D$  0.10, are listed in Table 1. Errors quoted in this table are estimated standard deviations, obtained in the least squares analysis, increased to allow for systematic errors and the

effects of the constraints of the molecular model. The least squares correlation matrix for this refinement is given in Table 2. Observed and final weighted difference intensity curves are shown in Fig. 3a-c.

Table 1. Molecular parameters for  $(CH_3)_3P=CH_2$

	Distance [pm]	Amplitude [pm]
Independent distances		
r1 (P=C)	164.0(6)	5.3(8)
r2 (P-C) (methyl)	181.5(3)	6.2(4)
r3 (C-H) (methyl)	109.9(5)	7.9(7)
r4 (C-H) (methylene)	106.0 (fixed)	7.1 (tied to <i>u</i> 3)
Dependent distances <sup>a)</sup>		
d5 (C...C)	281.2(34)	11.5(10)
d6 (C...C)	294.0(57)	
d7 (P...H) (methyl)	241.3(30)	11.6(6)
d8 (P...H) (methylene)	244.9(40)	
d9 (C...H) <sup>b)</sup>	374-396	17.8(16)
d10 (C...H) <sup>b)</sup>	277-342	15.0 (fixed)
Angles (degrees)		
1 (C=P-C)	116.5(6)	
2 (P-C-H) (methyl)	109.3(4)	
3 (P-C-H) (methylene)	128 (fixed)	
4 (methyl twist) <sup>c)</sup>	17 (see text)	
5 (methylene twist) <sup>c)</sup>	0 (fixed)	

<sup>a)</sup> Many H...H distances, not listed here, were included in the refinement.

<sup>b)</sup> C...H distances fell into two ranges. The limits of those ranges, and the amplitudes of vibration for individual distances, are given here.

<sup>c)</sup> For definition, see text.

Table 2. Least squares correlation matrix multiplied by 100

r1	r2	r3	<1	<2	u1	u2	u3	u5	u7	u9	k1	k2	k3	
100	31	-10	15	-23	-23	-31	-26	-40	-20	-4	-52	-38	-7	r1
	100	-6	12	-42	-14	1	1	0	1	13	2	12	9	r2
		100	-36	2	4	10	-3	28	-9	4	12	9	3	r3
			100	-72	-11	-10	1	-74	-13	-8	-12	-6	-1	<1
				100	4	-7	-2	36	24	-11	0	-17	-15	<2
					100	70	17	27	12	11	42	38	12	u1
						100	35	36	20	16	71	56	16	u2
							100	15	24	2	53	30	34	u3
								100	17	14	42	42	19	u5
									100	2	39	16	-10	u7
										100	14	19	13	u9
											100	53	12	k1
												100	18	k2
													100	k3



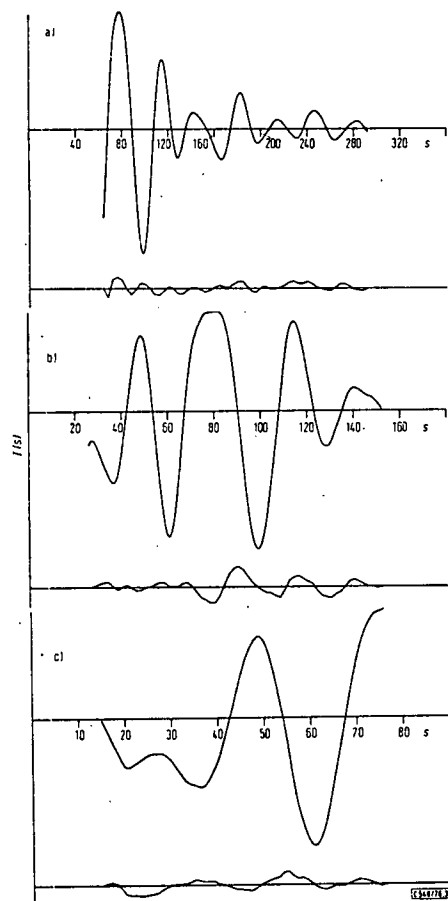


Fig. 3. Observed and final weighted difference molecular scattering intensities, obtained with nozzle-to-plate distances of a) 250, b) 500, and c) 1000 mm

### Discussion

In comparison with trimethylphosphine, trimethyl(methylene)phosphorane has short P—C(methyl) bonds [181.5(3) instead of 184.1(3) pm]<sup>8)</sup> and wide angles [101.6(5) instead

<sup>8)</sup> D. R. Lide and D. E. Mann, *J. Chem. Phys.* **29**, 914 (1958).

of 99.1(2)°] between these bonds. These are differences that are frequently observed between 3- and 4-coordinated phosphorus compounds, as, for example, in PF<sub>3</sub><sup>9)</sup> and PF<sub>3</sub>O<sup>10)</sup>. The corresponding parameters for trimethylphosphine oxide [180.9(2) pm and 104.1(8)°] and trimethylphosphine sulfide [181.8(2) pm and 104.5(3)°]<sup>11)</sup> are very close to those that we have determined.

The P—C(methylene) bond length of 164.0(6) pm is the shortest P—C distance involving a 3-coordinate carbon to be reported. This corresponds to a bond order of about 2.1, if one takes single, double, and triple bond distances to be 187, 166, and 153 pm, respectively — values derived from Pauling's covalent radii<sup>12)</sup>, with electronegativity corrections. There is also considerable distortion of the four bonds to phosphorus, away from a regular tetrahedral arrangement. Three CPC angles are 101.6°; the other three are 116.5°. This is consistent with the correlation between distortion of the phosphorus tetrahedron and shortening of the unique P—C bond in methylene-triphenylphosphorane derivatives that was mentioned above. There is no indication from these results as to the size of the P—C(methylene) bond dipole.

The methyl hydrogen atoms positions are reasonably well defined, and bond lengths and angles are as expected. The methylene hydrogen atoms positions unfortunately could not be determined. In particular, it was not possible to establish the planarity of the P=CH<sub>2</sub> group, although this would be expected in terms of our interpretation of the short P=C distance as implying sp<sup>2</sup> hybridisation of the carbon atom.

We thank Professor H. Schmidbaur and Dr. O. Gasser for providing the sample and experimental details. Professor D. W. J. Cruickshank and Dr. B. Beagley for the provision of experimental facilities, and Mrs. V. Ulbrecht for assistance in obtaining electron diffraction data. We thank the Science Research Council for a Research Studentship (T. E. F.) and the North Atlantic Treaty Organisation for a research grant.

### Experimental Part

A sample of trimethyl(methylene)phosphorane was prepared by the reaction of trimethyl(trimethylsilylmethylene)phosphorane with trimethylsilanol<sup>1)</sup>, and was purified by fractional condensation. Its purity was checked spectroscopically.

Electron diffraction scattering intensities were recorded photographically on Kodak Electron Image Plates, using a Balzers' KD.G2 diffraction apparatus at the University of Manchester Institute of Science and Technology. Data were obtained in digital form using a Joyce-Loebl automatic microdensitometer. The sample was maintained at 325 K and the nozzle at 347 K during exposures. Three camera heights were used, 250 mm (2 plates), 500 mm (2 plates) and 1000 mm (1 plate), giving data over a range of 15 to 292 mm<sup>-1</sup> in the scattering variable, *s*. The electron wavelength, determined from the diffraction pattern of gaseous benzene, was 5.672 ± 0.002 pm.

<sup>1)</sup> Y. Morino, K. Kuchitsu, and T. Moritani, *Inorg. Chem.* **8**, 867 (1969).

<sup>10)</sup> T. Moritani, K. Kuchitsu, and Y. Morino, *Inorg. Chem.* **10**, 344 (1971).

<sup>11)</sup> C. J. Wilkins, K. Hagen, L. Hedberg, Q. Shen, and K. Hedberg, *J. Am. Chem. Soc.* **97**, 6352 (1975).

<sup>12)</sup> L. Pauling, *The Nature of the Chemical Bond*, 3<sup>rd</sup> ed., Cornell University Press, Ithaca, New York 1960.

All calculations were carried out on an ICL 4-75 computer at the Edinburgh Regional Computing Centre, using established data reduction<sup>13)</sup> and least squares refinement<sup>14)</sup> programme. Weighting points used in setting up the off-diagonal weight matrix are given in Table 3, together with correlation parameters and scale factors. In all calculations, the complex scattering factors of Schäfer, Yates, and Bonham<sup>15)</sup> were used.

Table 3. Weighting functions, scale factors, and correlation parameters

Camera height mm	$\Delta s$ nm <sup>-1</sup>	$s_{\min}$ nm <sup>-1</sup>	$sw_1$ nm <sup>-1</sup>	$sw_2$ nm <sup>-1</sup>	$s_{\max}$ nm <sup>-1</sup>	$p/h$	scale factor
250	4	64	68	284	292	0.4611	0.704(19)
500	2	26	29	144	152	0.4975	0.728(16)
1000	1	15	18.5	72	76	0.4999	0.503(25)

<sup>13)</sup> D. M. Bridges, G. C. Holywell, D. W. H. Rankin, and J. M. Freeman, *J. Organomet. Chem.* **32**, 87 (1971).

<sup>14)</sup> G. C. Holywell, D. W. H. Rankin, B. Beagley, and J. M. Freeman, *J. Chem. Soc. A* **1971**, 785.

<sup>15)</sup> L. Schäfer, A. C. Yates, and R. A. Bonham, *J. Chem. Phys.* **55**, 3055 (1971).

[548/76]

## CHEMISCHE BERICHTE

Sonderdruck

## An Electron Diffraction Determination of the Molecular Structure of Hexamethylcarbodiphosphorane in the Gas Phase

E. A. V. Ebsworth\*, Thomas E. Fraser, and David W. H. Rankin

Department of Chemistry, University of Edinburgh,  
West Mains Road, Edinburgh, EH9 3JJ, Scotland, and

Oswald Gasser and Hubert Schmidbaur\*

Anorganisch-Chemisches Institut der Technischen Universität München,  
Arcisstr. 21, D-8000 München

Received December 30, 1976

The molecular structure of hexamethylcarbodiphosphorane,  $(\text{CH}_3)_3\text{P}=\text{C}=\text{P}(\text{CH}_3)_3$ , in the gas phase has been determined by electron diffraction. Principle bond lengths ( $r_e$ ) are: P–C, 181.4(3) pm, P=C, 159.4(3) pm; C–H, 108.9(4) pm. The angles between the P–C (methyl) bonds are 101.4(3)°, and the apparent P=C=P angle is 147.6(5)°. The single structure that fits the experimental data closest has  $C_2$  overall symmetry, but an even closer fit is obtained if free rotation about the P=C bonds is assumed. This and other evidence indicates that the molecule is probably a symmetric top, and that the P=C=P unit is linear in the average structure, with shrinkage caused by a low frequency bending vibration giving rise to the apparent non-linearity.

### Bestimmung der Molekülstruktur von Hexamethylcarbodiphosphoran in der Gasphase durch Elektronenbeugung

Die Molekülstruktur von Hexamethylcarbodiphosphoran,  $(\text{CH}_3)_3\text{P}=\text{C}=\text{P}(\text{CH}_3)_3$ , wurde in der Gasphase durch Elektronenbeugung bestimmt. Die hauptsächlichsten Bindungslängen ( $r_e$ ) sind P–C = 181.4(3) pm, P=C = 159.4(3) pm, C–H = 108.9(4) pm. Die Winkel zwischen den P–C (Methyl)-Bindungen betragen 101.4(3)°, der scheinbare P=C=P-Winkel 147.6(5)°. Die einzige fixierte Struktur, die die beste Anpassung an die Meßdaten ergibt, hat die Gesamtsymmetrie  $C_2$ , doch wird für ein Modell mit freier Drehbarkeit um die P=C-Achse eine noch bessere Übereinstimmung gefunden. Daraus und aus anderen Hinweisen kann geschlossen werden, daß das Molekül einen symmetrischen Kreisler bildet und daß die P=C=P-Einheit in der gemittelten Struktur linear ist. Die beobachtete Schrumpfung geht danach auf eine sehr niedrige Beugungsfrequenz zurück, die zur scheinbaren Nichtlinearität führt.

### Introduction

A study of the structure of trimethyl(methylene)phosphorane<sup>1)</sup> indicated that the P=C (methylene) bond is very short, corresponding to a bond order of at least 2, and that the methylene carbon atom can therefore be regarded as having  $sp^2$  hybridisation and a probable planar arrangement of its bonds to phosphorus and hydrogen. It is therefore possible that a carbon atom bonded to two phosphorus trialkyl groups would have  $sp$  hybridisation,

<sup>1)</sup> E. A. V. Ebsworth, T. E. Fraser, and D. W. H. Rankin, *Chem. Ber.* 110, 3494 (1977).

the PCP unit being linear. Crystalline hexaphenylcarbodiphosphorane has two molecules in the unit cell, with PCP angles of 143.8(6) and 130.1(6)°.<sup>2)</sup> In the ketene  $\text{Ph}_3\text{P}=\text{C}=\text{C}=\text{O}$ <sup>3)</sup> the P=C=C angle is 145.5(7)°, while in the analogous thioketene<sup>4)</sup> the corresponding angle is 168.0(7)°. Moreover, the related ion  $[\text{Ph}_3\text{P}=\text{N}=\text{PPh}_3]^+$  in most compounds has P=N=P angles ranging from 134.6 to 141.8°<sup>5,6)</sup>, depending on the counter anion; in one case,  $[\text{Ph}_3\text{P}=\text{N}=\text{PPh}_3]^+ [\text{V}(\text{CO})_6]^-$ , the PNP unit is crystallographically linear<sup>7)</sup>. This evidence suggests that in these systems there is only a small energy change involved in bending the chain by some 40–50° from the linear configuration. Thus it is to be expected that in the gas phase, free from packing constraints, hexamethylcarbodiphosphorane<sup>8)</sup> might well have a linear PCP unit, but that a large amplitude bending vibration would give rise to a large shrinkage effect, making the chain appear bent when studied by electron diffraction. However, if the average structure, rather than the structure determined from average distances, is in fact linear, the molecule is a symmetric top, and the orbitals available for  $\pi$  bonding, phosphorus  $d$ , and carbon  $p$  orbitals, are all members of degenerate pairs. In contrast to the situation in allenes, there should be no electronic barrier to rotation about the double bonds.

We present here the results of a study of the gas phase structure of hexamethylcarbodiphosphorane, and our interpretation of them in the light of the possibilities outlined above.

### Molecular Models

Two models were used to describe the molecular geometry of hexamethylcarbodiphosphorane,  $(\text{CH}_3)_3\text{P}=\text{C}=\text{P}(\text{CH}_3)_3$ , during least squares refinements. In both of them, the two  $(\text{CH}_3)_3\text{P}=\text{C}$  units were assumed to be identical, with overall  $C_3$  symmetry, and local  $C_{3v}$  symmetry for each  $\text{PCH}_3$  group. Geometrical parameters for this part were the P–C, P=C, and C–H bond lengths, the angles C=P–C and P–C–H, and the twist angle of the methyl groups, defined to be zero when one C–H bond was *trans* to the P=C bond. In one model, there were two further geometrical parameters, the angle P=C=P, and a twist angle. The latter was defined as the angle by which each  $(\text{CH}_3)_3\text{P}$  group was twisted away from the position in which one P–C bond was *cis* to the further P=C bond. Thus with zero twist the overall molecular symmetry was  $C_{2v}$ . The two end groups could be given twists of the same sign, giving overall  $C_2$  symmetry, or of opposite sign, giving  $C_s$  symmetry. In the second model, the P=C=P angle was defined in the same way, but instead of defining a twist angle and considering a single fixed conformation, free rotation about the P=C bonds was assumed. To do this, twist angles were defined for one P–C bond at each end of the molecule, and all possible combination of these, from 10 to 350° in steps of 20°, were considered. In this way, 9 different long P...C distances were calculated, but no less than 162 long C...C distances were involved, and an even

<sup>2)</sup> A. T. Vincent and P. J. Wheatley, *J. Chem. Soc., Dalton Trans.* 1972, 617

<sup>3)</sup> J. J. Duly and P. J. Wheatley, *J. Chem. Soc.* 1966, 1703.

<sup>4)</sup> J. J. Duly, *J. Chem. Soc.* A 1967, 1913.

<sup>5)</sup> J. K. Ruff, R. P. White, and I. F. Dahl, *J. Am. Chem. Soc.* 93, 2159 (1972), and references therein.

<sup>6)</sup> H. B. Chin, M. B. Smith, R. D. Wilson, and R. Bau, *J. Am. Chem. Soc.* 96, 5285 (1974).

<sup>7)</sup> R. D. Wilson and R. Bau, *J. Am. Chem. Soc.* 96, 7601 (1974).

<sup>8)</sup> O. Gasser and H. Schmidbaur, *J. Am. Chem. Soc.* 97, 6281 (1975). – <sup>8b)</sup> H. Schmidbaur, O. Gasser, and M. S. Hussain, *Chem. Ber.* 110, 3501 (1977), preceding.

greater number of C...H and H...H distances, and it seemed sensible to reduce these numbers to save computing time and space. For the C...C distances, the total range, from about 360 to 590 pm, was divided into 10 pm intervals and all those falling into one interval were replaced by a single composite "distance", being the weighted mean of its components, and having the appropriate total weight. The amplitudes of vibration for these distances represented the contributions to the real amplitudes arising from vibrations other than the torsion/internal rotation. For the C...H and H...H distances, even this method seemed to be unnecessarily complex, and these were therefore calculated assuming the same fixed conformation as was found using the first model.

### Results

The results of the best refinements using the two models are listed in table 1 as refinements A and B, respectively. Errors quoted in this table are estimated standard deviations, obtained in the least squares analysis, increased to allow for systematic errors. In both refinements, all geometrical parameters were included, and as many amplitudes of vibration as would refine satisfactorily. For the rotation model, these included the two types of C(P)C amplitude, constrained to be equal, and the "framework" amplitude of vibration, excluding effects due to torsion or internal rotation, of the long P...C distances.

Table 1. Molecular parameters of  $(\text{CH}_3)_3\text{P}=\text{C}=\text{P}(\text{CH}_3)_3$

	Refinement A		Refinement B	
	Distance (pm)	Amplitude (pm)	Distance (pm)	Amplitude (pm)
<b>Independent distances (<math>r_i</math>)</b>				
$r_1$ (P=C)	161.1(5)	5.6(8)	159.4(3)	6.9(8)
$r_2$ (P-C)	181.4(3)	5.5(5)	181.4(3)	6.1(4)
$r_3$ (C-H)	109.3(5)	7.6(7)	108.9(4)	7.4(7)
<b>Dependent distances<sup>a1</sup></b>				
$d_4$ (C...C)	283.8(30)	7.6(9)	280.6(16)	7.9(8)
$d_5$ (C...C)	289.6(31)		290.4(20)	
$d_6$ (P...H)	241.9(19)	11.6(7)	240.5(18)	11.3(6)
$d_7$ (P...P)	306.7(24)	8.0 (fixed)	306.0(22)	7.8(11)
$d_8$ (P...C)	382-447	14.1(13)	383-449	12.2(11) <sup>b1</sup>
(C...C)	406-565	20.9(18)	365-585	22.5 (fixed)
<b>Angles (degrees)</b>				
<1 (P=C=P)	144.3(6)		147.6(5)	
<2 (C=P-C)	115.4(6)		116.7(4)	
<3 (P-C-H)	110.1(8)		109.3(9)	
<4 (methyl twist) <sup>c1</sup>	37.7(18)		36.3(11)	
<5 (C <sub>3</sub> P twist) <sup>c1</sup>	31.4(6)		Free rotation	
$R_G$	0.131		0.113	
$R_D$	0.077		0.066	

<sup>a1</sup> Many C...H and H...H distances were included in refinements, but are not listed here.

<sup>b1</sup> "Framework" amplitude, refined for the group of P...C distances. See text.

<sup>c1</sup> For definition, see text.

The best value for the corresponding parameters for the long C...C distances was found earlier to be 22.5 pm, but this was not refined further. The least squares correlation matrix for refinement B is given in table 2.

Table 2. Least squares correlation matrix for refinement B, multiplied by 100

$r_1$	$r_2$	$r_3$	<1	<2	<3	<4	$u_1$	$u_2$	$u_3$	$u_4$	$u_6$	$u_7$	$u_8$	-1	$k_2$	$k_3$	
100	-54	-5	-62	29	7	15	7	-20	-10	-34	4	1	-4	-25	-42	-21	$r_1$
	100	-7	41	-14	24	-47	-2	19	7	24	-2	5	1	24	33	14	$r_2$
		100	14	-19	-24	22	-19	2	4	5	-13	-5	8	3	8	3	$r_3$
			100	-62	-2	-25	-7	24	10	17	-12	-41	6	24	38	21	<1
				100	-30	-24	-3	-4	4	-51	13	21	12	-1	-5	-6	<2
					100	-90	28	-5	-16	17	-27	-8	-14	-11	-23	-8	<3
						100	-25	-10	8	-16	27	16	10	-5	-1	-4	<4
							100	39	-12	11	-1	5	-4	11	5	4	$u_1$
								100	29	25	4	16	9	65	58	25	$u_2$
									100	10	11	11	8	40	35	11	$u_3$
										100	-5	50	-13	23	38	27	$u_4$
											100	9	0	26	8	-14	$u_6$
												100	-2	17	22	14	$u_7$
													100	10	13	6	$u_8$
														100	51	18	$k_1$
															100	31	$k_2$
																100	$k_3$

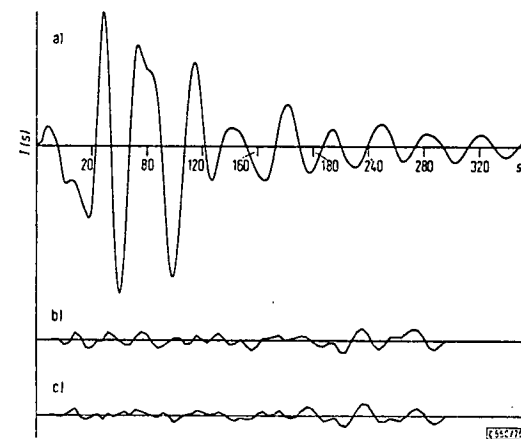


Fig. 1. Combined molecular scattering intensity curves: a) experimental, b) weighted difference, refinement A, c) weighted difference, refinement B

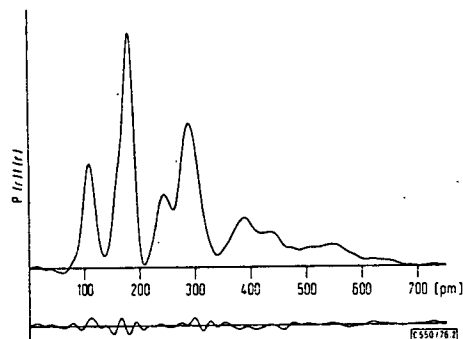


Fig. 2. Radial distribution curve,  $P(r)/r$ , and difference curve for refinement B. Before Fourier inversion, the data were multiplied by:  $s \cdot \exp[-0.00002 s^2/(z_p - f_p)(z_c - f_c)]$

With the fixed conformation model, there was one more geometrical parameter, and so amplitudes of vibration were not so easily refined. In this case, the amplitudes associated with long  $P \cdots C$  and  $C \cdots C$  distances include a contribution from the torsional vibrations, and so larger values were obtained. With this model, the lowest  $R$  factor ( $R_G$ ) obtained was 0.131 compared with 0.113 using the free rotation model. The molecular scattering intensities and final weighted differences for refinements A and B are shown in Fig. 1. The radial distribution curve,  $P(r)/r$ , and difference curve for refinement B, are shown in Fig. 2.

### Discussion

The parameters of the  $C_3P=C$  skeletons of the two halves of hexamethylcarbodi-phosphorane are very much as expected, when compared with corresponding parameters for trimethyl(methylene)phosphorane<sup>11</sup>. Thus the  $P=C$  distance is reduced from 164.0(6) to 159.4(3) pm, just as in the corresponding phenyl compounds, for which the change is from 166.1(8)<sup>9)</sup> to 163.1(3) pm<sup>2)</sup>. This shortening is consistent with a change of carbon atom hybridisation from  $sp^2$  to  $sp$ . The  $C=P-C$  angle [116.7(4)<sup>2)</sup>] corresponds to a  $C-P-C$  angle of 101.4<sup>2)</sup>, not much wider than that [99.1(2)<sup>2)</sup>] in trimethylphosphine itself<sup>10)</sup>. The  $P-C$  distances in the two phosphoranes are very similar, 181.4(3) and 181.5(3) pm, but they are considerably shorter than the equivalent distance in trimethylphosphine, 184.1(3) pm.

All parameters associated with the  $(CH_3)_3P=C$  groups are in excellent agreement with those for corresponding parameters reported for trimethylphosphine oxide and sulfide<sup>11)</sup>, including those involving hydrogen atom positions. These positions are much more reliably determined in the present study than in the work on trimethyl(methylene)phosphorane, as possible systematic errors arising from choice of methylene group parameters are avoided. As the agreement with

<sup>2)</sup> J. C. J. Bart, *J. Chem. Soc. B* 1969, 350.

<sup>10)</sup> D. R. Lile and D. E. Mann, *J. Chem. Phys.* 29, 914 (1958).

<sup>11)</sup> C. J. Wilkins, K. Hagen, L. Hedberg, Q. Shen, and K. Hedberg, *J. Am. Chem. Soc.* 97, 6352 (1975).

trimethylphosphine oxide and sulfide results was so good, the possibility of free rotation of methyl groups was not considered, as this had been found in the earlier work not to improve the fit of theoretical and experimental data.

The most interesting results of the present study are concerned with the relative positions and motions of the two  $(CH_3)_3P=C$  units. In both refinements, A and B, the PCP angle is very wide, 147.6(6)<sup>2)</sup>, in the preferred set of parameters. It should be emphasized that this angle is the one that gives the best fitting set of time-averaged interatomic distances ( $r_a$ ), and that it is not necessarily the angle in the average structure of either the ground vibrational state of the molecule, or the vibrational states populated at the temperature of the experiment.

In carbon suboxide<sup>12, 13)</sup>, a linear molecule with a low frequency ( $63 \text{ cm}^{-1}$ ) for the CCC bending vibration, the apparent CCC angle, determined by electron diffraction, is only 158<sup>2)</sup> and silyl isocyanate has an apparent SiNC angle of 151.7(12)<sup>2)</sup> when studied by electron diffraction<sup>14)</sup>, although a microwave study<sup>15)</sup> shows unequivocally that the ground state molecule is a symmetric top, with an SiNC angle of 180<sup>2)</sup>.

Thus shrinkages large enough to make a linear system appear to be bent by 30<sup>2)</sup> or more are well established, and we present two pieces of evidence to support the hypothesis that the present system may be similar. Firstly, in the linear  $[Ph_3P=N=PPH_3]^+$  cation, the  $P=N$  bonds are 153.9(2) pm long<sup>7)</sup>, compared with 157–158 pm in the same ion in situations where the PNP angle is 137–142<sup>3, 6)</sup>. A  $P=C$  bond of the same order as the short  $P=N$  bond would be approximately 159 pm long – almost exactly the same as is found in the carbodi-phosphorane. Secondly, in a linear  $R_3P=C=PR_3$  system, all the orbitals that could be involved in  $\pi$ -bonding are members of degenerate pairs, and there can be no electronic barrier to rotation about the  $P=C$  bonds. In a bent system the degeneracy would be lifted, and the electronic contribution to the barrier would in principle be expected to increase as the angle decreases. Theoretical calculations have shown that the barrier to rotation about the  $P-C$  bond in the hypothetical  $H_3PCH_2$  should be very small<sup>16, 17)</sup>. Most 6-fold barriers are small. In bent  $R_3PCPR_3$ , the barrier to rotation about the  $P-C$  bonds would be 3-fold. From the ratio of the  $R$  factors for our refinements B and A, and tabulated values for such ratios<sup>18)</sup>, we can reject, at the 99% confidence level, the single conformation model of refinement A. The radial distribution curve,  $P(r)$ , and difference curves for refinements A and B (Fig. 3) show how the free rotation model is superior. We conclude that rotation about the double bonds is effectively unrestricted; this would be most consistent with a model in which the average structure of the  $P=C=P$  chain were linear, at least for the vibrational states populated at the temperature of the experiment.

<sup>12)</sup> M. Tamimoto, K. Kuchitsu, and Y. Morino, *Bull. Chem. Soc. Jpn.* 43, 2776 (1970).

<sup>13)</sup> A. Almenningen, S. P. Arnesen, O. Bastiansen, H. M. Seip, and R. Seip, *Chem. Phys. Lett.* 1, 569 (1968).

<sup>14)</sup> C. Glidewell, A. G. Robiette, and G. M. Sheldrick, *Chem. Phys. Lett.* 16, 526 (1972).

<sup>15)</sup> J. A. Duckett, A. G. Robiette, and I. M. Mills, *J. Mol. Spectrosc.* 62, 74 (1976).

<sup>16)</sup> R. Hoffmann, D. B. Boyd, and S. Z. Goldberg, *J. Am. Chem. Soc.* 92, 3929 (1970) (Extended Hückel).

<sup>17)</sup> J. Absar and J. R. van Wazer, *J. Am. Chem. Soc.* 94, 2382 (1972) (*Ab-initio*).

<sup>18)</sup> W. C. Hamilton, *Acta Crystallogr.* 18, 502 (1965).

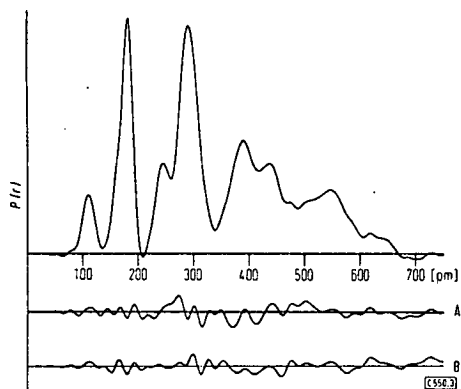


Fig. 3. Radial distribution curve,  $P(r)$ , and difference curves for refinements A (fixed conformation) and B (free rotation). The curves were obtained in the same way as those of Fig. 2

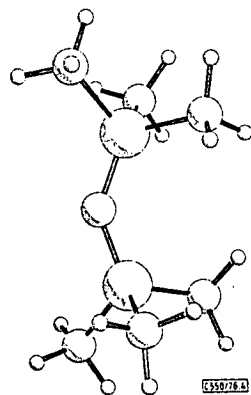


Fig. 4. Molecular model of  $(\text{CH}_3)_3\text{P}=\text{C}=\text{P}(\text{CH}_3)_3$

If the  $\text{P}=\text{C}=\text{P}$  unit is linear, then to account for the observed apparent angle, the PCP bending frequency, which is unknown, must be low, probably about  $80\text{ cm}^{-1}$ . This is not unreasonable, by analogy with carbon suboxide<sup>12, 13</sup>, which also has a central carbon atom with two double bonds, and a  $\pi$ -system derived from degenerate pairs of orbitals, in which the CCC bending frequency is  $63\text{ cm}^{-1}$ . Similarly, the wide range of PNP and PCP angles in  $\text{Ph}_3\text{P}=\text{C}=\text{PPh}_3$ <sup>21</sup> and  $[\text{Ph}_3\text{P}=\text{N}=\text{PPh}_3]^+$  cation<sup>5, 6, 7</sup> indicate that there is very little energy change involved in

bending the central chains by  $40-50^\circ$  from the linear structures, and the triboluminescence of hexaphenylcarbodiphosphorane has been attributed to a phase change associated with a change of PCP angle<sup>19</sup>. Thus it seems probable that in all these structures, the potential well for the bending coordinate is fairly flat-bottomed, rising steeply at about  $130-140^\circ$ , when the phosphorus atoms get close to each other. Indeed, it may well be this easy flexibility, leading to ease of packing into a lattice, that accounts for the remarkable properties of  $[\text{Ph}_3\text{P}=\text{N}=\text{PPh}_3]^+$ , which is used for stabilising reactive anions.

It should be noticed that hexamethylcarbodiphosphorane is iso-electronic with hexamethyldisiloxane. This molecule has an SiOSi angle, determined by electron diffraction<sup>20</sup>, of  $148(3)^\circ$ , but there is uncertainty about the SiOSi bending frequency, and the extent of shrinkage effects. The possibility cannot be excluded that this disiloxane also has a linear average structure for the SiOSi group.

Finally, it should be noted that in the  $\text{P}=\text{C}=\text{P}$  bending vibration of hexamethylcarbodiphosphorane, the atom that moves most is the central carbon atom. If this movement takes place without much relative movement of the two phosphorus atoms, then the  $\text{P}=\text{C}$  distance would change in the course of the vibration, but the  $\text{P}\cdots\text{P}$  distance would change relatively little. Our results show a surprisingly large amplitude of vibration,  $6.9(8)\text{ pm}$ , for the  $\text{P}=\text{C}$  atom pair, and an unusually small value,  $7.8(11)\text{ pm}$ , for the  $\text{P}\cdots\text{P}$  pair, although the latter value is correlated with  $\text{C}\cdots\text{C}$  amplitudes of vibration. These two observations therefore provide further evidence that this molecule is a symmetric top, but with a large amplitude bending vibration.

We thank Professor D. W. J. Cruickshank and Dr. B. Beagley for the provision of experimental facilities, and Mrs. V. Ulbrecht for recording the scattering data. We thank the Science Research Council for a research studentship (T. E. F.), the North Atlantic Treaty Organisation for a research grant, and the Deutsche Forschungsgemeinschaft for support.

### Experimental Part

A sample of hexamethylcarbodiphosphorane was prepared from difluorotrimethylphosphorane by the route that has been described previously<sup>8a</sup>, and purified by fractional distillation. Its purity was checked spectroscopically.

Electron diffraction scattering data were recorded photographically on Kodak Electron Image Plates using a Balzers' KD.G2 diffraction apparatus, and were converted to digital form with a Joyce-Loebl automatic microdensitometer. During experiments the temperature of the sample and inlet system were maintained at  $350\text{ K}$ . Camera heights of  $250\text{ mm}$  (3 plates),  $500\text{ mm}$  (3 plates) and  $1000\text{ mm}$  (3 plates) were used, giving data over a total range of  $10$  to  $296\text{ nm}^{-1}$  in the scattering variable,  $s$ . The electron wavelength,  $5.661(5)\text{ pm}$ , was determined from the diffraction pattern of gaseous benzene.

An ICL 4-75 computer at the Edinburgh Regional Computing Centre was used for all calculations, with our usual data reduction<sup>21</sup> and least squares refinement<sup>22</sup> programmes. Weighting points used in setting up the off-diagonal weight matrix, together with correlation parameters and scale

<sup>19</sup> J. I. Zink and W. C. Kaska, *J. Am. Chem. Soc.* **95**, 7510 (1973).

<sup>20</sup> B. Csákvári, Z. S. Wagner, P. Gümöry, F. C. Mijlhoff, B. Rozsondai, and I. Hargittai, *J. Organomet. Chem.* **107**, 287 (1976).

<sup>21</sup> D. M. Bridges, G. C. Holywell, D. W. H. Rankin, and J. M. Freeman, *J. Organomet. Chem.* **32**, 87 (1971).

<sup>22</sup> G. C. Holywell, D. W. H. Rankin, B. Beagley, and J. M. Freeman, *J. Chem. Soc. A* **1971**, 785.

factors, are given in Table 3. In all calculations, the scattering factors of Schäfer, Yates, and Bonham<sup>23)</sup> were used.

Table 3. Weighting functions, correlation parameters, and scale factors

Camera height mm	$\Delta s$ nm <sup>-1</sup>	$s_{min}$ nm <sup>-1</sup>	$s_w$ nm <sup>-1</sup>	$s_{w2}$ nm <sup>-1</sup>	$s_{max}$ nm <sup>-1</sup>	$p/h$	Scale factor
250	4	72	87	282	296	0.4193	0.417(14)
500	2	24	29	142	152	0.4687	0.747(12)
1000	1	10	11.5	76	78	0.4978	0.603(15)

<sup>23)</sup> L. Schäfer, A. C. Yates, and R. A. Bonham, J. Chem. Phys. 55, 3055 (1971).

[550/76]

## CHEMISCHE BERICHTE

Sonderdruck